FLUOROSULFATE DERIVATIVES OF NIOBIUM AND TANTALUM AND THEIR BEHAVIOR AS COMPONENTS OF NOVEL SUPERACID SYSTEMS

By

WALTER VLADIMIR CICHA

B.Sc., The University of British Columbia, 1984

A THESIS SUBMITTED IN PARTIAL FULFILLMENT OF

THE REQUIREMENTS FOR THE DEGREE OF

DOCTOR OF PHILOSOPHY

in

THE FACULTY OF GRADUATE STUDIES
(Department of Chemistry)

We accept this thesis as conforming
to the required standard

THE UNIVERSITY OF BRITISH COLUMBIA

August, 1989

In presenting this thesis in partial fulfilment of the requirements for an advanced degree at the University of British Columbia, I agree that the Library shall make it freely available for reference and study. I further agree that permission for extensive copying of this thesis for scholarly purposes may be granted by the head of my department or by his or her representatives. It is understood that copying or publication of this thesis for financial gain shall not be allowed without my written permission.

Department of CHEMISTRY

The University of British Columbia
Vancouver, Canada

Date August 18, 1989

DE-6 (2/88)

ABSTRACT

The goal of this study was to develop new superacid systems based on fluorosulfuric acid, HSO_3F, (the strongest monoprotonic Brönsted acid) and metal fluorosulfates capable of acting as Lewis acids. The in situ oxidation of niobium and tantalum in HSO_3F by bis(fluorosulfuryl) peroxide, $S_2O_6F_2$, resulted in the formation of the highly solvated Lewis acids $M(SO_3F)_5$ with M = Nb or Ta. Based on electrical conductivity measurements, both solutes were found to behave as moderately strong, monoprotonic acids in HSO_3F, with $Ta(SO_3F)_5$ the markedly stronger acid of the two. The Hammett Acidity Function, H_o, determined for the HSO_3F-$Ta(SO_3F)_5$ superacid system confirmed its high acidity, which clearly exceeds that of HSO_3F-SbF_5 ("Magic Acid"), the most frequently used superacid system. In addition, both the solubility and acidity in HSO_3F of the two new Lewis acids are vastly greater than those of the analogous fluorides, NbF_5 and TaF_5, in either HF or HSO_3F.

The high solubility of $Nb(SO_3F)_5$ and $Ta(SO_3F)_5$ allowed the study of their solution behavior, using ^1H, ^{19}F and ^{93}Nb NMR, as well as Raman spectroscopy. Evidence for the existence of $M(SO_3F)_5$, with M = Nb or Ta, comes from the synthesis of the salts $M_x'[M(SO_3F)_{5+x}]$, with M´ = Cs or Ba and x = 1 or 2, which were characterized by vibrational spectroscopy. Salts with anions of the types $[M(SO_3F)_6]^-$ or $[M(SO_3F)_7]^{2-}$ have previously not been isolated. In solution, multicomponent equilibria appeared to be present between the anions $[M(SO_3F)_6]^-$ and $[M(SO_3F)_7]^{2-}$ with M = Nb or Ta.

Synthesis of $TaF_4(SO_3F)$ from a 4:1 mixture of TaF_5 and $Ta(SO_3F)_5$ in HSO_3F as well as the formation of $NbF_2(SO_3F)_3$ from a concentrated solution of HSO_3F-$Nb(SO_3F)_5$ suggested the possibility of a new family of superacid systems of the type

HSO_3F-$MF_x(SO_3F)_{5-x}$, with x = 1-4. Initial investigations are reported. In addition, preliminary work dealing with analogous trifluoromethyl sulfuric acid (HSO_3CF_3) systems is also discussed.

During the course of this study, bis(fluorosulfuryl) peroxide ($S_2O_6F_2$) was found to behave as a weak base soluble only in acids stronger than 100% sulfuric acid. Addition of potassium fluorosulfate, KSO_3F, to reduce the acidity of HSO_3F also lowered the acid's ability to dissolve $S_2O_6F_2$. The HSO_3F-$S_2O_6F_2$ system was studied using Raman, ^1H and ^{19}F NMR, and ESR spectroscopy, which led to evidence for proton transfer, hydrogen-bridging and fluorosulfate exchange between the solvent (HSO_3F) and solute ($S_2O_6F_2$).

TABLE OF CONTENTS

LIST OF TABLES

Page

LIST OF FIGURES

Page

LIST OF ABBREVIATIONS AND SYMBOLS

as	asymmetric
b	broad
δ	vibrational deformation mode (IR), chemical shift (NMR)
Δ	difference between two values
DNFB	2,4 - dinitrofluorobenzene
dt	doublet
ϵ	extinction coefficient (molar absorptivity)
ESR	electron spin resonance
FT	Fourier transform
H	HSO_3F
H_o	Hammett Acidity Function
ΔH_{pp}	signal linewidth (ESR)
int.	integration
IR	infrared
K	equilibrium constant
κ	specific conductance
λ^*	molal conductance
λ_{max}	wavelength of maximum absorbance
m	medium (intensity), molality (concentration)
NMR	nuclear magnetic resonance
ν	vibrational frequency
ν_{as}	asymmetric vibrational stretching mode
ν_s	symmetric vibrational stretching mode
Ω	ohm

OX	$S_2O_6F_2$
prep.	preparation
redox	reduction-oxidation
s	strong
sh	shoulder
solv	solvated
st	singlet
stoich.	stoichiometry
sym	symmetric
temp.	temperature
TNT	2,4,6 - trinitrotoluene
v	very
w	weak
$w_{1/2}$	signal linewidth at half-height (NMR)

ACKNOWLEDGEMENTS

First and foremost, the guidance, wisdom and confidence-boosts provided by my scientific mentor, Professor Felix Aubke, were deeply appreciated during the years leading to this thesis. His unlimited generosity and kindness were only surmounted by his patience in bearing my more than sporadic somewhat-less-than-scientific rambling.

Many thanks are also due to the "boys (and occasionally girls) of 457", who made work a very pleasant and rewarding experience. Roshan Cader and Freddy Mistry deserve special mention for their invaluable comradeship, various eccentricities, and perseverance with my incurable habit of using the lab as a walk-in locker for the multitude of recreational hardware with which I have burdened myself (and those around me) over the years.

The exceptional service staff of this department are too numerous to list exhaustively here, but a few deserve special mention: Marietta and Orson (NMR Service Lab); Milan, Brian and Mike (Electronics); Ron, Bill and Graham (Mech. Shop); the graphics illustrators, who made my conference presentations presentable, and the entire staff of Chemistry Stores, where the entrance door handle has a permanent impression of my fingerprints. To forget the department's favorite Hungarians, Peter the microanalyst and Steve the glass-blower, is unthinkable. Their artistry brings a whole new dimension to the word "chemistry".

The helpful discussions of Professor Herring and the infinite know-how and good will of Ben Clifford (everyone's favorite laboratory instructor) are also appreciated.

The enlightening debates with Tim, Ian and Pete brought a whole new dimension to the concept of intellectual freedom, while Whistler and McLeery provided us with the physical equivalent. The "Bus Stop" sessions with Professor Wickenheiser and Rosh are also something to be remembered. The friendship of this lot is truly prized.

Although more detrimental to my hearing than all the explosions in which I have figured, the "music" of the Free Radicals will perpetually follow me about. Being part of this band with Ian, Jim and Dave provided a much needed distraction as well as a large handful of hang-overs.

Financial support from Moli Energy Ltd. and the British Columbia Research Council in the form of a Graduate Research Engineering and Technology Award (1986-1989) is gratefully appreciated.

Finally, I am (grateful)^{x} to Sherry, without whose support, understanding and multitude of sacrifices this work would not have been possible (at least not during this decade).

Dílo Jako Prase

For Sherry and my parents, Bohumila and Vladimír,
the three most important people in my life

CHAPTER 1
INTRODUCTION

1.A. General Overview

Fluorosulfuric acid has been extensively studied and widely used as a solvent, reagent and catalyst in a large assortment of organic and inorganic reactions since it was first prepared nearly a century ago by Thorpe and Kirman[1] according to:

$$HF + SO_3 \longrightarrow HSO_3F \qquad (1\text{-}1)$$

There have been various reviews published during the last forty years dealing with many aspects of the acid's characteristics and uses.[2-9]

An important feature of fluorosulfuric acid is its high acidity. It is in fact considered to be the strongest known simple Brönsted acid and is widely used as a component of superacid solvent systems, this name commonly given to any acid stronger than 100% H_2SO_4.[10] This, more than any other property, has been responsible for its frequent employment as a catalyst and chemical reagent in various chemical processes involving organic materials, such as alkylation, acylation, polymerization, sulfonation, isomerization and the production of organic fluorosulfates.[11] More specialized application of HSO_3F has involved the preparation of intercalation compounds with graphite.[11,12] The acid has also been used as a reagent and solvent for the preparation and characterization of a vast range of inorganic fluorosulfate and fluoride compounds.[9,13] The addition of strong Lewis acids in order to increase the acidity of HSO_3F has been studied since the early 1960's. The increased acidity has been used to stabilize unusual carbocations and many novel inorganic homo- and heteronuclear compounds.[11]

The last two decades have seen increased interest in the chemistry of fluorosulfates. The range of known fluorosulfate compounds in various oxidation states from +1 to +7 spans the majority of the metalloids, main group and transition metals in the periodic table.[13] The only exceptions among the transition metals are the group 3 metals, hafnium and technetium. However, *binary* fluorosulfates are somewhat rarer. Figure 1.1 shows their abundance among the transition metals in comparison to the better represented binary fluorides. Comparing the two groups MF_n and $M(SO_3F)_n$, a number of reasons for the greater abundance of the former become apparent: (i) The use of elemental fluorine is unique, with a wide range of reaction conditions and synthetic techniques having been employed. Besides metals, a large number of starting materials (e.g. halides, oxides and oxyacid salts) may be used. (ii) Fluorides display a wider range of oxidation states. For example, platinum fluorides[14] may have n values of 3, 4, 5 or 6, while only $Pt(SO_3F)_4$[15] is known among the fluorosulfates. (iii) Whereas hexa- and even heptafluorides are known for some transition metals, in binary fluorosulfates n appears to be limited to *four*, which may in part be due to steric reasons. (iv) Binary fluorosulfates have a more limited thermal stability. Four modes of decomposition are known:[8]

$$\text{a)}\ M(SO_3F)_n \longrightarrow MF_x(SO_3F)_{n-x} + x\,SO_3 \qquad (1\text{-}2a)$$

$$\text{b)}\ M(SO_3F)_n \longrightarrow MO_x(SO_3F)_{n-2x} + x\,S_2O_5F_2 \qquad (1\text{-}2b)$$

$$\text{c)}\ M(SO_3F)_n \longrightarrow M(SO_4)_x(SO_3F)_{n-2x} + x\,SO_2F_2 \qquad (1\text{-}2c)$$

$$\text{d)}\ M(SO_3F)_n \longrightarrow M(SO_3F)_{n-2x} + x\,S_2O_6F_2 \qquad (1\text{-}2d)$$

Only modes a) and b), however, are common.[16-19]

For this study, niobium and tantalum are chosen from amongst the other "available" early transition metals for three main reasons: (i) their compounds are known

III B	IV B	V B	VI B	VII B	——— VIII ———			I B	II B
3 Sc	3,4 Ti	3,4,5 V ③	2,3,4,5 Cr ③	2,3 Mn ②③	2,3 Fe ②③	2,3 Co ②	2 Ni ②	2 Cu ②	2 Zn ②
3 Y	4 Zr	3,4,5 Nb	3,4,5,6 Mo	5,6 Tc	3,4,5,6 Ru ③	3,4,5,6 Rh ③	2,3*,4 Pd ②	1,2 Ag ①②	2 Cd ②
3 La	4 Hf	3,5 Ta	4,5,6 W	4,5,6,7 Re	4,5,6,7 Os ③	3,4,5,6 Ir ③④	3*,4,5,6 Pt ④	3,5 Au ③	1,2 Hg ②

* denotes a mixed oxidation state + 2, + 4

Figure 1.1. Oxidation States of Known Binary Fluorosulfates (circled) and Fluorides (upper rows) of the Transition Metals

to exist preferentially in the +5 oxidation state[20,21] and are hence unlikely to cause oxidation as a side reaction in the presence of other materials; (ii) both the fluorides NbF_5 and TaF_5 have previously been used with HSO_3F as components of effective superacid systems, although their application has been somewhat restricted by lack of sufficient solubility and acidity in the Brönsted acid and (iii) compared to some of the other 4d and 5d metals, Nb and Ta are less expensive and their compounds should consequently see wider use. Besides considerable similarities between the physical properties of elemental niobium and tantalum, shown in Table 1.I, there is also comparable chemistry known for both. The nearly identical tetrameric structure and chemical behaviour of NbF_5 and TaF_5 are good examples of this.[20] Of all the properties listed, the identical lattice constant and atomic radii of the two metals best predict these similarities.

The remaining element in group 5, vanadium, was not included in this study for a number of reasons: (i) it tends to exist in more variable oxidation states ranging from +3 to +5; (ii) VF_5, which is a liquid at S.T.P., has not been investigated as a potential Lewis acid in HSO_3F, probably due to its fluorinating ability[22] and its tendency to undergo oxidative side reactions; (iii) $V(SO_3F)_3$ has been synthesized and found to be insoluble in HSO_3F[23,24] and (iv) vanadium exhibits a great tendency to form VO and VO_2 derivatives of oxyacids ($VO(SO_3F)_3$ is a well known example[18]), a tendency which is not shared to the same extent by niobium or tantalum.

There have been two precedents for the use of binary fluorosulfates in superacid systems, $Au(SO_3F)_3$[25] and $Pt(SO_3F)_4$,[15] both previously prepared in our laboratory. However, the metals' high cost has limited any widespread synthetic use.

Table 1.I. General Properties of Niobium and Tantalum[a]

Property	Niobium	Tantalum
Atomic #	41	73
Atomic weight	92.9064	180.9479
Electron configuration	$Kr4d^45s^1$	$Xe4f^{14}5d^36s^2$
Principal isotopes	^{93}Nb	^{180}Ta, ^{181}Ta
Relative abundance (%)	(100)	(0.0123), (99.988)
Nuclear spin, I	9/2	7/2
Crystal structure	bcc	bcc
$Radius_{metal}$ (Å)	1.43	1.43
Lattice constant	3.294	3.296
$Radius_{ion}$ (M^{5+}, Å)	0.69	0.68
Melting point	2468 ± 10	2996
Boiling point	5127	5427 ± 100
Density (20°C, g/cm^3)	8.66	16.64
Heat of fusion (kcal/g-atom)	6.4	7.5
Heat of vaporization (")	166.5	180
Heat of combustion (")	227.5	244
Principle oxidation states	5,4?,3,2	5,4?,3,2?
$\varepsilon^\circ_{1/2}$ for $M_2O_5 + 10H^+ \xrightarrow{+10e^-} 2M + 5H_2O$ (volts)	-0.65	-0.81
Natural abundance in earth's crust (% by weight)	4×10^{-5}	1.2×10^{-5}
Rank amongst elements	59th	64th

[a]references: 20 and 141

Structural characterization of fluorosulfate compounds has been limited; the existence of only seven reported x-ray crystal structure analyses[26-32] is indicative of this. Consequently, vibrational specroscopy has been used as the principal means of obtaining the majority of structural information for these compounds in the solid state.[13] In the case of tin fluorosulfates, ^{119}Sn Mössbauer spectroscopy has also found considerable

use.[33,34] Additional structural information has been obtained for many of these compounds in HSO_3F solution, given that they dissolve adequately in the acid. The techniques most relied upon in the latter case have been ^{19}F NMR, Raman and electronic spectroscopy, as well as conductivity.[13]

1.B. Properties of Fluorosulfuric Acid

In addition to its high acid strength, fluorosulfuric acid has a number of additional features which have contributed to its use. HSO_3F, unlike anhydrous HF,[35,36] can be handled in pyrex or similar borosilicate glasses without causing etching. The self-dissociation equilibrium:

$$HSO_3F \rightleftharpoons HF + SO_3 \qquad (1\text{-}3)$$

is only important at elevated temperatures and distillation for the purpose of purification is possible at atmospheric pressure in a pyrex apparatus.[37] While HSO_3F reacts rapidly and exothermically with most organic matter, it will not do so explosively, like $HClO_4$, for example.

Some properties of HSO_3F are summarized in Table 1.II. Properties of the three other protonic solvents H_2SO_4, HF and H_2O are also included for comparison. The liquid range of HSO_3F is nearly as wide as that of H_2SO_4, but more conveniently placed at a mean temperature of *37 °C*. It distills without extensive decomposition, can be used as a low and high temperature medium. Secondly, its viscocity is comparable to that of water, allowing easy isolation of acid-free solid products by filtration. It appears that the presence of only one proton per molecular unit causes reduced hydrogen bridging in HSO_3F compared to that found in H_2SO_4.[6] Consequently,

Table 1.II. Physical Properties[a] of HSO_3F, H_2SO_4, HF and H_2O

Property	HSO_3F	H_2SO_4	HF	H_2O
Freezing point (°C)	-88.98	10.371	-89.37	0
Boiling point (°C)	162.7	290.317	19.51	100
Liquid range (°C)	252	~300	109	100
Viscosity (centipoise)	1.56 (25°C)	24.54 (25°C)	0.256 (0°C)	0.8904 (25°C)
Density (g/cm^3)	1.726 (")	1.8269 (")	1.002 (")	1.00 (4°C)
Dielectric constant	~120 (")	100 (")	84 (")	78.5 (25°C)
Specific conductance (Ω^{-1}/cm)	1.085×10^{-4} (")	1.0439×10^{-2} (")	$\sim 10^{-6}$ (")	5×10^{-7} (")
Autoprotolysis constant	3.8×10^{-8}	2.7×10^{-4}	$\sim 2 \times 10^{-12}$	10^{-14} (")
Cryoscopic constant (deg mol^{-1} kg)	3.93 ± 0.05	6.12 ± 0.02	–	–

[a]references 6 and 40

electrolytes are more mobile in HSO_3F, making it much more suitable for electrical conductivity studies. Thirdly, the dielectric constant of HSO_3F is estimated to be higher than that found in H_2SO_4, which also makes it very suitable as an ionizing solvent. Finally, the autoprotolysis or proton transfer equilibrium[6] takes place according to:

$$2\,HSO_3F \overset{K_{ap}}{\rightleftharpoons} H_2SO_3F^+ + SO_3F^- \qquad (1\text{-}4)$$

with $K_{ap} = [SO_3F^-][H_2SO_3F^+] = 3.8 \times 10^{-8}$ mol^2 kg^{-2}. The acidium, $H_2SO_3F^+$, and base, SO_3F^-, ions produced are responsible for the acid's specific conductance of 1.08×10^{-4} ohm^{-1}cm^{-1} at 25.00 °C.[6] Molal conductance values at infinite dilution of 320 and 235 ohm^{-1}cm^{-1}mol^{-1} have been established for $H_2SO_3F^+$ and SO_3F^-, respectively,[37,38] and it has been postulated that pure HSO_3F, just like H_2SO_4, conducts via a proton transfer mechanism.

There are two other possible modes of dissociation for fluorosulfuric acid. The first involves the reverse of the reaction from which it is most commonly synthesized, shown earlier in Equation (1-3). The equilibrium constant is expected to be very small and hence this mode of dissociation is not significant at room temperature.[6] A less likely route of dissociation suggested to occur via the equilibrium:[39]

$$HSO_3F \rightleftharpoons HSO_3^+ + F^- \qquad (1\text{-}5)$$

lacks any evidence. It appears that at 25 °C, HSO_3F is only subject to autoprotolysis. For H_2SO_4, self-dissociation is appreciable as well, with the H_2O and SO_3 so formed acting as base or acid, respectively, leading to the formation of six ionic species which make up a significant total molar concentration of 0.0424 M at 25 °C in this system.[40]

Due to the strong proton donating ability, most solutes behave as bases in HSO_3F and only very few solutes are known to behave as non-electrolytes or as acids in this solvent. Basic ionization in HSO_3F leads to an increase in the system's SO_3F^- concentration, by one of two pathways:[7]

$$MSO_3F \xrightarrow{HSO_3F} M^+ + SO_3F^- \qquad (1\text{-}6)$$

$$B + HSO_3F \overset{K_b}{\rightleftharpoons} BH^+ + SO_3F^- \qquad (1\text{-}7)$$

Even H_2SO_4 and HF act as bases in HSO_3F according to equilibrium (1-7),[9] although the magnitude of K_b for the latter has been shown to be very small in a recent report concerning the ionization of HSO_3F in HF.[36] H_2O also initially ionizes according to Equilibrium (1-7) when dissolved in HSO_3F (with an extremely large K_b value), but it is the secondary equilibrium[11] that gives water its notoriously unwelcome character:

$$H_3O^+ + SO_3F^- \rightleftharpoons HF + H_2SO_4 \qquad (1\text{-}8)$$

There are two important consequences of Equilibrium (1-8): (i) purification of partly hydrolysed fluorosulfuric acid is possible by distillation because HF is significantly more volatile than H_2SO_4, with the separation being most efficient at atmospheric pressure and (ii) solutes capable of forming H_2O (e.g. by dehydration) will present complications.

This study is concerned with the less common but somewhat more interesting *acidic ionization* mode:

$$A + 2\,HSO_3F \overset{K_a}{\rightleftharpoons} [A(SO_3F)]^- + H_2SO_3F^+ \qquad (1\text{-}9)$$

While other Brönsted acids are not capable of protonating HSO_3F appreciably, very strong Lewis acids (stronger than anhydrous $AlCl_3$)[11] are used to ionize as acids in this solvent.

1.C. Superacid Systems and Their Applications

1.C.1. Establishing the Hammett Acidity Function

The fundamental difference between "acids" and "superacids" lies in their relative protonating ability, or acid strength. By far the most common method used to express acid strength in aqueous media is the pH scale,[11] with pH defined as:

$$pH = -\log[HS^+] \tag{1-10}$$

where $[HS^+]$ is the concentration of the solvated proton. However, the practical range of this scale is limited by the self-dissociation (autoprotolysis) of H_2O, with K_{ap} of 10^{-14}. With the pH scale intimately connected to the aqueous medium, in non-aqueous and more acidic solvents, a more widely applicable acidity function is needed.

The method of Hammett and Deyrup[41] has been adopted as the most useful means of measuring elevated acidity. They employed a series of weakly basic primary aromatic amine indicators and measured their degree of protonation in H_2SO_4-H_2O mixtures of varying composition by using ultraviolet-visible spectroscopy to monitor the protonation-induced color changes. Subsequently, the Hammett Acidity Function, H_o, was defined as:

$$H_o = pK_{BH+} - \log\frac{[BH^+]}{[B]} \tag{1-11}$$

where: $pK_{BH+} = \log([B][H+]/[BH+])$, in very dilute solutions

[BH+] = concentration of protonated indicator in acid solution

[B] = concentration of unprotonated indicator in acid solution

and postulated to be unique for a particular series of solutions of changing acidity.

For an indicator to qualify as a Hammett base, the plot of log[BH+]/[B] vs. H_0 in Equation (1-11) should give a straight line with negative unit slope.[11] This was originally established for a whole series of primary aromatic amines,[42] and has more recently[43,44] been shown to approximate the behavior for a much less basic family of aromatic nitro compounds. Their functional indicator range begins at about the acidity of 100% sulfuric acid ($-H_0 = 11.93$),[43] which is where the onset of superacidity is taken to occur.[10] The pK_{BH+} values for the latter group of indicators that have commonly been employed are listed in Table 1.III. It appears that the only major limitation to the Hammett Acidity scale is the availability of adequately weak Hammett bases.

Although the most reliable experimental method used to measure H_0 values of superacid solutions has been spectrophotometry, other techniques such as NMR spectroscopy, electrochemistry, chemical kinetics and heat of protonation studies of weak bases have also more recently been reported.[11] Advantages of these methods are that they can be used with colored acid systems and with indicators that remain colorless upon protonation. In some cases, they also allow for the estimation of H_0 values that are too high to be determined by spectrophotometric methods. However, none of these other techniques are as convenient to use nor do they always give H_0 values of comparable reliability.

Table 1.III. pK_{BH^+} Values of Aromatic Nitro-Compound Indicators[a]

Indicator	$-pK_{BH^+}$
p-Nitrotoluene	11.35
m-Nitrotoluene	11.99
Nitrobenzene	12.14
p-Nitrofluorobenzene	12.44
p-Nitrochlorobenzene	12.70
m-Nitrochlorobenzene	13.16
2,4-Dinitrotoluene	13.76
2,4-Dinitrofluorobenzene	14.52
2,4,6-Trinitrotoluene	15.60
1,3,5-Trinitrobenzene	16.04
2,4,6-Trinitrochlorobenzene	16.12
(2,4-Dinitrofluorobenzene)H+	17.35
(2,4,6-Trinitrotoluene)H+	18.36[b]
(1,3,5-Trinitrobenzene)H+	18.93[c]
(2,4,6-Trinitrochlorobenzene)H+	19.76[c]
(1,3-Dichloro-2,4,6-Trinitrobenzene)H+	20.23[c]

[a]reference 44, except [b]ref. 50; [c]ref. 36

1.C.2. Superacid Systems

Superacids were originally defined as acids of a higher proton strength than 100% H_2SO_4. This definition has been extended and for practical reasons division into four general classes of superacids is suggested:[11]

(i) Brönsted Superacids e.g. HSO_3F;

(ii) Lewis Superacids e.g. SbF_5;

(iii) Brönsted-Lewis Conjugate Superacids e.g. $HF\text{-}SbF_5$;

(iv) Solid Superacids e.g. $SbF_5 : TiO_2 : ZrO_2$.

This thesis is concerned with the first three classes. The most common Brönsted superacids are listed in Table 1.IV, along with some other common protonic solvents. Both their $-H_o$ and pK_{ap} (see Equation (1-4)) values are shown. The use of $HClO_4$ has been limited by its explosive nature, while self-dissociation presents a serious problem for HSO_3Cl. The other four acids have all seen extensive use in organic and inorganic synthesis. NH_3 can be thought of as a "superbase", as its $-H_o$ value clearly indicates.

Table 1.IV. Acidity Range of Some Protonic Solvents

Solvent	$-H_o$	$-\log K_{ap}$	Ref.
NH_3	-15	~26-30 (-35°C)	40,142
H_2O	-7.0	14 (25°C)	40
H_2SO_4	11.9	3.6 (25°C)	40,43
$HClO_4$	~13.0[a]	–	11
HSO_3Cl	13.8	–	43
CF_3SO_3H	13.8, 14.0, 14.1	–	36,143,144
$H_2S_2O_7$	14.1, 14.4	1.7 (25°C)	36,43,142
HF	15.1	~12 (0°C)	36,40
HSO_3F	15.1	7.4 (25°C)	6,43

[a]estimated

The term Lewis acid generally refers to electron pair acceptors. In this thesis, only *molecular Lewis acids* are considered, but not the rather large group of metal cations

M^{n+}. The most relevant feature of these molecular Lewis acids is that they are coordinatively unsaturated. It is recognized that good molecular Lewis acids, where the central atom is bonded to electronegative, potentially polydentate ligands (like F or SO_3F) will also show a tendency to polymerize, so much so that use in superacid systems is severely curtailed by an apparent lack of solubility in the Brönsted acid. $Sn(SO_3F)_4$ exemplifies this behavior.[33]

The vast majority of Lewis acids which have been reported to be stronger than $AlCl_3$ and hence termed *Lewis superacids* (arbitrary definition[11]) are binary fluorides of the general type MF_n. Here, the M-F bond is resistant to solvolytic cleavage by strong protonic acids when their use in superacid systems is considered. The relative strength of these acids is now reasonably well established although the exact order may differ, depending on the method of study and the Lewis base used. For the same reason, it has not been possible to derive an absolute quantitative scale. In HSO_3F, their relative strength has been reported to be $SbF_5 > AsF_5 \sim BiF_5 \sim TiF_4 \geq TaF_5 > BF_3 > NbF_5 \sim PF_5$, as measured using spectrophotometry,[44,45] electrical conductivity[46] and vibrational spectroscopy.[47] Other binary fluorides capable of acting as Lewis acids include WF_6, SiF_4, CrF_3, AlF_3, HfF_4, OsF_5, ReF_5, MoF_5, SnF_4 and TiF_4.[11] However, due to both their high intrinsic acidity and stability, TaF_5, NbF_5, SbF_5 and AsF_5 have been the most widely studied and used Lewis superacids. Their properties are given in Table 1.V. Furthermore, solid superacids based on NbF_5 and TaF_5 are more stable than those based on SbF_5 because of their resistance to reduction.[48]

Table 1.V. Physical Properties of Some Lewis Superacids[a]

Properties	NbF_5	TaF_5	SbF_5	AsF_5
Melting point (°C)	72-73	97	7.0	-79.8
Boiling point (°C)	236	229	142.7	-52.8
Specific gravity (15°C, g/cm3)	2.7	3.9	3.145	2.33[b]
Structure	tetramer[c]	tetramer[c]	polymer[d]	monomer[e]

[a]reference 11; [b]at the bp; [c]solid; [d]liquid; [e]gas

Of greatest relevance to the present study are the Brönsted-Lewis conjugate superacids. They have proven to be most useful in organic synthesis as catalysts and as stabilizers of various unusual and unstable carbocation intermediates. The systems of greatest importance are shown in Table 1.VI, together with the Lewis acid concentration and H_0 values.[11] Of these superacid systems, the ones based on HSO_3F or HF as the Brönsted acid component have found the greatest application. The HF-SbF_5 system is considered to be the strongest liquid superacid system, as indicated in Table 1.VI. However, the acidity values obtained for it at higher concentrations are *estimated*, and the highest *measured* $-H_0$ value to date for any superacid system is 26.5, found for a 90 mole % solution of SbF_5 in HSO_3F.[11] In either case, there is no doubt that HF-SbF_5 is more acidic per mole SbF_5 than the analogous HSO_3F system.

Table 1.VI. Hammett Acidity of Some Brönsted-Lewis Superacids

Superacid System	Mole % Lewis Acid	$-H_0$	Ref.
H_2SO_4 - $HB(HSO_4)_4$	30	13.6	11
H_2SO_4 - SO_3	70.00	14.92	11
HF - BF_3	7	16.6	11
HF - NbF_5	0.40	16.98	36
HF - TaF_5	0.40	18.60	36
HF - AsF_5	0.40	19.31	36
HF - TaF_5	0.90	19.32	36
HF - AsF_5	0.70	19.89	36
HF - SbF_5	0.40	20.64	36
"	0.60	21.13	36
HSO_3CF_3 - TaF_5	15	16.5	45
HSO_3CF_3 - SbF_5	10	~18	11
HSO_3CF_3 - $B(SO_3CF_3)_3$	22	~18.5	11
HSO_3F - SO_3	4	15.5	11
HSO_3F - AsF_5	5	16.61	44
HSO_3F - TaF_5	10	16.7	45
HSO_3F - SbF_5	5	18.28	44
HSO_3F - $SbF_5 \cdot 3SO_3$	5	19.10	44
HSO_3F - SbF_5	90	26.5	140

The conjugate HSO_3F superacid systems are understandably of special interest. They are best represented by the HSO_3F-SbF_5 system, which has been most thoroughly investigated and most widely used for spectroscopic observation of unstable carbocations[11] (to be briefly discussed later). For this reason, this system was named "Magic Acid" shortly after its detailed characterization was reported in 1965.[38] This initial study used electrical conductivity measurements to establish that at dilute

concentrations, SbF_5 is a weak acid in HSO_3F; a dissociation constant of 3.7×10^{-3} mol kg-1 was estimated for the monomeric acidic dissociation equilibrium shown in Equation (1-9) with A = SbF_5. As the SbF_5 concentration is increased, the apparent degree of ionization of the acid increases due to the increasing concentration of a stronger dimeric acid in equilibrium,[6,38] according to:

$$2\,H[SbF_5(SO_3F)] \overset{K_d}{\rightleftharpoons} [(SbF_5)_2SO_3F]^- + H_2SO_3F^+ \qquad (1\text{-}12)$$

with K_d estimated as 7×10^3. ^{19}F NMR studies at -67 °C suggested that a bidentate SO_3F group is present in $[(SbF_5)_2SO_3F]^-$. Later studies[10,49-51] using ^{19}F NMR and Raman spectroscopy suggested a more complicated nature for this system at higher concentrations, with the number of ionic species and their relative abundance being a function of the SbF_5 concentration. The resulting complexity of the 1:1 HSO_3F-SbF_5 system is depicted in Figure 1.2. It should be noted that the presence of species **B_2** and **B_3** is in conflict with the earlier study,[38] where fluorosulfate bridges were assigned to the structure of the dimeric anion.

The acidity of SbF_5 in HSO_3F increases dramatically[10,38,44] when 3 moles of SO_3 per mole SbF_5 are added to the solutions, presumably leading to species of the type $SbF_{5-x}(SO_3F)_x$. The strongest of these solvated acids is $H[SbF_2(SO_3F)_4]$ (see Table 1.VI) which is completely dissociated in HSO_3F according to Equation (1-9). At higher concentrations, the dimeric form of this acid also undergoes complete dissociation, with the monomer/dimer equilibrium constant estimated[38] at 4×10^{-3}. These acids form a multitude of monomeric and oligomeric anions in solution, as a result of F vs. SO_3F interchange and bridging via both fluorine and fluorosulfate.[44] Widespread use of these latter SO_3-containing acids has been limited by their complexity and tendency to cause

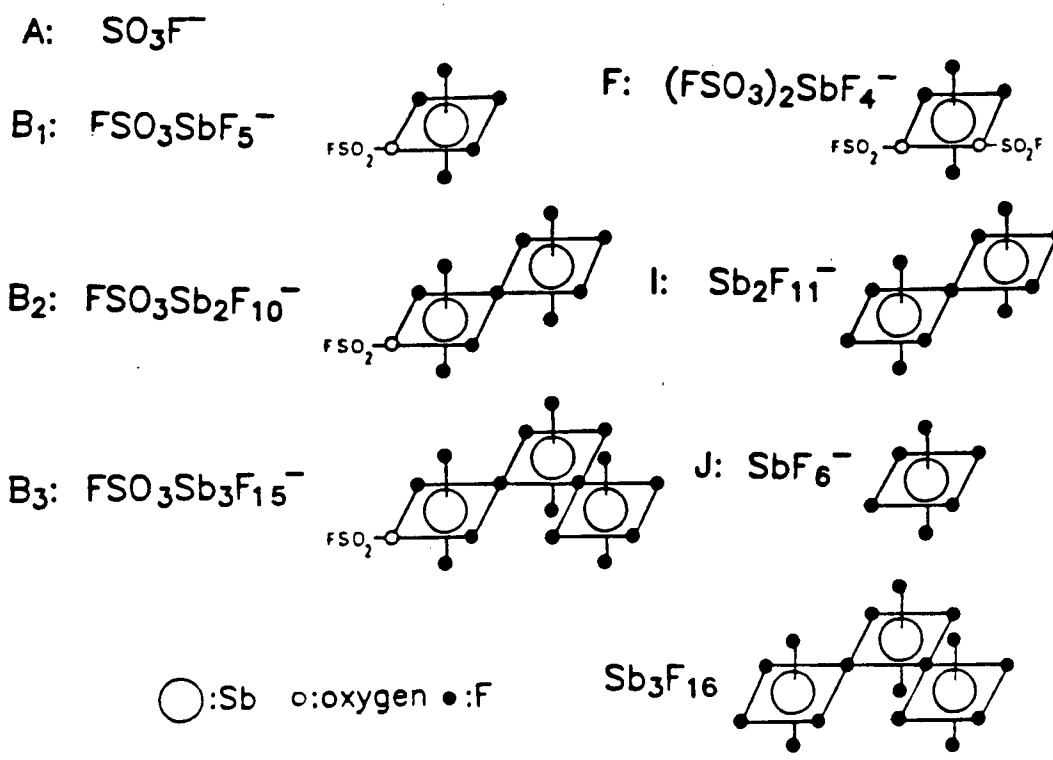

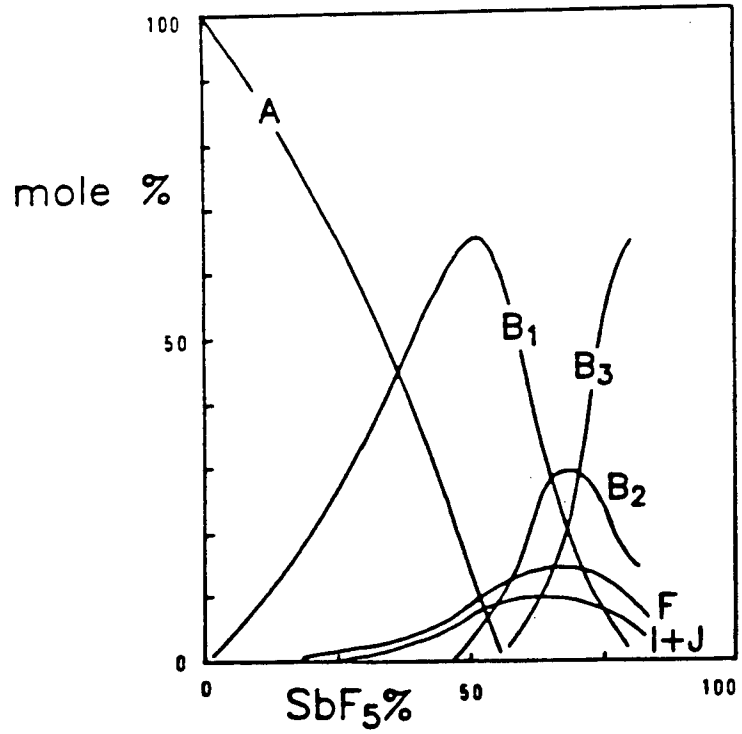

Variation of the composition of HSO_3F–SbF_5 depending on the SbF_5 content

Figure 1.2. The HSO_3F-SbF_5 "Magic Acid" System

extensive oxidative side reactions when in contact with organic compounds, possibly due to the presence of free SO_3.

AsF_5 has considerably lower acidity in HSO_3F than SbF_5.[11] Addition of up to three moles of SO_3 results in enhanced acidity, with values however well below those found for the SbF_5 system. High toxicity of gaseous AsF_5 as well as its less than optimal acidity has led to limited study and use of this superacid system.

NbF_5 and especially TaF_5 have both been used extensively as Lewis acids in conjugate HSO_3F, and more so, HF superacid systems. In fact, reports of their use (to be discussed later) are more extensive than the fundamental studies done on them. The only direct acidity study[46] of either Lewis acid in HSO_3F has involved the conductivity measurements of dilute NbF_5 solutions, which indicated very minimal acidic dissociation. In HF as the Brönsted acid, the acidity of both NbF_5 and TaF_5 has been studied in some detail,[11] with TaF_5 being found the stronger of the two acids, but considerably weaker than SbF_5 in this medium. A comprehensive study[45,52] on hydrocarbon solutions of all three of these as well as other Lewis acids in both HF and HSO_3F resulted in the devolpment of a so-called *"selectivity parameter"* which was defined as follows:

$$I/E = \frac{\text{rate of isomerization of hydrocarbon}}{\text{rate of proton exchange}} \qquad (1\text{-}13)$$

In terms of its carbocation stabilizing ability, the greater the above ratio, the better the acid. Two relevant and interesting results came from this study: (i) in any given Brönsted acid, the I/E parameter of the different Lewis acids correlates very well with their independently measured H_0 values, but the correlation is *very dependent on the acid*

used and (ii) TaF_5 has an unexplainably higher parameter value than SbF_5 at the highest studied HF concentrations. The subsequent conclusion arrived at was that the I/E parameter cannot be used to predict accurately the proton donating ability of a given conjugate superacid system while the H_0 value cannot be applied as an accurate means of gauging its ion stabilizing properties. It should however be noted that many of the H_0 values obtained in this study have since been proven to be too low, especially for the HF systems.[11]

The greatest detriment to the use and study of NbF_5 and TaF_5 in these acid systems has been their lack of solubility,[11] which is in part due to their tetrameric solid state structure.[53] They both, however, coordinate the fluoride ion in *alkaline* HF solutions to form $[MF_6]^-$ or even $[MF_7]^{2-}$ anions, indicating their acceptor properties.[21] The solubility limit[11,35] of TaF_5 in HF is only 0.9 mole % (0.5 M) at 19 °C and that of NbF_5 an even lower 0.7 mole % (0.4 M); although there are no exact data available, the limit for TaF_5 appears to be slightly higher in HSO_3F.[45] However, in the presence of dissolved alkanes, up to 2 M solutions of MF_5 can be formed[52] in both HF and HSO_3F with both metals. This general lack of solubility has in large part been counteracted by the use of *heterogeneous* mixtures of these Lewis acids with the Brönsted acid in organic synthesis. The high redox potential[54] and limited volatility of both Lewis acids has made them catalysts of choice in certain hydrocarbon conversions, to be briefly discussed in the next subsection.

In summary, it is intriguing to note that both NbF_5 and TaF_5 have found use in superacid systems in spite of obvious limitations posed by the stated lack of solubility. It should be possible to modify both in order to increase their solubility without losing their acceptor ability and intrinsic acidity.

1.C.3. Synopsis of Superacid Applications

Superacids have been used for three important, general applications:

(i) to stabilize carbocations which cannot be prepared in less acidic media;

(ii) as catalysts in organic reactions which may proceed via transient cationic intermediates;

(iii) to generate unusual "inorganic" cations.

All three of these processes have been discussed elsewhere in a methodological manner[11] and will hence only be highlighted here.

Two general types of carbocations have been generated in superacid media: "classical" trivalent carbenium ions and "nonclassical" pentavalent (or higher) carbonium ions. Examples are numerous but a very brief general summary[48] of some generated carbenium ions is shown in Figure 1.3. An interesting representative of the many higher valent carbonium ions which can be prepared in superacid media is the $(CH)_6^{2+}$ - type hexamethyl cation.[11] It can be generated by more than one pathway and is shown in the same Figure. An equally interesting synthetic process is the conversion of benzene to cyclohexane by hydrogenation in a HF-TaF_5/iso-pentane superacid solvent medium.[48]

As catalysts, superacids have seen many applications. Among the processes in which they have shown exceptional efficiency are electrochemical oxidations, isomerization of alkanes, alkylation of alkanes, oligocondensation of lower alkanes, alkylation of aromatic hydrocarbons and acylation of aromatics. Carboxylation, formylation, sulfonation, nitration, halogenation, amination and polymerization of a

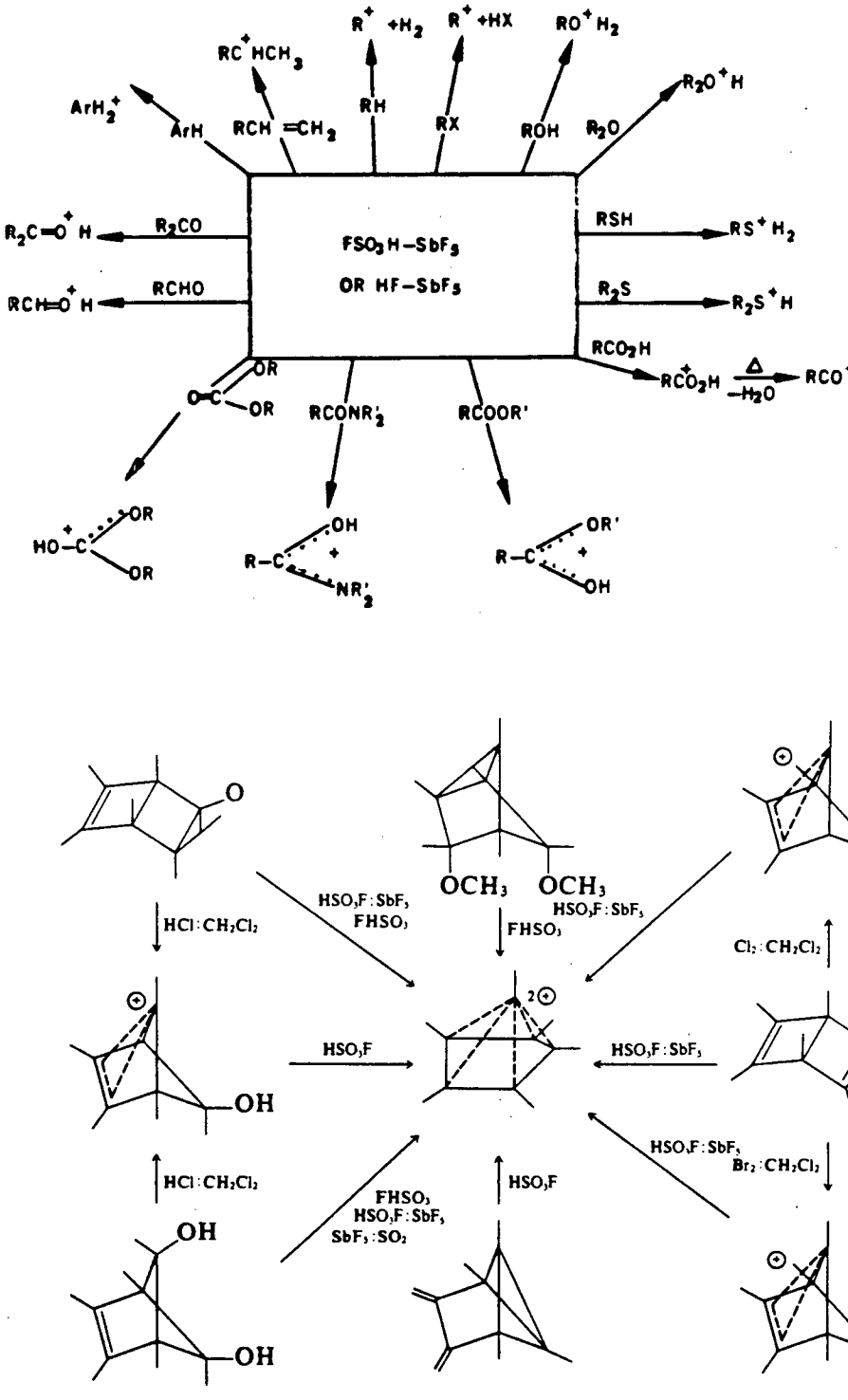

Figure 1.3. Examples of Carbenium and Carbonium Ions Generated in Superacidic Media

variety of organic materials are also efficient in superacid media.[11,55] Their industrial importance has consequently been very well established.

Of greater relevance to this study are the various examples of interesting inorganic and organometallic cations which are mostly only observable in or isolable out of very weakly basic superacid media due to their high electrophilicity. Many different types of cations have been generated and they can be broadly categorized as follows:

(i) onium ions;

(ii) halogen cations;

(iii) homopolyatomic cations of group 6 (chalcogens);

(iv) miscellaneous cations.

Their chemistry has been reviewed.[11,56,57] Table 1.VII lists a selection of interesting examples from each category.

To generate the cations shown, three general processes are used:

(i) protonation of suitable substrates to generate onium cations;

(ii) oxidation reactions involving various oxidizing agents;

(iii) halide or preferably fluoride ion abstraction.

A very well explored[56] method is the second above, which makes use primarily of $S_2O_6F_2$, SO_3, and SbF_5 or AsF_5 as the oxidizing agents in HSO_3F, H_2SO_4/oleum and SO_2 systems, respectively.

Table 1.VII. Examples of Some Inorganic and Organometallic Cations Generated in Superacidic Media

Substrate	Cation Generated	Salt Isolated	Superacidic-Oxidizing/ Protonating Medium	Cation Category	Ref.
H_2O	H_3O^+	YES	HSO_3F-SbF_5 or HF-AsF_5	i	11
H_2O_2	$H_3O_2^+$	NO	HSO_3F-SbF_5	i	11
H_2S	H_3S^+	YES	HF-SbF_5	i	145
HNO_3	NO_2^+	YES	oleum	i	127
I_2	I_2^+	YES	SO_2-SbF_5	ii	58
	I_4^+	YES	SO_2-SbF_5 or SO_2-AsF_5	ii	11
	I_3^+	YES	AsF_3-AsF_5 or HSO_3F-$S_2O_6F_2$	ii	146
	I_5^+	YES	SO_2-AsF_5 or HSO_3F-$S_2O_6F_2$	ii	146
	I_{15}^+	YES	SO_2-SbF_5	ii	62
Br_2	Br_2^+	YES	BrF_5-SbF_5	ii	64
	Br_3^+	YES	BrF_5-AsF_5 or		147
			HSO_3F-SO_3/$S_2O_6F_2$/SbF_5	ii	148
	Br_5^+	YES	$Au_{(s)}$/$BrSO_3F$	ii	149
Cl_2	Cl_3^+	YES	ClF-AsF_5	ii	65
ClO_2F or	ClO_2^+	YES	AsF_5 or $S_2O_6F_2$/$Sn(SO_3F)_4$	i/ii	150
ClO_2SO_3F					132
XF_3	XF_2^+	YES	SbF_5	ii	11
(X=Cl or Br)					
ICl	I_2Cl^+	YES	ISO_3F	ii	151
O_2	O_2^+	YES	F_2/SbF_5 or F_2/AsF_5	iii	11
			F_2/MnO_2	iii	71
S_8	S_4^{2+}	YES	SO_2-AsF_5 or HSO_3F-$S_2O_6F_2$	iii	152
	S_8^{2+}	YES	SO_2-SbF_5 or HSO_3F-$S_2O_6F_2$	iii	153
	S_{16}^{2+}	NO	HSO_3F-$S_2O_6F_2$	iii	68
	S_{19}^{2+}	YES	SO_2/SO_2ClF-AsF_5	iii	69
	S_5^+	NO	65% oleum	iii	61
Se	Se_4^{2+}	YES	SO_2-AsF_5 or HSO_3F-$S_2O_6F_2$	iii	154
	Se_8^{2+}	YES	SO_2-SbF_5 or HSO_3F-$S_2O_6F_2$	iii	155
	Se_{10}^{2+}	YES	SO_2-MF_5 (M=As or Sb)	iii	156
Te	Te_4^{2+}	YES	SO_2-$S_2O_6F_2$ or SO_2-AsF_5	iii	11
	Te_6^{2+}	NO	SO_2-AsF_5	iii	157
	Te_6^{4+}	YES	SO_2/AsF_3-AsF_5	iii	158
XeF_4	XeF_3^+	YES	SbF_5	iv	159
B_2H_6	$B_2H_5^+$,$B_2H_7^+$	NO	HSO_3F-SbF_5	iv	160
$(CH_3)_2SnF_2$	$(CH_3)_2Sn^{2+}$	YES	HF-MF_5 (M=Nb,Ta,Sb)	iv	161

Of the cations listed in Table 1.VII, some merit special mention:

a) Halogen cations

In particular, the I_2 system has yielded a number of interesting cations. The crystal structures of $I_2^+(Sb_2F_{11}^-)$, $I_3^+(AsF_6^-)$, $I_5^+(AsF_6^-)$, $I_{15}^{3+}(SbF_6^-)_3$, $I_4^{2+}(AsF_6^-)_2$, $I_4^{2+}[SbF_6^-(Sb_3F_{14})^-]$ and $[I(SO_3F)_2]^+I^-$ have all been reported[11,28,58-63] with many of the cations first identified in superacid solution. Of the other halogen cations, only $Br_2^+(Sb_3F_{16}^-)$ has a known[64] molecular structure while Cl_3^+ has been identified[65] solely by vibrational spectra. There is seemingly an increase in electrophilicity on going from I to Cl and consequently Cl_2^+ (well known in the gas phase) has remained elusive in the condensed phase.[66]

A very recently reported[67] study has established the acidity threshholds above which the cations I_2^+, I_3^+, and I_5^+ can be generated in anydrous HF solutions. NaF and the Lewis acids MF_5, with M = Nb, Ta and Sb, were used to fix precisely the acidity.

b) Chalcogen cations

Besides square planar cations of the type E_4^{2+}, with E = S, Se or Te, a number of unusual species exist for each element:[56] Te_6^{4+} with a trigonal prismatic structure, Se_{10}^{2+} with a six-membered ring bridged by a Se_4 chain to give a bicyclic system, and S_{19}^{2+} are such examples. The latter had originally been indentified[68] in solution as S_{16}^{2+}, and its crystal structure[69] as $S_{19}^{2+}(AsF_6^-)_2$ came as a bit of a surprise. This serves to illustrate the general point that many more species may exist in superacid solution than are actually isolable.

The last member, O_2^+, is unusual for a number of reasons:

(i) its identification[70] in $O_2^+(PtF_6^-)$ triggered off noble gas chemistry;

(ii) It does not appear to exist in superacid solution;

(iii) Even though over a dozen O_2^+ salts with different fluoroanions are known,[11,56] the only existing x-ray crystal structure study, that of $O_2^+(Mn_2F_9^-)$, was solved quite recently.[71]

A possible O_3^+ species derived from ozone has remained elusive and a rather interesting S_5^+ is only identifiable[61] by ESR.

c) Interhalogen cations and cations formed by xenon and krypton fluorides

In the former group, tri-, penta- and heptaatomic systems dominate, with the triatomic cations involving any one of the four halogens and the latter two groups restricted to fluorocations.[11] Only a few are listed in Table 1.VII, and structural studies have been reported on some but not on all. The same can be said for the two chemically active noble gases.[11]

As in any of the preceding groups, there are a number of challenges left for the synthetic and structural chemist: (i) diatomic interhalogen cations such as ICl^+ and IBr^+, both well known[72] in the gas phase, have not been generated in liquid nor in solid state; (ii) a number or pentaatomic cations of the type XY_4^+ with X = I or Br and Y = Br or Cl should be obtainable and (iii) a postulated Xe_2^+ has remained an enigma.[73]

d) Organotin(IV) cations

This is the last class significant enough to merit special attention. Dimethyl tin(IV) derivatives of very strong protonic or Lewis acids have recently been extensively studied via ^{119}Sn Mössbauer and the relative basicity or nucleophicity of the conjugate weak anionic Lewis bases has been approximately established.[34] Furthermore, the $(CH_3)_2Sn^{2+}$ moiety can be thought of as the simplest representative of a more general class of R_2Sn^{2+} type organotin cations, whose study in superacidic media is presently underway.[74]

As a final note, it may be of interest that the most recent liquid superacid system to be reported[75] is the rather complex $HCl/AlCl_3$-1-ethyl-3-methyl-1H-imidazolium chloride system, which has been claimed to have an arene protonating ability similar to that of anhydrous HF ($-H_o = 15.1$).

1.D. Some Properties of $S_2O_6F_2$

The usefulness of bis(fluorosulfuryl) peroxide, $S_2O_6F_2$, as oxidizing agent to generate cations in HSO_3F has already been mentioned in the preceding section. This section will deal with some of its properties. Since HSO_3F will be the principal reaction medium in this study, the two electron oxidizer:

$$S_2O_6F_2 + 2e^- \longrightarrow 2\,SO_3F^- \qquad (1\text{-}14)$$

becomes a natural reagent, generating the base ion SO_3F^- in the process.

$S_2O_6F_2$ was first prepared in 1957 by Dudley and Cady[76] via the fluorination of SO_3 at elevated temperature in the presence of AgF_2 as catalyst. A number of alternative routes have been reported,[77] but this method has been adopted, modified and optimized by us, with details discussed in the experimental section. Its chemistry has been extensively explored[77-82] and its physical properties (m.p.: -55.4 °C, b.p.: +67.1 °C) found convenient for synthetic use. It is obtainable in high purity to allow its stoichiometric use in reactions.

Thorough characterization has been obtained via vapour density measurements, vapour pressure curves,[83] as well as vibrational[76,84] and ^{19}F NMR spectroscopy (singlet at 40.4 ppm)[85]. The IR and Raman spectra are consistent with a structure of the point group C_2 (also found for H_2O_2), consisting of two O-SO_2F fragments singly-bonded via the oxygens, with the O-O-S-F grouping being planar. Hence, $S_2O_6F_2$ is structurally related to HSO_3F and to other halogen fluorosulfates where the X-O-S-F group is found to be planar.[84]

$S_2O_6F_2$ does not react with glass and is conveniently stored in glass ampoules. Upon heating well beyond its boiling point, the material produces a brownish gas which has been shown[86] to result from the following reversible equilibrium:

$$S_2O_6F_2 \rightleftharpoons 2\ SO_3F^{\cdot} \qquad (1\text{-}15)$$

It is the presence of the radical shown in the above equilibrium that is generally thought to be responsible for this material's oxidizing ability. The radical $SO_3F^{\cdot}$ has been studied by ESR,[87] its electronic, vibrational and rotational spectra are known[88] and it has been isolated[89] in an argon matrix. Its photochemistry has also been discussed.[83] The enthalpy

of dissociation of $S_2O_6F_2$ into the two radicals has been found to be 23 ± 1 kcal/mole by a number of different techniques.[86,87,90]

The electronegativity of the fluorosulfate group has been estimated from ^{119}Sn Mössbauer studies[91,92] of $K_2[SnX_6]$ type complexes, with X = F, Cl and SO_3F. Using the Pauling electronegativities of 3.98 and 3.16 for F and Cl, respectively, this value was found to be 3.83 for SO_3F. A calculation[93] based on Mulliken's definition of electronegativity led to a very comparable value of 3.88, suggesting that SO_3F is closer to fluorine in this regard than to chlorine. The Taft inductive constant,[94] which is a measure of a ligand's ability to withdraw electronic charge via σ and π effects, was also estimated for the fluorosulfate group by using ^{119}Sn Mössbauer to study a specifically chosen set of tin fluorosulfate complexes.[95] The value of 3.68 obtained is significantly greater than that of 3.08 found for fluorine and indicates that the fluorosulfate group is better suited to delocalize charge over the entire group.[93] The anion SO_3F has been shown to be a stronger field ligand than chloride, much more comparable to fluoride in this respect.[96] Evidence for its ability to delocalize electronic charge comes from its relative position[93] in the nephelauxetic series:

$$Cl^- > SO_3F^- > H_2O > F^-$$

In summary, the strong oxidizing power of $S_2O_6F_2$ makes the synthesis of a variety of compounds with the metal in high oxidation states very promising. This brief summary has centered around the physical and chemical properties of this versatile reagent. Some of its chemical reactions have been summarized by DeMarco and Shreeve.[77] Additional aspects will be mentioned throughout this thesis and its interaction with HSO_3F will be dealt with in Chapter 3.

1.E. Preparation of Metal Fluorosulfates

A number of preparative methods leading to metal fluorosulfates have been thoroughly reviewed previously[6,8,9,13,77,97] and a detailed account is hence not needed. Only more recent pathways relevant to the present work will be introduced here.

1.E.1. Solvolysis in HSO_3F

There are several general points of importance here which will be mentioned first. Most of these guidelines are valid for reactions of other strong acids as well:

a) The oxidation state of the metal is retained;

b) The reaction temperature must be sufficiently low to avoid self-dissociation of HSO_3F to HF and SO_3 with ensuing problems;

c) The leaving group must be readily separable, allowing two simple and practical alternatives:

(i) $MX_n + n\,HSO_3F \longrightarrow M(SO_3F)_{n(s)} + HX_{(g)}$ (1-16)

with X = Cl, F, CH_3, etc.

The main product can be obtained by distillation or removal of volatiles.

(ii) $M(O_2CR)_n + 2n\,HSO_3F \longrightarrow M(SO_3F)_{n(s)} + n\,[RCO_2H_2]^+_{(solv)} + n\,SO_3F^-_{(solv)}$ (1-17)

with R = CH_3, CF_3, C_6H_5, etc.

The main product here is best isolated by filtration;

e) As a general rule, solvolysis works well where n is low (e.g. 1 to 3);

f) The availability of suitable precursors limits this route's versatility.

Some examples of this synthetic pathway follow. Alkali metal fluorosulfate salts are easily made at room temperature[8,97,98-100] as are $Sn(SO_3F)_2$ and $Pb(SO_3F)_2$,[98] for example. Reports of higher oxidation state metal fluorosulfates prepared by this route are quite rare.

$In(SO_3F)_3$[101] and the tin(IV) species, $(CH_3)_2Sn(SO_3F)_2$[102] (starting with $(CH_3)_2SnCl_2$, $(CH_3)_3SnCl$ or $(CH_3)_4Sn$), have been prepared, the former using elevated temperatures. Chlorofluorosulfates can also form upon incomplete ligand substitution; some examples are $TiCl_2(SO_3F)_2$, $SnCl_3(SO_3F)$, $SnCl_2(SO_3F)_2$ and $SbCl_4(SO_3F)$.[97] $Th(SO_3F)_4$,[103] $Bi(SO_3F)_3$,[104] $Al(SO_3F)_3$,[105] $Pb(SO_3F)_4$[106] and $U(SO_3F)_4$[107] have all been prepared as well, albeit with a little more difficulty.

1.E.2. The Use of $S_2O_6F_2$

More convenient routes to fluorosulfate compounds with the central metal in a +3 or +4 oxidation state make use of the strong oxidizing ability of $S_2O_6F_2$. They can be classified into three general categories:

(i) oxidative halide substitution;

(ii) direct metal oxidation;

(iii) solvent-aided metal oxidation.

Route (i) has seen limited use, due to frequently encountered mixed reaction products. A few binary fluorosulfate derivatives have, however, been synthesized according to:

$$MCl_n + n/2\ S_2O_6F_2 \longrightarrow M(SO_3F)_n + n/2\ Cl_2 \qquad (1\text{-}18)$$

$Ga(SO_3F)_3$[108] and $U(SO_3F)_4$[109] can be obtained in pure form at room temperature according to the above, whereas $Sn(SO_3F)_4$ can be prepared by heating the reaction mixture to 120 °C.[110] Reaction of $SnCl_4$ with an excess of $S_2O_6F_2$ at room temperature yields $SnCl(SO_3F)_3$[111] whereas the reactions of $NbCl_5$ or $TaCl_5$ with excess $S_2O_6F_2$ at 60 °C have resulted in the isolation of the oxyfluorosulfates $MO(SO_3F)_3$ with both metals.[18]

The substitution of chloride by $S_2O_6F_2$ however suffers from a serious deficiency. With solid products formed, an excess of $S_2O_6F_2$ is required, being used as reagent as well as reaction medium. At elevated temperatures, a sequence of side reactions occurs, resulting in the initial formation of $ClSO_3F$:

$$Cl_2 + S_2O_6F_2 \longrightarrow 2\ ClSO_3F \qquad (1\text{-}19a)$$

with further oxidation possible according to:

$$ClSO_3F + 2\ S_2O_6F_2 \longrightarrow ClO_2SO_3F + 2\ S_2O_5F_2 \qquad (1\text{-}19b)$$

Such chloronium fluorosulfate or other intermediates formed during oxidation may interfere in two ways. Firstly, there is a chance of an explosion occurring, as has actually happened in the reaction of $SnCl_4$ with $S_2O_6F_2$. Secondly, ClO_2SO_3F may act as an SO_3F^- donor; the first accidental discovery of $[Sn(SO_3F)_6]^{2-}$ has occurred in this manner.[92]

A milder, rather elegant version of this substitution reaction involves the use of $BrSO_3F$ instead of $S_2O_6F_2$, as first reported by DesMarteau.[112]

Fluorides have also been employed instead of chlorides in these types of reactions. The reaction of UF_5 with $S_2O_6F_2$ in $CFCl_3$ at 40 °C yields $UF_3(SO_3F)_2$[113], whereas the reaction of SbF_3[114] or AsF_3[115] with excess $S_2O_6F_2$ leads to the respective antimony or arsenic analogs with the same composition, both of which are viscous liquids; oxidative addition rather than substitution is involved here. Non-statistical ligand redistribution reactions employing SbF_5 have also been used[114] in the antimony system to prepare the species $SbF_4(SO_3F)$ and $Sb_2F_9(SO_3F)$. The reaction of $SnCl_2F_2$ with $S_2O_6F_2$ yields $SnF_2(SO_3F)_2$.[116]

Route (ii) above has been somewhat limited by the lack of solubility of the M° species in the peroxide. At elevated temperatures (60 - 130 °C), $Ag(SO_3F)_2$[117,118] and very recently $Os(SO_3F)_3$[119] have however been prepared according to:

$$M + \text{excess } S_2O_6F_2 \longrightarrow M(SO_3F)_n \qquad (1\text{-}20)$$

The advantage of this method, when feasible, is the simplicity of product isolation, since the excess $S_2O_6F_2$ is very easily removed in vacuo.

Route (iii) is perhaps the most efficient and most frequently and successfully used of all pathways leading to binary fluorosulfates, according to:

$$M + n/2\ S_2O_6F_2 \xrightarrow[25\text{-}120\ °C]{HSO_3F} M(SO_3F)_n \qquad (1\text{-}21)$$

A variety of species with n ranging from 2 to 4 have been prepared by this route: $Pd(SO_3F)_2$,[120,121] $Ir(SO_3F)_3$,[122] $Ru(SO_3F)_3$,[123] $Au(SO_3F)_3$,[25] $Mn(SO_3F)_3$,[17] $Rh(SO_3F)_3$,[119] $Sn(SO_3F)_4$,[33] $Pt(SO_3F)_4$[15] and $Ir(SO_3F)_4$.[122] These reactions usually proceed very smoothly over a period of a few days. The versatility of this method combined with the

absence of any by-products makes it very useful; the products can usually be isolated by removing the solvent and excess $S_2O_6F_2$ in vacuo. This pathway has encountered limitations, however. In one case, the unique +7 oxidation state fluorosulfate $ReO_2(SO_3F)_3$ was obtained as a viscous yellow liquid.[17] A binary fluorosulfate with this metal could not be isolated. Similarly, only the fluorofluorosulfate $GeF_2(SO_3F)_2$ could be isolated.[33]

In addition to the above binary fluorosulfates, Reaction (1-21) can be expanded to prepare a variety of ternary fluorosulfates, usually by introducing a desired fluorosulfate salt to the reaction mixture:

$$x\,M'(SO_3F) + M + n/2\,S_2O_6F_2 \xrightarrow[25\text{-}120\ ^\circ C]{HSO_3F} M_x'[M(SO_3F)_{n+x}] \qquad (1\text{-}22)$$

where x = 1 or 2 and M′ = Cs, K, or ClO_2, among others.

Most of the binary species made via Reactions (1-20) and (1-21) can be converted to their respective ternary fluorosulfate according to the above. In some cases, such as with $Pt(SO_3F)_4$[15] and $Sn(SO_3F)_4$,[33] both the $[M(SO_3F)_5]^-$ and $[M(SO_3F)_6]^{2-}$ anions can be stabilized. However, for many of the listed binary fluorosulfates, only the $M'[M(SO_3F)_{n+1}]$ type salts are isolable. The ruthenium system[123] is somewhat interesting in that the salts $K_2[Ru(SO_3F)_6]$, $Cs_2[Ru(SO_3F)_6]$, and $Cs[Ru(SO_3F)_5]$ have been prepared although the parent species $Ru(SO_3F)_4$ has not. Dipositive cations, such as Ba^{2+} or Pd^{2+} have also been used in Reaction (1-22) to stabilize salts with $[M(SO_3F)_{n+2}]^{2-}$ type anions.[15,121] The preparation of both $Cs_2[Sn(SO_3F)_6]$[33] and $Cs_2[Pt(SO_3F)_6]$[15] by this route suggests by analogy that $Sn(SO_3F)_4$ is probably an acid of

the HSO_3F system (HSO_3F-$Pt(SO_3F)_4$ forms a very powerful superacid system),[15] although its virtual insolubility in this solvent precludes any solution studies.

1.E.3. SO_3 Insertion Reactions

This route is limited to substrates with weak and/or polar enough metal-fluorine bonds to allow insertion of SO_3; bridging fluorines are targets and indeed this reaction has been attempted with SbF_5,[16] NbF_5,[21] TaF_5,[21] and UF_5,[113] leading to the respective species $SbF_4(SO_3F)$, $NbF_5 \cdot 2.1SO_3$ ("$NbF_3(SO_3F)_2$"), $TaF_5 \cdot 2.6SO_3$ ("$TaF_3(SO_3F)_2$") and $UF_3(SO_3F)_2$. The presence of excess, unremoved SO_3 was claimed as the cause of the composition discrepancy[107] in the Nb and Ta materials. The reaction of $U^{VI}F_6$ with SO_3 in $CFCl_3$ is quite interesting, yielding $U^{V}F(SO_3F)_4$[113] between -60 and -50 °C whereas at higher temperatures, $UF_2(SO_3F)_3$[124] is formed; both compounds were obtained in an analytically pure state. $S_2O_6F_2$ was identified as a by-product during the unusual reduction of the uranium from +6 to +5 in both instances.

As is evident from the previous discussion, some binary metal fluorosulfates are prone to decomposition, which occurs via one or both of the following primary pathways: (i) SO_3 elimination, resulting in a fluoro(fluorosulfate) or (ii) $S_2O_5F_2$ evolution, resulting in an oxyfluorosulfate. Both of these decomposition products are volatile and hence removable in vacuo. The preparation of $GeF_2(SO_3F)_2$[33] is an example of the first pathway whereas the formation of $ReO_2(SO_3F)_3$,[17] $NbO(SO_3F)_3$[18] and $TaO(SO_3F)_3$[18] are examples of the second. When $SbCl_5$ was reacted with $S_2O_6F_2$,[19] both decomposition routes were suggested as an explanation for the very complex nature of the resulting system.

Many other synthetic pathways[13] have been used to make metal fluorosulfates, which were not touched upon in the above discussions for the sake of brevity. The last two sections of this introduction will deal with two important techniques that have been employed to characterize fluorosulfate compounds, both in solid state and in solution.

1.F. Vibrational Characterization of the Fluorosulfate Group

The fluorosulfate group is suitable for characterization via vibrational spectroscopy for the following reasons:

(i) its fundamental modes spread conveniently over the mid- to far-IR region (1500 - 300 cm^{-1});

(ii) stretching modes, found between 1500 and 700 cm^{-1}, are primarily used in structural interpretation;

(iii) S-O and S-F are good Raman scattering groups.

1.F.1. Symmetry Considerations

The free SO_3F^- ion has C_{3v} symmetry, giving rise to *six* fundamental vibrational modes, 3A´ + 3E. However, upon coordination through one or two oxygens, the symmetry is reduced to C_s or C_1 and *nine* fundamental vibrations, 6A´ + 3A˝, result. If the third oxygen as well as the fluorine are also involved in the coordination, C_{3v} symmetry is restored and *six* fundamental modes are expected. Furthermore, strongly polarizing or aspherical cations such as NO^+, NO_2^+ or ClO_2^+ can partially lift the degeneracy of the E modes if C_{3v} symmetry of the fluorosulfate group is involved. All of the vibrational modes of SO_3F are both IR and Raman active.

Relative band positions in the S-O and S-F stretching regions (~750 - 1450 cm^{-1}) reflect the type of SO_3F group that is present. Coordination of either oxygen or fluorine weakens and thus lowers the stretching frequency of the respective S-O or S-F bond. Electron withdrawal effects[125] resulting from the coordination of oxygen in turn strengthen the other uncoordinated S-O and S-F bonds, causing their vibrational modes to occur at higher frequencies. The occurrence of the S-F stretching mode in an unobscured region of the spectra makes it very useful as an indicator of whether an ionic or covalently bound SO_3F group is present.

1.F.2. Effect of Various Fluorosulfate Coordination on Vibrational Frequencies

A very general schematic representation showing the effect of the different possible fluorosulfate coordination types on band frequencies is given in Figure 1.4. Each type is briefly discussed below.

a) Ionic (C_{3v})

Simple crystalline ionic salts such as KSO_3F[29] give vibrational spectra whose band frequencies are nearly at identical positions to those calculated from a normal coordinate analysis[126] of the SO_3F^- ion's $^1A_1$ electronic ground state: 1287 (ν_4, as. S-O stretch), 1082 (ν_1, sym. S-O stretch), 786 (ν_2, S-F stretch), 592 (ν_5, SO_3F deformation), 566 (ν_3, SO_3F deformation) and 409 (ν_6, SO_3F deformation) cm^{-1}. The only significant difference is in the position of the S-F stretching mode, which occurs at a somewhat lower frequency of 741 cm^{-1} in KSO_3F.

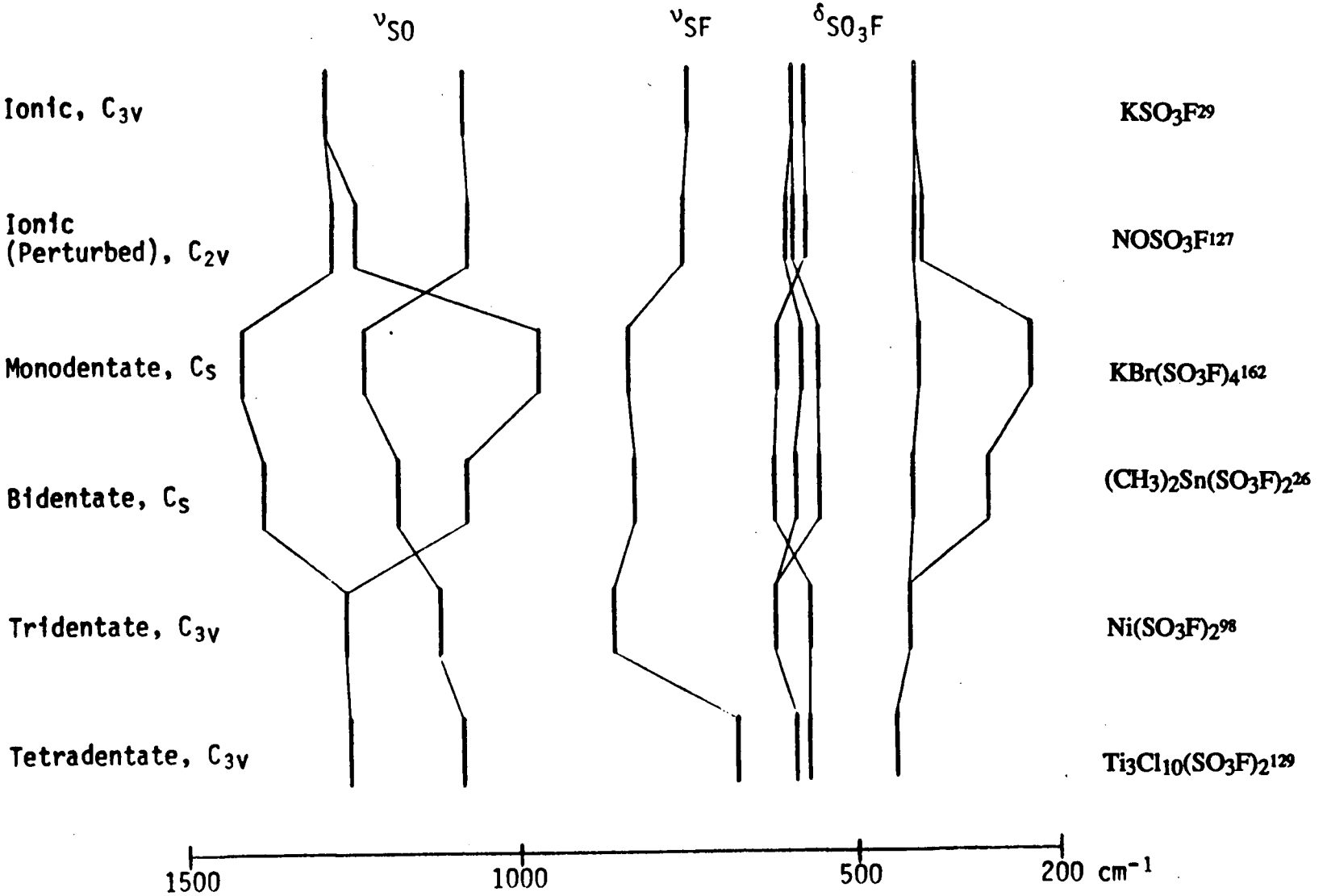

Figure 1.4. Effect of Coordination on the Vibrational Band Pattern of the SO_3F Group

b) Perturbed Ionic (C_{3v})

As already mentioned, strongly polarizing monatomic and/or asymmetric polyatomic cations can cause up to about a 30 cm^{-1} splitting of one or more of the three doubly degenerate E modes. $NOSO_3F$ is an example of such a species.[127]

c) Covalent Monodentate (C_s)

This type of coordination is very common among ternary fluorosulfate complexes, such as $Cs[Au(SO_3F)_4]$ and $Cs_2[M(SO_3F)_6]$ with M = Pd, Pt, Sn or Ge, and is also found among halogen fluorosulfates such as FSO_3F.[128] Typically, the three S-O stretching modes are found[15] at about 1450, 1230 and 1000 cm^{-1}, although the latter can occur as low as 900 cm^{-1} in complexes of very low ionicity. The S-F stretching mode can be found anywhere in the range 850 ± 40 cm^{-1}.

d) Covalent Bidentate (C_s)

Bridging bidentate SO_3F groups are found in, for example, the binary fluorosulfates $M(SO_3F)_3$, with M = Ge, Fe or Mn, as well as in the compounds $(CH_3)_3Sn(SO_3F)_2$ (verified by x-ray crystal structure),[26] $SnF_2(SO_3F)_2$ and $GeF_2(SO_3F)_2$. Typical frequencies for the S-O stretching modes are about 1400, 1130 and 1070 cm^{-1}, and hence are quite distinguishable from those found for covalent monodentate groups;[15,128] the position of the S-F stretching mode, however, is not.

e) Covalent Tridentate (C_{3v})

This type of coordination is usually found among the polymeric bis(fluorosulfates) of the 3d transition metals, with each SO_3F group being coordinated

via the oxygens to three different metal centers. It is easily distinguishable from the ionic fluorosulfates by its high S-F stretching frequency, usually occurring in the range 840-890 cm^{-1}.

f) Covalent Tetradentate (C_{3v})

$Ti_3Cl_{10}(SO_3F)_2$[129] is the only compound for which coordination of all three oxygens and the fluorine has been postulated. The C_{3v} symmetry for the SO_3F group suggested from the vibrational spectra as well as the occurrence of the S-F stretching mode at an unprecedently low frequency of 660 cm^{-1} were the basis for this assignment.

A number of fluorosulfate compounds, such as $Au(SO_3F)_3$,[25] $Pt(SO_3F)_4$,[15] and $Sn(SO_3F)_4$,[33,110] involve both covalent monodentate and bridging bidentate SO_3F groups to allow the metal center to exist in a higher coordinated, more symmetric ligand environment. This has been concluded from the presence of representative S-O stretching frequencies from both categories *c)* and *d)* above, and from the proliferation of the S-F stretching mode. In addition, compounds of the type $M'(II)[M(IV)(SO_3F)_6]$,[118,121] with M′ = Ag or Pd and M = Sn, Pd or Pt, involve "aniso-bidentate bridging", where the fluorosulfate group may be bridging between both the +2 and +4 metal ions, with a stronger bond to M^{4+}; spectra of these species also show evidence for both monodentate and bidentate SO_3F coordination. Furthermore, the co-existence of bidentate and tridentate SO_3F coordination has been tentatively suggested for the presumably eight-coordinated $UF_2(SO_3F)_3$[125] and $UF_3(SO_3F)_2$[113] species from the vibrational spectral data.

Complications in exactly assigning the aformentioned diagnostic spectral bands can arise from solid state band splitting or broadening that is caused by cation-anion

interactions. The resulting spectra tend as a result to look much more complex than expected, as has been observed[33] in the Raman spectrum of the ternary complex $Cs_2[Ge(SO_3F)_6]$.

As may be apparent from Figure 1.4, the SO_3F deformation region is not very practical as a means of differentiating among the various fluorosulfate groups. In addition, this spectral region is often obscured by coincidentally overlapping M-O stretching modes.

In summary, the diagnostic vibrational bands that have been discussed together with their intensities provide a means of qualitatively probing the structural backbones of a variety of fluorosulfate compounds. In light of the paucity of reported X-ray crystal structures, this is very fortunate and lends this technique additional significance.

1.G. Multinuclear NMR Spectroscopy Studies in HSO_3F

Few NMR spectroscopy studies are reported with fluorosulfuric acid as the solvent. With few exceptions, these studies have involved the investigation of the acceptor properties of strong Lewis acids in HSO_3F. The nuclei that have been studied are ^{1}H, ^{19}F, ^{13}C, ^{119}Sn and ^{129}Xe.

An important NMR study in this solvent has involved the "Magic Acid" system HSO_3F-SbF_5. An initial study[38] of ~1-3 molal SbF_5 solutions assigned the ^{19}F signals found in the Sb-F and -OSO_2F resonance regions at -66 °C to the solvated species $[SbF_5(SO_3F)]^-$ and $[(SbF_5)_2SO_3F]^-$ (bridged via SO_3F). Addition of 1-3 moles of SO_3 to the HSO_3F-SbF_5 solutions led to the identification of species of the type

$[SbF_{5-x}(SO_3F)_x]SO_3F^-$, with x = 1, 2 or 3. A more detailed ^{19}F NMR study[50] of the HSO_3F-SbF_5 solutions at -60 ± 5 °C (with the molar fraction of SbF_5 ranging from 0.4 to 0.8) suggested a more complicated system. In addition to the species already shown earlier in Figure 1.2 and mentioned above, $[(SbF_4(SO_3F))_2SO_3F]^-$ and $[(SbF_5)_4SO_3F]^-$ were also identified. In all of the above solutions, both the terminal and bridging SO_3F resonances were assigned within 4 ppm downfield of the solvent resonance, which was itself however reported[50] at an unusually low field position of 44.9 ppm (relative to $CFCl_3$) compared to 41.0 ± 0.5 ppm that has been reported elsewhere.[15,25,130,131]

The presence of both fluorides and fluorosulfates in the above system make it suitable for this type of structural investigation. Furthermore, the high solubility (miscibility) of SbF_5 in HSO_3F allowed high solute concentrations to be reached. The lack of one or both of these features has frequently been at the head of factors limiting wider applicability of this technique with other fluorosulfate systems.

A number of other systems have been studied via multinuclear NMR and will be briefly summarized. Two molar solutions of $Au(SO_3F)_3$ and $Cs[Au(SO_3F)_4]$ both exhibit[25] a singlet resonance at the same position (slightly downfield of the solvent peak), supporting the acceptor behaviour of the former. Similarily, 0.2 M solutions of $Pt(SO_3F)_4$, $Cs[Pt(SO_3F)_5]$ and $Cs_2[Pt(SO_3F)_6]$ give rise[15] to the same singlet resonance a few ppm downfield of the solvent signal. This helped establish HSO_3F-$Pt(SO_3F)_4$ as the first and only known dibasic superacid system in fluorosulfuric acid.

Although the lack of solubility of $Sn(SO_3F)_4$ precluded its study, the ternary salts $K[Sn(SO_3F)_5]$ and $K_2[Sn(SO_3F)_6]$ have been studied[33,132] by both ^{19}F and ^{119}Sn NMR. Rapid solvent/solute fluorosulfate exchange was found for the former salt, leading to one

combined signal, whereas the latter gave rise to a singlet solute resonance again marginally downfield of the solvent signal. This provided the best evidence for the suspected superacidity of $Sn(SO_3F)_4$ in HSO_3F.

Rapid solvent/solute fluorosulfate exchange has given rise to only single combined solvent/solute resonances down to -80 or -90 °C in the ^{19}F NMR of all other reported systems. These are $I(SO_3F)_3$,[133] $Cs_2[Ge(SO_3F)_6]$,[33] $Cs_x[(CH_3)_2Sn(SO_3F)_{2+x}]$,[134] with x = 0, 1 or 2, $XeF_5(SO_3F)$ (fluorosulfate region of spectrum only) and $Xe(SO_3F)_2$.[130,135] The last species listed was also found to be in rapid equilibrium with $Xe(SO_3F)^+$. ^{129}Xe NMR investigations in HSO_3F at temperatures ranging from -70 to -100 °C have also been reported for these as well as other xenon-containing solutes.[136,137]

The dimethyltin(IV) anions, $[(CH_3)_2Sn(SO_3F)_{2+x}]^{x-}$, with x = 1 or 2, have also been studied[134] in HSO_3F solution using ^1H, ^{13}C and ^{119}Sn NMR in the temperature range -90 to +25 °C. The electronic structure of the $(CH_3)_2Sn^{2+}$ moiety was found to be nearly identical in each case, with the coordination number of tin being six via coordination from either fluorosulfate ions or the solvent itself.

Only one signal was seen in the ^1H NMR of the HSO_3F-SbF_5[38] and HSO_3F-$Au(SO_3F)_3$[25] systems. This is consistent with a rapid proton transfer process occurring in these and presumably other protonic superacid systems.

The main limitations of conventional NMR techniques (especially ^{19}F NMR) in the study of fluorosulfuric acid solutions can be summarized:

(i) lack of solubility of the desired solute;

(ii) rapid solvent/solute fluorosulfate exchange minimizing the structural information available;

(iii) tendency of coordinated fluorosulfate ^{19}F resonances to occur in close proximity to the solvent signal, resulting in potential overlap.

^{1}H Dynamic Nuclear Magnetic Resonance (^{1}H DNMR) techniques[11] have been used to study the acidity of the HSO_3F-SbF_5 ("Magic Acid") system at concentrations beyond 11 mole %, which is where the indicator method described in Section 1.C. meets its limit. The acidity of this system was established in the 12 - 90 mole % SbF_5 range by systematically investigating the thermodynamic[138,139] and kinetic[140] behaviour of various aromatic aldehydes and ketones in these media. A $-H_0$ value of 26.5 was thus established[140] for the 90 mole % solution, which remains to date as the highest acidity measured in solution.

REFERENCES

1. T.E. Thorpe and W. Kirman, *J. Chem. Soc. London,* 921 (1892).

2. W. Lange, in *"Fluorine Chemistry"*, J.H. Simons, Ed., Academic Press, New York, Vol.I, 1950.

3. G.H. Cady, *Adv. Inorg. Chem. Radiochem.* **2**, 105 (1960).

4. A. Engelbrecht, *Angew. Chem. Int. Ed. Engl.* **4**, 641 (1965).

5. S.M. Williamson, *Prog. Inorg. Chem.* **7**, 39 (1968).

6. R.C. Thompson, in *"Inorganic Sulphur Chemistry"*, G. Nickless, Ed., Elsevier, Amsterdam, 1968.

7. R.J. Gillespie, *Acc. Chem. Res.* **1**, 202 (1968).

8. A.W. Jache, *Adv. Inorg. Chem. Radiochem.* **16**, 177 (1974).

9. S Natarajan and A.W. Jache, in *"The Chemistry of Non-Aqueous Solvents"*, Vol.VB J.J. Lagowski, Ed., Academic Press, N.Y., 1978.

10. R.J. Gillespie and T.E. Peel, *Adv. Phys. Org. Chem.* **9**, 1 (1972).

11. G.A. Olah, G.K.S. Prakash and J. Sommer, *"Superacids"*, J. Wiley & Sons, N.Y., 1985 (and references herein).

12. S. Karunanithy and F. Aubke, *Materials Science and Engineering* **62**, 241 (1984).

13. G.A. Lawrence, *Chem. Rev.* **86**, 17 (1986).

14. P. Hagenmüller, *"Inorganic Solid Fluorides"*, Academic Press, N.Y., 1985.

15. K.C. Lee and F. Aubke, *Inorg. Chem.* **23**, 2124 (1984).

16. R.J. Gillespie and R.A. Rothenbury, *Can. J. Chem.* **42**, 416 (1964).

17. S.P. Mallela and F. Aubke, *Inorg. Chem.* **24**, 2969 (1984).

18. G.C. Kleinkopf and J.M. Shreeve, *Inorg. Chem.* **4**, 607 (1964).

19. R.E. Noftle and G.H. Cady, *J. Inorg. Nucl. Chem.* **29**, 969 (1967).

20. F. Fairbrother, *"The Chemistry of Niobium and Tantalum"*, Elsevier, London, 1967.

21. D. Brown, *Chemistry of Niobium and Tantalum* in *"Comprehensive Inorganic Chemistry"*, Pergamon Press, N.Y., Vol.III, 1973.

22.a) H.C. Clark and H.J. Emeléus, *J. Chem. Soc.*, 2119 (1957).
b) L.E. Trevorrow, J. Fischer and R.K. Steunenberg, *J. Am. Chem. Soc.* **79**, 5167 (1957).

23. R.C. Paul, R.C. Kumar and R.D. Verma, *J. Fluor. Chem.* **11**, 203 (1978).

24. S. Singh, M.S. Gill and R.D. Verma, *J. Fluor. Chem.* **27**, 133 (1985).

25. K.C. Lee and F. Aubke, *Inorg. Chem.* **18**, 389 (1979).

26. F.A. Allen, J. Lerbscher and J. Trotter, *J. Chem. Soc. A*, 2507 (1971).

27. R.J. Gillespie, G.J. Schrobilgen and D.R. Slim, *J. Chem. Soc., Dalton Trans.*, 1003 (1977).

28. M.J. Collins, G Dénès and R.J. Gillespie, *J. Chem. Soc., Chem. Commun.*, 1296 (1984).

29. K. O'Sullivan, R.C. Thompson and J. Trotter, *J. Chem. Soc. A*, 2024 (1967).

30. K. O'Sullivan, R.C. Thompson and J. Trotter, *J. Chem. Soc. A*, 1814 (1970).

31. Å. Kvick, P.-G. Jönsson and I. Olovsson, *Inorg. Chem.* **8**, 2775 (1969).

32. N. Bartlett, M. Wechsberg, G.R. Jones and R.D. Burbank, *Inorg. Chem.* **11**, 1124 (1972).

33. S.P. Mallela, K.C. Lee and F. Aubke, *Inorg. Chem.* **23**, 653 (1984).

34. S.P. Mallela, S. Yap, J.R. Sams and F. Aubke, *Inorg. Chem.* **25**, 4327 (1986).

35. H.H. Hyman and J.J. Katz, in *"Non-Aqueous Solvent Systems"*, T.C. Waddington, Ed., Academic Press, London, Chapter 2, 1965.

36. R.J. Gillespie and J. Liang, *J. Am. Chem. Soc.* **110**, 6053 (1988).

37. J. Barr, R.J. Gillespie and R.C. Thompson, *Inorg. Chem.* **3**, 1149 (1964).

38. R.C. Thompson, J. Barr, R.J. Gillespie, J.R. Milne and R.A. Rothenbury, *Inorg. Chem.* **4**, 1641 (1965).

39. A.A. Woolf, *J. Chem. Soc.* 433 (1955).

40. T.C. Waddington, *"Non-Aqueous Solvents"*, Appleton-Century-Crofts, N.Y., 1969.

41. L.P. Hammett and A.J. Deyrup, *J. Am. Chem. Soc.* **54**, 2721 (1932).

42. M.A. Paul and F.A. Long, *Chem. Rev.* **57**, 1 (1957).

43. R.J. Gillespie, T.E. Peel and E.A. Robinson, *J. Am. Chem. Soc.* **93**, 5083 (1971).

44. R.J. Gillespie and T.E. Peel, *J. Am. Chem. Soc.* **95**, 5173 (1973).

45. G.M. Kramer, *J. Org. Chem.* **40**, 302 (1975).

46. R.J. Gillespie, R. Ouchi and G.P. Pez, *Inorg. Chem.* **8**, 63 (1969).

47. F.O. Sladky, P.A. Bolliner and N. Bartlett, *J. Chem. Soc. A*, 2179 (1969).

48. G.A. Olah, G.K.S. Prakash and J. Sommer, *Science* **206**, 13 (1979).

49. G.A. Olah and A. Commeyras, *J. Am. Chem. Soc.* **91**, 2929 (1969).

50. D. Brunel, A. Germain and A. Commeyras, *Nouv. J. Chim.* **2**, 275 (1978).

51. P.A.W. Dean and R.J. Gillespie, *J. Am. Chem. Soc.* **92**, 2362 (1970).

52. G.M. Kramer, *J. Org. Chem.* **40**, 298 (1975).

53. A.J. Edwards, *J. Chem. Soc.*, 3714 (1964).

54. J.O. Hill, I.G. Worsley and L.G. Hepler, *Chem. Rev.* **71**, 127 (1971).

55. G.A. Olah, O. Farooq, S.M.F. Farnia and J.A. Olah, *J. Am. Chem. Soc.* **110**, 2560 (1988).

56. N. Burford, J. Passmore and J.C.P. Sanders, in *"Molecular Structure and Energetics"*, VCH, Accepted, 1989.

57. A.A. Woolf, *Adv. Inorg. Chem. Radiochem.* **9**, 217 (1966).

58. C.G. Davies, R.J. Gillespie, P.R. Ireland and J.M. Sowa, *Can. J. Chem.* **52**, 2048 (1974).

59. J. Passmore, G. Sutherland and P.S. White, *Inorg. Chem.* **20**, 2169 (1981).

60. A. Apblett, F. Grein, J.P. Johnson, J. Passmore and P.S. White, *Inorg. Chem.* **25**, 422 (1986).

61. H.S. Low and R.A. Beaudet, *J. Am. Chem. Soc.* **98**, 3849 (1976).

62. J. Passmore, P. Taylor, T. Whidden and P.S. White, *Can. J. Chem.* **57**, 968 (1979).

63. R.J. Gillespie, R. Kapoor, P. Faggiani, C.J.L. Lock, M.J. Murchie and P. Passmore, *J. Chem. Soc., Chem. Commun.*, 8 (1983).

64. A.J. Edwards and G.R. Jones, *J. Chem. Soc.* 2318 (1971).

65. R.J. Gillespie, M.J. Morton, *Inorg. Chem.* **9**, 811 (1970).

66. R.J. Gillespie and M.J. Morton, *Inorg. Chem.* **11**, 591 (1972).

67. J. Besida and A. O'Donnell, *Inorg. Chem.* **28**, 1669 (1989).

68. J. Barr, R.J. Gillespie and P.K. Uminat, *J. Chem. Soc., Chem. Commun.*, 264 (1970).

69. R.C. Burns, R.J. Gillespie and J.F. Sawyer, *Inorg. Chem.* **19**, 1423 (1980).

70. N. Bartlett and D.H. Lohmann, *Proc. Chem. Soc. London*, 115 (1962).

71. B.G. Müller, *J. Fluor. Chem.* **17**, 409 (1981).

72. A.B. Cornford, Ph.D. Thesis, University of British Columbia, 1972.

73. K. Seppelt and D. Lentz, *Prog. Inorg. Chem.* **29**, 167 (1982).

74. F. Aubke, unpublished results.

75. G.P. Smith, A.S. Dworkin, R.M. Pagni and S.P. Zingg, *J. Am. Chem. Soc.* **111**, 525 (1989).

76. F.B. Dudley and G.H. Cady, *J. Am. Chem. Soc.* **79**, 513 (1957).

77. R.A. DeMarco and J.M. Shreeve, *Adv. Inorg. Chem. Radiochem.* **16**, 109 (1974).

78. E.L. Muetterties and D.D. Coffman, *J. Am. Chem. Soc.* **80**, 5914 (1958).

79. J.M. Shreeve and G.H. Cady, *J. Am. Chem. Soc.* **83**, 4521 (1961).

80. J.M. Shreeve and G.H. Cady, *Inorg. Syn.* **7**, 124 (1963).

81. F.B. Dudley, *J. Chem. Soc.*, 3407 (1963).

82. J.K. Ruff and R.F. Merritt, *Inorg. Chem.* **6**, 1219 (1968).

83. E.C. Zimmermann and J. Ross, *J. Chem. Phys.* **80**, 720 (1984).

84. A.M. Qureshi, L.E. Levchuk and F. Aubke, *Can. J. Chem.* **49**, 2544 (1971).

85. G. Franz and F. Neumayr, *Inorg. Chem.* **3**, 921 (1964).

86. F.B. Dudley and G.H. Cady, *J. Am. Chem. Soc.* **85**, 3375 (1963).

87. P.M. Nutkowitz and G. Vincow, *J. Am. Chem. Soc.* **91**, 5956 (1969).

88. G.W. King and C.H. Warren, *J. Mol. Spect.* **32**, 121 (1969).

89. E.M. Suzuki, J.W. Nibler, K.A. Oakes and D. Eggers, Jr., *J. Mol. Spect.* **58**, 201 (1975).

90. E. Castellano, R. Gatti, J.E. Sicre, and H.I. Schumacher, *Z. Physik. Chem. (Frankfurt)* **42**, 174 (1964).

91. H.A. Carter, A.M. Qureshi, J.R. Sams and F. Aubke, *Can. J. Chem.* **48**, 2853 (1970).

92. P.A. Yeats, J.R. Sams and F. Aubke, *Inorg. Chem.* **12**, 328 (1973).

93. P.C. Leung, Ph.D. Thesis, University of British Columbia, 1979.

94. R.W. Taft in *"Steric Effects in Organic Chemistry"*, M.S. Newman, Ed., Wiley, N.Y., 1956.

95. P.A. Yeats, J.R. Sams and F. Aubke, *Inorg. Chem.* **11**, 2634 (1972).

96. D.A. Edwards, M.J. Stiff and A.A. Woolf, *Inorg. Nucl. Chem. Lett.* **3**, 427 (1967).

97. A.A. Woolf in *"New Pathways in Inorganic Chemistry"*, E.A.V. Ebsworth, A.G. Maddock and A.G. Sharpe, Eds., Cambridge University Press, U.K., 1968.

98. C.S. Alleyne, K. O'Sullivan-Mailer and R.C. Thompson, *Can. J. Chem.* **52**, 336 (1974).

99. S.P. Mallela and F. Aubke, *Can. J. Chem.* **62**, 382 (1984).

100. A.A. Woolf, *J. Chem. Soc. A*, 335 (1967).

101. R.C. Paul, R.D. Sharma, S. Singh and R.D. Verma, *J. Inorg. Nucl. Chem.* **43**, 1919 (1981).

102. P.A. Yeats, B.F.E. Ford, J.R. Sams and F. Aubke, *Chem. Commun.*, 791 (1969).

103. R.C. Paul, S. Singh and R.D. Verma, *J. Indian Chem. Soc.* **58**, 24 (1981).

104. R.C. Paul, S. Singh, R.C. Kumar, R.D. Sharma and R.D. Verma, *Ind. J. of Chem.* **17A**, 273 (1979).

105. S. Singh and R.D. Verma, *Polyhedron* **2**, 1209 (1983).

106. H.A. Carter, C.A. Milne and F. Aubke, *J. Inorg. Nucl. Chem.* **37**, 282 (1975).

107. R.C. Paul, S. Singh and R.D. Verma, *J. Fluor. Chem.* **16**, 153 (1980).

108. A. Storr, P.A. Yeats and F. Aubke, *Can. J. Chem.* **50**, 452 (1972).

109. L.M. Emme and G.L. Gard, *J. Fluor. Chem.* **12**, 77 (1978).

110. P.A. Yeats, B.L. Poh, B.F.E. Ford, J.R. Sams and F. Aubke, *J. Chem. Soc. A*, 2188 (1970).

111. M. Lustig and G.H. Cady, *Inorg. Chem.* **3**, 714 (1962).

112. D.D. DesMarteau, *Inorg. Chem.* **7**, 434 (1968).

113. J.P. Masson, C. Naulin, P. Charpin and R. Bougon, *Inorg. Chem.* **17**, 1858 (1978).

114. W.W. Wilson and F. Aubke, *J. Fluor. Chem.* **13**, 431 (1979).

115. H. Imoto and F. Aubke, *J. Fluor. Chem.* **15**, 59 (1980).

116. L.E. Levchuk and F. Aubke, *Inorg. Chem.* **11**, 43 (1972).

117. P.C. Leung and F. Aubke, *Inorg. Nucl. Chem. Letters* **13**, 263 (1977).

118. P.C. Leung and F. Aubke, *Inorg. Chem.* **17**, 1765 (1978).

119. P.C. Leung, G.B. Wong and F. Aubke, *J. Fluor. Chem.* **35**, 607 (1987).

120. K.C. Lee and F. Aubke, *Can. J. Chem.* **55**, 2473 (1977).

121. K.C. Lee and F. Aubke, *Can. J. Chem.* **57**, 2058 (1979).

122. K.C. Lee and F. Aubke, *J. Fluor. Chem.* **19**, 501 (1982).

123. P.C. Leung and F. Aubke, *Can. J. Chem.* **62**, 2892 (1984).

124. W.W. Wilson, C. Naulin and R. Bougon, *Inorg. Chem.* **16**, 2252 (1977).

125. D.W.J. Cruickshank and B.C. Webster, *"Inorganic Sulfur Chemistry"*, G. Nickless, Ed., Elsevier, Amsterdam, 1968.

126. S.P. So, *Mol. Phys.* **23**, 1147 (1972).

127. A.M. Qureshi, H.A. Carter and F. Aubke, *Can. J. Chem.* **49**, 35 (1971).

128. K.C. Lee, Ph.D. Thesis, University of British Columbia, 1980.

129. J.R. Dalziel, R.D. Klett, P.A. Yeats and F. Aubke, *Can. J. Chem.* **52**, 231 (1974).

130. N. Keller and G.J. Schrobilgen, *Inorg. Chem.* **20**, 2118 (1981).

131. R. Mews and H.C. Braeuer, *Z. Anorg. Allg. Chem.* **447**, 126 (1978).

132. P.A. Yeats, J.R. Sams and F. Aubke, *Inorg. Chem.* **12**, 328 (1973).

133. R.J. Gillespie and J.B. Milne, *Inorg. Chem.* **5**, 1236 (1966).

134. S.P. Mallela, S. Yap, J.R. Sams and F. Aubke, *Inorg. Chem.* **25**, 4074 (1986).

135. R.J. Gillespie and G.J. Schrobilgen, *Inorg. Chem.* **13**, 765 (1974).

136. G.J. Schrobilgen in *"NMR and the Periodic Table"*, R.K. Harris and B. E. Mann, Ed., Academic Press, London, 1978.

137. G.J. Schrobilgen, J.H. Holloway, P. Ganger and C. Brevard, *Inorg. Chem.* **17**, 980 (1978).

138. J. Sommer, P. Rimmelin and T. Drakenberg, *J. Am. Chem. Soc.* **98**, 2671 (1976).

139. J. Sommer, S. Schwartz, P. Rimmelin and P. Canivet, *J. Am. Chem. Soc.* **100**, 2576 (1978).

140. V. Gold, K. Lali, K.P. Morris and L.Z. Zdunek, *J. Chem. Soc., Chem. Commun.*, 769 (1981).

141. H. Remy, *"Lehrbuch der Anorganische Chemie"*, Akademische Verlagsgeselschaft, Leipzig, Geest und Partig K-G, 1949.

142. R.P. Bell, *"Acids and Bases: Their Quantitative Behaviour"*, Methuen and Co., Ltd., London, 1969.

143. J. Grondin, R. Sagnes and A. Commeyras, *Bull. Soc. Chim. Fr.*, 1779 (1976).

144. V.A. Engelbrecht and E. Tschager, *Z. Anorg. Allg. Chem.* **433**, 19 (1977).

145. K.O. Christie, *Inorg. Chem.* **14**, 2230 (1975).

146. R.J. Gillespie and J.B. Milne, *Inorg. Chem.* **5**, 1577 (1966).

147. O. Glemser and A. Smalc, *Angew. Chem. Int. Ed. Engl.* **8**, 517 (1969).

148. R.J. Gillespie, M.J. Morton, *J. Chem. Soc., Chem. Commun.*, 1565 (1968).

149. K.C. Lee and F. Aubke, *Inorg. Chem.* **19**, 119 (1980).

150. P.A. Yeats and F. Aubke, *J. Fluor. Chem.* **4**, 243 (1974).

151. W.W. Wilson and F. Aubke, *Inorg. Chem.* **13**, 326 (1974).

152. J. Passmore, G. Sutherland and P.S. White, *J. Chem. Soc., Chem. Commun.*, 330 (1980).

153. C.G. Davies, R.J. Gillespie, J.J. Park and J. Passmore, *Inorg. Chem.* **10**, 2781 (1971).

154. R.C. Burns and R.J. Gillespie, *Inorg. Chem.* **21**, 3877 (1982).

155. R.K. McMullen, D.J. Prince and J.D. Corbett, *Inorg. Chem.* **10**, 1749 (1971).

156. R.C. Burns, W.L. Chan, R.J. Gillespie, W.C. Luk, J.F. Sawyer and D.R. Slim, *Inorg. Chem.* **19**, 1432 (1980).

157. J. Barr, R.J. Gillespie, G.P. Pez, P.K. Ummat and O.C. Vaidya, *Inorg. Chem.* **10**, 362 (1971).

158. R.J. Gillespie, W. Luk and D.R. Slim, *J. Chem. Soc., Chem. Commun.*, 791 (1976).

159. R.J. Gillespie, B.Landa and G.J. Schrobilgen, *Inorg. Chem.* **15**, 1256 (1976).

160. G.A. Olah, R. Aniszfeld, G.K.S. Prakash and R.E. Williams, *J. Am. Chem. Soc.* **110**, 7885 (1988).

161. S.P. Mallela, S. Yap, J.R. Sams and F. Aubke, *Rev. Chim. Min.* **23**, 572 (1986).

162. H.A. Carter, S.P.L. Jones and F. Aubke, *Inorg. Chem.* **9**, 2485 (1970).

CHAPTER 2

GENERAL EXPERIMENTAL

2.A. Introduction

General experimental techniques as well as the sources, purification and, where necessary, preparation of starting materials used in this study will be dealt with in this section. Specific syntheses and procedures will be described in the appropriate chapters.

The extreme moisture sensitive nature of nearly all of the purchased and synthesized chemicals necessitated handling them either by using standard vacuum line techniques, or, in the case of less volatile liquid or solid materials, manipulating and storing them in an inert atmosphere drybox. The high toxicity of the various species encountered required a well ventilated working environment, necessitating the use of fume hoods at all times.

Where possible, reactions were monitored by weight difference in the reaction vials. Removal of volatile by-products was usually carried out at, or slightly below, room temperature. Complete removal of less volatile materials, such as HSO_3F, which requires elevated temperatures even under vacuum conditions,[1] was not always possible using this method, owing to the thermal instability of a large number of the prepared compounds. Product isolation by filtration was employed in instances where solids formed, resulting necessarily in reduced yields, and precluded obtaining a mass balance of the reaction by weight.

Fluorolube grease Series 25÷10M, $CF_2Cl(CF_2\text{-}CFCl)_nCF_2Cl$, obtained from

Halocarbon Products Corporation, was sparingly used to lubricate all ground glass connections. Its low volatility and reactivity toward halogen-containing compounds made it very suitable.

2.B. Apparatus

2.B.1. Reaction Vessels

To facilitate the isolation of products by vacuum filtration, two-part Pyrex reactors were used. A typical reactor consisted of a 25, 50, or 100 ml round bottom flask with a B19 ground glass cone, fitted with a "drip lip" to trap any grease-contaminated volatiles. The corresponding adaptor top had a Kontes Teflon stem stopcock between a B19 socket and a B10 cone (see Fig. 2.1.a). During reaction work-up, the adaptor could be substituted for a vacuum adapted sintered-glass "space-satellite" filter and the product was isolated by prolonged vacuum filtration. Alternatively, a slightly modified filtration apparatus allowed for the solution to be cooled prior to filtration, using either a dry ice/acetone or an ice bath, in order to optimize the yield (see illustrations in Figure 2.2).

The reaction products were also isolated by removing all volatiles in vacuo whenever possible. One-piece reactors were employed in these instances. If high pressures were anticipated during the reaction, 3 mm thick-walled tubular Pyrex reactors of ~ 30 ml maximum capacity fitted with a Kontes Teflon stem stopcock with a sidearm extending to a B10 ground glass cone (see Figure 2.1.b) were used; otherwise, 50 or 100 ml round bottom flasks fitted with the same type stopcock and cone were employed, as shown in Figure 2.1.c. Reagents were loaded most efficiently into these reactors via a

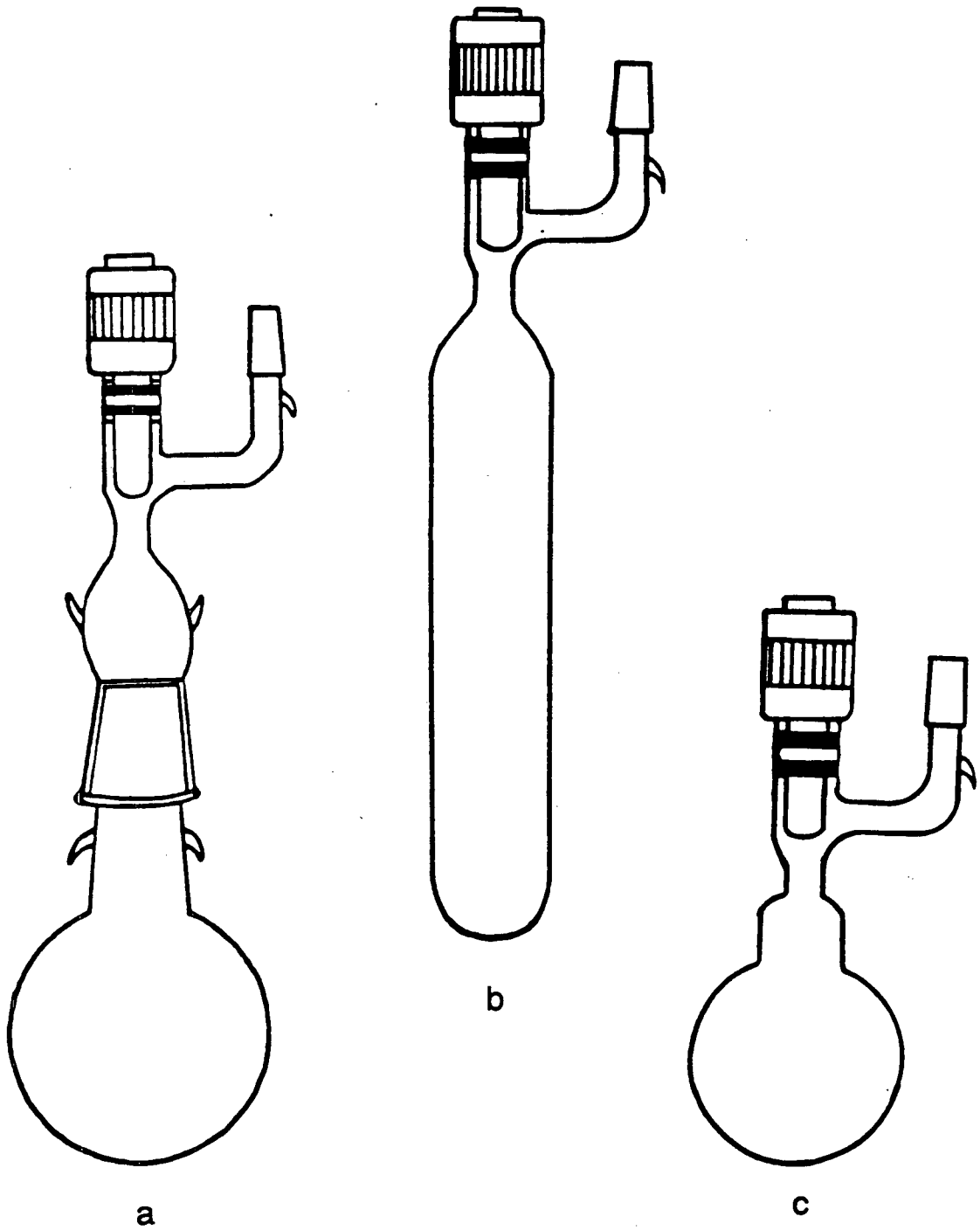

Figure 2.1. Typical Pyrex Reaction Vessels

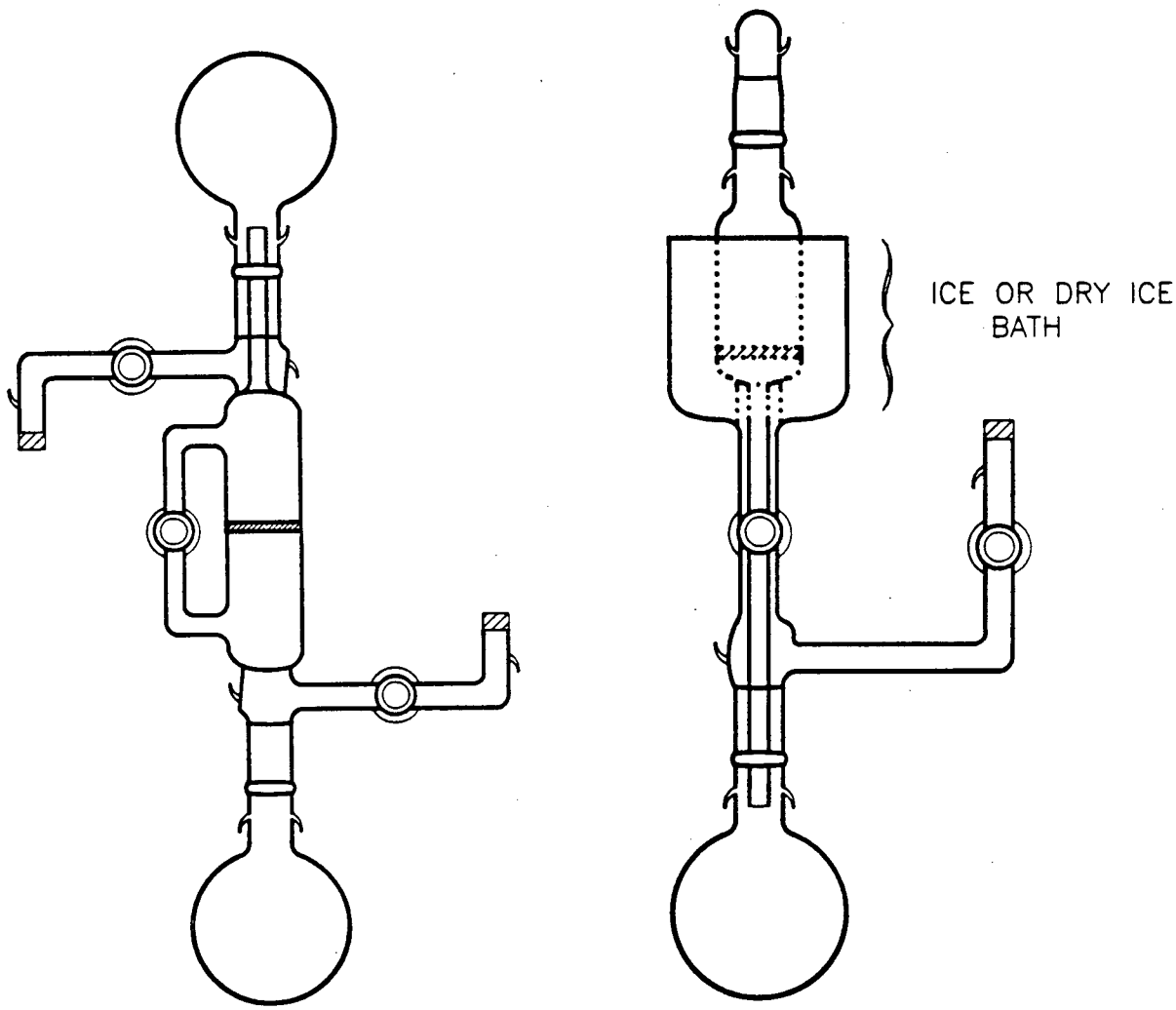

Figure 2.2. Vacuum-Adapted Filtration Apparatus

small diameter funnel, to prevent contamination of the Teflon stem area and to ensure proper vacuum seal.

On occasion, neither product isolation technique proved adequate and complete solvent removal was accomplished by passing a stream of N_2 gas over the "wet" product. A vacuum adaptor fitted with two Teflon stopcock B10 outlet cones was used. Materials known to be reactive with glass were handled in semi-transparent Kel-F reactors. The monel top attachment was equipped with a stainless steel Whitey valve, a standard tapered B10 cone, and fittings to retain the Kel-F tube.

2.B.2. $S_2O_6F_2$ - Addition Trap

Where exact volumes of $S_2O_6F_2$ had to be used, a 4.00 ml graduated pipette equipped with an overflow bulb and fitted on top with a Kontes Teflon stem stopcock attached via sidearm to a B10 cone was employed. The $S_2O_6F_2$ was transferred at room temperature under static vacuum directly from this vessel to the reactor. Larger volumes of $S_2O_6F_2$ could be estimated by using a thick-walled tubular one-piece vessel (described earlier) instead and calibrating the cylinder's walls to approximately 0.25ml/mm length. Determination of the precise amount of $S_2O_6F_2$ used was obtained by weight difference.

2.B.3. Ultraviolet/Visible Optical Cells

To allow various manipulations of solutions without exposing them to the atmosphere, 1 mm quartz Spectrosil precision optical cells were attached via a Pyrex bridge to a 25 ml round bottom flask fitted with a B19 cone. In addition, the apparatus was fitted with a Kontes Teflon stem stopcock and sidearm attached to a B10 cone. A matching adaptor consisting of a Kontes Teflon stem stopcock between a B10 cone and a

B19 socket was also provided, as shown in Figure 2.3. Sample solutions were usually loaded into the solvent-containing flask in the drybox, mixed thoroughly and then transferred into the optical cell chamber by tilting the apparatus. Reproducibility was tested by repeating the above mixing procedure a few times between readings. On some occasions, it was adequate to use 10 mm Spectrosil precision optical cells, fitted with Teflon plugs and sealed with Teflon tape.

2.B.4. Pyrex Vacuum Line

A general purpose Pyrex vacuum line consisting of five B10 outlets with Kontes Teflon stem stopcocks was employed. It was equipped with a safety trap cooled to liquid N_2 temperature and situated between the vacuum pump and the manifold. A leak valve to the atmosphere was also provided. Most volatile liquid transfers were afforded with a T-connection bridge under static vacuum; it consisted of B10 sockets at both ends and a B10 cone connecting it to the main manifold via a Kontes Teflon stopcock. Typical vacuum generated on this line was of the order of about 10^{-2} torr.

2.B.5. Metal Vacuum Line

For corrosive materials, a metal vacuum line was employed. It was constructed of 1/4 inch O.D. monel tubings equipped with Whitey valves (IKS 4) and was operated in a manner similar to that used with the Pyrex line. Copper tubing (1/4 inch O.D.) was used in connections to the manifold to gain more flexibility. A more "customized" metal line for preparing $S_2O_6F_2$ is described in Section 2.D.3..

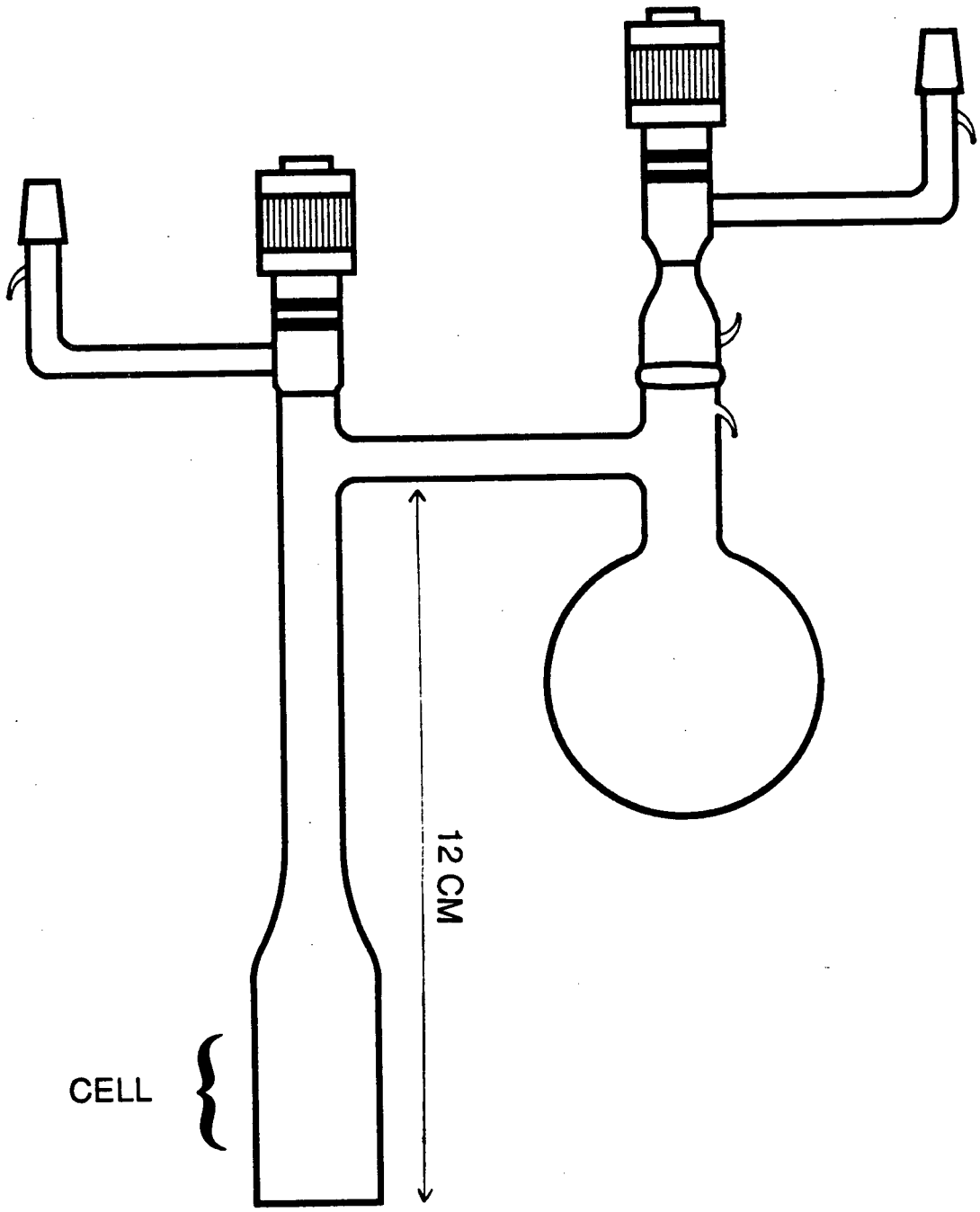

Figure 2.3. Ultraviolet/Visible Optical Cell

2.B.6. Drybox

For the handling and storage of hygroscopic solids and low-volatility liquids, a *Vacuum Atmospheres Corporation* "Dri-Lab" Model HE-493 was employed, filled with K-grade N_2 gas. The dryness of the atmosphere was ensured by circulation over molecular sieves, which were regenerated about once per month by heating over a Cu catalyst contained within the HE-493 "Dri-Train" purifier. Fresh P_2O_5 was also kept inside the glove box to act as a moisture indicator.

2.B.7. Balances

Three balances of varying precision and load capacities were involved. Primarily, a Mettler Gram-atic analytical balance #1-910 with precision to about ± 0.5 mg and a 200 g maximum load limit was employed. For heavier and/or bulkier weights, a Sartorius top-loading balance with a maximum capacity of 1 kg was used, precise to about ± 50 mg. A top-loading Mettler PC440 balance with a 440 g maximum capacity and precise to about ± 5 mg was kept inside the drybox.

2.C. Instrumentation and Methods

2.C.1. Electrical Conductivity

Detailed description of the general methods and apparatus involved has been given previously.[1,2] The conductivity cells used are shown in Figure 2.4. Two different sizes were employed to accommodate the varying sample volumes, ranging from ~ 7 ml in the small cell (Fig. 2.4.a) to ~ 50 ml in the large one. The platinum-black coating of the electrodes was renewed after every two runs, electroplating from H_2PtCl_6.[3] Cell

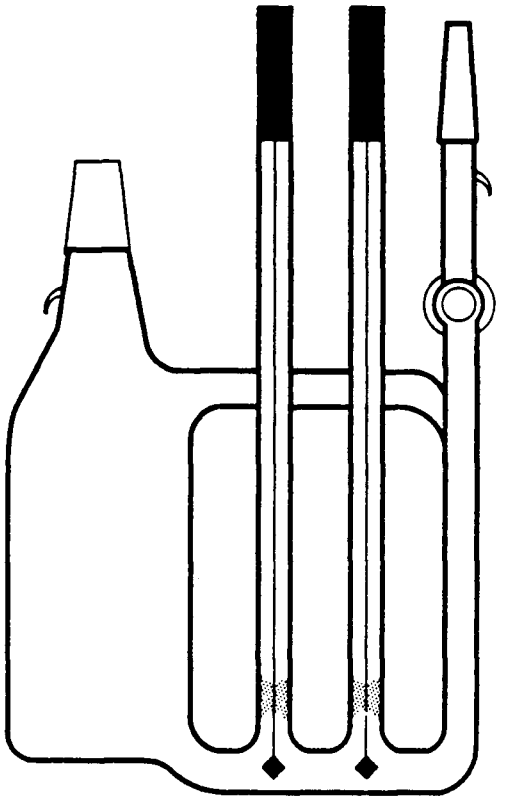

a. SMALL VOLUME CELL

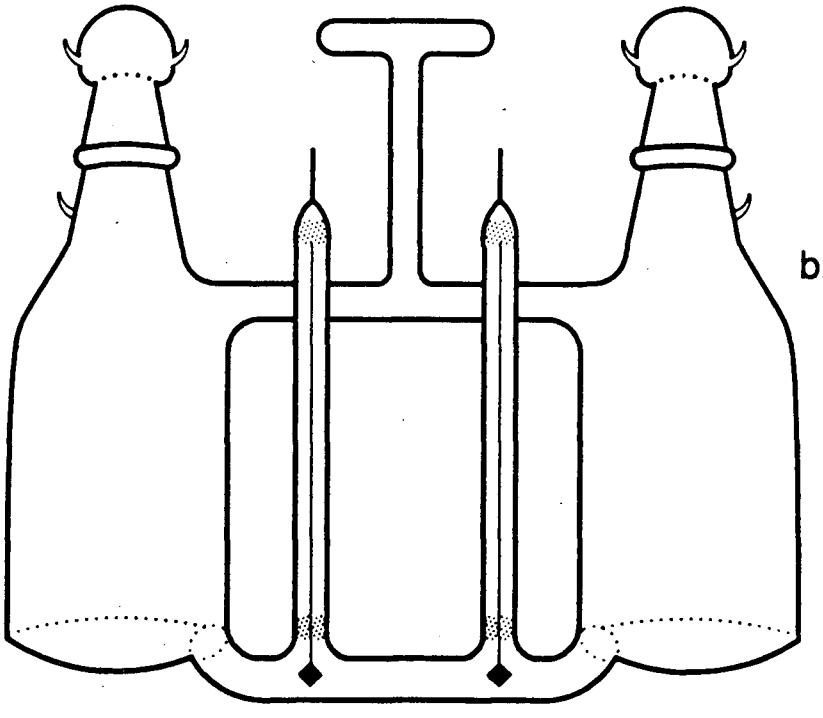

b. LARGE VOLUME CELL

Figure 2.4. Electrical Conductivity Cells

constants were determined using dilute (~0.01 M) KCl solutions[4] and had values ranging from 5.400 $\pm$ 0.013 cm^{-1} to 7.896 $\pm$ 0.016 cm^{-1}.

A specially fitted buret (shown in Figure 2.5) of ~20 ml maximum capacity was filled with the acidic or basic solutions of known concentration in the drybox and quickly attached to the conductivity cell in the fume hood. The buret contents were added stepwise to the cell and conductivity readings were taken after each addition. The solution concentrations were then calculated as fractions of the total volume added, with the prime source of error being in the buret calibration uncertainty ($\pm$ 0.02 ml). The solutions were well shaken and allowed to equilibrate for ~ 5-10 minutes to the constant oil bath temperature of 25.00 $\pm$ 0.01 °C before readings were taken. A Sargent Thermonitor Model ST maintained the temperature while the actual conductivity measurements were obtained using a Wayne-Kerr Universal Bridge, Model B221A. Solutes were not introduced directly into the cell in order to prevent the periodic exposure of the cell's contents to the atmosphere and the subsequent formation of basic impurities.

2.C.2. Infrared Spectroscopy

IR spectra of well-powdered solids and occasionally Nujol mulls were recorded on Perkin Elmer Model 598 or Model 783 spectrophotometers, operating in the range 4000 to 250 cm^{-1} and 4000 to 200 cm^{-1}, respectively. The samples were pressed in the drybox between two AgBr or AgCl windows with an approximate transmission range down to 300 or 400 cm^{-1}, respectively. The use of mulling agents or other window materials was not always possible, owing to the reactivity of the species studied. Spectra of gaseous samples were recorded using a monel cell of 7 cm path length, fitted with AgCl windows and a Whitey valve. All spectra were calibrated with a polystyrene

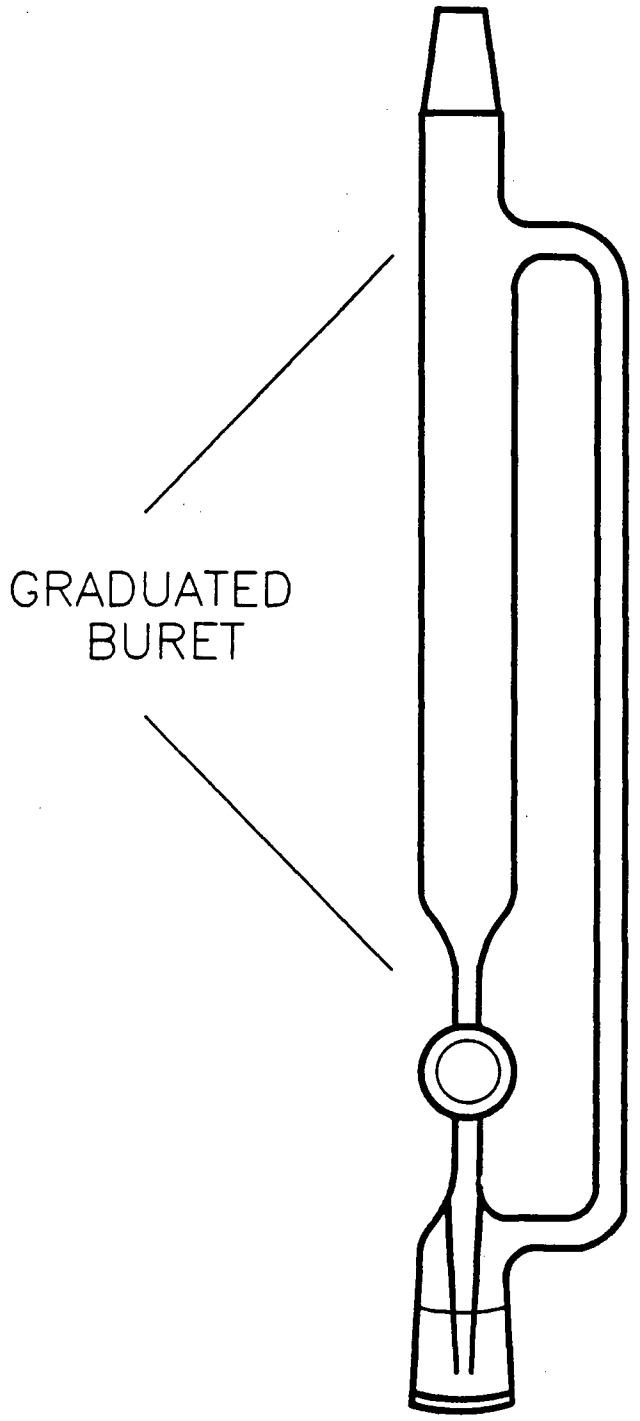

Figure 2.5. Addition Buret Used During Conductivity Measurements

reference. Error in the position of narrow bands was estimated at ± 2 cm^{-1}, whereas positions of the broader bands were only certain to within ± 10-15 cm^{-1}. Gas pressure was monitored via a closed-ended manometer, equipped with two Kontes Teflon stem stopcocks and a B10 cone.

2.C.3. Raman Spectroscopy

Raman spectra were obtained using a Spex Ramalog 5 spectrophotometer equipped with a Spectra Physics 164 argon ion laser, with the 514.5 nm green line as the excitation line. Solid samples were packed in the drybox into melting point capillaries, temporarily sealed with fluorolube grease and then immediately flame-sealed. Liquid samples were loaded into 5 mm NMR tubes and stoppered with Teflon plugs which were wrapped with Teflon tape. Error in band positions was found comparable to that stated above.

2.C.4. Electronic Spectroscopy

Electronic spectra were recorded on a Hewlett Packard Single-Cell Mode Array Spectrophotometer, Model 8452A, incorporating HP Vectra computer hardware and a HP Think Jet printer. Software was available for internal sample referencing. The apparatus and methods used have been described in Section 2.B.3.

2.C.5. Nuclear Magnetic Resonance

The vast majority of FT spectra were obtained on a Varian XL-300 multinuclear spectrometer, operating at the following frequencies and using the listed external references:

^{1}H = 300 MHz, TMS;

^{19}F = 282.231 MHz, $CFCl_3$;

^{93}Nb = 73.329 MHz, $LiNbF_6$ in propylene carbonate.

Either $CDCl_3$ or D_6-acetone was used as the external lock source in each case. Using DSO_3F as internal lock source was attempted on occasion, but the very marginal improvement in spectral quality and reproducibility did not justify the expense and inconvenience incurred. For some of the ^{1}H and ^{19}F spectra, the solvent (HSO_3F) signal served as a convenient reference point by which to verify the reproducibility of the various runs. Some of the FT spectra were also obtained on either a Bruker-Nicolet HXS 270 MHz or on a 400 MHz Bruker WH-400 instrument.

Solutions were either loaded into 5 mm NMR tubes in the drybox or, in the case of highly volatile liquids, transferred via static vacuum into NMR tubes equipped with a B10 ground glass cone and then flame-sealed. Low temperature spectra were obtained by cooling the probe with liquid N_2 and exactly controlling the temperature with a high precision thermocouple. In all spectra obtained, *positive values* are assigned to chemical shifts *downfield* of the external reference.

2.C.6. Electron Spin Resonance Spectroscopy

ESR measurements were made using an X-band (9.0 GHz) homodyne spectrometer employing a Varian 12 inch magnet equipped with a MK II Fieldial control. Phase-sensitive detection at 100 kHz was achieved with an Ithaco Dynatrac 391A lock-in amplifier. The temperature was controlled to ± 0.1 °C using a Varian E-257 temperature controller. Computational details have been reported previously.[5]

Solutions were syringed under inert atmosphere into 100 μl Pyrex tubes using a teflon-tipped needle. Separate tubes containing N_2 and HSO_3F were used for background correction.

2.C.7. X-ray Diffraction

Well-powdered solids were loaded into 0.5 mm O.D. Lindemann glass capillary tubes in the drybox, temporarily sealed with fluorolube grease and then immediately and carefully flame-sealed. X-ray diffraction patterns were obtained using a Phillips powder camera of 57 mm radius with conventional Straumanis arrangement. Cu-K_α radiation (1.5405 Å) was used with a Ni filter to minimize K_β radiation. Kodak NS-392T film was employed to obtain photographs, with exposure times of about 6 hours. On rare occasions, crystals were also grown, but owing to their poor quality, single crystal x-ray diffraction studies were not possible.

2.C.8. Melting Points

Melting points and decomposition temperatures were determined using a Thomas Hoover capillary melting point apparatus, equipped with an oil bath containing high flash point oil, in which the sample capillary and thermometer were both submerged.

2.C.9. Computer-Generated Plots

The two-dimensional plots shown in some of the figures have all been generated using the graphics program *TELLEGRAF*, available on the University of British Columbia General MTS Computer Network. Unless stated otherwise, data point smoothing curves were generated using the iterative algorithm *Delta*, and a *QMS* plotter was employed to print the output.

2.D. Chemicals

2.D.1. Materials Used Without Purification

Many chemicals used during this study were obtainable from the respective supplier in a user-ready form. These are listed in Table 2.I, along with their source and percentage purity.

2.D.2. Purifications Required

a) $BaCl_2$ was obtained by dehydration from $BaCl_2 \cdot 2H_2O$ (99.0 %, *BDH*) in a 110 °C oven.

b) KCl (> 99%, *MCB*) was dried in the oven for about one week at 110 °C.

c) HSO_3F, from *Allied Chemical* and more recently *Orange County Chemical*, was carefully purified by double distillation in a Pyrex apparatus under 1 atm. of P_2O_5-dried N_2.[2] The constant boiling fraction at 162-163 °C was either collected into a conductivity cell, into a 100 ml pyrex storage vessel or directly into a reactor for synthetic use. The freshly distilled acid had a specific conductance of $1.4 - 1.7 \times 10^{-4}\ \Omega^{-1}cm^{-1}$.

d) HSO_3CF_3, from the *Ventron Corporation*, was purified by repeated vacuum distillations.

e) HF, from *Matheson Ltd.*, was dried by bubbling F_2 gas through it immediately prior to use.

f) CH_3CN (reagent grade, *MCB*) was dried over CaH_2 for one week and then vacuum distilled.

Table 2.I. Chemicals Used Without Further Purification

Chemical	Source	Purity (%)
Ta, -22 or -60 mesh	*Ventron*	99.99, 99.9
Nb, -60 mesh	*Ventron*	99.9
TaF_5	*Ozark Mahoning*	99.9
NbF_5	*Ozark Mahoning*	99.5
$TaCl_5$	*Strem*	99.9
$NbCl_5$	*Strem*	99.9
CsCl	*BDH*	99.9
LiCl	*Fisher*	99.9
LiF	*Ventron*	99.5
P_2O_5	*BDH*	98.0
CaH_2	*BDH*	reagent grade
$CaCl_2$	*Fisher*	97.1
$K_2Cr_2O_7$	*Analar*	reagent grade
H_2PtCl_6	*Aldrich*	8 wt % water sol'n
SO_3	*Allied*	unavailable
DSO_3F	*Sigma*	98+
H_2SO_4	*J.T. Baker*	96.5
CH_3OH	*Aldrich*	99+
N_2	*Union Carbide*	dry K-grade

g) 2,4,6-Trinitrotoluene (reagent grade, *Eastman Organic Chemicals*) and 2,4-Dinitrofluorobenzene (reagent grade, *MCB*) were both recrystallized from methanol and dried under vacuum over P_2O_5.[6]

2.D.3. Preparative Reactions

a) $S_2O_6F_2$ was prepared by the reaction of SO_3 and F_2 using AgF_2 as catalyst and N_2 as carrier gas. The general apparatus is shown in Figure 2.6. Some modifications to the method reported by Shreeve and Cady[7] were made to increase the yield: (i) the reactor was kept at ~180 °C instead of 150 °C and the SO_3 was heated gently to about 40 °C, to increase the rate of reaction; (ii) collection vessel **A** was kept at room temperature to allow gradual cooling of the gas mixture and to visually detect posssible non-volatile materials such as SO_3, while vessel **C** was cooled with dry-ice (-78 °C) instead of liquid O_2 (-183 °C) to prevent the collection of dangerous amounts of the potentially explosive[8] by-product FSO_3F[9], and (iii) the crude product was collected in the two pyrex vessels **B** and **C** (see Figure 2.6) and cooled to -78 °C by solid dry ice. Excess F_2 and the by-product FSO_3F were destroyed by reaction with sodalime contained in the metal reactor. Unreacted SO_3 was removed by washing the crude product with concentrated H_2SO_4 and separating the two resulting immiscible layers. Further purification was achieved by pumping on the product overnight at -78 °C to remove any residual FSO_3F. The purified $S_2O_6F_2$ was vacuum distilled into large, one-part storage traps equipped with Kontes Teflon Valves. Purity was checked by both IR and ^{19}F NMR spectra. Some $S_2O_5F_2$[10] (≤ 5 %) was found as an impurity in products washed with conc. H_2SO_4. It was found inert in subsequent reactions and hence its removal was not attempted.

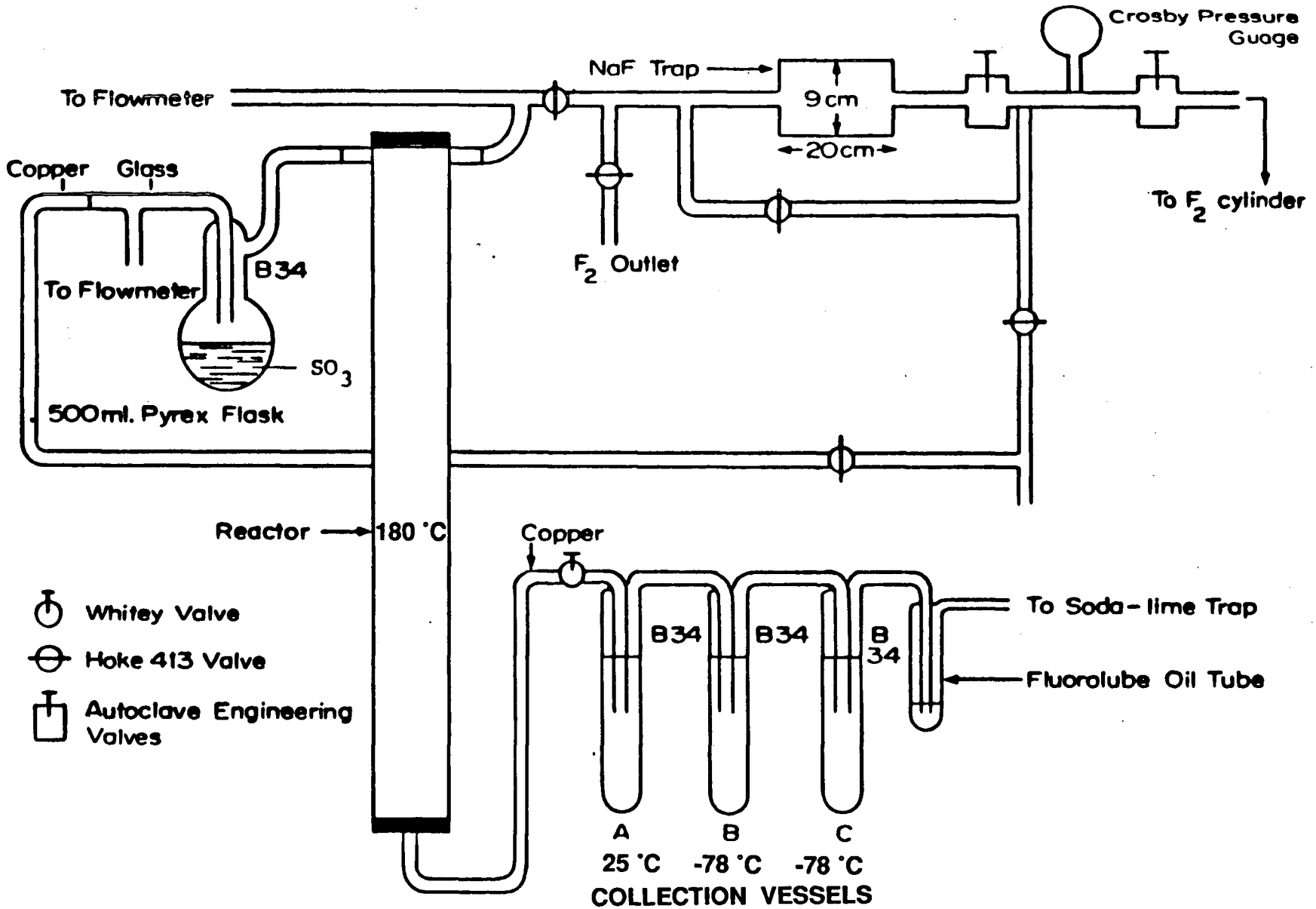

Figure 2.6. General Apparatus for Preparing $S_2O_6F_2$

While the catalytic fluorination of SO_3 was found to be a convenient route for the large scale production of $S_2O_6F_2$, allowing preparations of ~1 kg over one week of operation, a number of problems surfaced over the last 5 years requiring some modifications to the apparatus, then in operation in our laboratory for almost 20 years:

(i) Changes in the F_2 flow rate caused by a badly corroded valve caused overheating of the reactor due to the burning of copper wool used as carrier for AgF_2, resulting ultimately in the melting of some copper and a blocking of the gas outlet by a copper plug. The resulting back pressure caused extensive SO_3 leakage. Copper had fused to the reactor walls and the reactor had to be discarded.

(ii) Fluorination of silver-plated copper in order to prepare new catalyst went out of control and melting of the copper wall in one spot caused leakage of F_2. The reactor had to be discarded as well.

(iii) The use of chore balls provided by the *Metal Corporation* as recommended[7] to produce new catalyst caused an additional problem: the manufacturer had added a polymeric resin as support and catalytic fluorination of SO_3 resulted in large quantities of SO_2F_2 being formed.

(iv) For the reactor in use, built in 1967, asbestos paper and asbestos had been extensively used. Both are now regarded as hazardous.

A new reactor was subsequently built and the following modifications to the original design were made:

(i) The copper tube was replaced by a 1/16" wall monel tube.

(ii) The reactor design was changed in four important ways:

a) At the bottom and top, 1/4" monel tubes of about 10" length, with ends sealed off, were welded in the center section to allow better monitoring of the temperature inside the reactor. In addition, two thermocouples were attached to the outside and temperatures at all four locations were routinely checked during operation.

b) The gas outlet tube was welded to the side rather than the bottom of the lower section to prevent plugging.

c) The top and bottom parts of the reactor tube were left empty to allow better mixing of reactants and cooling of the reaction products.

d) A removable top with Teflon gaskets was used to fill the catalyst.

(iii) Copper turnings purchased from *Johnson and Mathey* were used to prepare silver-plated copper, which was subsequently fluorinated in a slow stream of undiluted F_2 while carefully monitoring the temperature by reducing or increasing the flow rate.

(iv) Two rather than one heating zones were produced by heating the upper and lower parts of the reactor independently.

(v) The monel reactor tube was wrapped in Fiberfrax insulating paper,

bonded with sodium silicate. The Chromel heating wire was subsequently wrapped around and pyrex wool was used as insulating material, held in place by a 0.020" thick stainless steel casing and clamps. In addition, design and size of the NaF trap, used to remove HF impurities from technical grade fluorine, had to be changed because the contents of the previous trap had fused during regeneration to a solid mess.

A detailed illustration of the new improved reactor is shown in Figure 2.7, with most of the aforementioned features indicated.

b) $CsSO_3F$ was prepared by either reacting CsCl with excess HSO_3F[2] or with excess $S_2O_6F_2$. The product was isolated by removing volatiles in vacuo.

c) KSO_3F, $LiSO_3F$ and $Ba(SO_3F)_2$ were prepared by reacting the respective chloride with excess HSO_3F.[2] The products were isolated by removing the volatiles in vacuo.

2.D.4. Elemental Analyses

Carbon, hydrogen, chlorine, and some of the sulfur analyses were carried out by Mr. Peter Borda of the Chemistry Department, University of British Columbia. All other elemental analyses were performed by Analytische Laboratories, Gummersbach, F.R.G..

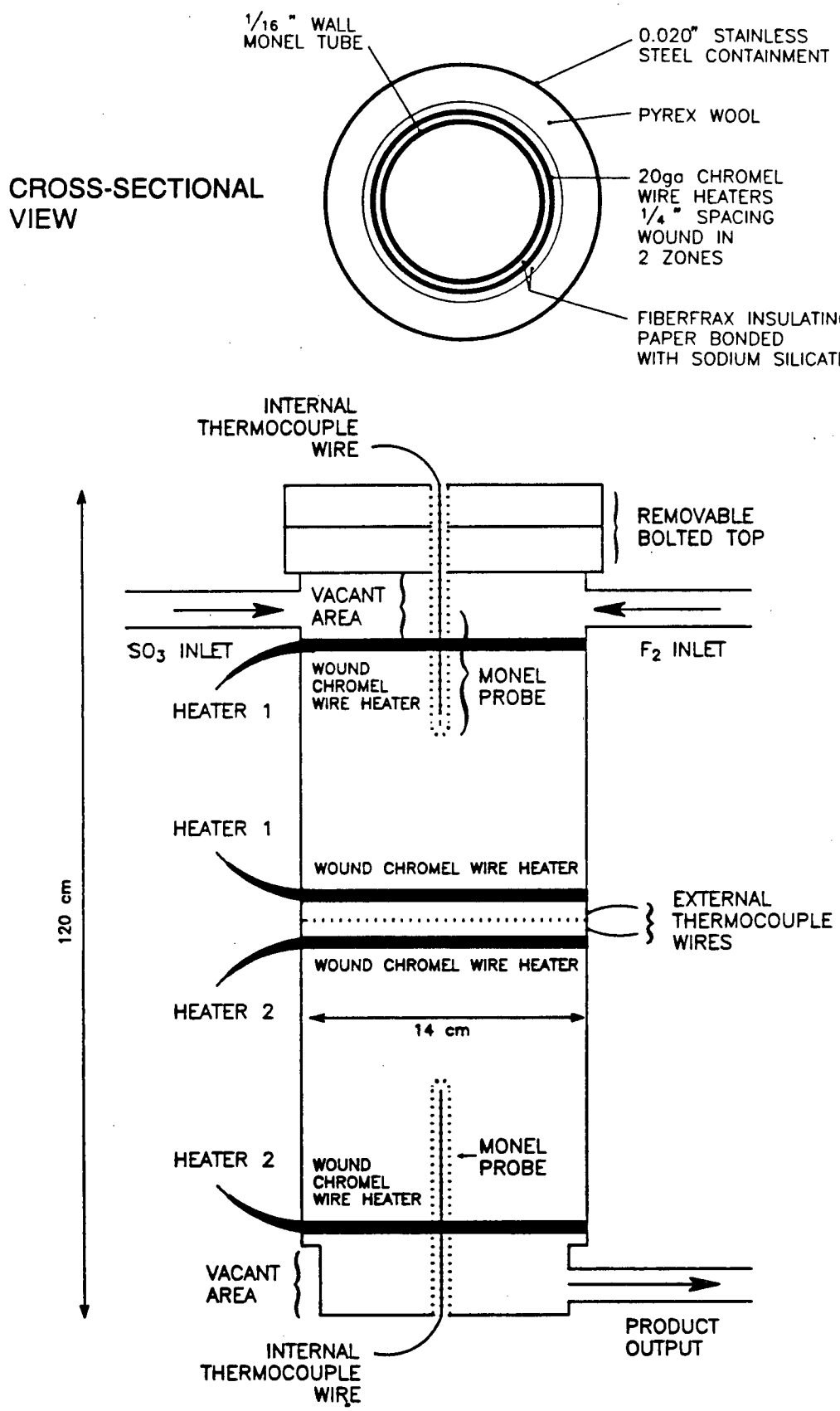

Figure 2.7. $S_2O_6F_2$ Reactor

REFERENCES

1. K.C. Lee, Ph.D. Thesis, University of British Columbia, 1980.

2. J. Barr, R.J. Gillespie and R.C. Thompson, *Inorg. Chem.* **3**, 1149 (1964).

3. A. Vogel, in *"Quantitative Inorganic Analysis"*, 3rd ed., J. Wiley & Sons, N.Y., 1961.

4. J.E. Lind, Jr., J.J. Zwolenik and R.M Fuoss, *J. Am. Chem. Soc.* **81**, 1557 (1959).

5. P.S. Phillips and F.G. Herring, *J. of Magn. Reson.* **57**, 43 (1984).

6. W.A. Gey, E.R. Dalbey and R.W. Van Dolah, *J. Am. Chem. Soc.* **78**, 1803 (1956).

7. J.M. Shreeve and G.H. Cady, *Inorg. Synth.* **7**, 124 (1963).

8. G.H. Cady, *Inorg. Synth.* **11**, 155 (1968).

9. F.B. Dudley, G.H. Cady and D.F. Eggers, Jr., *J. Am. Chem. Soc.* **78**, 290 (1956).

10. E.L. Muetterties and D.D. Coffman, *J. Am. Chem. Soc.* **80**, 5914 (1958).

CHAPTER 3

THE SYSTEM FLUOROSULFURIC ACID (HSO_3F) AND BIS(FLUOROSULFURYL) PEROXIDE ($S_2O_6F_2$): A SOLUTION STUDY

3.A. Introduction

While the principal oxidizing agent in the well studied[1-9] HSO_3F-$S_2O_6F_2$ metal-oxidizing reagent combination is $S_2O_6F_2$, the role of HSO_3F is also significant. Its purpose is three-fold: (i) it allows an expansion of the reaction temperature range well beyond the boiling point[10] of $S_2O_6F_2$, 67.1 °C; (ii) it maintains in solution and hence at the reactive site a high concentration of $SO_3F^{\cdot}$ radicals formed by the reversible dissociation of $S_2O_6F_2$[11] and (iii) it dissolves freshly formed reaction product from the metal surface. All three factors contribute to fast, complete oxidation reactions where $S_2O_6F_2$ alone often gives only incompletely reacted products or requires excessively long reaction times. $S_2O_6F_2$ and HSO_3F are completely miscible together at 25 °C in any proportion to give clear colourless solutions. On the other hand, $S_2O_6F_2$ is virtually insoluble at 25 °C in the related protonic acid H_2SO_4. This is found very useful when crude $S_2O_6F_2$, formed in the catalytic fluorination of SO_3[12], is purified by extracting SO_3 with concentrated 96.5% H_2SO_4.[13] This rather puzzling behaviour inspired the present investigation into the HSO_3F-$S_2O_6F_2$ system. Equally puzzling is the observation, made during the synthesis of $Au(SO_3F)_3$,[1] that an excess of $S_2O_6F_2$ well above the stoichiometrically required amount is needed to ensure fast and complete metal oxidation.

Previous studies of this system by cryoscopy and conductivity by Gillespie et al.[14] allow preliminary conclusions to be drawn regarding the extent of this interaction. Gillespie et al. reported that $S_2O_6F_2$ essentially exists in its molecular form in HSO_3F at 25 °C, which allowed its use in the determination of the cryoscopic constant of HSO_3F. Obviously, the second observation is only strictly valid for temperatures at or around the melting point of HSO_3F (-88.98 °C).

These observations appear to invalidate two possible interaction pathways between HSO_3F and $S_2O_6F_2$: (i) extensive ionizing solvation of $S_2O_6F_2$ in HSO_3F, with protonation the most probable initial process according to:

$$HSO_3F + S_2O_6F_2 \overset{HSO_3F}{\rightleftharpoons} HS_2O_6F_2^{+}{}_{(solv)} + SO_3F^{-}{}_{(solv)} \qquad (3\text{-}1)$$

and (ii) electron transfer between the $SO_3F^{\cdot}$ radical and the self-ionization ion SO_3F^{-}, according to:

$$SO_3F^{\cdot}{}_{(solv)} \underset{-e^-}{\overset{+e^-}{\rightleftharpoons}} SO_3F^{-}{}_{(solv)} \qquad (3\text{-}2)$$

The conductivities measured[14] on solutions of $S_2O_6F_2$, although quite small, do increase with increasing $S_2O_6F_2$ concentration (see Figure 3.2 in the next section), suggesting that $S_2O_6F_2$ behaves as a weak electrolyte in HSO_3F. It should be noted that a true, soluble non-electrolyte is expected to reduce proton mobility via a structure breaking effect, which would be expected to cause a slight concentration-dependent *drop* in the conductance values. An ESR study[15] on pure $S_2O_6F_2$ led to the conclusion that $SO_3F^{\cdot}$ radicals are present at ambient temperature and may persist to 4 °C, which suggests that a similar study of the HSO_3F-$S_2O_6F_2$ solutions is warranted, to demonstrate whether or not appreciable dissociation of $S_2O_6F_2$ into radicals occurs at room temperature.

To address these points, three studies are described in this chapter: (i) Ambient temperature Raman spectroscopy on solutions of $S_2O_6F_2$ in HSO_3F. The vibrational spectra of the individual compounds are well known.[16-18] (ii) NMR spectroscopy of both the ^1H and ^{19}F nuclei in the temperature range -75 to +45 °C. (iii) ESR spectroscopy of the system in the temperature range -90 (freezing point of HSO_3F) to +50 °C to detect the onset of $SO_3F^{\cdot}$ radical formation. The ESR spectrum of the $SO_3F^{\cdot}$ radical in the temperature range 4 to 180 °C has been previously reported.[15] Furthermore, the effect of varying the acidity of HSO_3F by the addition of the standard base, KSO_3F[19], will be described.

3.B. Experimental

$S_2O_6F_2$ and then HSO_3F of varying exact stoichiometries were vacuum distilled into reactor flasks to make up a series of about 5 ml "neutral" solutions, which were then thoroughly agitated before being transferred to NMR tubes in the drybox prior to obtaining the Raman and NMR spectra.

"Basic" solutions were obtained by introducing accurately weighed amounts of KSO_3F[19] to some of the above solutions and ensuring complete dissolution before transferring to NMR tubes. The molar ratio HSO_3F:$S_2O_6F_2$ for each solution is designated as "H/OX" throughout the chapter, with "H" representing HSO_3F and "OX" representing $S_2O_6F_2$. The solubility studies of $S_2O_6F_2$ in HF were handled in a Kel-F (poly fluoro-chloro-carbon) reactor.

3.C. Results and Discussion

3.C.1. Raman Spectroscopy

The Raman spectrum recorded on a 1:2 (by volume) solution of $S_2O_6F_2$ in HSO_3F is shown in Figure 3.1. A comparison with previously reported Raman spectra data for HSO_3F[16,17] and $S_2O_6F_2$,[16], as well as with a re-recorded spectrum on freshly distilled $S_2O_6F_2$ (see Table 3.I for data), allows the following conclusions: (i) The solution spectrum is at first approximation a composite spectrum of the two major components as judged from band positions and relative intensities. (ii) The relatively strong, polarized vibrational bands of $S_2O_6F_2$ are unperturbed and clearly recognizable. Some of the very weak bands, however, are not observed. It is clear that the bulk of bis(fluorosulfuryl) peroxide is present in solution of HSO_3F. (iii) The symmetric O-O stretching band at 801 cm^{-1} is unchanged in both position and relative intensity. It appears that the O-O bond strength is not altered in HSO_3F solution. This suggests that at room temperature no change in reactivity of $S_2O_6F_2$ in solution has occurred. (iv) The OH stretching mode is observed as a broad band centered at 3096 ± 10 cm^{-1}, a position comparable to the reported IR band at 3125 cm^{-1} in liquid HSO_3F.[18] This implies that intramolecular interaction between HSO_3F and $S_2O_6F_2$ effects νOH in a very similar way as intermolecular association does in liquid HSO_3F. (v) Besides bands due to $S_2O_5F_2$,[20] the only other new, weak bands found at 1281 and 774 cm^{-1} are attributed to the presence of SO_3F^- in solution, based on a precedent[21] and the fact that addition of KSO_3F (see Table 3.I for data) results in an increase in intensity for both bands. The Raman data for an aqueous solution of KSO_3F are included in Table 3.I for comparison.

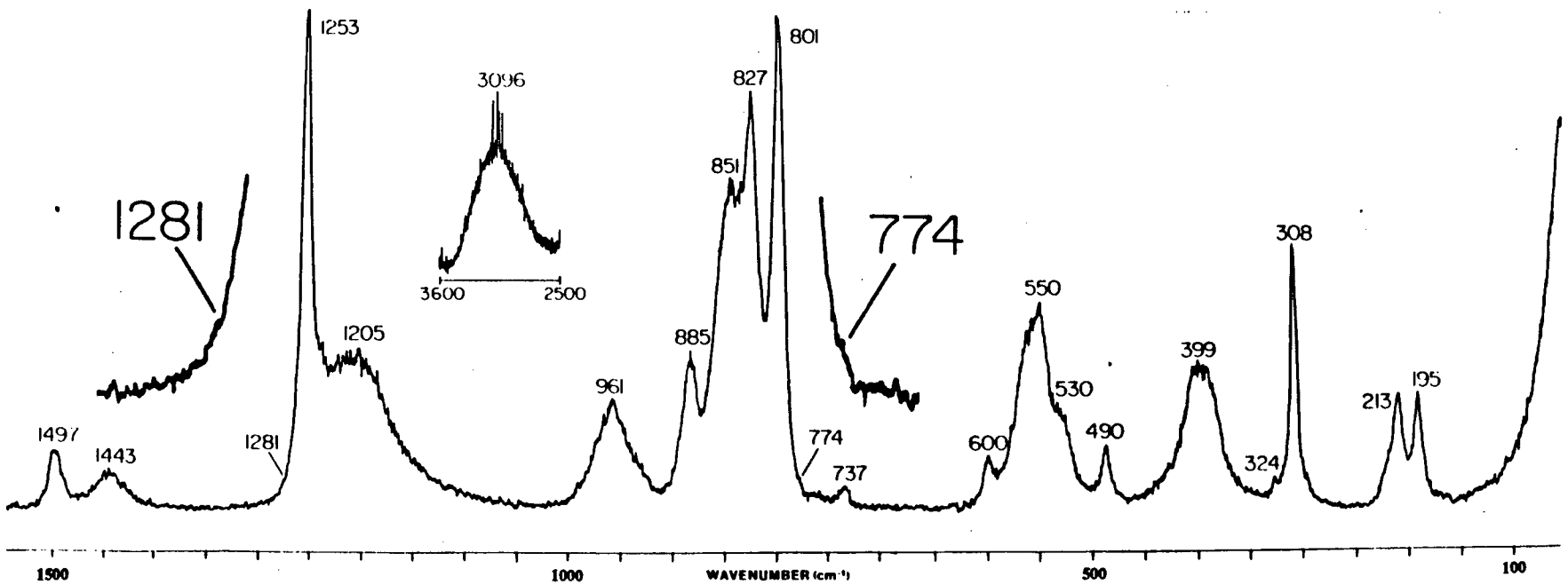

Figure 3.1. Raman Spectrum of $S_2O_6F_2$ in HSO_3F (1:2 solution by volume) at 20 °C

Table 3.I. Raman Vibrational Frequencies ($\Delta\nu$, cm^{-1}) for HSO_3F-$S_2O_6F_2$, HSO_3F,[c,d] $S_2O_6F_2$ and KSO_3F_{aq}[e,f] at Ambient Temperature

H-OX (H/OX=4.44)[a]	K-H-OX (H/OX=1.82)[b]	$S_2O_6F_2$	HSO_3F	KSO_3F_{aq}	Assign.
3096 w,b			3125 (IR)		ν (O-H)
	1509 w,sh				$S_2O_5F_2$
1497 w,b	1499 w,b	1498 w			
1443 w,vb			1444 w,b		
1281 vw,sh	1276 vw,sh			1287[e]	
1253 s	1254 s	1252 vs	1230[d] m,b,sh	1250[f]	ν (SO_3)
1205 m,vb	1200 w		1205[c] m,b,sh		
	1101 w		1179 m,b		
	1093 w,b			1082	
961 m,b	962 vw,b		961 m		
885 m	885 m	883 m			ν (S-F)
851 s,b	850 w		851 s		
827 s	828 s	826 s			ν (S-O)
801 s	803 s	801 vs			ν (O-O)
774 vw,sh	774 w,sh			786	ν (S-F)
737 vw,b	741 w				?
			686[c] vw		
600 w	603 w	600 w		592	
	592 w				
550 m,b	555 w,b		560 s,sh	566	
			553 s		
530 w,b,sh	531 w,b	530 w,b			
490 w	491 w	488 w	490[c] vw		δ (SO_3F)
		434 vw,b	405 m	409	
399 m,b	398 w,b	393 w,b	392 m,sh		
324 w,sh	328 w,sh				?
308 m	311 m	308 s			
213 w	213 m	212 m			lattice
192 w	194 m	192 m			modes

[a]H = HSO_3F, OX = $S_2O_6F_2$, H/OX = molar ratio; [b]K = KSO_3F, [KSO_3F] = 3.21 M
[c]ref.16, [d]ref.17, [e]ref.50, [f]ref.21

The presence of spectroscopically observable (although marginal) amounts of SO_3F^- in the *neutral* solution suggests at least weakly basic behaviour of $S_2O_6F_2$ via Equation (3-1). The previously reported[14] electrical conductivity of $S_2O_6F_2$ in HSO_3F, shown in Figure 3.2 along with other weak electrolytes, is most likely due to this type of ionizing solvation. Two things should be noted concerning Figure 3.2: (i) the slope of the κ vs. molality plot of $S_2O_6F_2$ slightly increases with concentration and (ii) the maximum concentration of $S_2O_6F_2$ studied was only 0.04 m. The solutions studied here had $S_2O_6F_2$ concentrations of about 7 m. Even a very weakly basic electrolyte in HSO_3F would be expected to form significant amounts of $SO_3F^-_{(solv)}$ at this concentration.

If hydrogen bonding or even proton transfer plays a role, it is then prudent to question how HSO_3F is capable of interacting with $S_2O_6F_2$ in this manner while H_2SO_4 appears unable to do so. There are two plausible, interrelated explanations: (i) HSO_3F is a better proton donor than H_2SO_4 (this is reflected in their respective $-H_o$ values: 15.07 for HSO_3F;[22] 11.93 for 100% H_2SO_4[23] and 10.09 for 96.5% "concentrated" H_2SO_4[24]) and (ii) tight intermolecular hydrogen bonding in H_2SO_4, which causes its high viscosity,[25] is not effectively broken up by the insufficiently basic $S_2O_6F_2$ molecule.

If these conclusions are correct, it should be possible to dissolve $S_2O_6F_2$ in acids stronger than H_2SO_4 using the H_o value as a guideline and moreover to reduce the acidity of HSO_3F by addition of KSO_3F to a point where $S_2O_6F_2$ will no longer be soluble. The next section will deal with these points.

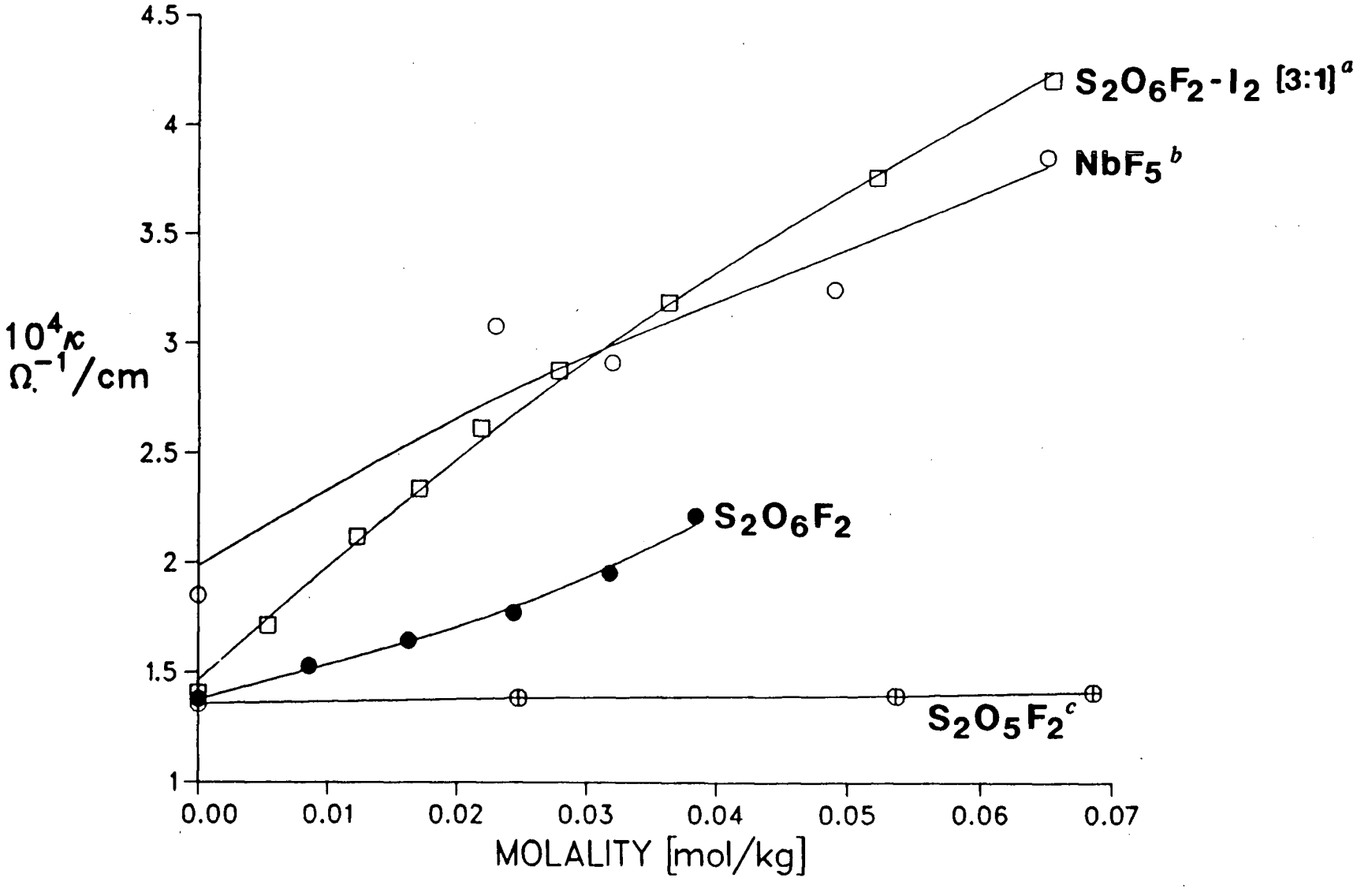

Figure 3.2. Specific Conductance of Weak Electrolytes in HSO_3F at 25.00 °C; *a*ref.48, *b*ref.49, *c*ref.14

3.C.2. Solubility Studies of $S_2O_6F_2$ in Strong Protonic Acids

There are, in addition to HSO_3F, two simple protonic acids which are of higher acidity than H_2SO_4, available in anhydrous form, that do not decompose at room temperature as do HSO_3Cl or $HClO_4$. These are anhydrous HF ($-H_o$ = 15.1)[26] and HSO_3CF_3 ($-H_o$ = 14.1),[27] both widely used protonic solvents. The latter, trifluoromethyl sulfuric acid, is similar in acidity to a number of additional sulfonic acids with various other fluorocarbon substituents on sulfur.[27]

As has been reported some time ago,[28] $S_2O_6F_2$ is extremely soluble in HSO_3CF_3. These solutions, however, are metastable and slowly give rise to the evolution of heat as well as volatile products, among them CF_3OSO_2F. There is also sufficient evidence from the reported interaction of the two acids HSO_3F and HSO_3CF_3 and from the thermal instability of the peroxide $(CF_3)_2S_2O_6$ to conclude that oxidative cleavage of the S-C bond occurs.[29] It appears then, that HSO_3CF_3 is not a suitable solvent for $S_2O_6F_2$ in spite of its high solubility. Furthermore, synthetic use of the mixture is only indicated where oxidation reactions proceed quickly.[28]

In anhydrous HF, the solubility of $S_2O_6F_2$ is found to be somewhat lower than in either HSO_3F or HSO_3CF_3 but is still appreciable, with about 25 mole % $S_2O_6F_2$ in anhydrous HF being the point of saturation. Its $-H_o$ value of 15.1 would suggest a higher solubility than is actually observed in this acid. This Hammett acidity value, however, has not been obtained directly but rather by interpolation during the course of a study on HF-SbF_5 and other related systems.[26] On account of small amounts of H_2O acting as a base in "anhydrous" HF, measured $-H_o$ values have ranged as low as ~11.[27] Difficulties encountered in removing the last traces of water from HF,[30] its low boiling point, and the

possibility of F^- vs. SO_3F^- exchange during synthesis all refute extensive synthetic use of the HF-$S_2O_6F_2$ system.

Addition of the standard base KSO_3F[19] to a solution of $S_2O_6F_2$ in HSO_3F (molar ratio of acid to peroxide = 1.72) at room temperature results in a separation into two phases once the concentration of KSO_3F is in excess of 1.8 M. Assuming that KSO_3F is the only base in the system, this corresponds to a reduced $-H_0$ value of 11.8, calculated by exponentially extrapolating data for previously reported KSO_3F solutions in HSO_3F.[22] Thus, the solubility of $S_2O_6F_2$ in strong protonic acids closely correlates with the relative acid strength, best given as:

$$\underset{\textit{highly soluble}}{HSO_3F} \geq \underset{\textit{soluble}}{HSO_3CF_3} > \underset{}{HF} > \underset{\textit{insoluble}}{H_2SO_4}$$

As is expected from the reported densities of 1.726 g-cm^{-3} for HSO_3F[31] and 1.645 g-cm^{-3} for $S_2O_6F_2$,[32] the latter is the principal constituent of the upper layer. The volume of this upper layer increases steadily with increasing KSO_3F concentration in the acid phase and contains the bulk of the $S_2O_6F_2$ for 3.1 M KSO_3F solutions, thus allowing physical separation of both phases by pipetting inside the inert atmoshpere box, a procedure used to accommodate the NMR studies described in the next section.

The observed solubility loss of $S_2O_6F_2$ in HSO_3F can be explained by the lowered acidity of HSO_3F as previously argued. Alternatively, one may view the strongly basic SO_3F^- as competing successfully with $S_2O_6F_2$ for HSO_3F to form solvates. The strength of the SO_3F^-- HSO_3F interaction is evident from the isolation and

structural characterization of solid solvates of the type $M'[H(SO_3F)_2]$, with M' = Na or Cs.[33,34]

In addition, the solubility loss discussed has some implications regarding the synthetic use of $S_2O_6F_2$ solutions in HSO_3F. Metal oxidation reactions in the presence of alkali metal fluorosulfates, aimed at forming ternary fluorosulfato complexes according to Equation (1-22) of Chapter 1, at least initially show the same phase separation. It becomes important then to choose reaction conditions and reactant concentrations such that sufficient $S_2O_6F_2$ remains in the acid phase to effect oxidation of the metal.

The qualitative solubility study described here has indicated conditions where $S_2O_6F_2$ ceases to be soluble in HSO_3F, and the role acidity plays in solvent-solute interaction has been investigated. The subsequent section will probe more deeply into the nature of the interaction using NMR as the principal tool. There are now two aspects to the system: (i) the acid phase where $S_2O_6F_2$ is the solute and HSO_3F the solvent and (ii) the upper phase formed under basic conditions, where the roles may be reversed.

3.C.3. ^{19}F and ^{1}H NMR Spectroscopy Studies

To probe into the HSO_3F-$S_2O_6F_2$ interaction discussed above, solutions of varying $HSO_3F/S_2O_6F_2$ molar ratios (0.1-4.5) were studied over a >100 K temperature range (198-318 K). In addition, solutions containing KSO_3F ("basic") were studied under similar conditions. The results will be discussed first for the acid phase ($-H_o$ > 11.8) and then for the dual acid/peroxide phase ($-H_o \leq 11.8$) systems.

3.C.3.a. Single Acid-Phase Systems

Both $S_2O_6F_2$ and HSO_3F yield sharp, single line resonances in the ^{19}F NMR spectra, which at 298 K occur at 39.03 and 40.74 ppm relative to $CFCl_3$, respectively. Both resonances show only very small temperature dependence over the temperature range studied. The $S_2O_6F_2$ line gradually shifts from 39.04 ppm at 318 K to 38.83 ppm at 198 K, while the ^{19}F resonance line of HSO_3F shifts from 40.77 to 40.61 ppm in the same temperature range. The peak separation between both lines remains reasonably constant at 1.72 ± 0.04 ppm over the entire range.

The ^{1}H resonance of HSO_3F also shifts very gradually from 10.47 ppm relative to TMS at 298 K to 10.67 ppm at 198 K. Satellite resonances due to ^{33}S and ^{34}S isotopes have been observed in the ^{19}F NMR for both HSO_3F and $S_2O_6F_2$,[35,36] but the low natural abundance (0.76% for ^{33}S and 4.22% for ^{34}S) and ^{19}F-^{33}S coupling result in very weak signals,[37-39] which will be of no consequence in this study.

It therefore appears that in the anticipated absence of spin-spin interactions (^{19}F-^{1}H), only single lines are expected and any evidence for solvent-solute interaction will have to come from two sources: (i) chemical shifts, ^{19}F and ^{1}H, relative to their positions in pure HSO_3F and $S_2O_6F_2$ and (ii) the integration of peak areas of the ^{19}F resonances obtained from mixtures of known composition. Of these two, chemical shift information obtained on a 300 MHz instrument should be more accurate and reliable than peak area integration. However, the latter technique is useful for the detection of SO_3F^- group exchange between solvent and solute.

From previous studies on the KSO_3F-HSO_3F system,[40] it is expected that increased SO_3F^- concentration, due to the solute's basic behaviour, will cause a small,

concentration dependent upfield shift of the ^{19}F solvent resonance line. Such a shift is indeed noticed at 298 and 318 K for mixtures of HSO_3F and $S_2O_6F_2$ of various molar ratios, as seen in Table 3.II. The solute resonance, on the other hand, shifts gradually downfield but the magnitude of this shift decreases with decreasing temperature. Below 298 K the ^{19}F resonance due to HSO_3F begins to move downfield as well, and at 198 K the initial peak separation is nearly restored. A downfield shift of the ^{19}F resonances, indicative of reduced shielding, is expected for protonated bis(fluorosulfuryl) peroxide, $HS_2O_6F_2^+$, as well as for its hydrogen bridged solvate, formulated tentatively as $S_2O_6F_2 \cdot HSO_3F$.

The observations made for various mole ratios and temperatures, summarized in Table 3.II, may be expressed in terms of two simple processes, *solvate formation* and subsequent *ionic dissociation of the solvate* according to the overall reaction scheme:

$$S_2O_6F_2 + HSO_3F \rightleftharpoons S_2O_6F_2 \cdot HSO_3F \rightleftharpoons S_2O_6F_2H^+_{(solv)} + SO_3F^-_{(solv)} \quad (3\text{-}3)$$

It appears that ionic dissociation is reduced in favour of solvate formation at lower temperatures. Consistent with this view is a noticeable upfield shift of the ^1H resonance by about 0.5 to 0.6 ppm which is best observed at 218 and 198 K for solutions with HSO_3F in excess.

The overall process (3-3) involving hydrogen bonding and proton transfer from HSO_3F to $S_2O_6F_2$ is not the only exchange process in the system, however. The peak area integrations summarized in Table 3.II indicate that the "acid" ^{19}F resonance is increased at the expense of the signal attributed to $S_2O_6F_2$ over the whole temperature range (318 to 198 K), with no pronounced temperature dependency recognizable. It appears that fluorosulfate exchange involving the acid, its self-ionization ions

Table 3.II. Summary of ^{19}F and ^{1}H NMR Data for $S_2O_6F_2$-HSO_3F Solutions

Temperature (Kelvin)	Molar Ratio (H/OX)[a]	I/S[b]	Δ ^{19}F $S_2O_6F_2$ (ppm) A[c]	Δ ^{19}F HSO_3F (ppm) B[c]	B-A (ppm)	Δ ^{1}H HSO_3F (ppm)[c]
318	4.44	1.33	+0.31	-0.20	-0.51	-
298		1.34	+0.24	-0.16	-0.40	0
253		1.32	+0.19	+0.05	-0.14	+0.01
218		1.34	+0.18	+0.12	-0.06	-0.52
198		1.30	+0.18	+0.12	-0.06	-0.41
318	1.86	1.40	+0.32	-0.15	-0.47	-
298		-	-	-	-	-0.09
253		-	-	-	-	-0.09
218		-	-	-	-	-0.61
198		1.26	+0.10	+0.06	-0.04	-0.57
318	0.96	1.44	+0.31	-0.12	-0.43	-
298		1.39	+0.13	-0.14	-0.27	-
253		1.46	+0.05	0	-0.05	-
198		1.28	+0.11	+0.12	+0.01	-
298	0.078	0.95	-0.06	-0.07	-0.01	-0.65
198		0.89	0	+0.06	+0.06	-0.09

[a] H = HSO_3F, OX = $S_2O_6F_2$

[b] I = Integration peak area H/OX ratio, S = H/OX fluorine content ratio from stoichiometry

[c] difference between signal position of pure species and that found in solution

$H_2SO_3F^+$ and more so SO_3F^-, the solute ion $S_2O_6F_2H^+$ and the solvate, formulated as $S_2O_6F_2 \cdot HSO_3F$, occurs in addition to proton exchange. As seen from the tabulated integration ratios, SO_3F^- exchange is consistently observed, apparently independent of temperature and molar ratio of solute to solvent, and involves about 10 to 20 % of the $S_2O_6F_2$ present in the mixture, increasing slightly with temperature and/or molar ratio of acid to peroxide.

Addition of KSO_3F to the HSO_3F-$S_2O_6F_2$ mixture does not have a dramatic effect on either proton or SO_3F exchange at concentrations of less than 1.8 M. The ^1H and ^{19}F NMR data for the various *basic* solutions studied are summarized in Table 3.III. Both the ^1H and ^{19}F NMR shifts have been corrected for the downfield and upfield chemical shift effect on the solvent resonance, respectively, caused by KSO_3F.[40] The only significant remaining effect is seen in the ^1H NMR spectra, where the single proton resonance already tends to be shifted upfield of the pure HSO_3F signal at ambient temperature, indicative of additional hydrogen-bridging between the acid and peroxide according to Equation (3-3) . This is consistent with an expected shift of this equilibrium further to the left upon addition of the basic SO_3F^- species. The slight effect on the ^{19}F NMR resonances is exhibited in Figures 3.3 and 3.4, where the observed relative chemical shifts and measured integrated peak areas for chosen "basic" solutions are compared to a typical "neutral" solution. Solutions with similar H/OX ratios were purposely chosen, since there is a slight dependence in the trends observed on this value (see Tables 3.II and 3.III). The relative chemical shifts of unmixed HSO_3F and $S_2O_6F_2$ are also shown in Figure 3.3. When the concentration of KSO_3F is raised beyond 1.8 M, a dual phase system results, as discussed earlier, and the ^{19}F NMR spectrum becomes more complicated.

Table 3.III. Summary of ^{19}F and ^{1}H NMR Data for KSO_3F-$S_2O_6F_2$-HSO_3F Solutions

Sample[a]	Temp. (K)	[KSO_3F] (mol/L)	Molar Ratio (H/OX)[b]	I/S[c]	Δ ^{19}F $S_2O_6F_2$ (ppm) A[d]	Δ ^{19}F HSO_3F (ppm) B[d]	B-A (ppm)	Δ ^{1}H HSO_3F (ppm)[d]
2P	298	3.21	1.82	4.38	+0.22	-0.29	-0.51	-0.37
	198			2.67	0	-0.11	-0.11	-0.41
2P	298	3.14	1.72	2.24	+0.37	-0.22	-0.59	-
	253			1.21	+0.20	-0.16	-0.36	-
	198			0.87	+0.05	-0.12	-0.17	-
2P	298	~2.0	0.170	0.19	-0.04	-0.09	-0.05	-
	198			0.12	+0.05	+0.12	+0.07	-
1P	298	2.43	2.22	1.89	+0.40	-0.05	-0.45	-
	198			1.85	+0.82	+0.52	-0.30	-
1P	298	1.47	2.22	1.42	+0.13	-0.21	-0.34	-
	198			1.08	+0.10	+0.03	-0.07	-
1P	298	0.86	1.68	1.32	+0.24	-0.14	-0.38	-
	253			1.28	+0.14	-0.03	-0.17	-
	198			1.11	+0.16	+0.01	-0.15	-
1P	298	0.45	1.70	1.26	+0.18	-0.16	-0.34	-
	253			1.19	+0.06	-0.04	-0.10	-
	198			1.11	+0.10	+0.05	-0.05	-

[a]1P = single phase, 2P = dual phase; [b]H = HSO_3F, OX = $S_2O_6F_2$
[c]I = Integration peak area H/OX ratio, S = H/OX fluorine content ratio from stoichiometry
[d]difference between signal position of pure species and that found in solution

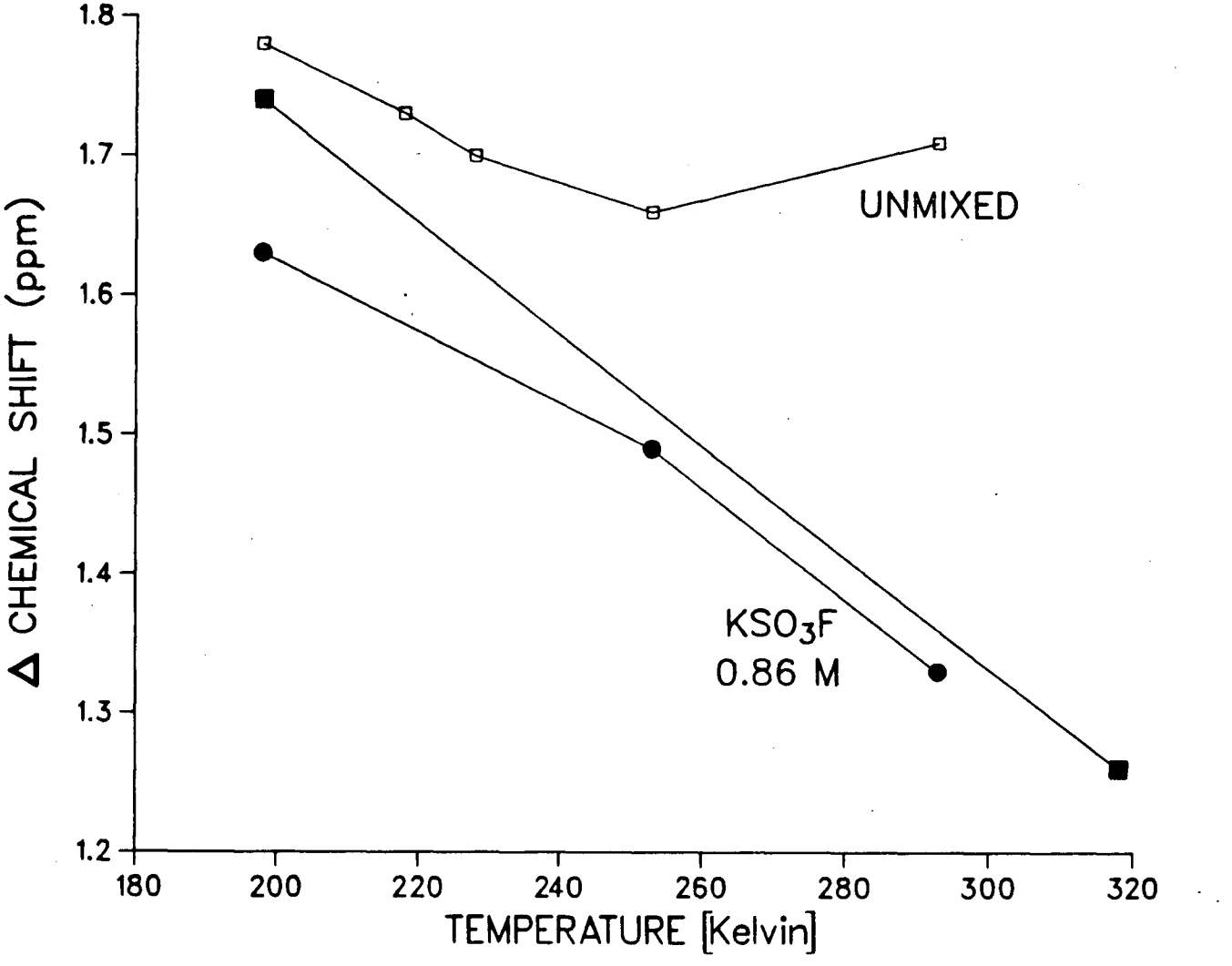

Figure 3.3. Temperature Dependence of the Separation Between HSO_3F and $S_2O_6F_2$ ^{19}F NMR Signals (■: "neutral", H/OX molar ratio = 1.86; ●: "basic", H/OX molar ratio = 1.68)

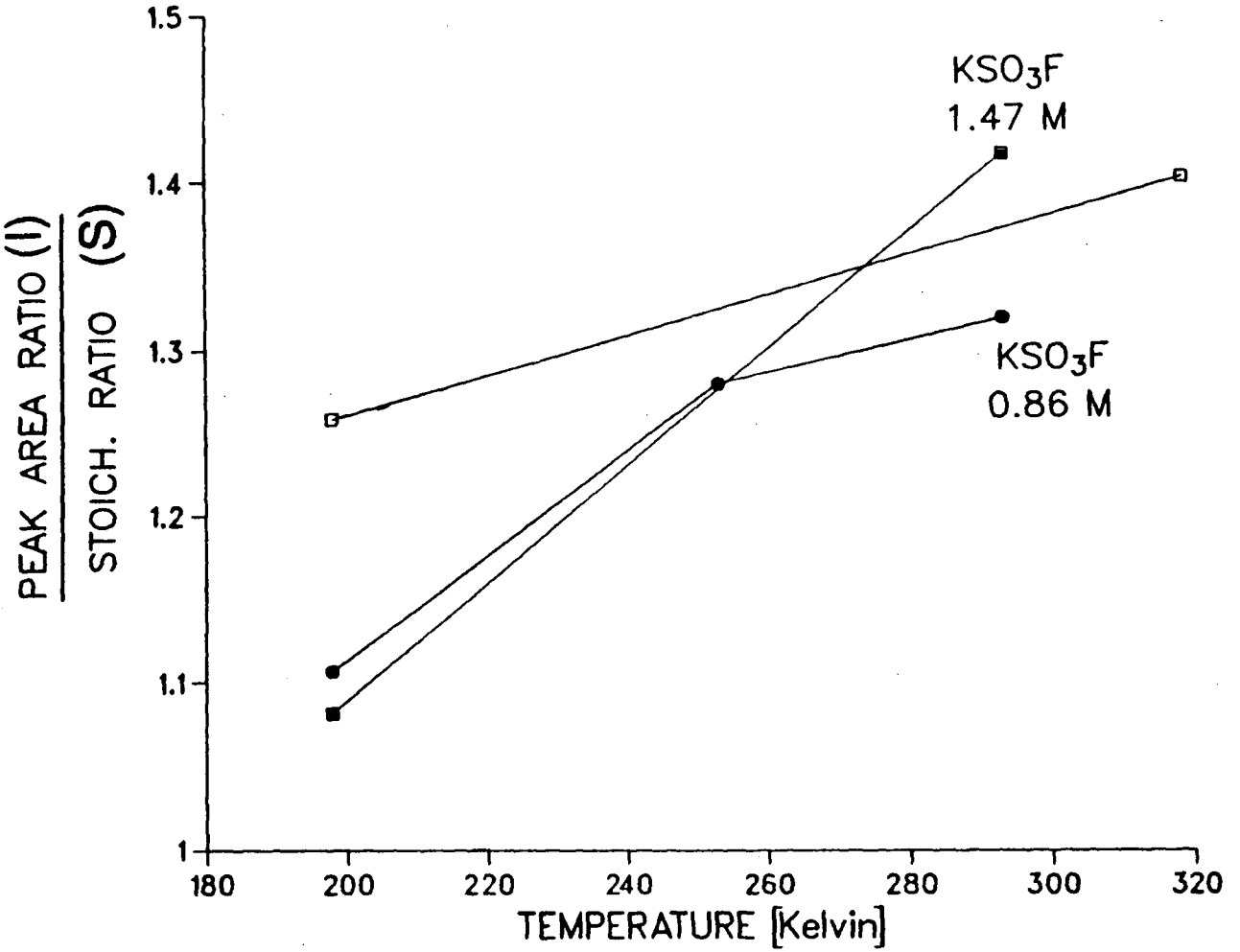

Figure 3.4. Temperature Dependence of $HSO_3F/S_2O_6F_2$ ^{19}F NMR Integration Peak Area Ratio Relative to the Stoichiometric Fluorine Content Ratio (□: "neutral", H/OX molar ratio = 1.86; ■: "basic", H/OX molar ratio = 2.22; ●: "basic", H/OX molar ratio = 1.68)

3.C.3.b. Dual Phase Systems

Figure 3.5 shows the ^{19}F NMR spectrum of a typical two phase system, with a KSO_3F concentration of 3.14 M, and a molar H/OX ratio of 1.72. As the temperature is lowered from 298 to 198 K, peak **A** gets less intense and eventually completely vanishes, while peak **B** increases in intensity. The intense, unlabelled peak at ~40 ppm is due to HSO_3F while the two resonances labelled **A´** and **B´** at ~47 ppm are assigned to $S_2O_5F_2$, present as an impurity. Resonances **A** and **A´** are attributed to $S_2O_6F_2$ and $S_2O_5F_2$, respectively, dissolved in HSO_3F, while **B** and **B´** resonances are again due to the same respective species found in the upper phase. As the temperature is lowered, the solubility of both $S_2O_6F_2$ and $S_2O_5F_2$ in HSO_3F decreases while the upper phase increases in volume.

Peak **B** and the downfield **B´** resonance are both distorted *triplets*, indicative of comparable perturbation affecting both the $S_2O_6F_2$ and $S_2O_5F_2$ resonances. Similar triplets are observed in all solutions studied with KSO_3F concentrations greater than about 3 M. Unequal spacings and relative intensities within the triplet pattern argue against any coupling as the cause. Therefore, the most likely cause of the triplet patterns is hydrogen bridging from the HSO_3F dissolved in the upper phase to both $S_2O_6F_2$ and $S_2O_5F_2$. *A possible* bridging conformation is shown in Figure 3.5-inset for $HSO_3F{\bullet}S_2O_6F_2$, where the acid proton is involved in a hydrogen bridge to one of the S=O bonds of $S_2O_6F_2$, creating different environments for each of the three fluorine atoms present. The most intense middle peak of the triplet is assigned to $\mathbf{F_2}$ in Figure 3.5-inset, since its chemical shift is within ± 0.05 ppm of the free $S_2O_6F_2$ resonance. Accordingly, the presence of free, unsolvated $S_2O_6F_2$ in the upper phase would contribute to this middle peak, accounting for its greater relative intensity, seen especially at 198 K. A similar interpretation applies for the $S_2O_5F_2$ resonance **B´**.

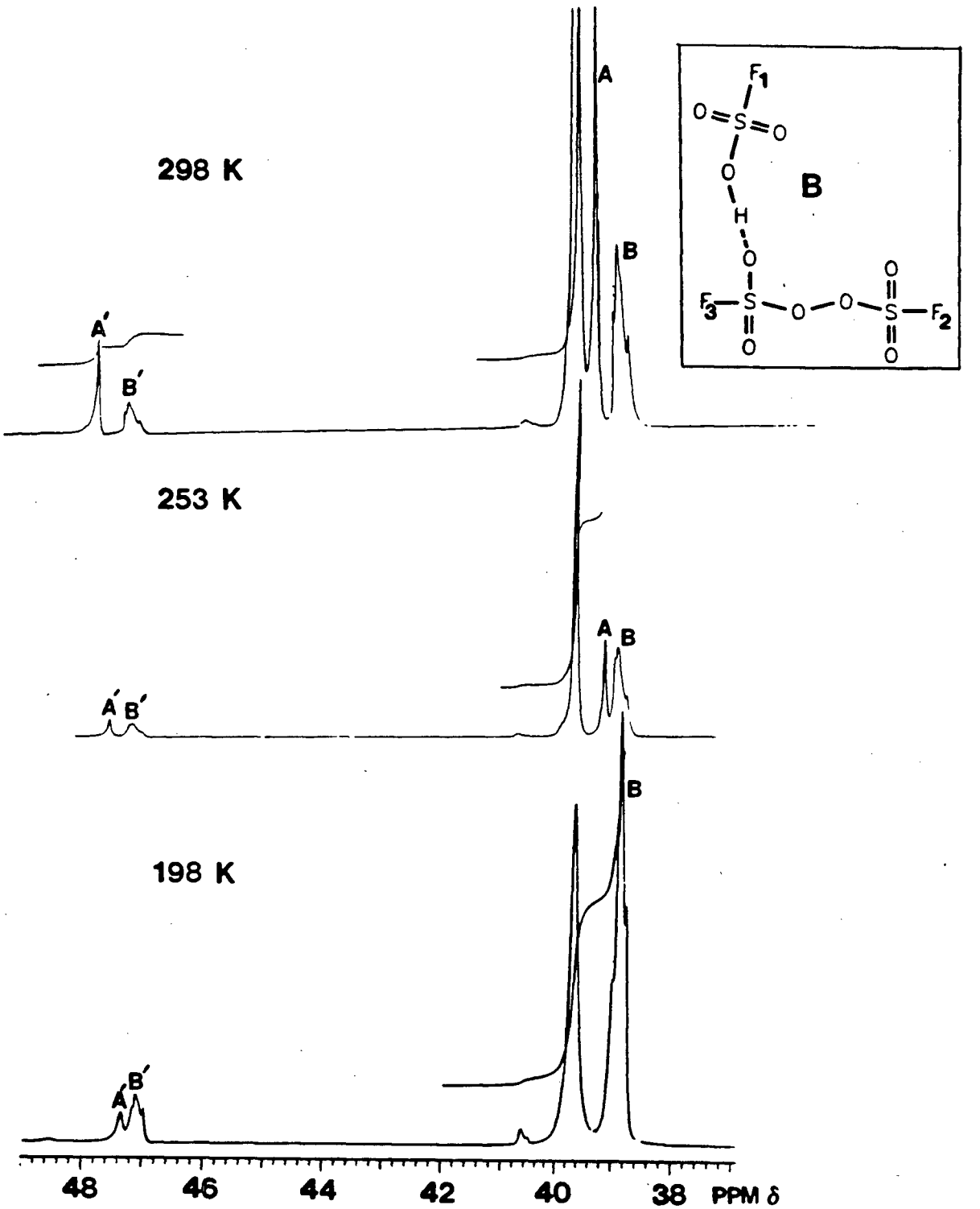

Figure 3.5. ^{19}F NMR Spectra of 2-Phase KSO_3F-$S_2O_6F_2$-HSO_3F Solution ([KSO_3F] = 3.14 M, H/OX molar ratio = 1.72)

The last feature of interest in Figure 3.5 is the very small peak at ~40.6 ppm, whose intensity increases with decreasing temperature. The HSO_3F resonance which usually occurs at this chemical shift is being shifted upfield by dissolved KSO_3F[35] in the *lower* acid phase. Consequently, the most likely assignment for this resonance is small amounts of HSO_3F, possibly present as dimers (as suggested by Savoi and Giguère[18]) in the *upper* peroxide phase. This in turn suggests that KSO_3F is insoluble in $S_2O_6F_2$. The ^1H and ^{19}F NMR data of various two phase solutions are summarized in Table 3.III.

The structure observed for both $S_2O_6F_2$ and $S_2O_5F_2$ resonances in the upper phase also implies the absence of exchange or ionization processes and the presence of well defined solvates at low temperatures with both sulfur(VI) oxyfluorides acting as proton acceptors. In the acid phase, with solvent and solute roles reversed, only single, reasonably sharp signals **A** and **A´** are seen (see Figure 3.5), permitting no deductions to be made regarding the structure of the solvates in the strongly ionizing medium. The mechanism of SO_3F exchange between HSO_3F and $S_2O_6F_2$, reflected in the peak area integrations for both, remains unclear, and the question arises whether cleavage of the O-O bond may be facilitated in the solvate, resulting in the formation of radicals like $SO_3F^{\cdot}_{(solv)}$ and their subsequent recombination. The NMR spectra discussed have provided no evidence for the presence of radicals in concentrations high enough to affect peak positions, with respect to previous reports,[41] or to cause line broadening, as has been observed in liquid $S_2O_6F_2$ at elevated temperatures.[42] The probability of finding radicals in HSO_3F solutions at lower concentrations should therefore be increased by using ESR. These results are discussed in the subsequent section.

3.C.4. ESR Spectroscopy Study of the Solvated Fluorosulfate Radical

The reversible dissociation of bis(fluorosulfuryl) peroxide into radicals according to:

$$S_2O_6F_2 \rightleftharpoons 2\ SO_3F^{\cdot} \qquad (3\text{-}4)$$

has previously been studied by ESR with the radical $SO_3F^{\cdot}$ observed in the liquid,[15] gaseous[43] and solid[42,44] state. In addition, the radical has been studied in a solid $CFCl_3$ matrix at 77 K and generated by photolysis of fluorine fluorosulfate, $FOSO_2F$.[44] All reports agree on a g-value of close to 2.011, with hyperfine splitting observed in the solid state.[42] In the liquid phase, a single, structureless component with a *temperature dependent* linewidth of ~25 G at 290 K is observed. Slightly broader linewidths are reported for the gas phase spectrum of the radical.[43]

Our own observations for liquid $S_2O_6F_2$ at 293 K differ only slightly and probably not significantly from the previous reports, considering differences in computational analyses and magnetic field calibrations of the spectra.[45] A slightly higher g-value of 2.0207 ± 0.0005 is obtained, but the band shape of $\Delta H_{pp} \approx 26$ G is similar to previous reports.[15]

When $S_2O_6F_2$ is dissolved in HSO_3F, a single, inhomogeneously broadened line is observed, which shows very little change in linewidth and g-value between 283 and 323 K, with g_{iso} having a value of 1.9693 at 322 K. The signal persists when the temperature is gradually lowered and the spectrum obtained at 183 K is shown in Figure 3.6. As can be seen, g is clearly anisotropic with g_{iso} found to be 1.97267. Hyperfine splitting is not observed.

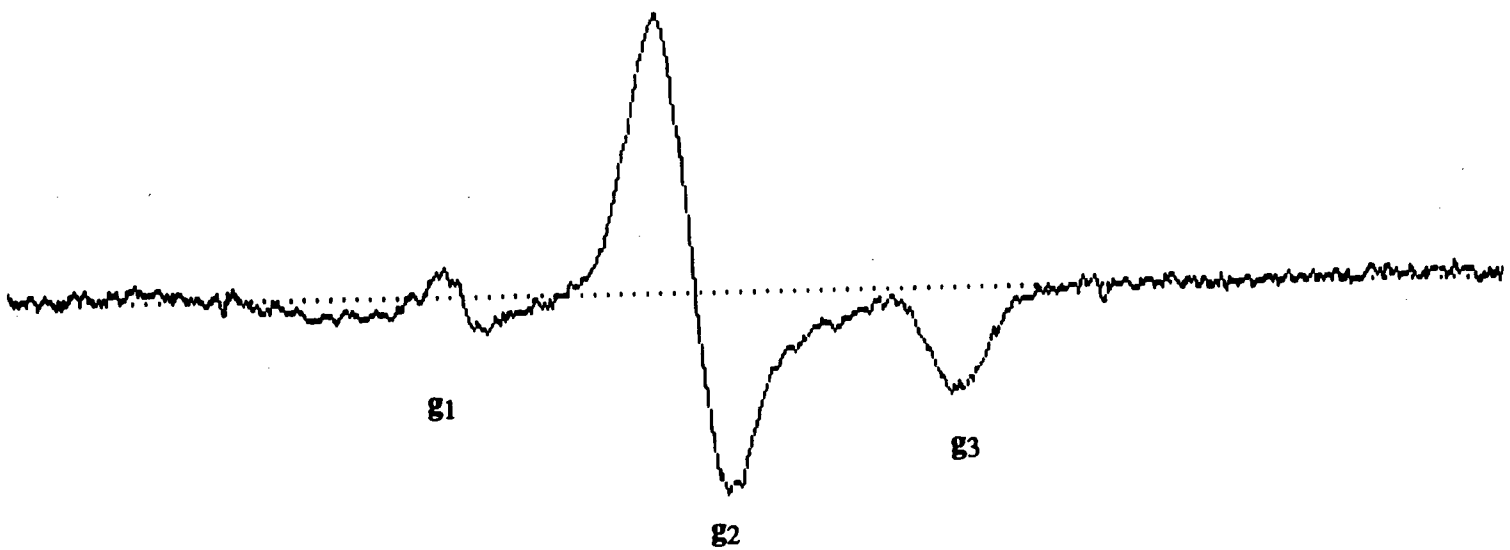

$g_1 = 1.99310$

$g_2 = 1.97264$

$g_3 = 1.95227$

$g_{iso} = 1.97267$

Figure 3.6. ESR Spectrum of $S_2O_6F_2$ in HSO_3F (1:2.12 solution by volume) at 183 K

The radical observed in solution is clearly not identical with $SO_3F^{\cdot}$ as reported previously[15,42-44] or observed by us in liquid $S_2O_6F_2$. Consistent with the observance of three g-values (see Fig. 3.6), it can be concluded that the symmetry of the radical in HSO_3F solution is below C_{2v}. On the other hand, $SO_3F^{\cdot}$ has C_{3v} symmetry for both the electronic ground state ($^2A_2$) and the nearest excited state (^2E), according to the vibrational analysis of the electronic spectrum[46] or to its vibrational spectrum studied in an inert gas matrix.[47] Conversion of $SO_3F^{\cdot}$ to other radicals such as $FSO_2^{\cdot}$ in solution (via a reduction) is rather unlikely because this species is short lived and highly reactive, while the radical encountered here is persistent. Furthermore, $FSO_2^{\cdot}$ reportedly[44] has a g-value of 2.005. It is more likely that the fluorosulfate radical, just like SO_3F^-[34] and to a lesser extent its dimer $S_2O_6F_2$ as discussed in the previous section, will form a solvate with HSO_3F which may subsequently undergo a temperature dependent ionic dissociation, as follows:

$$SO_3F^{\cdot} + HSO_3F \rightleftharpoons [FSO_3 \cdot HSO_3F]^{\cdot} \rightleftharpoons [HSO_3F^+]^{\cdot} + SO_3F^- \qquad (3\text{-}5)$$

For both the solvated or protonated radical, the overall symmetry would be expected to be very low, whether protonation and hydrogen bridging involve oxygen, the more basic site, or fluorine on the $SO_3F^{\cdot}$ radical. Hence, three g-values were observed. However, the actual solution environment around the radical is expected to be more complex than has been depicted in the first-order approximation shown above. In addition to the previously postulated radical displacement reaction in liquid $S_2O_6F_2$[15] according to:

$$SO_3F^{\cdot} + S_2O_6F_2 \rightleftharpoons S_2O_6F_2 + SO_3F^{\cdot} \qquad (3\text{-}6)$$

a similar displacement with HSO_3F:

$$SO_3F^{\cdot} + HSO_3F \rightleftharpoons [FSO_3 \cdot HSO_3F]^{\cdot} \rightleftharpoons HSO_3F + SO_3F^{\cdot} \qquad (3\text{-}7)$$

could compete effectively with the recombination reaction to again give $S_2O_6F_2$ and account for its persistence shown to 183 K, a temperature close to the melting point of HSO_3F. In addition, a radical mediated SO_3F group exchange involving $S_2O_6F_2$ and HSO_3F could well explain observations made in the preceding NMR section concerning peak area integrations. However, in view of the anticipated low radical concentration, alternate exchange pathways may also be involved.

Finally, $SO_3F^{\cdot}$ radical migration via Equilibria (3-6) and (3-7) together with SO_3F^- migration involving the proton transfer account for the fast and efficient metal oxidation performed in $HSO_3F/S_2O_6F_2$.[1-9] Hence, postulated hydrogen bridging to and protonation of the $SO_3F^{\cdot}$ radical does not only explain the observed ESR spectrum, but also the radical's persistence in HSO_3F and its reactivity in this medium.

The proposed interaction of $SO_3F^{\cdot}$ with HSO_3F is reversible, which accounts for the fact that both the solvent, HSO_3F, and the solute, $S_2O_6F_2$, can be separated quantitatively by distillation.[32] Therefore, irreversible degradation of the $SO_3F^{\cdot}$ radical to $FSO_2^{\cdot}$, for example, or into other radical fragments is rather unlikely.

3.D. Summary and Conclusions

The principal solute $S_2O_6F_2$ and its monomeric radical $SO_3F^{\cdot}$ behave as very weak bases in HSO_3F. All manifestations of the acid-base interaction are rather subtle with the possible exception of the ESR spectrum of solvated $SO_3F^{\cdot}$, where a change in symmetry and electronic structure is apparent. Ironically, two principal conclusions

reached in an earlier study of the HSO_3F-$S_2O_6F_2$ system,[14] that $S_2O_6F_2$ is a non-electrolyte and is present in undissociated form in HSO_3F, are found to be not entirely valid. However, the solvated radical, which is detectable at the freezing point of HSO_3F, appears to be present in an extremely low concentration, and would not interfere when $S_2O_6F_2$ is used to determine the cryoscopic constant of HSO_3F.[14]

The spectroscopic techniques of Raman, ^1H and ^{19}F NMR, and ESR used in this study show increasing usefulness (in the listed order) in studying the two very weak bases. The solubility loss found for $S_2O_6F_2$ in HSO_3F-KSO_3F is very helpful in two respects: (i) it reveals the key role that acidity or proton donor strength plays in the weak acid-base interaction and (ii) it leads to the study of $S_2O_6F_2$ and HSO_3F in reversed roles, with $S_2O_6F_2$ now the solvent, using ^{19}F and ^1H NMR spectroscopy.

The formulation of monosolvated $S_2O_6F_2$ and $SO_3F^{\cdot}$ is chosen because such hydrogen-bridged solvates are known[33] for the related SO_3F^- ion and in the case of $Cs[SO_3F{\bullet}HSO_3F]$, have been structurally characterized. Solvation of the $SO_3F^{\cdot}$ radical is seen to increase the lifetime and mobility of this species in HSO_3F and in turn contributes to the synthetic usefulness of the HSO_3F-$S_2O_6F_2$ system, which has been demonstrated in the past.[1-9] In agreement with the Raman spectra, there is no evidence for a weakening of the O-O bond and the consequently more facile formation of radicals in HSO_3F. There is evidence, however, for a longer radical lifetime at low temperatures due to solvate formation. Further applications will be discussed in upcoming chapters.

REFERENCES

1. K.C. Lee and F. Aubke, *Inorg. Chem.* **18**, 389 (1979).
2. K.C. Lee and F. Aubke, *Inorg. Chem.* **23**, 2124 (1984).
3. S.P. Mallela, K.C. Lee and F. Aubke, *Inorg. Chem.* **23**, 653 (1984).
4. P.C. Leung and F. Aubke, *Can. J. Chem.* **62**, 2892 (1984).
5. S.P. Mallela and F. Aubke, *Inorg. Chem.* **24**, 2969 (1984).
6. K.C. Lee and F. Aubke, *J. Fluor. Chem.* **19**, 501 (1982).
7. K.C. Lee and F. Aubke, *Can. J. Chem.* **55**, 2473 (1977).
8. K.C. Lee and F. Aubke, *Can. J. Chem.* **57**, 2058 (1979).
9. M.S.R. Cader, S. Karunanithy and F. Aubke, *Synth. Metals* **30**, 9 (1989).
10. F.B. Dudley and G.H. Cady, *J. Am. Chem. Soc.* **79**, 513 (1957).
11. F.B. Dudley and G.H. Cady, *J. Am. Chem. Soc.* **85**, 3375 (1963).
12. J.M. Shreeve and G.H. Cady, *Inorg. Syn.* **7**, 124 (1963).
13. F. Aubke, unpublished observation.
14. R.J. Gillespie, J.B. Milne and R.C. Thompson, *Inorg. Chem.* **5**, 468 (1966).
15. P.M. Nutkowitz and G. Vincow, *J. Am. Chem. Soc.* **91**, 5956 (1969).
16. A.M. Qureshi, L.E. Levchuk and F. Aubke, *Can. J. Chem.* **49**, 2544 (1971).
17. G.A. Olah, A. Commeyras, *J. Am. Chem. Soc.* **91**, 2929 (1969).
18. R. Savoi and P.A. Giguère, *Can. J. Chem.* **42**, 277 (1964).
19. J. Barr, R.J. Gillespie and R.C. Thompson, *Inorg. Chem.* **3**, 1149 (1964).
20. R.J. Gillespie and E.A. Robinson, *Can. J. Chem.* **39**, 2179 (1961).
21. R.J. Gillespie and E.A. Robinson, *Can. J. Chem* **40**, 644 (1962).
22. R.J. Gillespie and T.E. Peel, *J. Am. Chem. Soc.* **95**, 5173 (1973).

23. R.J. Gillespie, T.E. Peel and E.A. Robinson, *J. Am. Chem. Soc.* **93**, 5083 (1971).

24. C.R. Johnson, A.R. Katvitzki and S.A. Shapiro, *J. Am. Chem. Soc.* **91**, 6654 (1969).

25. T.C. Waddington, *"Non-Aqueous Solvents"*, Appleton-Century-Crofts, N.Y., 1969.

26a. R.J. Gillespie and J. Liang, *J. Am. Chem. Soc.* **110**, 6053 (1988).
b. T.A. O'Donnell, *J. Fluor. Chem.* **25**, 75 (1984).

27. G.A. Olah, G.K.S. Prakash and J. Sommer, *"Superacids"*, J. Wiley & Sons, N.Y., 1985 (and references herein).

28. J.R. Dalziel and F. Aubke, *Inorg. Chem.* **12**, 2707 (1973).

29. S.P. Mallela, J.R. Sams and F. Aubke, *Can. J. Chem.* **63**, 3305 (1985).

30. M.F.A. Dove and A.F. Clifford, in *"Chemistry in Non-Aqueous Ionizing Solvents"*, Vol.2.I, J.Jander, H. Spandau and C.C. Addison, Eds., Vienweg, Braunschweig, 1971.

31. R.C. Thompson, in *"Inorganic Sulphur Chemistry"*, G. Nickless, Ed., Elsevier, Amsterdam, 1968.

32. G.H. Cady, *Adv. Inorg. Chem. Radiochem.* **2**, 105 (1960).

33. C. Josson, M. Deporcq-Stratmains and P.Vast, *Bull. Soc. Chim. Fr.*, **9-10**, 820 (1977).

34. C. Belin, M Charbonnel and J. Potier, *J. Chem. Soc., Chem. Commun.* 1036 (1981).

35. R.J. Gillespie and J.W. Quail, *J. Chem. Phys.* **39**, 2555 (1963).

36. R.A. Stewart, S. Fujiwara and F. Aubke, *ibid.* **49**, 965 (1968).

37. D. Rehder, in *"Multinuclear NMR"*, J. Mason, Ed., Plenum Press, N.Y., 1988.

38. *"NMR and the Periodic Table"*, R.K. Harris and B.E. Mann, Eds., Academic Press, London, 1978.

39. *"Handbook of Chemistry and Physics"*, 57th Edition, R.C. Weast, Ed., C.R.C. Press, U.S.A., 1976-1977.

40. A.M. Qureshi, H.A. Carter and F. Aubke, *Can. J. Chem.* **49**, 35 (1971).

41. F.A. Hohorst and J.M. Shreeve, *Inorg. Chem.* **5**, 2069 (1964).

42. R.A. Stewart, *J. Chem. Phys.* **51**, 3406 (1969).

43. R.A. Stewart, S. Fujiwara and F. Aubke, *ibid.* **48**, 5524 (1968).

44. F. Neumayr and N. Vanderkooi, Jr., *Inorg. Chem.* **4**, 1234 (1965).

45. P.S. Phillips and F. G. Herring, *J. Magn. Reson.* **57**, 43 (1984).

46. G.W. King and C.H. Warren, *J. Mol. Spect.* **32**, 121 (1969).

47. E.M. Suzuki, J.W. Nibler, K.A. Oakes and D. Eggers, Jr., *ibid.* **58**, 201 (1975).

48. R.J. Gillespie and J.B. Milne, *Inorg. Chem.* **5**, 1236 (1966).

49. R.J. Gillespie, R. Ouchi and G.P. Pez, *Inorg. Chem.* **8**, 63 (1969).

50. H. Siebert, *Z. Anorg. U. Allgem. Chem.* **289**, 15 (1957).

CHAPTER 4

FLUOROSULFATE DERIVATIVES OF NIOBIUM(V)

4.A. Introduction

Niobium predominantly exhibits the oxidation states +2 to +5 among its known compounds. Furthermore, only tri-, tetra- and pentavalent halides or oxyhalides are known to exist. Reports of redox chemistry are very uncommon and the pentahalides of this metal are difficult to reduce.[1-3]

Structural data have been reported for a number of pentavalent niobium halides and oxyhalides,[2] including NbF_5.[4] This hygroscopic, tetrameric (distorted octahedral coordination to Nb via cis-fluorine bridges), volatile white solid (see listing of general properties in Table 1.I) is prepared by the reaction of fluorine gas with either the metal or with the pentachloride at elevated temperature.[1,3] NbF_5 has found use as the Lewis acid in HF, HSO_3F or HSO_3CF_3 superacid systems.[5] Whereas the resistance of NbF_5 to reduction[1] has been a clear advantage, its limited solubility in all three protonic solvents has severely limited its use as a Lewis acid.

The ability of NbF_5 to behave as an acceptor has been demonstrated using ^{19}F NMR spectroscopy. The $[NbF_6]^-$ ion is observed in > 30 mole % aqueous HF solutions and may be formed by dissolution of NbF_5 or Nb_2O_5. The $[NbF_7]^{2-}$ ion was detected only when the HF_{aq} concentration was increased beyond 95 mole %.[6] In addition, a number of alkali metal salts of the type $M^I_3NbF_8$, $M^I_2NbF_7$, M^INbF_6 (with M^I = Na, K or NH_4) as well as $(CH_3)Sn(NbF_6)_2$[7] have been obtained by reaction of stoichiometric amounts of NbF_5 and the respective M^IF salt in aqueous HF.[2] The formation of the

anions $[NbF_7]^{2-}$ and $[NbF_8]^{3-}$ species serves as good illustration of niobium's ability to expand its coordination sphere beyond the "traditional" six coordination.[8] Fluoride ions in particular allow such an expansion, although the existence of $[NbCl_7]^{2-}$ has also been claimed.[9] With Br or I as the halogens, only monomeric, octahedral $[NbX_6]^-$ anions are known.[10]

The high acidity and solubility of the binary fluorosulfates $Au(SO_3F)_3$[15] and $Pt(SO_3F)_4$[11] in HSO_3F and the fluorosulfate ion acceptor ability of NbF_5 (in spite of its limited solubility) in this solvent[5] led to interest in the synthesis, characterization and use of the fluorosulfate $Nb(SO_3F)_5$. Previous attempts to prepare this species have been unsuccessful, but two fluorosulfate derivatives of Nb(V) have been reported: (i) the reaction of NbF_5 with excess SO_3[12] is said to yield a viscous liquid of the composition $NbF_5 \cdot 2.1SO_3$, which may be viewed as $NbF_3(SO_3F)_2$ with residual SO_3 present. Heating to 175 - 225 °C leads to decomposition of this material to $NbOF_3$ and $S_2O_5F_2$; (ii) the reaction of $NbCl_5$ with $S_2O_6F_2$ is claimed to yield a viscous, yellow liquid of the composition $NbO(SO_3F)_3$ at room temperature.[13] In both cases, neither spectroscopic nor structural information was reported and hence the presence of the SO_3F group was not clearly established.

Metal oxidation by bis(fluorosulfuryl) peroxide in HSO_3F has been used successfully to prepare binary fluorosulfates of a variety of metals (see Chapter 1). This method is simple, straightforward and should allow oxidation of niobium to the +5 state, and hopefully the isolation of $Nb(SO_3F)_5$. Furthermore, the preparation of salts containing the $[Nb(SO_3F)_{5+x}]^{x-}$ anion should be possible if the oxidation of Nb is carried out in the presence of fluorosulfate anions. The existence[2] of salts of the type $M^I_x[NbF_{5+x}]$, with x = 1 - 3, suggests that an analogous series of fluorosulfate salts may

be obtainable. Previously, metal oxidation has only yielded *binary* fluorosulfates where the oxidation state of the metal does not exceed +4. Wherever oxidation to a higher state occurred, either oxy- or fluoro-fluorosulfates were obtained instead.[12,13] It is difficult to predict which one of these mixed fluorosulfates will form, should $Nb(SO_3F)_5$ prove to be thermally labile. As mentioned in Chapter 1, the two principal decomposition modes of fluorosulfates leading to these types of materials involve formation of volatile SO_3 or $S_2O_5F_2$. Should the SO_3F group turn out to be very labile, even ternary fluorides or oxides are anticipated.

4.B. Experimental

4.B.1. In Situ Synthesis of Pentakis(fluorosulfato)niobium(V), $Nb(SO_3F)_5$

Typically, 236 mg (2.54 mmol) of niobium metal powder was treated with an approximate 7 ml mixture of $S_2O_6F_2$ and HSO_3F (2:1 by volume) and the mixture stirred at 25 °C for 2 days, by which time all the metal was consumed and a colorless solution was obtained. Excess $S_2O_6F_2$ was removed in vacuo at room temperature. Attempts at completely removing the acid in vacuo at room temperature led to product decomposition when the temperature was raised. The product did not precipitate, even when the volume of acid was reduced as far as possible (as judged by weight) with the temperature lowered to -10 °C.

4.B.2. In Vacuo Degradation of $Nb(SO_3F)_5$

In an attempt to remove all the HSO_3F from $Nb(SO_3F)_5$ solutions in vacuo at 25 °C, $Nb(SO_3F)_5$ decomposed, presumably via SO_3 elimination, to form species of the form $NbF_x(SO_3F)_{5-x}$, with x being primarily 2 or 3. This process was monitored by weight and periodically by analyzing for sulfur.

Analytical Data for $NbS_{5-x}O_{15-3x}F_x$:

S(%) Calculated x = 2	S(%) Calculated x = 3	S(%) Found (chronologically)
22.47	18.42	20.68
		18.50
		21.41
		21.50

4.B.3. Derivatives of $Nb(SO_3F)_5$

a) Cesium Hexakis(fluorosulfato)niobate(V)

Typically, 265 mg (2.85 mmol) of niobium metal powder was added to 661 mg (2.85 mmol) of $CsSO_3F$. To this mixture about 4 ml of $S_2O_6F_2$ and about 3 ml of HSO_3F were added in vacuo. The grey slurry was stirred for 2 days at room temperature, by which time all the metal was consumed and the slurry appeared white. The white powder was collected by vacuum filtration. Excess solvent and $S_2O_6F_2$ were removed and the product was dried in vacuo for 24 hours at room temperature (isolated yield 77%). The hygroscopic $Cs[Nb(SO_3F)_6]$ decomposed at 115-119 °C.

Analytical Data for $CsNbS_6O_{18}F_6$:

	Nb(%)	S(%)	F(%)
Calculated:	11.33	23.45	13.90
Found:	10.95	23.46	14.11
S:F = 1.0003			

b) Cesium Heptakis(fluorosulfato)niobate(V)

Typically, 227 mg (2.44 mmol) of niobium metal powder was added to 1.105 g (4.76 mmol) of $CsSO_3F$. 4 ml of $S_2O_6F_2$ and 3 ml of HSO_3F were then added in vacuo. The grey slurry was stirred at room temperature for 3 days, by which time all the metal was consumed and a thick, white slurry had formed. The reaction vessel was cooled to 0 °C for one hour and a fine white hygroscopic powder was collected by vacuum filtration. Excess solvent and $S_2O_6F_2$ were removed and the product was dried in vacuo for 24 hours at room temperature (70% isolated yield). $Cs_2[Nb(SO_3F)_7]$ melted at 78-82 °C .

This material was also prepared by an alternative method: On to 500 mg (1.85 mmol) of $NbCl_5$ and 620 mg (3.56 mmol) of CsCl was vacuum distilled exactly 1.67 ml (14.5 mmol) of $S_2O_6F_2$. The white paste was stirred at 25 °C for 4 hours, during which time the gases which vigorously evolved were periodically removed in vacuo. The reaction appeared to be completed shortly after the vigorous bubbling ceased, and the product was dried in vacuo overnight at 25 °C to ensure complete removal of all volatile by-products. Isolated yield of the white powder was 95%. Chloride tests were negative.

Analytical Data for $Cs_2NbS_7O_{21}F_7$:

	Nb(%)	S(%)	F(%)
Calculated:	8.83	21.33	12.64
Found:	9.05	21.46	12.85
S:F = 1.016			

c) Barium Heptakis(fluorosulfato)niobate(V)

727 mg (2.17 mmol) of $Ba(SO_3F)_2$ was added to 194 mg (2.09 mmol) of niobium metal powder to which was then vacuum distilled about 4 ml of $S_2O_6F_2$ and 3 ml of HSO_3F. The mixture was stirred at 25 °C for 2 days by which time all the metal was consumed and a white slurry appeared. A fine white powder was collected by vacuum filtration at room temperature. Excess solvent and $S_2O_6F_2$ were removed and the product was dried in vacuo for 1 day at room temperature. $Ba[Nb(SO_3F)_7]$ was isolated in 20% yield and decomposed at 130-135 °C.

Analytical Data for $BaNbS_7O_{21}F_7$:

	Ba(%)	Nb(%)	F(%)
Calculated:	14.87	10.06	14.40
Found:	14.65	9.93	14.60

Successful isolation of $Ba[Nb(SO_3F)_7]$ was only possible when the product mixture was filtered. Attempts to evaporate excess HSO_3F in vacuo resulted in evolution of volatiles and led to mixed products, suggesting partial decomposition.

4.B.4. Attempted Syntheses of Additional $Nb(SO_3F)_5$ Derivatives

a) Cesium Octakis(fluorosulfato)niobate(V)

Repeated preparation attempts using a synthetic route analogous to the above led to wax-like, colorless materials of uncertain composition.

Analytical Data for $Cs_3NbS_8O_{24}F_8$:

S(%): Calculated = 19.97, Found = 22.98

b) Lithium Hexakis(fluorosulfato)niobate(V)

Repeated preparations of $Li[Nb(SO_3F)_6]$ were attempted by the previously described pathway. A wax-like material of uncertain composition was obtained each time.

Analytical Data for $LiNbS_6O_{18}F_6$:

S(%): Calculated = 27.71, Found = 23.03

c) Lithium or Potassium Heptakis(fluorosulfato)niobate(V)

Using metal oxidation, very viscous, colorless oils were obtained with lithium, whereas paste-like materials were isolated with potassium as counter-cation. The materials crystallized near 0 °C, but appeared to be of mixed composition. They melted to very viscous oils upon warming to room temperature. Complete removal of the solvent HSO_3F was not possible, even upon extended periods in vacuo. Employing heat during the attempted solvent removal led to seemingly decomposed brown products.

4.B.5. Synthesis of Difluorotris(fluorosulfato)niobium(V), $NbF_2(SO_3F)_3$

Two related routes led to the isolation of this species, with one leading to a powder and the other to a crystalline product.

a) Crystalline $NbF_2(SO_3F)_3$

394 mg (4.24 mmol) of niobium metal powder was treated with 3.17 ml (27.6 mmol) of $S_2O_6F_2$ and 2.31 ml (39.8 mmol) of HSO_3F and allowed to react at 25 °C for 3 days, by which time all the metal was consumed and a colorless, slightly murky solution was obtained. Excess $S_2O_6F_2$ was removed in vacuo at 0 °C and the solution was stored in the drybox for two months, during which time a crystalline product precipitated from solution. The crystals were isolated by slowly removing the liquid first in vacuo at 0 °C and then by passing a stream of dry N_2 over the product for 4 days. The crystals were mounted in Lindemann tubes for an X-ray diffraction study, but were found to be of poor quality.

b) Finely-Powdered $NbF_2(SO_3F)_3$

1.289 g (13.87 mmol) of niobium metal powder was treated with about 9 ml of $S_2O_6F_2$ and 13 ml of HSO_3F and the mixture allowed to stir at 25 °C for 4 days, during which time the metal was completely consumed and a murky, colorless solution was obtained. Excess $S_2O_6F_2$ was removed in vacuo at -5 °C. A fine, white powder precipitated out of the resulting solution after sitting at room temperature for one day and was collected by vacuum filtration. The product was dried in vacuo at 25 °C overnight and was isolated in 15% yield. The white, hygroscopic $NbF_2(SO_3F)_3$ melted at 126-129 °C.

Analytical Data for $NbS_3O_9F_5$:

	Nb(%)	S(%)	F(%)
Calculated:	21.70	22.47	22.19
Found:	21.40	22.52	21.85

4.C. Results and Discussion

4.C.1. Synthesis and General Discussion

4.C.1.a. In Situ Synthesis of $Nb(SO_3F)_5$

A general synthetic route to binary metal fluorosulfates[11,14,15] which combines the oxidizing power of bis(fluorosulfuryl) peroxide, $S_2O_6F_2$, with the solvating ability of HSO_3F was applied to prepare the desired species. The reaction proceeded according to:

$$2\ Nb + 5\ S_2O_6F_2 \xrightarrow[2\ days,\ 25°C]{HSO_3F} 2\ Nb(SO_3F)_{5(solv)} \qquad (4\text{-}1)$$

yielding a clear, colorless solution. More concentrated solutions (≥1 M) were of a gel-like consistency, but unlike the synthesis of $Pt(SO_3F)_4$[11] or $Sn(SO_3F)_4$,[14] no precipitate formed. Excess $S_2O_6F_2$ was readily removed in vacuo at room temperature. The results of Chapter 3 suggested the need for using greater than a 1:1 $S_2O_6F_2/HSO_3F$ ratio by volume, to ensure the efficient oxidation of the metal; indeed reactions using a less than 1:1 ratio did not appear to proceed nearly as smoothly. 1.0 M solutions of the product undergo rapid fluorosulfate exchange between solute and solvent (single solvent/solute resonance in ^{19}F NMR spectra to be discussed in more detail later in Chapter 6) at temperatures as low as -55 °C, which is believed to be in part responsible for the species' high solubility.

Complete removal of the solvent HSO_3F in vacuo at room temperature failed owing to the solute's extremely high solubility. At +60 °C, partially decomposed materials of lower than expected weight formed. The presence of ν(Nb-F) bands (at ~700 cm^{-1})[16] in the IR spectrum and the sulfur analyses of the product at various stages of decomposition (see Section 4.B.3) suggested the general overall composition

$NbF_x(SO_3F)_{5-x}$, most likely due to SO_3 elimination. This decomposition pathway has previously been postulated for the very unstable $Sb(SO_3F)_5$ species,[17] and would be expected to reduce the steric crowding around the metal centers.

$Nb(SO_3F)_5$ solutions of greater than one molar concentration appeared to decompose, again with loss of SO_3, to form less soluble species of the type $NbF_2(SO_3F)_3$. Precipitation and characterization of solid $NbF_2(SO_3F)_3$ from a 1.1 M solution and solution NMR studies discussed later support this postulate. In summary, the evidence for $Nb(SO_3F)_5$ being formed in Reaction (4-1) is three-fold: (i) salts of the general composition $M'[Nb(SO_3F)_{5+x}]$, with x = 1 or 2 and M´ = Cs or Ba, have been isolated from the $Nb(SO_3F)_5$ solutions and are discussed in Section 4.C.1.c; (ii) to obtain materials of the average composition $NbF_2(SO_3F)_3$ from Nb and $S_2O_6F_2$, a precursor of the type $Nb(SO_3F)_5$ or at least $NbF(SO_3F)_4$ must form and (iii) $NbF_2(SO_3F)_3$ is a minor product obtained in low yield. This suggests that undissociated $Nb(SO_3F)_5$ exists in solution at very low concentrations, with ~1 M concentrations already appearing to be too high.

4.C.1.b. Alternative Attempts to Isolate $Nb(SO_3F)_5$

Four other synthetic routes were tried in an attempt to isolate $Nb(SO_3F)_5$:

(i) the reaction of NbF_5 with excess HSO_3F;

(ii) the reaction of $NbCl_5$ with excess HSO_3F;

(iii) the reaction of $NbCl_5$ with excess $S_2O_6F_2$, according to the previously reported unsuccessful attempts at making $Nb(SO_3F)_5$[13] and $Sb(SO_3F)_5$;[17]

(iv) the reaction of $Nb(SO_3F)_5/HSO_3F$ with CH_2Cl_2.

None of the above routes were successful, usually leading to a mix of unidentifiable species, in the -75 °C to +45 °C temperature range that was investigated.

The failure of pathway (i) was not very surprising since NbF_5 appears to be inert enough to resist solvolysis by HSO_3F even at elevated temperature.[1,2] Route (ii) led to the formation of chlorine-containing products, as judged by the yellow/orange color of the viscous oil that was isolated and by positive chloride tests. The chlorine-containing solids could not be separated from more desirable products that may have formed. Reaction (iii) led to similar but somewhat more interesting results. Invariably, a viscous yellow/orange oil was also isolated. In addition, the volatiles that were pumped off and collected with the excess $S_2O_6F_2$ were deep red in color. Very similar observations were previously reported during the reaction of $SbCl_5$ with excess $S_2O_6F_2$.[17] The viscous oil was attributed to a mix of species of the type $[SbF_x(SO_3F)_{6-x}]^-$, whereas the red volatile liquid was judged to be chloryl fluorosulfate,[18,19] ClO_2SO_3F, or its complex with the above series of anions. The formation of these chlorine-oxygen derivatives is thought to result from the reaction of the excess $S_2O_6F_2$ with the evolved chlorine:

$$5\ S_2O_6F_2 + Cl_2 \longrightarrow 2\ ClO_2SO_3F + 4\ S_2O_5F_2 \qquad (4\text{-}2)$$

The ClO_2SO_3F salt thus formed can in turn stabilize any possible product of pathway (iii) above. The use of stoichiometric amounts of $S_2O_6F_2$ was not feasible here, since the reaction would not go to completion. Finally, pathway (iv) was attempted in order to find out whether CH_2Cl_2 is capable of reducing the solubility of $Nb(SO_3F)_5$ in HSO_3F significantly enough to lead to an isolable precipitate. A precipitate did not form, and ^{19}F NMR spectra of the resulting solution showed that CH_2Cl_2 may have reacted with the HSO_3F solution, leading to a mixture of unidentified materials.

4.C.1.c. Derivatives of $Nb(SO_3F)_5$

The high solubility of $Nb(SO_3F)_5$ in HSO_3F suggested that it may behave as an SO_3F acceptor in solution. The simplest explanation for its solubility may be described in terms of solvation reactions such as:

$$Nb(SO_3F)_5 + HSO_3F \xrightarrow{HSO_3F} H[Nb(SO_3F)_6]_{(solv)} \qquad (4\text{-}3)$$

To test this assumption, $CsSO_3F$, acting as a base in HSO_3F, was mixed in stoichiometric amounts with niobium metal. The following reaction was observed:

$$2\,CsSO_3F + 2\,Nb + 5\,S_2O_6F_2 \xrightarrow[2\text{ days, }25^\circ C]{HSO_3F} 2\,Cs[Nb(SO_3F)_6] \qquad (4\text{-}4)$$

$Cs[Nb(SO_3F)_6]$ was isolated by filtration with a yield of 77%, which may be largely a result of some limited solubility. Once isolated, the salt does not re-dissolve in HSO_3F very readily and saturated solutions are about 0.2 M in concentration. Evidence for $Cs[Nb(SO_3F)_6]$ rests on chemical analysis and on the vibrational spectra.

It was found possible to carry out this reaction (viewed as an acid($Nb(SO_3F)_5$) - base($CsSO_3F$) reaction) further, based on the assumption that Nb unlike Sb is well capable of expanding its coordination sphere beyond six:[8]

$$4\,CsSO_3F + 2\,Nb + 5\,S_2O_6F_2 \xrightarrow[3\text{ days, }25^\circ C]{HSO_3F} 2\,Cs_2[Nb(SO_3F)_7] \qquad (4\text{-}5)$$

$$2\,Ba(SO_3F)_2 + 2\,Nb + 5\,S_2O_6F_2 \xrightarrow[2\text{ days, }25^\circ C]{HSO_3F} 2\,Ba[Nb(SO_3F)_7] \qquad (4\text{-}6)$$

These reactions proceeded in a very similar fashion to that of Equation (4-4), with the products isolated by filtration. The use of filtration obviously lowers the yield of isolated product, but helps in the identification of the precipitate. Since $CsSO_3F$ is very soluble in HSO_3F,[20] the product cannot be viewed as a mixture of $CsSO_3F$ and $Cs[Nb(SO_3F)_6]$. The use of $CsSO_3F$ in reactions of this type offers two additional advantages: (i) Cs^+, unlike K^+ or Li^+, is best capable of stabilizing large anions and (ii) the ν(S-F) vibrational mode in $CsSO_3F$ is unusually low (715 cm^{-1}),[21] allowing its easy detection in product mixtures. $Cs_2[Nb(SO_3F)_7]$ was obtained in a 70% yield, whereas the yield of $Ba[Nb(SO_3F)_7]$ was 20%. Neither species re-dissolved in HSO_3F very readily once isolated, with solutions formed being of ~0.2 M maximum concentration.

Alternatively, $Cs_2[Nb(SO_3F)_7]$ could be prepared in the absence of HSO_3F as well, according to:

$$4\,CsCl + 2\,NbCl_5 + 7\,S_2O_6F_2 \xrightarrow[4\text{ hrs.}]{25^\circ C} 2\,Cs_2[Nb(SO_3F)_7] + 7\,Cl_2 \qquad (4\text{-}7)$$

The product was isolated by removing all volatiles in vacuo and it was very important to use an exact stoichiometric amount of $S_2O_6F_2$ in this reaction. Any excess led to further oxidation of Cl_2 generating by-products, as described in Section 4.C.2.b. On occasion, small amounts of residual chloride were detected even after the products had attained constant weight. This observation suggests that the reaction does not always go to completion. This was the case for all the attempts to prepare $Cs[Nb(SO_3F)_6]$ by this general route, where chloride-containing wax-like materials formed. For these reasons,

metal oxidation appeared to be the route of choice to both the hexakis and heptakis(fluorosulfato) niobiate(V) salts of cesium.

All three salts described here melted or decomposed at temperatures ranging from a maximum of ~135 °C ($Ba[Nb(SO_3F)_7]$) to a minimum of ~78 °C ($Cs_2[Nb(SO_3F)_7]$); $Cs[Nb(SO_3F)_6]$ fell about halfway, decomposing at ~117 °C. Although there are no known $[M(SO_3F)_7]^{2-}$ precedents, salts of the type $Cs_2[M(SO_3F)_6]$, with M = Pt,[11] Ge[14] or Sn,[14] all melt at much higher temperatures (260 °C, 242 °C and 249 °C, respectively). All three salts, however, contain a -2 charged anion, which has been shown via vibrational and/or ^{119}Sn Mössbauer spectroscopy to exist with octahedral coordination around the metal. The lower thermal stability of the Nb salts, resulting perhaps from significantly different structural backbones, would be expected for the $[Nb(SO_3F)_7]^{2-}$ salts, but not so much for $Cs[Nb(SO_3F)_6]$.

The isolation of $Cs_2[Nb(SO_3F)_7]$ and $Ba[Nb(SO_3F)_7]$ is of interest, since species with more than six SO_3F groups per central atom have not previously been reported. In light of the well-known existence of heptacoordinate fluorocomplexes of the type $M^I_2[NbF_7]$, with M^I = an alkali metal or NH_4,[1,2] their preparation here is not totally surprising and underlines once again the similarity between F and SO_3F in their coordinating ability.

4.C.1.d. Attempted Syntheses of Other $Nb(SO_3F)_5$ Salts

Reactions with either $LiSO_3F$ or KSO_3F as base in HSO_3F led to wax-like or oily products when used in either a 1:1 or 2:1 molar ratio with $Nb(SO_3F)_5$. In some cases, the solvent HSO_3F could not be separated from the product mixture, even after prolonged periods and elevated temperatures (~50-60 °C), indicating a very strong degree of

solvation. The weights of the products isolated, the sulfur analyses obtained, as well as results from vibrational spectroscopy (see Section 4.C.2) indicated that these materials tend to decompose.

It appears that very large, electropositive countercations[22,23] such as Cs^+ or Ba^{2+} are needed to successfully stabilize the $[Nb(SO_3F)_6]^-$ or $[Nb(SO_3F)_7]^{2-}$ anions, resulting in isolable salts. The reported[24] existence of Na_3NbF_8 suggested the possible existence of $Cs_3[Nb(SO_3F)_8]$, but synthetic attempts were unsuccessful. Wax-like, partly decomposed materials of variable composition were formed when nearly all HSO_3F had been removed in vacuo, as indicated by the sulfur analysis and the weight of the isolated product. Both the metal oxidation and the oxidative chloride substitution routes were equally unsuccessful.

4.C.1.e. Synthesis of $NbF_2(SO_3F)_3$

Crystalline $NbF_2(SO_3F)_3$ precipitated out of a 2.4 M "$Nb(SO_3F)_5$" solution after two months storage at room temperature. $NbF_2(SO_3F)_3$ powder precipitated directly out of a 1.1 M "$Nb(SO_3F)_5$" solution at -5 °C. They had identical compositions and vibrational spectra (see Section 4.C.2). The melting point (126-129 °C) was slightly higher than that of $Cs[Nb(SO_3F)_6]$. For comparison, the tetrameric NbF_5 melts at 72-73 °C.[25] These observations suggest that $NbF_2(SO_3F)_3$ is thermodynamically favoured in these systems.

Only one complex of the type $MF_2(SO_3F)_3$, where M = metal or metalloid, has previously been reported, with uranium as the central metal.[26] It was prepared by reacting a 4:1 molar mixture of SO_3 and UF_6, with the surprising formation of $S_2O_6F_2$ as by-product. Solely on the basis of chemical analysis data, Kleinkopf and Shreeve[13]

reported the preparation of oxyfluorosulfates of the composition $MO(SO_3F)_3$ (M = Nb or Ta), by reaction of MCl_5 with $S_2O_6F_2$. $VO(SO_3F)_3$ was also prepared from $VOCl_3$ and $S_2O_6F_2$. However, their data for $NbO(SO_3F)_3$ agree much better with the composition $NbF_2(SO_3F)_3$. Description of "$NbO(SO_3F)_3$" as a yellow oil, however, does not agree with $NbF_2(SO_3F)_3$ obtained in this study. While $VO(SO_3F)_3$ is certainly a genuine compound, the existence of its Nb and Ta analogues is still uncertain.

4.C.2. Vibrational Spectroscopy

4.C.2.a. $Cs_x[Nb(SO_3F)_{5+x}]$, with x = 1 or 2

The principal source of structural information for the two salts $Cs[Nb(SO_3F)_6]$ and $Cs_2[Nb(SO_3F)_7]$ comes from the infrared and Raman spectra data compiled in Table 4.I. The Raman spectra of $Cs[Nb(SO_3F)_6]$ and $Cs_2[Nb(SO_3F)_7]$ are also shown in Figure 4.1. The spectra of both $[Nb(SO_3F)_6]^-$ and $[Nb(SO_3F)_7]^{2-}$ are rather similar. If presence of monodentate $-OSO_2F$ groups in both salts is assumed, the similarity in the region of the SO_3F stretches is not surprising, since differences in symmetry around Nb will only be relayed to a limited degree into this region.

If *only* monodentate coordination of $-OSO_2F$ groups was present, three bands would be expected in the 1000-1500 cm^{-1} region (at ~1450, ~1230, and 900-1000 cm^{-1}) as the highest frequency modes of the monodentate SO_3F groups. Especially in the IR spectra, there are a few extra bands and band shoulders present, and they fall at the approximate frequencies where the three *bidentate* $-OSO_2F$ groups' modes normally occur, namely ~1400, ~1120 and ~1070 cm^{-1}.[11] Combined with the similarity of both the IR and Raman band positions found here to that of the polymeric (via bidentate SO_3F groups), octahedrally coordinated $Pt(SO_3F)_4$,[11] it would seem that neither $[Nb(SO_3F)_6]^-$ nor $[Nb(SO_3F)_7]^{2-}$ exists as a monomer in solid state. Even though *monomeric* salts

Table 4.I. Vibrational Frequencies of $Cs_x[Nb(SO_3F)_{5+x}]$, with x = 1 or 2

$Cs[Nb(SO_3F)_6]$				$Cs_2[Nb(SO_3F)_7]$				
Raman ($\Delta\nu$, cm^{-1})		IR (ν, cm^{-1})		Raman ($\Delta\nu$, cm^{-1})		IR (ν, cm^{-1})		Approx. Assignment
1433	w,b	1432	s,b	1431	w,b	1434	s,b	
		1403	s,b			1410	s,b	ν_{as} (SO_3)
						1338	m,b,sh	
1263	s	1258	m	1262	s	1256	m	ν_s (SO_3) monodentate
1233	w	1221	s	1230	w	1217	s	
1106	w,b	1153	m,b,sh	1102	w,b	1153	w,b,sh	ν (SO_2) polydentate
		1083	w,b,sh			1085	w,b	
928	w,b	~910	s,vb	924	w	~980	s,vb	ν (O-SO_2F)
						~905	m,vb,sh	
847	w,b	~830	s,vb	846	w	830	s,b	ν (S-F)
643	w	651	m	641	w	648	w,b	ν_s (Nb-O) + δ (SO_3F)
562	w	554	m,b	560	w	555	m	δ (SO_3F)
552	w			548	w			
434	w	434	m,sh	432	w	433	m,sh	
		423	m			424	m	ν_{as} (Nb-O) + δ (SO_3F)
		412	m,sh	406	vw,b	412	m,sh	
						405	m,sh	
253	m			250	m			skeletal and
193	m			192	m			lattice vibrations

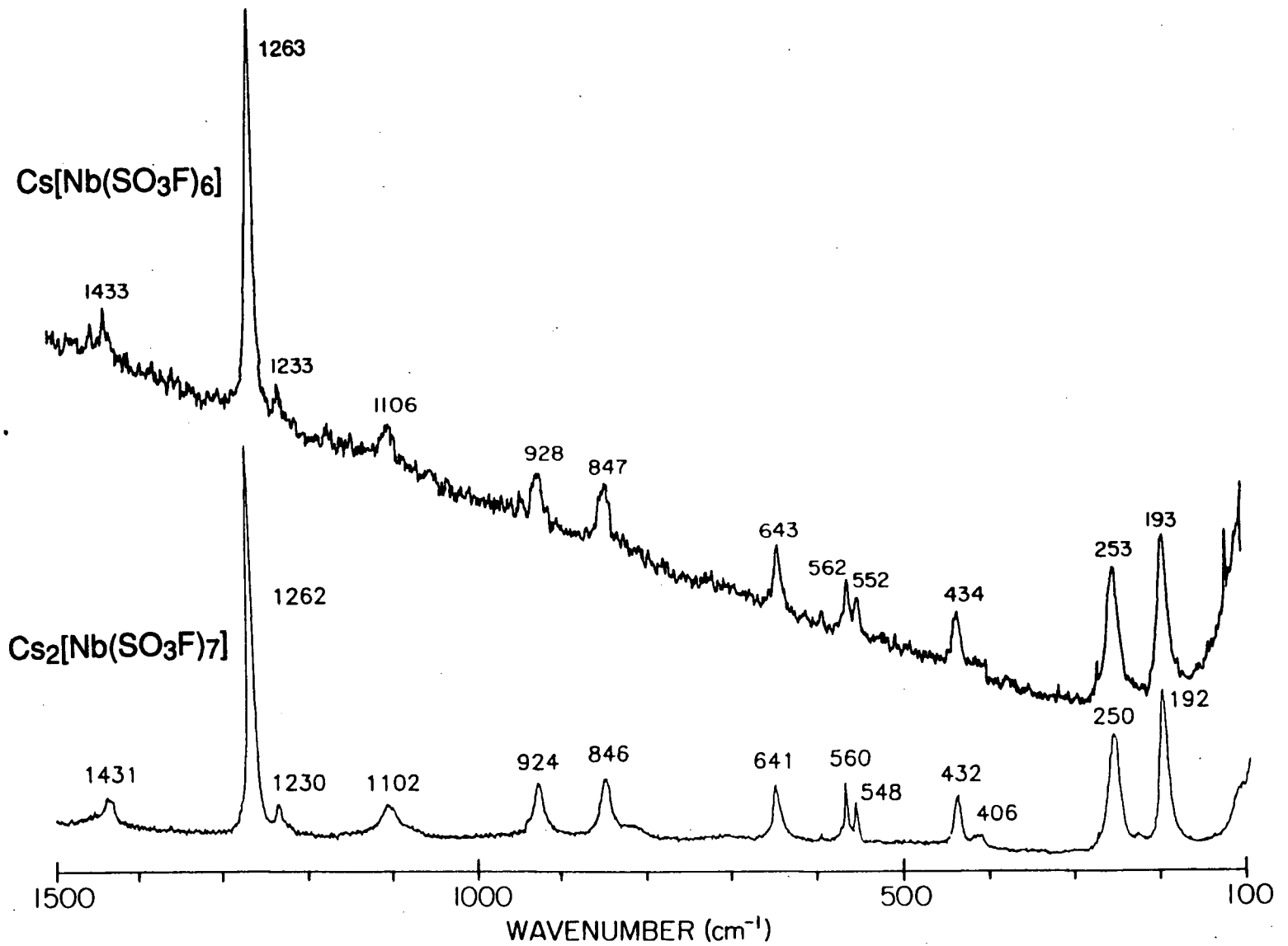

Figure 4.1. Raman Spectra of $Cs[Nb(SO_3F)_6]$ and $Cs_2[Nb(SO_3F)_7]$ from 100 to 1500 cm^{-1}

such as $Cs_2[Ge(SO_3F)_6]$[14] exhibit similar *Raman* spectra, their *IR* spectra are much less complex, supporting the above conclusion. Furthermore, the IR spectrum of the supposedly oligomeric $Cs[Pt(SO_3F)_5]$[11] salt and the Raman spectrum of the likewise oligomeric $Cs[Sn(SO_3F)_5]$[14] salt are very similar to the respective spectra of the present salts.

For a mixed mono/bidentate $-OSO_2F$ environment, multiple ν(S-F) bands would be expected.[11,14] Although this is not seen in either of the salts' spectra, the ν(S-F) band found in each case at ~830 cm^{-1} is very broad, especially in the case of $Cs[Nb(SO_3F)_6]$, suggesting that multiple bands may be partially overlapped. It is interesting to note that bands present in both the IR and Raman spectra at 1430-1450 and 900 cm^{-1} have previously also been found for $Pt(SO_3F)_4$[11] and $Sn(SO_3F)_4$[14] but not for their respective salts $Cs_x[M(SO_3F)_{4+x}]$, with x = 1 or 2.

Observed splitting of some of the vibrational modes may be due to vibrational mixing or slight non-equivalency among various SO_3F groups[27] in the anion. The vibrational data, however, indicate that in both salts, nearly identical conformations of the SO_3F groups are found and that monodentate as well as bridging polydentate SO_3F groups are present. The broadness of many of the bands present in the IR spectra prevents a more definite assignment for the bands due to the latter, although bidentate coordination is most likely.[14] A higher than six-coordinate environment for Nb and oligomeric structural units are implied, which is given some precedent by the existence of the eight-coordinate Na_3NbF_8 salt.[24] K_2NbF_7, on the other hand, exists with monomeric $[NbF_7]^{2-}$ units and Nb in a seven-coordinate, capped trigonal (C_{2V}) coordination environment.[2] For Nb to have the same coordination environment in $Cs[Nb(SO_3F)_6]$ as it has in $Cs_2[Nb(SO_3F)_7]$, it would require a highly oligomerized structure, leading ultimately to an eight-coordinate environment around the metal centers in both cases.

4.C.2.b. Ba[Nb(SO$_3$F)$_7$] and Other Derivatives

The infrared data for Ba[Nb(SO$_3$F)$_7$] are listed in Table 4.II, along with the approximate band assignments. The presence of both monodentate and bidentate -OSO$_2$F groups is indicated. However, a much greater complexity of the spectrum compared to that of Cs[Nb(SO$_3$F)$_6$] and Cs$_2$[Nb(SO$_3$F)$_7$] is observed and it appears that Ba^{2+} unlike Cs^+ is a good acceptor and is involved in coordination to oxygen. It should be pointed out that the IR spectrum of Ba(SO$_3$F)$_2$ has been reported and all the E-modes appear to be split, with C_s rather than C_{3v} symmetry indicated.[28] Coordination to Ba^{2+} is seen as a possible cause. The presence of a broad band at ~700 cm^{-1} in the present spectrum, which is normally the region of terminal Nb-F stretching modes[16] (also see Section 4.C.2.c), and a region in which fluorosulfate bands are not usually found, is puzzling and as yet not easily explained.

The rest of the discussion here will briefly deal with the spectra of some of the salts for which good analytical data have not been obtained, as a result of either incomplete reaction or decomposition (see Section 4.C.1.d). The most promising of these is Cs$_3$[Nb(SO$_3$F)$_8$], prepared from NbCl$_5$ in the absence of HSO$_3$F, whose IR spectrum is somewhat *simpler* in the 800-1450 cm^{-1} region than the spectra of Cs[Nb(SO$_3$F)$_6$] or Cs$_2$[Nb(SO$_3$F)$_7$]. There is no sign of bidentate -OSO$_2$F bands, suggesting the presence of monomeric $[Nb(SO_3F)_8]^{3-}$ units. Unfortunately, chlorine-free, undecomposed samples could not be isolated. Attempts at isolating this salt from HSO$_3$F led again to partially decomposed materials, as indicated by the presence of a band at ~700 cm^{-1}, which is attributable to a terminal Nb-F stretching mode.[16] Very similar spectra were obtained for "Li[Nb(SO$_3$F)$_6$]" and "K$_2$[Nb(SO$_3$F)$_7$]", both giving rise to a very prominent Nb-F stretching band at ~700 cm^{-1} indicative of partial decomposition; neither

Table 4.II. Infrared Vibrational Frequencies of $Ba[Nb(SO_3F)_7]$

ν (cm^{-1})		Approx. Assignment
1390	vs	ν_{as} (SO_3)
1342	s,sh	
1282	s,b	ν (SO_3)
1233	s,sh	
1221	s	
1213	s,sh	
1152	w,b	
1115	m	
1097	w,b,sh	
1008	s	ν (O-SO_2F)
997	s,b,sh	
867	m,sh	ν (S-F)
853	s,sh	
842	s	
824	s	
~700	m,b	(?)
670	w,sh	ν_s (Nb-O) + δ (SO_3F)
632	m	
610	m,sh	δ (SO_3F)
599	m,sh	
583	s,sh	
563	s	
443	m	ν_{as} (Nb-O) + δ (SO_3F)
423	w,sh	
415	w,sh	

salt precipitates out of solution to allow isolation by filtration. IR spectra of both of these materials look similar to those of the cesium salts, however with less pronounced evidence for bidentate SO_3F groups.

4.C.2.c. $NbF_2(SO_3F)_3$

The seemingly incomplete Raman and infrared data for this species are shown in Table 4.III. The Raman spectrum is of poor quality on two accounts: (i) Raman bands are observed on a strong, broad fluorescence envelope and show a sloping baseline and (ii) a number of glass and plasma lines are observed but are for the most part identifiable. The principal feature of the IR spectrum shown in Figure 4.2 is its complexity.

The absence of a constraint to coordination number six for Nb and the unavailability of other structural techniques such as Mössbauer spectroscopy allow only tentative band assignments. A number of uranium(V) fluorosulfato derivatives such as $UF_2(SO_3F)_3$,[26] a direct analogue to $NbF_2(SO_3F)_3$, and also $UF_3(SO_3F)_2$, $UF(SO_3F)_4$ and $UO(SO_3F)_3$[29] provide some help, however. Uranium, just like niobium, may well exhibit seven- or eight-coordination. More reliable Raman spectra have been obtained and magnetic measurements have confirmed the oxidation state +5 for uranium.[26] Relative IR and Raman exclusion of the two extremely intense ν(F-U-F) modes at 636 (asymmetric) and 606 cm^{-1} (symmetric) is interpreted in terms of a linear or nearly linear UF_2 group and is seen as evidence for a more symmetrical environment. Such a feature, however, is not apparent for $NbF_2(SO_3F)_3$, with ν_{as}(F-Nb-F) at 712 and ν_s(F-Nb-F) at 666 cm^{-1} both seen in the IR. The latter band has only a rather weak counterpart in the Raman spectrum. These bands occur at 734 and 688 cm^{-1} for $[NbF_5]_4$[16] and at 722 and 710 cm^{-1} for $(CH_3)_2Sn(NbF_6)_2$,[7] respectively.

The SO_3F band spacings found for $NbF_2(SO_3F)_3$ allow some tentative assignments and limited structural conclusion. Based on the above, cited precedents such

Table 4.III. Vibrational Frequencies of $NbF_2(SO_3F)_3$

Raman ($\Delta\nu$, cm^{-1})		IR (ν, cm^{-1})		Approx. Assignment
~1435	vw,b	1434	s	
		1407	s	ν_{as} (SO_3)
		1394	s,sh	
		1378	s	
		1216	s,b	ν_s (SO_3)
1161	m	1164	s	
~1112	w,b,sh	1115	m,b,sh	
1104	m			
1080	w	1090	s,sh	
1070	w	1069	s	
~1050	w,b	1046	s,sh	ν (SO_2 + O-SO_2F)
1006	s	1002	s	
		~970	m,vb,sh	
884	m,sh	888	m,b,sh	
874	m	854	s,b	ν (S-F)
869	m,sh	837	s,b,sh	
		712	m,b	ν_{as} (Nb-F)
669	vw,b	666	s	ν_s (Nb-F)
		634	m,sh	
		621	s	ν_s (Nb-O) + δ (SO_3F)
		605	m,sh	
		592	m	
566	vw,b	571	m,sh	δ (SO_3F)
561	vw,b	562	m	
		475	w	ν_{as} (Nb-O) + δ (SO_3F)
		450	w	
386	vw,b			
310	w,b			lattice vibrations
288	w			+
269	m			torsion modes
250	m			

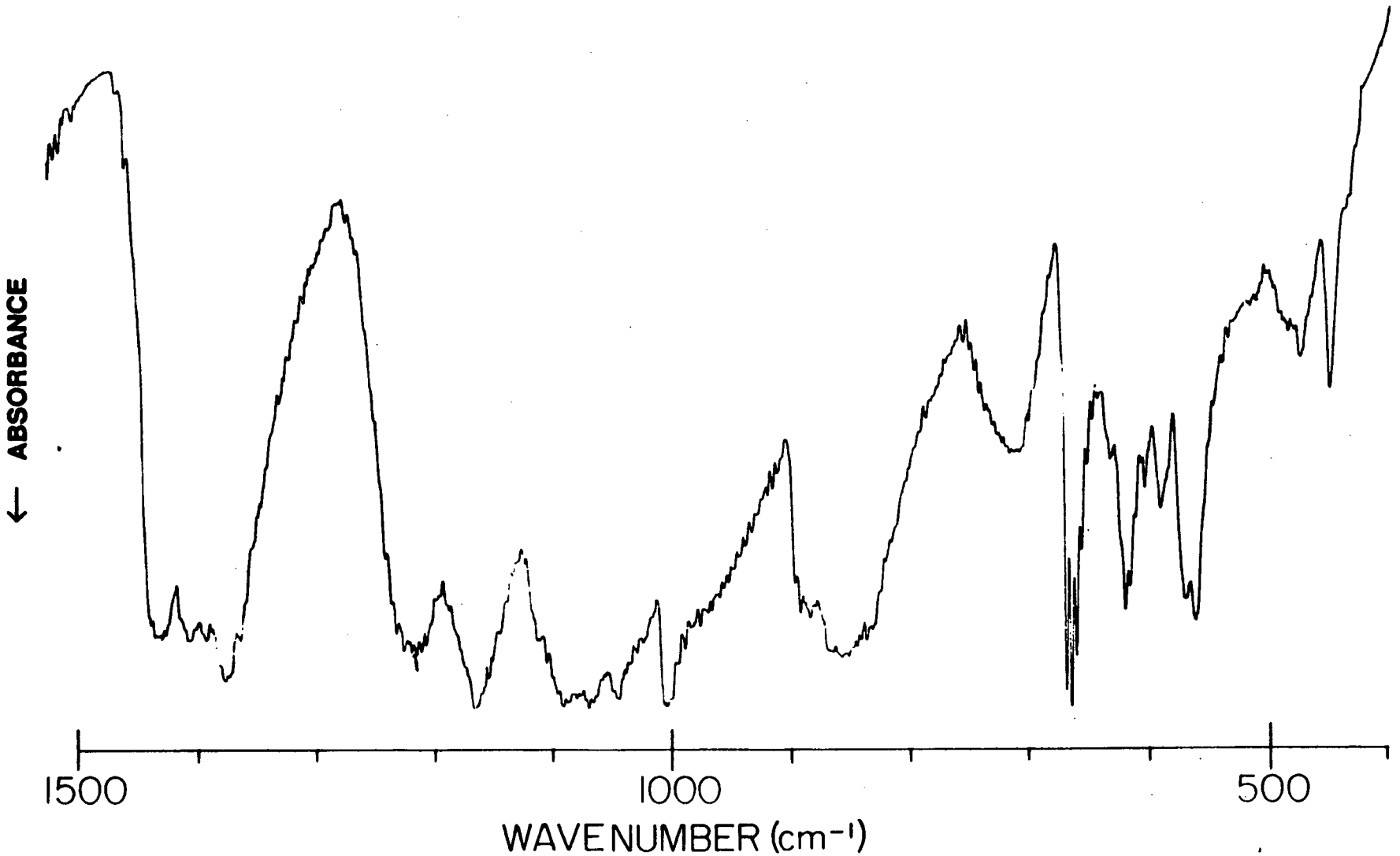

Figure 4.2. Infrared Spectrum of $NbF_2(SO_3F)_3$ from 400 to 1500 cm^{-1}

as $MF_2(SO_3F)_2$, with M = Sn,[14,30] Ge,[14] Sb[31] or As,[32] $Pt(SO_3F)_4$[11] and the uranium(V) fluorosulfates just discussed, bands at ~1380-1410, ~1160 and ~1070 cm^{-1} are assignable to a symmetrically bidentate, presumably bridging SO_3F group. For the remaining bands at ~1430, ~1220 and ~1000 cm^{-1}, the band positions suggest a monodentate group. The observed band intensities, however, do not support this conclusion. The supposedly symmetrical SO_3 stretch is barely detectable in the Raman spectrum, while a Raman band with $\Delta\nu$ of 1006 cm^{-1} has the highest overall intensity. No clear assignment is possible and either tridentate or unsymmetrical, aniso-bidentate coordination remain feasible. The presence of more than one type of fluorosulfate group is further supported by the very broad ν(S-F) bands in the ~830-900 cm^{-1} region of the spectrum.

Whereas the evidence for fluorosulfate bridges is abundant, fluorine bridges are more difficult to detect, since they would occur in a cluttered region of the spectrum (~450-550 cm^{-1}, based on the ν(Nb-F-Nb) bands found at 514 or 479 cm^{-1} in the spectrum of $[NbF_5]_4$).[16] The only such band in the spectrum of $NbF_2(SO_3F)_3$ is found at 475 cm^{-1}, but an unambiguous assignment is not possible. Besides, it is difficult to envision the existence of both fluoro- and fluorosulfate-bridges in this compound, especially since only the latter are present in previously studied $MF_x(SO_3F)_y$ type species.[14,26,27,31]

The conclusions reached here are three-fold: (i) the coordination number of Nb in $NbF_2(SO_3F)_3$ appears higher than six, possibly seven or even eight; (ii) the coordination environment of Nb appears to be of low symmetry and (iii) consistent with other fluorides or fluorosulfates studied by us and others, SO_3F-bridging appears to take precedence over F-bridging. The poor quality of the Raman spectrum, the poor match with the $UF_2(SO_3F)_3$ vibrational data and the lack of auxiliary techniques preclude more

detailed conclusions. Crystals of $NbF_2(SO_3F)_3$ have been obtained, but were unfortunately found to exist in clusters, making them unsuitable for single crystal X-ray diffraction studies. An interesting structure is suspected for this compound based on its vibrational spectra, and further pursuit of a single crystal appears worthwhile in the future.

4.C.3. Powder X-ray Diffraction Studies

A powder X-ray diffraction photograph was obtained for $Ba[Nb(SO_3F)_7]$ and the resulting lines are listed in Table 4.IV. The assignment of Miller indices was not attempted, since, to the author's knowledge, there are no suitable studies available for comparison. The most significant features of the pattern are the presence of the second and third most intense lines at unusually high d_{ex} values of 9.83 and 8.08 Å. Salts of the type M^INbF_{5+x},[24] where MI = alkali metal and x = 1, 2 or 3, as well as $UF_2(SO_3F)_3$,[26] for example, do not possess any high intensity lines with $d_{ex} > 8.00$ Å. This *may* suggest an unusual unit cell for $Ba[Nb(SO_3F)_7]$.

Table 4.IV. X-ray Powder Pattern for $Ba[Nb(SO_3F)_7]$

d_{ex} (Å)	Intensity
9.83	m
8.08	s
6.71	m
4.72	m
4.45	w
3.98	m
3.46	w
3.25	vs

Unfortunately, an adequate X-ray diffraction line pattern could not be obtained for amorphous $NbF_2(SO_3F)_3$, owing to its inefficient X-ray scattering and its tendency to decompose after only one or two hours of X-ray exposure.

4.D. Conclusion

Extremely soluble $Nb(SO_3F)_5$ has been generated in situ in HSO_3F, with its solutions thermally stable at least at low concentrations (≤1 M). Higher concentrations led to the precipitation of $NbF_2(SO_3F)_3$, which was isolated and characterized. Formation of oxyfluorosulfates, such as $NbO(SO_3F)_3$, was not observed. Since no $S_2O_5F_2$ was detected, its formation as by-product is also judged unlikely.

The existence of $Nb(SO_3F)_5$, at least in "basic" solution, is supported by the isolation and characterization of the ternary salts $Cs[Nb(SO_3F)_6]$, $Cs_2[Nb(SO_3F)_7]$ (two different pathways) and $Ba[Nb(SO_3F)_7]$. Their isolation demonstrates the ability of $Nb(SO_3F)_5$ to act as a Lewis acid or SO_3F^- ion acceptor in HSO_3F. Its solubility in HSO_3F appears to be good and the HSO_3F-$Nb(SO_3F)_5$ system emerges as a promising superacid system. However, proof of superacidity still requires conductometric and spectroscopic studies. Expanded coordination spheres via fluorosulfate bridging are apparent in all three salts from their IR and Raman spectra, with eight-coordination being very likely and at least seven coordination present. $Cs_2[Nb(SO_3F)_7]$ and $Ba[Nb(SO_3F)_7]$ are the first salts reported with definite existence of a higher than six-coordinated fluorosulfato metallate.

The next chapter will describe an analogous investigation of niobium's "father metal",[25] tantalum.

REFERENCES

1. F. Fairbrother, *"The Chemistry of Niobium and Tantalum"*, Elsevier, London, 1967.

2. D. Brown, *Chemistry of Niobium and Tantalum* in *"Comprehensive Inorganic Chemistry"*, Pergamon Press, N.Y., Vol.III, 1973.

3. F.A. Cotton and G. Wilkinson, *"Advanced Inorganic Chemistry"*, 5th Edition, J. Wiley & Sons, N.Y., 1988.

4. A.J. Edwards, *J. Chem. Soc.*, 3714 (1964).

5. G.A. Olah, G.K.S. Prakash and J. Sommer, *"Superacids"*, J. Wiley & Sons, N.Y., 1985 (and references herein).

6. J.A.S. Howell and K.C. Moss, *J. Chem. Soc. A*, 2481 (1971).

7. S.P. Mallela, S. Yap, J.R. Sams and F. Aubke, *Rev. Chim. Min.* **23**, 572 (1986).

8. S.J. Lippard, *Prog. Inorg. Chem.* **8**, 109 (1967).

9. H. Funk, W. Weiss and K.P. Roethe, *Z. Anorg. Chem.* **301**, 271 (1959).

10. D.L. Kepert, *"The Early Transition Metals"*, Academic Press, London, Chapt. 3, 1972.

11. K.C. Lee and F. Aubke, *Inorg. Chem.* **23**, 2124 (1984).

12. H.C. Clark and H.J. Emeléus, *J. Chem. Soc.*, 190 (1958).

13. G.C. Kleinkopf and J.M. Shreeve, *Inorg. Chem.* **4**, 607 (1964).

14. S.P. Mallela, K.C. Lee and F. Aubke, *Inorg. Chem.* **23**, 653 (1984).

15. K.C. Lee and F. Aubke, *Inorg. Chem.* **18**, 389 (1979).

16. I.R. Beattie, K.M.S. Livingston, G.A. Ozin and D.J. Reynolds, *J. Chem. Soc. A.*, 958 (1969).

17. R.E. Noftle and G.H. Cady, *J. Inorg. Nucl. Chem.* **29**, 969 (1967).

18. W.P. Galbraith and G.H. Cady, *Inorg. Chem.* **2**, 496 (1963).

19. H.A. Carter, A.M. Qureshi and F. Aubke, *J. Chem. Soc., Chem. Commun.*, 1461 (1968).

20. A.W. Jache, *Adv. Inorg. Chem. Radiochem.* **16**, 177 (1974).

21. A. Ruoff, J.B. Milne, G. Kaufmann and M.Z. Leroy, *Z. Anorg. Allg. Chem.* **372**, 119 (1970).

22. R.T. Sanderson, *Inorg. Chem.* **25**, 3518 (1986).

23. R.G. Pearson, *Inorg. Chem.* **27**, 734 (1988).

24. D. Bizot and M. Malek-Zadeh, *Rev. Chim. Min.* **11**, 710 (1974).

25. *"Handbook of Chemistry and Physics"*, 57th Edition, R.C. Weast, Ed., C.R.C. Press U.S.A., pp. B-34 and B-50, 1976-1977.

26. W.W. Wilson, C. Naulin and R. Bougon, *Inorg. Chem.* **16**, 2252 (1977).

27. L.E. Levchuk, J.R. Sams and F. Aubke, *Inorg. Chem.* **11**, 43 (1972).

28. C.S. Alleyne, K.O. Mailer and R.C. Thompson, *Can. J. Chem.* **52**, 336 (1974).

29. J.P. Masson, C. Naulin, P. Charpin and R. Bougon, *Inorg. Chem.* **17**, 1858 (1978).

30. P.A. Yeats, B.L. Poh, B.F.E. Ford, J.R. Sams and F. Aubke, *J. Chem. Soc. A*, 2188 (1970).

31. W.W. Wilson and F. Aubke, *J. Fluor. Chem.* **13**, 431 (1979).

32. H. Imoto and F. Aubke, *J. Fluor. Chem.* **15**, 59 (1980).

CHAPTER 5

FLUOROSULFATE DERIVATIVES OF TANTALUM(V)

5.A. Introduction

The similarity between the chemical behaviour of tantalum and that of niobium can be predicted from the assortment of physical properties listed earlier in Table 1.I and some general comments can be made. Pentavalent halides of tantalum are harder to reduce than those of niobium and hence the tri- and tetrahalides are less well known. TaF_4 has not been prepared, whereas TaF_3 only forms as a minor by-product during the synthesis of TaF_5.[1]

The very stable TaF_5[2] has been among the numerous halides or oxyhalides of tantalum for which the structure has been reported.[3] It exists as a hygroscopic, white solid and is isostructural with NbF_5 as a cis-fluorine bridged tetramer. Its melting point of 95-97 °C[1,4] is however higher. The high resistance of TaF_5 towards reduction and its higher acidity has resulted in its more frequent use as the Lewis acid component in HF, HSO_3F or HSO_3CF_3 superacid systems[5] compared to NbF_5.

The anions $[TaF_6]^-$ and $[TaF_7]^{2-}$ have both been detected in aqueous HF solutions of Ta(V) and NH_4F via Raman spectroscopy.[6] A similar ^{19}F NMR study[7] gave evidence for the presence of the same two species. Tentative evidence for the $[TaF_9]^{4-}$ ion in aqueous HF media has also been established,[2] while $[TaF_8]^{3-}$ has not been observed. Even more so than with NbF_5, these results give evidence for the excellent acceptor ability of TaF_5, which is the basis of its superacidity. Salts of the type $M_3^ITaF_8$, $M_2^ITaF_7$, M^ITaF_6 (M^I = Na, K or NH_4), and $(CH_3)_2Sn(TaF_6)_2$[8] have also been isolated.

Single crystal X-ray structures of Na_3TaF_8 and more recently K_2TaF_7 have also been reported.[9,10] The anions in both salts exist as discrete monomeric units. This tendency to exhibit higher coordination numbers than six is seemingly even more pronounced for tantalum than it is for niobium. Salts of only the octahedral, monomeric anions $[TaX_6]^-$ have been obtained with the other halides, Cl^-, Br^-, and I^-.[11]

The resistance of TaF_5 towards reduction to lower fluorides and its promising superacidic behavior led to interest in the preparation of the binary $Ta(SO_3F)_5$; success encountered with the analogous niobium system in the previous chapter reinforced this. In addition, this species is expected to be even more acidic than the niobium analog, and, due to its expected ability to support a more crowded coordination sphere, should be less prone to the type of decomposition that led to $NbF_2(SO_3F)_3$. The solubility of $Ta(SO_3F)_5$ in HSO_3F is also expected to be comparable to that of $Nb(SO_3F)_5$ and hence significantly greater than that of TaF_5. As was the case with niobium, both $TaF_5 \cdot 2.6SO_3$ ("$TaF_3(SO_3F)_2$" with excess SO_3)[12] and $TaO(SO_3F)_3$[13] have previously been reported, although neither compound was properly characterized. In addition, the reaction of $TaCl_5$ with the very toxic $C_2H_5SO_3F$ has been claimed[14] to yield $TaCl_3(SO_3F)_2$.

5.B. Experimental

5.B.1. In Situ Synthesis of Pentakis(fluorosulfato)tantalum(V), $Ta(SO_3F)_5$

Typically, 411 mg (2.27 mmol) of tantalum metal powder was treated with an approximate 7 ml mixture of $S_2O_6F_2$ and HSO_3F (2:1) and allowed to react at 40 °C for 5 days, by which time all the metal was consumed and a colorless solution was obtained. Excess $S_2O_6F_2$ was removed in vacuo at room temperature. Attempts to completely remove the acid in vacuo failed at room temperature, whereas the application of heat

resulted in decomposition of the product. The product did not precipitate, even when the acid volume was reduced as much as possible and cooling down to -10 °C was applied.

5.B.2. Derivatives of $Ta(SO_3F)_5$

a) Cesium Hexakis(fluorosulfato)tantalate(V)

Two different forms were obtained, depending on the synthetic route used. They are termed forms α and β.

α-FORM

617 mg (3.41 mmol) of tantalum metal powder was added to 781 mg (3.37 mmol) of $CsSO_3F$ to which was then distilled 5 ml of $S_2O_6F_2$ and 4 ml of HSO_3F in vacuo. The mixture was allowed to stir at 35 °C for 3 days, by which time the dark grey metal powder was completely consumed and a white slurry had formed. The fine white powder was collected by vacuum filtration. Excess solvent and $S_2O_6F_2$ were removed and the product was dried in vacuo for 24 hours at room temperature. α-$Cs[Ta(SO_3F)_6]$ was isolated in 64% yield and decomposed at 120-124 °C.

Analytical Data for α-$CsTaS_6O_{18}F_6$:

	Cs(%)	Ta(%)	S(%)	F(%)
Calculated:	14.63	19.92	21.18	12.55
Found	14.45	20.00	20.96	12.31
S:F = 0.991				

β-FORM

763 mg (2.13 mmol) of $TaCl_5$ was added to 360 mg (2.14 mmol) of CsCl to which was then vacuum distilled exactly 2.30 ml of $S_2O_6F_2$ and the white, paste-like material was allowed to stir at 25 °C for 5 hours. Vigorous evolution of yellow to deep-orange gaseous by-products occurred during the course of the reaction, and the reaction vessel was periodically vented in vacuo. Following the visible completion of the reaction (end of bubbling), volatile by-products were removed overnight in vacuo. A paste-like white material was isolated in 89% yield. This material's texture prevented the measurement of an accurate melting point.

Analytical Data for β-$CsTaS_6O_{18}F_6$:

	Cs(%)	Ta(%)	S(%)	F(%)
Calculated:	14.63	19.92	21.18	12.55
Found:	14.90	19.80	20.40	12.65
S:F = 0.956				

b) Cesium Heptakis(fluorosulfato)tantalate(V)

Typically, 310 mg (1.71 mmol) of tantalum metal powder was added to 824 mg (3.55 mmol) of $CsSO_3F$. About 3 ml of $S_2O_6F_2$ and 2 ml of HSO_3F were then distilled onto the solids. The resulting mixture was allowed to stir at 40 °C for 2 days, by which time all the dark grey metal was consumed and a white slurry appeared. The reaction vessel was cooled to 0 °C. A fine white powder was collected by vacuum filtration. Excess solvent and $S_2O_6F_2$ were removed and the product was dried in vacuo for 3 days

at room temperature. The isolated yield was 70%. $Cs_2[Ta(SO_3F)_7]$ decomposed at 77-79 °C.

$Cs_2[Ta(SO_3F)_7]$ was alternatively prepared as follows. 717 mg (2.00 mmol) of $TaCl_5$ was added to 665 mg (3.95 mmol) of CsCl to which was then vacuum distilled 1.8 ml of $S_2O_6F_2$. The white, paste-like mixture was stirred at 25 °C for 3 hours, during which time vigorous evolution of gaseous by-products occurred, requiring periodic venting of the reactor in vacuo. Once all bubbling had ceased, additional pumping overnight on the product at 0 °C was applied, to ensure the complete removal of all volatile by-products without product deomposition. The white, powdery product was isolated in quantitative yield and gave a negative chloride test.

Analytical Data for $Cs_2TaS_7O_{21}F_7$:

	Ta(%)	S(%)	F(%)
Calculated:	15.87	19.68	11.66
Found:	15.60	19.40	11.61
S:F = 1.010			

5.B.3 Attempted Syntheses of Additional $Ta(SO_3F)_5$ Derivatives

a) Cesium Octakis(fluorosulfato)tantalate(V)

The preparation of $Cs_3[Ta(SO_3F)_8]$ was attempted via both general routes described earlier. The synthesis from $TaCl_5$ led to a mixed product of uncertain composition, whereas the metal oxidation route led to a product which was prone to fairly rapid degradation.

Analytical Data for $Cs_3TaS_8O_{24}F_8$:

	Cs(%)	Ta(%)	S(%)	F(%)
Calculated:	29.06	13.19	18.69	11.08
Found ($TaCl_5$ prep.):	–	17.10	17.31	10.37
Found (Ta prep.):	14.60	19.65	18.40	12.26

b) Barium Heptakis(fluorosulfato)tantalate(V)

Synthetic attempts along the same lines as the successful synthesis of $Ba[Nb(SO_3F)_7]$ were carried out repeatedly. Products of mixed composition were obtained each time due to partial decomposition.

Analytical Data for $BaTaS_7O_{21}F_7$:

	Ba(%)	Ta(%)	S(%)	F(%)
Calculated:	13.57	17.89	22.18	13.15
Found:	7.05	28.95	16.28	17.02

c) Lithium Salts of Heptakis(fluorosulfato) and Octakis(fluorosulfato)tantalate(V)

Attempts to use metal oxidation in the presence of $LiSO_3F$ led either to very viscous oils or paste-like materials of uncertain composition. Complete solvent (HSO_3F) removal was difficult in both instances.

5.B.4. The Synthesis of Tetrafluoro(fluorosulfato)tantalum(V), $TaF_4(SO_3F)$

1.50 g (5.44 mmol) of TaF_5 was added to 0.73 ml of a 1.88 M $Ta(SO_3F)_5$ in HSO_3F solution (1.36 mmol $Ta(SO_3F)_5$) in the drybox. The heterogeneous mixture was stirred for 18 hours at room temperature, by which time all of the TaF_5 had dissolved and a clear, colorless solution resulted. A white, powdery product was isolated in 52% yield by pumping on the solution for 2 days at room temperature and thus evolving all volatiles. $TaF_4(SO_3F)$ decomposed at 210-220 °C.

Analytical Data for TaF_5SO_3:

	Ta(%)	S(%)	F(%)
Calculated:	50.83	9.01	26.68
Found:	51.10	9.16	26.54
S:F = 0.205			

5.C. Results and Discussion

5.C.1. Synthesis and General Discussion

5.C.1.a. In Situ Synthesis of $Ta(SO_3F)_5$

The same general route that was used to obtain $Nb(SO_3F)_5$ in Chapter 4 was applied to prepare $Ta(SO_3F)_5$:

$$2\,Ta + 5\,S_2O_6F_2 \xrightarrow[2\text{ days, }40^\circ C]{HSO_3F} 2\,Ta(SO_3F)_5 \qquad (5\text{-}1)$$

Slightly higher temperatures and longer reaction times were needed than in the preparation of $Nb(SO_3F)_5$, reflecting a greater resistance of Ta towards oxidation. This

trend seemed independent of the metal powders' mesh or exact purity (see Table 2.I). Clear, colorless solutions resulted, with more concentrated solutions (≥ 2 M) tending to be of a gel-like consistency. Once again, no precipitate formed. Excess $S_2O_6F_2$ was readily removed in vacuo at room temperature. As observed during the synthesis of $Nb(SO_3F)_5$ and $Au(SO_3F)_3$,[15,16] it was found that the $S_2O_6F_2$ volume in the $S_2O_6F_2/HSO_3F$ mixture must be larger than that of HSO_3F to ensure that the reaction proceeds efficiently. 0.9 M solutions of the product were observed to undergo rapid fluorosulfate exchange between the solute and solvent, giving rise to a single solvent/solute resonance in the ^{19}F NMR spectra even at temperatures of -55 °C. This exchange is believed to be responsible for the noted high solubility of $Ta(SO_3F)_5$.

Because of the solute's extremely high solubility, complete removal of the solvent (HSO_3F) in vacuo was not possible at room temperature. Heating the reaction mixture to about 45 °C led to a decomposed product of a lower than expected weight. Infrared spectra were obtained at various stages prior to and at the point when the product reached constant weight. As constant weight was approached, a gradual reduction in intensity and increased proliferation of the fluorosulfate bands as well as the appearance of a ν(Ta-F) band (at ~700 cm^{-1})[17] suggested decomposition via SO_3 loss to form species of the type $TaF_x(SO_3F)_{5-x}$. However, the spectra of volatiles collected during this process showed very similar bands, suggesting that some of these $TaF_x(SO_3F)_{5-x}$ decomposition products may be volatile. The species isolated at the end of this decomposition process was a white powder, whose weight was lower than that expected for TaF_5, even though its IR spectrum still contained some SO_3 stretching bands.

Solutions of $Ta(SO_3F)_5$ in HSO_3F were found to be clear at considerably higher concentrations than those of $Nb(SO_3F)_5$. No apparent evidence for the dissociation of

$Ta(SO_3F)_5$ in HSO_3F solution up to concentrations of about 2 M was obtained and only highly concentrated (12 - 13 M) solutions have shown signs of precipitation and possible decomposition. As was the case with $Nb(SO_3F)_5$, the isolation of salts of the type $M'_x[Ta(SO_3F)_{5+x}]$, with x = 1 or 2 and M′ = Cs or Ba, from solution supports the existence of undecomposed $Ta(SO_3F)_5$, at least at low concentrations.

5.C.1.b. Additional Attempts to Obtain $Ta(SO_3F)_5$

The same four synthetic routes that had been tried in attempts to isolate solid $Nb(SO_3F)_5$ were explored here:

(i) the reaction of TaF_5 with excess HSO_3F;

(ii) the reaction of $NbCl_5$ with excess HSO_3F;

(iii) the reaction of $NbCl_5$ with excess $S_2O_6F_2$;

(iv) the reaction of $Ta(SO_3F)_5/HSO_3F$ with CH_2Cl_2.

None of these routes was entirely fruitful in the temperature range -45 to +45 °C, usually leading to mixtures.

There is however some evidence for the formation of $TaF_4(SO_3F)$ at 25 °C after one week via reaction (i), based on weight measurements, the product's IR spectrum and its decomposition at 210 °C (see Section 5.B.4). However, microanalysis of the product isolated after all the HSO_3F was removed showed a 4.04:1 F/Ta ratio, with F and Ta analytical data suggesting the composition $TaF_{3.2}(SO_3F)_{0.8}O_{0.5}$. The discrepancy may be due to some Si_xO_y type materials being left behind from the reaction of the by-product HF with the glass.

The other three attempted reaction routes proceeded very similarily to those already described for the niobium analogs, and therefore will not be discussed again. It appears that neither $Nb(SO_3F)_5$ nor $Ta(SO_3F)_5$ is obtainable as a stable entity separable from the solvent HSO_3F, which is due in part to their high degree of solvation and in part to their thermal instability.

5.C.1.c Derivatives of $Ta(SO_3F)_5$

As in the case of $Nb(SO_3F)_5$, synthesis of alkali metal fluorosulfato derivatives of tantalum was also successful. The base $CsSO_3F$ was again chosen, and initial reaction was found to proceed according to:

$$2\ CsSO_3F + 2\ Ta + 5\ S_2O_6F_2 \xrightarrow[3\ days,\ 35°C]{HSO_3F} 2\ Cs[Ta(SO_3F)_6] \qquad (5\text{-}2)$$

The analytically pure product was obtained by filtration as a white powder in slightly lower isolated yield (64%) than the analogous niobium salt, possibly due to greater solubility in HSO_3F, which was also indicated by the product's ability to re-dissolve once isolated to give about 0.3 M solutions.

A salt of the same composition was prepared in the absence of HSO_3F, according to:

$$CsCl + TaCl_5 + 3\ S_2O_6F_2 \xrightarrow[5\ hrs.]{25°C} Cs[Ta(SO_3F)_6] + 3\ Cl_2 \qquad (5\text{-}3)$$

Even though analytical data obtained were satisfactory (except for a low sulfur value), there are reasons to view the material with suspicion:

(i) a mass balance of the reaction was unsatisfactory, with only 89% of the expected product weight found;

(ii) occasional samples gave a positive chloride test;

(iii) the paste-like consistency of the product suggested a mixture.

It does appear that preparations from HSO_3F via metal oxidation are the better route. It must be noted however that the reaction of $TaCl_5$ with $S_2O_6F_2$ takes a different course in the presence of CsCl (or $CsSO_3F$) than in its absence, where $TaO(SO_3F)_3$ reportedly[13] forms. For convenience, the products formed via Reactions (5-2) and (5-3) are referred to as "Form α" and "Form β", respectively.

As is the case with niobium, the coordination sphere of tantalum is also expandable. Accordingly, the following reaction was attempted:

$$4\ CsSO_3F + 2\ Ta + 5\ S_2O_6F_2 \xrightarrow[2\ days,\ 40°C]{HSO_3F} 2\ Cs_2[Ta(SO_3F)_7] \qquad (5\text{-}4)$$

$Cs_2[Ta(SO_3F)_7]$ was isolated by filtration, to discriminate against a possible mixture of $Cs[Ta(SO_3F)_6]$ and $CsSO_3F$ being present, the latter being very soluble in HSO_3F.[18] Once isolated, $Cs_2[Ta(SO_3F)_7]$ redissolves only sparingly (up to ~ 0.1 M) in HSO_3F.

$Cs_2[Ta(SO_3F)_7]$ was also prepared in the absence of HSO_3F by an alternative procedure, according to:

$$2\ CsCl + TaCl_5 + 7/2\ S_2O_6F_2 \xrightarrow[3\ hrs.]{25°C} Cs_2[Ta(SO_3F)_7] + 7/2\ Cl_2 \qquad (5\text{-}5)$$

The product was isolated by removing the volatiles in vacuo and an exact weight balance

was obtained. The salts isolated by Reaction (5-4) and (5-5) both appeared to have the same structure, the same melting point, and gave rise to nearly identical infrared and ^{19}F NMR spectra, as will be discussed later.

The thermal stabilities of α-$Cs[Ta(SO_3)F)_6]$ and $Cs_2[Ta(SO_3F)_7]$ were found to be very comparable to that of their niobium analogs, with the former melting at about five degrees higher while the latter melted about two degrees lower.

The successful isolation of the unusual heptakis(fluorosulfato) tantalate(V) salt, $Cs_2[Ta(SO_3F)_7]$, is not surprising in view of the known heptacoordinate fluorocomplexes of the type $M^I_2[TaF_7]$,[1,2] where M^I = an alkali metal or NH_4. Nevertheless, both the Nb and Ta salts provide the first examples of heptakis(fluorosulfato) anions.

5.C.1.d. Attempted Syntheses of Other $Ta(SO_3F)_5$ Derivatives

Most puzzling is the failure to synthesize $Ba[Ta(SO_3F)_7]$. Whereas $Ba[Nb(SO_3F)_7]$ could be isolated by filtration from HSO_3F solution, multiple attempts at the isolation of $Ba[Ta(SO_3F)_7]$ by filtration and by removal of volatiles in vacuo led to partially decomposed products as gauged by weight measurements, microanalysis, and infrared spectroscopy. Analysis for all elements except oxygen led to the conclusion that the products obtained by filtration were a mixture of the desired product and some other fluoro(fluorosulfato) species, perhaps of the form $TaF_x(SO_3F)_{5-x}$. This was supported by the high fluorine value, the low sulfur value, and the extremely high tantalum and correspondingly low cesium values (see Section 5.B.3.b). The obtained yields were always lower than expected (when isolated in vacuo) and the various products' infrared spectra invariably gave evidence for the presence of Ta-F bonds. There is at present no satisfactory explanation for this difference in behavior between Nb and Ta.

The synthesis of $Cs_3[Ta(SO_3F)_8]$, by both oxidative chloride substitution and metal oxidation, was unsuccessful. The existence of the target material was suggested by the known Na_3TaF_8.[2] Products (isolated in vacuo) were contaminated by either the presence of chloride or by unreacted $CsSO_3F$, as evident from microanalysis and infrared spectra. The chloride substitution, it seems, does not go to completion. Products obtained by metal oxidation (isolated by filtration) are of "ambiguous" composition. Repeatedly, sulfur analyses agreed very well with the expected composition, but the cesium, tantalum and fluorine values all agreed with $Cs[Ta(SO_3F)_6]$. Furthermore, the infrared spectrum (see Section 5.C.2.b) has characteristics of both the α- and β- forms of the latter salt.

To gain further understanding of the effect of changing the countercation, the syntheses of $Li_x[Ta(SO_3F)_{5+x}]$, with $x = 2$ or 3, type salts were attempted. Unfortunately, very viscous oils or paste-like materials were obtained, which could not be completely separated from the solvent without the onset of visible decomposition. No characterization could consequently be undertaken.

It hence appears that the large, electropositive Cs^+ is the only cation that is capable of stabilizing the $[Ta(SO_3F)_{5+x}]^{x-}$ anions ($x = 1$ or 2), indicating their somewhat unstable nature. This will be further discussed in Chapter 6.

5.C.1.e. Synthesis of $TaF_4(SO_3F)$

The preparation of impure $TaF_4(SO_3F)$ from the solvolysis of TaF_5 in HSO_3F pointed to the possible existence of this compound. A concentrated (1.9 M) solution of $Ta(SO_3F)_5$ in HSO_3F was used as one of the reagents in its successful preparation, according to:

$$[TaF_5]_4 + Ta(SO_3F)_5 \xrightarrow[18\ hrs.,\ 25°C]{HSO_3F} 5\ TaF_4(SO_3F) \qquad (5\text{-}6)$$

Exact stoichiometry was very important here, since the product was isolated by removal of all volatiles in vacuo. The success of the reaction indicates that facile F vs. SO_3F interchange occurred with tantalum as the central metal, as had been reported previously for the SbF_5-SO_3F systems.[19,20] The successful removal of all HSO_3F at room temperature in vacuo suggested that $TaF_4(SO_3F)$ is less strongly solvated than $Ta(SO_3F)_5$ in the acid. It is noteworthy that the presence of $Ta(SO_3F)_{5(solv)}$ enhanced the solubility of TaF_5 in fluorosulfuric acid.

Two very unusual features of this reaction and its product deserve mention: (i) the obtained yield was only 52% and (ii) the product was thermally stable up to a much higher temperature (200 - 220 °C) than $NbF_2(SO_3F)_3$ (126 - 129 °C) or any of the salts (~70 - 130 °C). The first feature can best be explained by assuming that either the product or some reaction intermediate(s) together with excess HSO_3F are volatile. The high melting point of $TaF_4(SO_3F)$ is however not consistent with any significant volatility. It is likely that ligand redistribution occurred in solution via Equation (5-6). The solvated, possibly mono- or dimeric species is partly volatile in the presence of HSO_3F and will partly polymerize to remain as an involatile, high melting solid. The known melting point of 96.8 °C[4] for $[TaF_5]_4$ and the low thermal stability of $Ta(SO_3F)_5$

(see Section 5.C.1.a-b) makes the high decomposition point of $TaF_4(SO_3F)$ even more unexpected. To the author's knowledge, there are surprisingly no known species of the form $Ta^{V}F_4X$, with X = any ligand, reported in the literature.

5.C.2. Vibrational Spectroscopy

5.C.2.a. $Cs_x[Ta(SO_3F)_{5+x}]$, with x = 1 or 2

As was the case with $Nb(SO_3F)_5$ earlier in Chapter 4, the high solubility of $Ta(SO_3F)_5$ in HSO_3F and its extensive solvation in this medium precluded its study in solid state via vibrational spectroscopy. The results of some limited solution studies are discussed in Chapter 6. Both infrared and Raman spectra were obtained for $Cs[Ta(SO_3F)_6]$ and $Cs_2[Ta(SO_3F)_7]$, with the data compiled in Table 5.I. Many of the band assignments suggested are identical to those already discussed for the analogous niobium salts. As mentioned, the hexakis(fluorosulfato) tantalum salts appear to exist in two different structural forms, whose respective IR spectra are also shown in Figure 5.1. In spite of the relatively poor quality of the spectra, due mostly to solid state effects, the differences between them is quite apparent. The most obvious difference is the presence of the unique bands at 1263 cm^{-1} in the α-form and at 1090 cm^{-1} in the β-form. Secondly, the band complexity and the lack of resolution in the ~600 - 1000 cm^{-1} region of the α-form spectrum is not observed for the β-form. The similarities between the spectrum of α-$Cs[Ta(SO_3F)_6]$ and that of $Cs[Nb(SO_3F)_6]$ suggest similar structures and a comparable tendency to form oligomers or polymers for both.

The Raman spectrum of α-$Cs[Ta(SO_3F_6)]$, shown in Figure 5.2, although very similar, is not quite identical to that of $Cs[Nb(SO_3F)_6]$, shown in Figure 4.1. The major difference is the absence of a band at 1106 cm^{-1}, usually assigned to the $\nu(SO)_3$ mode of

Table 5.I. Vibrational Frequencies of $Cs_x[Ta(SO_3F)_{5+x}]$, with x = 1 or 2

α-$Cs[Ta(SO_3F)_6]$				β-$Cs[Ta(SO_3F)_6]$		$Cs_2[Ta(SO_3F)_7]$				
Raman ($\Delta\nu$, cm^{-1})		IR (ν, cm^{-1})		IR (ν, cm^{-1})		Raman ($\Delta\nu$, cm^{-1})		IR (ν, cm^{-1})		Approx. Assign.
1436	w	1433	s,b	1425	s			~1415	s,b	ν_{as} (SO_3)
		~1390	s,vb,sh							
1269	vs	1263	m			1272	s	1255	m,b,sh	ν_s (SO_3) monodentate
1233	w	1221	s,b	1220	s			1215	s	
		~1120	m,br,sh	1112	m,sh					ν (SO_2) bidentate
				1090	m,sh	1080	vw,b	1080	m	
953	m	~930	s,vb	~955	s,vb	956	m	955	s,b	ν (O-SO_2F)
844	m	~840	s,vb	830	s	851	m	~830	m,b	ν (S-F)
~825	w,b,sh									
				682	m	686	m	688	m,sh	
645	m	638	s	635	m,sh	656	w	660	m	ν_s (Ta-O) + δ (SO_3F)
		610	s,b,sh					625	m,sh	
563	m	556	s	560	m	569	w	560	m	δ (SO_3F)
552	m	524	s,b,sh							
436	w	435	s	434	m	442	vw	430	w	
								420	w,sh	ν_{as} (Ta-O) + δ (SO_3F)
406	vw	413	s	412	m			411	w,sh	
255	m					257	s			skeletal and
194	s					198	s			lattice vibrations

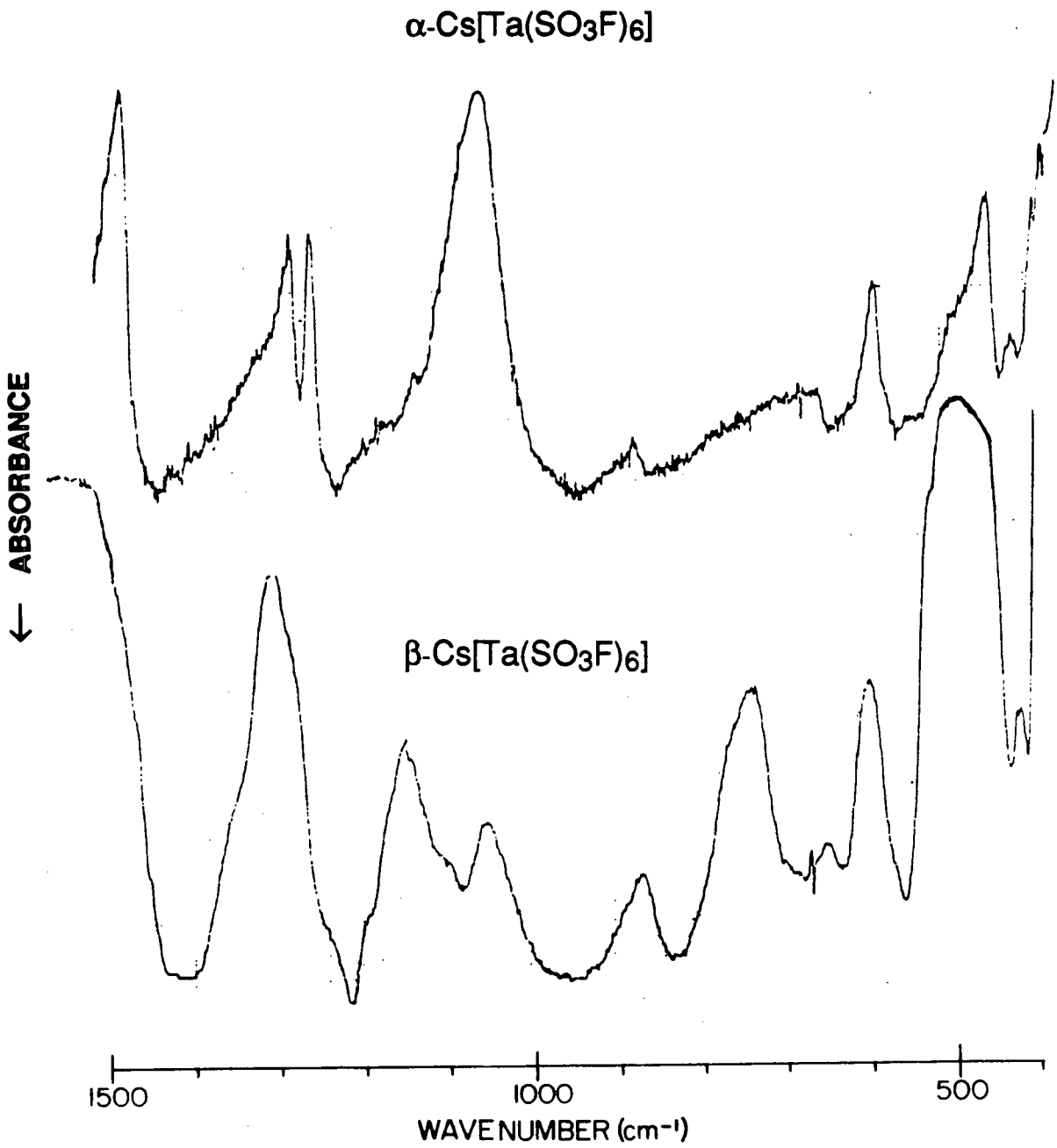

Figure 5.1. Infrared Spectra of the α- and β-Form of $Cs[Ta(SO_3F)_6]$ from 400 to 1500 cm^{-1}

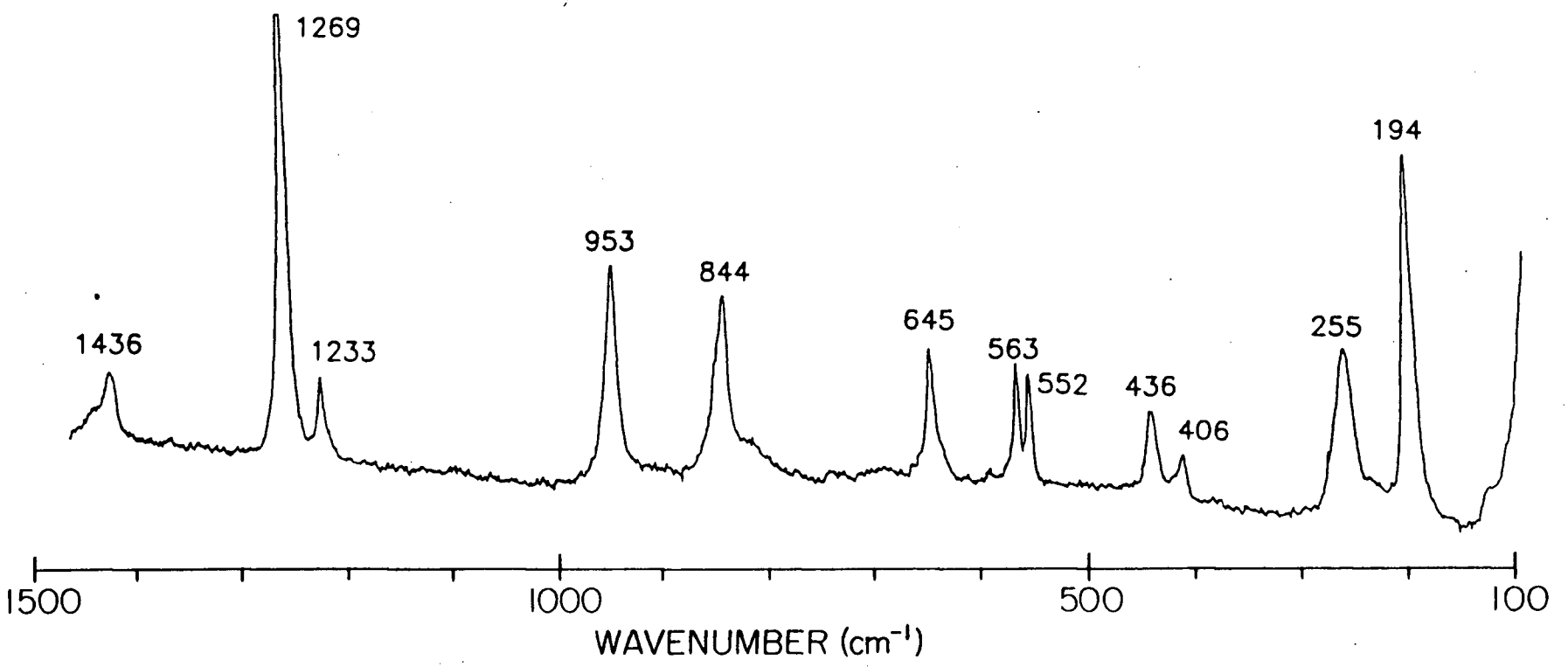

Figure 5.2. Raman Spectrum of α-Cs[Ta(SO_3F)$_6$] from 100 to 1500 cm^{-1}

a bidentate SO_3F group.[21,22] However, bands due to the ν(S-F) mode at both 844 cm^{-1} and ~825 cm^{-1} (weak, broad shoulder) indicate the presence of two different SO_3F groups, which would be expected if both monodentate and bridging bidentate ligands were present. An extremely broad, poorly resolved ν(S-F) band is also present in the IR spectrum (Figure 5.1) at about 840 cm^{-1}, which may partly be the result of multiple S-F environments, consistent with the above reasoning.

The simplicity of the IR spectrum of β-$Cs[Ta(SO_3F_6)]$ suggests the presence of the expected monomeric structure, possibly with octahedrally coordinated tantalum. Unfortunately, a Raman spectrum could not be obtained for this material. Two spectral features appear to argue against the exclusive presence of monodentate groups, namely the *shoulders* at 1112 and 1090 cm^{-1}, which fall in a region of $\nu(SO_3)$ modes due to bidentate SO_3F groups. However, both $Cs_2[Sn(SO_3F)_6]$ and $Cs_2[Ge(SO_3F)_6]$, where no bridging is expected,[22] show strong bands at 1091 and 1098 cm^{-1}, respectively, in their Raman spectra.

Both the Raman and IR spectra data of $Cs_2[Ta(SO_3F)_7]$ listed in Table 5.I are simpler than those obtained for $Cs_2[Nb(SO_3F)_7]$ in Chapter 4. However, the poor quality of the Raman spectrum necessitates caution. Although both band shapes and positions of $Cs_2[M(SO_3F)_7]$, with M = Nb or Ta, are reasonably similar, the latter displays a smaller degree of band proliferation. Except for the band at 1080 cm^{-1} in both the Raman and IR spectra, there is no additional evidence for any bidentate SO_3F groups, as there was in the $Cs_2[Nb(SO_3F)_7]$ spectra.

A band at 688 cm^{-1} (IR) and 686 cm^{-1} (Raman) is found for $Cs_2[Ta(SO_3F)_7]$ and β-$Cs[Ta(SO_3F)_6]$ (682 cm^{-1}). This band may be due to a Ta-F stretching mode, although

decomposition via SO_3 elimination is not apparent from the chemical analysis. Alternatively, this band may be attributed to a combined vibration of ν(Ta-O) + $\delta(SO_3F)$, which may occur at this somewhat higher than normal energy as a result of an *exclusively monodentate* SO_3F coordination environment around the metal leading to an increase in the average Ta-O bond strength. Hence, it is possible that $Cs_2[Ta(SO_3F)_7]$ exists with discrete $[Ta(SO_3F)_7]^{2-}$ anionic units, even though the analogous $Cs_2[Nb(SO_3F)_7]$ salt appears to involve bidentate SO_3F groups.

It is very unfortunate that suitable crystals for X-ray diffraction studies have not been isolable for any of these salts, since it is apparent that vibrational spectroscopy is not quite sufficient for understanding their structure. Nevertheless, vibrational spectra do allow some insight into the coordination of SO_3F groups in these salts.

5.C.2.b. Other $Ta(SO_3F)_5$ Derivatives

Infrared spectra of products obtained from various attempts to synthesize $Ba[Ta(SO_3F)_7]$ all showed extensive band complexity in the 800 - 1450 cm^{-1} region. This is not too surprising, since the spectrum of analytically pure $Ba[Nb(SO_3F)_7]$, described in Chapter 4, showed comparable band proliferation. Partial decomposition is suggested and the lack of good analytical data precludes any further discussion.

Attempts to obtain $Cs_3[Ta(SO_3F)_8]$ via oxidative chloride substitution led to impure materials, as indicated by the presence of $CsSO_3F$ vibrational modes at ~1400, 1075, 720, and 590 cm^{-1} in the IR spectrum. Metal oxidation yielded products of uncertain composition and evidence for $CsSO_3F$ was again found in the IR spectrum.

5.C.2.c. $TaF_4(SO_3F)$

Data from the infrared and Raman spectra of $TaF_4(SO_3F)$ are listed in Table 5.II, while its Raman spectrum is shown in Figure 5.3. Some difficulties are encountered in

Table 5.II. Vibrational Frequencies of $TaF_4(SO_3F)$

Raman ($\Delta\nu$, cm^{-1})		IR (ν, cm^{-1})		Approx. Assignment
		1403	m	ν_{as} (SO_3)
1191	w	1180	s	
1123	s	1112	s,b	ν (SO_3)
1105	w,sh			
1083	m	1075	s,sh	
		895	m,sh	ν (S-F)
		879	m,sh	
748	vs			ν_s (Ta-F)
725	m	733	m	
716	m	708	m	ν (Ta-F)
691	m	684	m	+
671	m			ν_s (Ta-O)
660	vw,sh	663	m,sh	+
648	w	644	m	δ (SO_3F)
620	vw,b	611	w	
488	w	486	w	ν_{as} (Ta-O) + δ (SO_3F)
470	w	464	vw,sh	
308	w			
283	m,sh			
268	m			lattice vibrations
241	w			+
228	w			torsion modes
220	w,sh			
200	w			

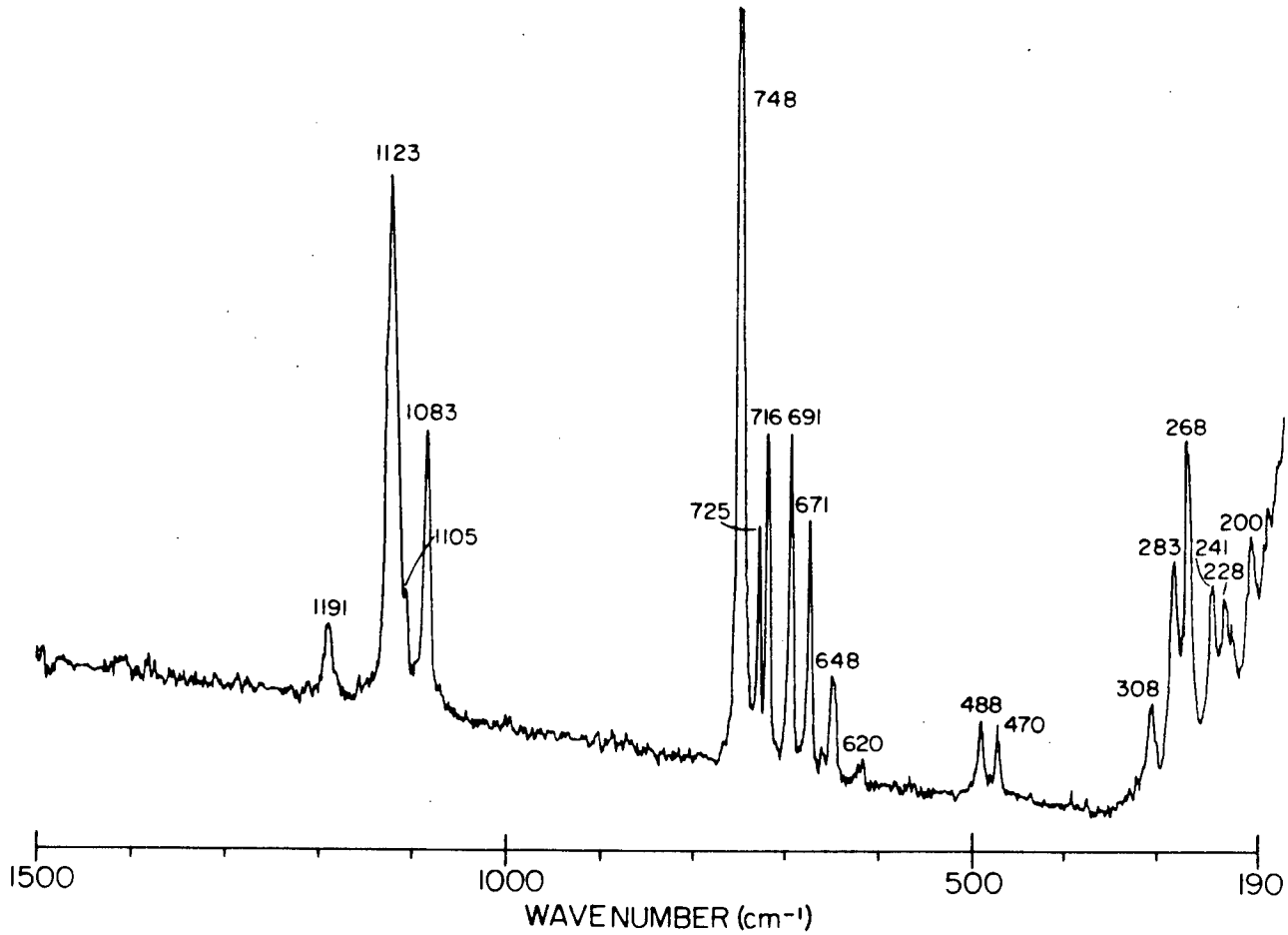

Figure 5.3. Raman Spectrum of $TaF_4(SO_3F)$ from 190 to 1500 cm^{-1}

arriving at a consistent and convincing interpretation for a number of reasons: (i) The spectra are not optimal; bands at about 1400 and 900 cm^{-1} are seemingly too weak to be picked up in the Raman spectrum and SO_3F deformation modes found consistently between 600 and 400 cm^{-1}, regardless of the SO_3F group conformation, are not clearly identifiable in either the IR or Raman spectrum. (ii) Precedents like $SbF_4(SO_3F)$[23] or $MF_2(SO_3F)_2$,[22,24] with M = Sn or Ge, are clearly not useful because in all instances the central atom has the coordination number six. This is not the case for tantalum nor for the previously discussed niobium. Thus, $NbF_2(SO_3F)_3$ and fluoro(fluorosulfate) derivatives of pentavalent uranium serve as more appropriate precedents. (iii) Support from auxiliary structural techniques, such as ^{119}Sn Mössbauer spectroscopy in the case of tin, are not available for solid state compounds with tantalum as the metal.

There are nevertheless some general observations possible which should be expandable once more examples of this structural type become available. Band positions and intensities in the SO_3F stretching region strongly suggest presence of bidentate (less pronounced $\nu(SO_3)$ at 1400, 1120 and 1080 cm^{-1}) and tridentate (more prominent bands at 1180 and 1120 cm^{-1}) SO_3F^- groups. There are two ν(S-F) bands at 895 and 879 cm^{-1}, but a clear, unambiguous attribution to either of the two bonding modes is difficult. A Raman band, $\Delta\nu$ = 748 cm^{-1}, in the Ta-F stretching region is of remarkably high intensity, suggesting a reasonably symmetric environment for Ta. There is no conclusive evidence for Ta-F-Ta bridging and only terminal Ta-F groups (ν(Ta-F) ≈ 650-750 cm^{-1}) are discernible. The coordination number of Ta appears to be seven or eight but clear distinction is not possible. Finally, in spite of the simple molecular formula $TaF_4(SO_3F)$, the material may be polynuclear with two or more different tantalum atoms in an overall oligo- or polymeric structure.

5.D. Conclusion

Although it was not possible to isolate $Ta(SO_3F)_5$ from HSO_3F solution, this material was found to be more resilient towards decomposition via SO_3 elimination than $Nb(SO_3F)_5$. Reaction of solvated $Ta(SO_3F)_5$ with one mole equivalent of $(TaF_5)_4$ in HSO_3F led to the isolation and vibrational characterization of $TaF_4(SO_3F)$ as an analytically pure, stable, and most likely polymeric solid. The course of reaction (5-6) allows the following concluding remarks to be made:

(i) successful isolation of $TaF_4(SO_3F)$ provides further proof for the initial presence of $Ta(SO_3F)_5$ and for the occurrence of F vs. SO_3F exchange in solution;

(ii) the solubility of $TaF_4(SO_3F)$ should allow solution studies in HSO_3F via ^{19}F NMR;

(iii) ligand redistribution is an efficient means of enhancing the solubility of TaF_5 in HSO_3F, resulting in enhanced interest in this solvent system.

The ternary salts $Cs[Ta(SO_3F)_6]$ and $Cs_2[Ta(SO_3F)_7]$ have also been isolated and characterized using IR and Raman spectroscopy. Tentative evidence for the preparation of $Cs_3[Ta(SO_3F)_8]$ was gathered but the impure products obtained (with no possibility of purification) precluded its characterization. Evidence was obtained via vibrational spectroscopy for the presence of oligomeric tantalates in both the salts α-$Cs[Ta(SO_3F)_6]$ and $Cs_2[Ta(SO_3F)_7]$. Conversely, the β-form of $Cs[Ta(SO_3F)_6]$ appeared to exist with tantalum in the expected octahedral coordination environment.

The high solubility of $Ta(SO_3F)_5$ in HSO_3F makes it ideal for a systematic solution study in HSO_3F. The next chapter will deal with these studies, which will serve to illustrate, among other things, to what extent these two species enhance the acidity of the already superacidic fluorosulfuric acid.

REFERENCES

1. F. Fairbrother, *"The Chemistry of Niobium and Tantalum"*, Elsevier, London, 1967.

2. D. Brown, *Chemistry of Niobium and Tantalum* in *"Comprehensive Inorganic Chemistry"*, Pergamon Press, N.Y., Vol.III, 1973.

3. A.J. Edwards, *J. Chem. Soc.*, 3714 (1964).

4. *"Handbook of Chemistry and Physics"*, 57th Edition, R.C. Weast, Ed., C.R.C. Press, U.S.A., 1976-1977.

5. G.A. Olah, G.K.S. Prakash and J. Sommer, *"Superacids"*, J. Wiley & Sons, N.Y., 1985 (and references herein).

6. O.L. Keller, Jr. and A. Chetham-Strode, Jr., *Inorg. Chem.* **5**, 367 (1966).

7. N.A. Matwiyoff, L.B. Asprey and W.E. Wageman, *Inorg. Chem.* **9**, 2014 (1970).

8. S.P. Mallela, S. Yap, J.R. Sams and F. Aubke, *Rev. Chim. Min.* **23**, 572 (1986).

9. J.L. Hoard, W.J. Martin, M.E. Smith and J.F. Whitney, *J. Am. Chem. Soc.* **76**, 3820 (1954).

10. R.B. English, A.M. Heyns and E.C. Reynhard, *J. Phys. C: Solid State Phys.* **16**, 829 (1983).

11. D.L Kepert, *"The Early Transition Metals"*, Academic Press, London, Chapt. 3, 1972.

12. H.C. Clark and H.J. Emeléus, *J. Chem. Soc.*, 190, (1958).

13. G.C. Kleinkopf and J.M. Shreeve, *Inorg. Chem.* **4**, 607 (1964).

14. E. Hayek, J. Puschmann and A. Czaloun, *Montash. Chem.* **85**, 360 (1954).

15. K.C. Lee and F. Aubke, *Inorg. Chem.* **18**, 389 (1979).

16. K.C. Lee, Ph.D. Thesis, University of British Columbia, 1980.

17. I.R. Beattie, K.M.S. Livingston, G.A. Ozin and D.J. Reynolds, *J. Chem. Soc. A.*, 958 (1969).

18. A.W. Jache, *Adv. Inorg. Chem. Radiochem.* **16**, 177 (1974).

19. R.C. Thompson, J. Barr, R.J. Gillespie, J.R. Milne and R.A. Rothenbury, *Inorg. Chem.* **4**, 1641 (1965).

20. R.J. Gillespie and T.E. Peel, *Adv. Phys. Org. Chem.* **9**, 1 (1972).

21. K.C. Lee and F. Aubke, *Inorg. Chem.* **23**, 2124 (1984).

22. S.P. Mallela, K.C. Lee and F. Aubke, *Inorg. Chem.* **23**, 653 (1984).

23. W.W. Wilson and F. Aubke, *J. Fluor. Chem.* **13**, 431 (1979).

24. L.E. Levchuk, J.R. Sams and F. Aubke, *Inorg. Chem.* **11**, 43 (1972).

CHAPTER 6

SOLUTION STUDIES IN HSO_3F

6.A. INTRODUCTION

Although the high solubility and strong solvation of both $Nb(SO_3F)_5$ and $Ta(SO_3F)_5$ in HSO_3F has prevented their isolation, detailed solution studies in this solvent are possible. The isolation of cesium salts of the type $M_x'[M(SO_3F)_{5+x}]$ (x = 1 or 2 and M = Nb or Ta) suggested that both $M(SO_3F)_5$ species exist in solution and behave as fluorosulfate acceptors. Furthermore, the isolation of the species $[M(SO_3F)_7]^{2-}$ with both metals suggested that $Nb(SO_3F)_5$ and $Ta(SO_3F)_5$ may behave as diprotonic acids in HSO_3F. This characteristic is significant since only one other diprotonic super acid has been reported in the literature: the HSO_3F-$Pt(SO_3F)_4$ system.[1] The solution studies in HSO_3F-$M(SO_3F)_5$ solutions to be discussed in this chapter will consist of:

(i) Electrical conductivity and conductometric titration measurements;

(ii) Hammett acidity (H_0) determination for $Ta(SO_3F)_5$;

(iii) ^1H, ^{19}F and ^{93}Nb variable temperature NMR spectroscopy;

(iv) Raman spectroscopy.

A brief introduction to each of the sections follows, although some of the basic aspects have already been covered in Chapter 1.

(i) Electrical Conductivity Measurements

Initial determinations of acidity in HSO_3F have previously been obtained using electrical conductivity for the Lewis acids SbF_5,[2] $SbF_5 \cdot nSO_3$ ($n \leq 3$),[2] NbF_5,[3] AsF_5,[3] $AsF_5 \cdot nSO_3$ ($n \leq 3$),[3] and more recently, $Au(SO_3F)_3$[4] and $Pt(SO_3F)_4$.[1] Of all these species, only $SbF_2(SO_3F)_3$ is completely dissociated in HSO_3F and therefore ranks as the strongest known acid in HSO_3F.[2,5]

The determination of a solute's mode of dissociation via conductometry in a given protonic solvent requires two steps:[6] (i) measurement of the solution's conductivity to establish that the solute behaves as an electrolyte in the solvent and (ii) conductometric titration of the solution with a strong base to determine whether the solute behaves as an acid or a base.

The behaviour of ternary salts in solution can also be investigated in this manner, as has been done previously in HSO_3F with potassium salts of the type $K_x[M(SO_3F)_{n+x}]$, where $x = 1$ or 2, $n = 3$ or 4, and M = Au,[4] Pt,[1] or Sn.[7] These types of salts (derived from strong bases) will be at best neutral but more likely basic, thus providing an additional measure of a superacid's acidity.

(ii) Hammett Acidity (H_o) Measurements

As stated in Chapter 1, the Hammett Acidity Function (H_0) is the accepted quantitative indicator of acidity in very concentrated aqueous or non-aqueous acids. The definition of H_0 is given in Equation (1-9) of Chapter 1. The reliability of this function as an acidity indicator rests primarily on the proper selection of aromatic Hammett base indicators. The very critical pK_{BH+} value (Equation (1-9)) can be *directly* obtained for a

given base only in very dilute aqueous acid solutions,[8,9] since only then is the H_0 scale equal to the pH scale. At higher acid concentrations or for non-aqueous acids, a set of indicators of decreasing basicity must be used and the pK_{BH+} values calculated from their degree of overlap with each other. Each indicator is only reliable over a range of about 2 log units and therefore a different indicator is necessary per each log unit in order to establish a set of accurate pK_{BH^+} values.[8] These values have been collected for a large range of indicators.[8] A sampling corresponding to the weaker bases in this range is listed in Table 1.III.

From a set of Hammett bases with known pK_{BH+} values, a selection can be made to determine the H_0 values for a given acid or superacid system. These bases must be selected to provide sufficient overlap between the acidity range over which each base is used. From Equation (1-9), it follows that the term log[BH+]/[B] restricts the range of a given indicator to ±1 log unit, so that three or four different indicators are required to accurately study an acidity range spanning 4 log units.

It has been previously reported[8,9,10] that the pK_{BH+} of a given Hammett indicator is nearly constant among different solvents of similar acidity and it is therefore unnecessary to determine pK_{BH+} for a new solvent system. The determination of H_0 for a given acid system then involves the calculation of the ionization ratio, log[BH+]/[B], by using a series of indicators with overlapping acidity detection ranges. Determination of log I may be accomplished via uv/vis spectrophotometry, as described in the upcoming sections 6.B and 6.C.2., or by dynamic NMR spectroscopic methods.[8]

(iii) Multinuclear Variable Temperature NMR Spectroscopy of Niobium(V) and Tantalum(V) Superacid Systems

The Lewis acids NbF_5 and TaF_5, as well as some respective MI_xMF_{5+x} (x = 1 or 2) type alkali salts, have been studied via ^{19}F NMR in aqueous HF solutions of various strengths.[11,12] Although signals due to both $[NbF_6]^-$ and $[NbF_7]^{2-}$ were observed in solutions of HF/NbF_5, only one signal, attributed to $[TaF_6]^-$, was present in the HF/TaF_5 solutions even when using K_2TaF_7 as solute.

More detailed ^{19}F NMR investigations of the $[NbF_6]^-$ anion in the inert organic solvents acetonitrile[13] and dimethylformamide[14] have also been reported. Interesting decet patterns of various temperature-dependent shapes were observed due to coupling of the equivalent, octahedrally coordinated fluorine atoms to ^{93}Nb, which has a nuclear spin of 9/2. The quadrupole moment of ^{93}Nb ($(-0.26 \pm 0.6) \times 10^{-28}$ m2)[15-17] is small enough to allow the observation of ligand coupling in compounds of high symmetry. Conversely, the quadrupole moment of ^{181}Ta (I = 7/2) is more than ten times greater, explaining the uncoupled ^{19}F signals of $[TaF_6]^-$ in aqueous HF solutions.[12]

The ^{19}F NMR spectra of $[NbF_5(SO_3F)]^-$ and $[TaF_5(SO_3F)]^-$ in SO_2 at -70 °C have also been reported.[18] The singlet fluorosulfate fluorine resonance was observed 41.2 ppm downfield from $CFCl_3$ in both cases. In addition, two other singlet signals were observed further downfield in both systems, attributable to cis- and trans-fluorines.

The moderate quadrupole moment, 100% abundance and very high receptivity (third among all the elements, after ^1H and ^{19}F) of ^{93}Nb make symmetric niobium compounds suitable for ^{93}Nb NMR investigations. Surprisingly, ^{93}Nb is not an extensively studied nuclide, perhaps due to the significant line-broadening found for

molecules of lower symmetry. For example, the highly symmetric $[NbCl_6]^-$ in acetonitrile gives the smallest reported linewidth ($w_{1/2}$) of 50 Hz, but $NbOCl_3$, with a lower degree of symmetry, yields linewidths of 1000 Hz. This problem is further illustrated by the unsymmetrical, "open metal sandwich" compound $CpNb(CO)_4$, which is characterized by linewidths approaching 6 kHz.[19]

Previous ^{93}Nb NMR studies have frequently involved mixed halogen or oxyhalogen compounds.[19] However, $[NbF_6]^-$ has also been studied extensively in different solvents, such as ethanol,[20] acetonitrile,[13] dimethylformamide,[14] aqueous HF[20] and anhydrous HF.[11] The signals obtained have ranged from septets reflecting the coupling of ^{93}Nb to six equivalent spin 1/2 (^{19}F) nuclides, to singlets of varying linewidths. This solvent dependency has restricted the use of $[NbF_6]^-$ as a ^{93}Nb NMR reference, although it is the most highly shielded of all species studied to date. Consequently, $[NbCl_6]^-$ has replaced $[NbF_6]^-$ as the most commonly used reference standard in acetonitrile.[15] The chemical shift range for ^{93}Nb NMR is in excess of 2000 ppm.[16]

Due to its relatively low receptivity (less than 1/10 that of ^{93}Nb) and high quadrupole moment, ^{181}Ta NMR reports are extremely uncommon.[15,16] The only successful report[21] involved a solution of Ta metal dissolved in a 1:1 mixture of HF/HNO_3, in which the extremely broad signal ($w_{1/2}$ = 36 kHz) observed at ambient temperature was assigned to $[TaF_6]^-$. Interestingly, ^{181}Ta has the highest quadrupole moment of any nucleus whose NMR signal has been observed in solution.[16]

(iv) Raman Spectroscopy

The study of fluorosulfate compounds in fluorosulfuric acid solutions using vibrational spectroscopy is restricted by the presence of overlapping solvent bands and signal broadening. Nevertheless, the superacid systems HSO_3F-$Au(SO_3F)_3$[4] and HSO_3F-$Pt(SO_3F)_4$[1] have both been studied in this manner, and it was concluded that coordinatively fully saturated species of the type $[Au(SO_3F)_4]^-$ and $[Pt(SO_3F)_6]^{2-}$ were present in solution, results consistent with the respective ^{19}F NMR and electrical conductivity studies. In this report, Raman spectroscopy studies of superacid solutions are used only to verify results obtained from other more primary techniques, such as those mentioned above.

6.B. Experimental

6.B.1. Electrical Conductivity Studies

$Nb(SO_3F)_5$ and $Ta(SO_3F)_5$ solutions in HSO_3F were prepared as described in Chapters 4 and 5, respectively, except that HSO_3F was distilled directly into the reactors from the distillation apparatus. Following synthesis, the removal of excess $S_2O_6F_2$ from the solutions was monitored by weight loss, and ensured by obtaining the infrared spectra of the gas phase and Raman or ^{19}F NMR spectra of each solution prior to measuring their conductivities. The $M(SO_3F)_5$-MF_5 (M = Nb or Ta) solutions were prepared by distilling first $S_2O_6F_2$ and then HSO_3F onto a 1:1 molar mixture of the respective metal pentafluoride and metal powder. After complete dissolution of all solids, removal of $S_2O_6F_2$ was ensured as described above.

The various potassium salts studied were not isolated, but were studied in situ by obtaining electrical conductivities directly from the $S_2O_6F_2$-free solutions. To ensure reproducibility, the experiments described in this section were repeated at least twice.

6.B.2. Hammett Acidity Studies

H_0 functions were determined in accordance with the procedures described by Gillespie et al.,[10,22] except for a few minor changes. The apparatus used and the purification of the aromatic nitro indicators have been described earlier.

Solutions were prepared in the drybox by dissolving 0.01 - 0.02 g. of accurately weighed indicator in a known volume (~2 ml) of the stock acid mixture (~4 - 6 mole % in $Ta(SO_3F)_5$). An approximately 0.03 ml aliquot was then pipetted into another stock acid mixture of approximately 2 ml volume. After thorough mixing at both dilution stages, solutions were pipetted step-wise into the uv/vis cell described earlier, where they were diluted prior to each measurement by a small volume (~1 ml) of HSO_3F of identical indicator concentration. A reference sample containing the same $Ta(SO_3F)_5$ concentration as the sample studied was prepared at the same time from the stock acid mixture. Either 5 or 10 ml volumetric flasks were used for the preparation of all the solutions, and 0.2 - 2.0 ml pipets were employed for carrying out transfers. Reproducibility of the results was tested by carrying out the entire experiment twice.

The Beer-Lambert Law[23] was used to convert absorbance measurements into extinction coefficients:

$$\varepsilon = \frac{A}{CL} \qquad (6\text{-}1)$$

where: ε = extinction coefficient (molar absorptivity)
A = absorbance
L = cell path length
C = indicator concentration

6.B.3. Multinuclear NMR and Raman Spectroscopy Studies

Experimental methods for these studies were described in part earlier. $LiNbF_6$ was used as external reference for the ^{93}Nb experiments and was prepared from a 1:1 mixture of LiF and NbF_5 in anhydrous HF at room temperature. The identity of the sample was checked by X-ray powder diffraction[24] and by the absence of NbF_5 bands in the IR spectrum. Furthermore, the ^{19}F NMR decet line pattern of the material dissolved in propylene carbonate matched the pattern reported for $[NbF_6]^-$ in acetonitrile[13] or dimethylformamide.[14] $LiNbF_6$ was chosen as the external reference because it yields relatively sharp ^{93}Nb NMR signals in a diverse variety of solvents.[16] Propylene carbonate was chosen as the solvent for two reasons: (i) its ability to dissolve >5 molar $LiNbF_6$ and (ii) its compatability with the solute. Free NbF_5 caused propylene carbonate to polymerize within a few hours, as was evident from the solution's deep red colour and the increase in its viscosity.

All solutions were prepared in the drybox, as described earlier, with solute concentrations made very close to the saturation point. An 8 molal "$Ta(SO_3F)_5$" solution was obtained from a 1.6 M solution by removing HSO_3F in vacuo and thus reducing the *total* weight of the solution below that expected for acid-free $Ta(SO_3F)_5$. Residual HSO_3F in the resulting liquid indicated decomposition of $Ta(SO_3F)_5$.

6.C. Results and Discussion

6.C.1. Electrical Conductivity Studies

6.C.1.a. Electrical Conductance Measurements

The specific conductance data measured for solutions of $Nb(SO_3F)_5$ and $Ta(SO_3F)_5$ at 25 °C in the concentration range 0 to 0.05 molal are listed in Table 6.I. Both species behave as electrolytes in HSO_3F, as indicated by the concentration dependent increase in their specific conductance. Both solutions were also titrated with HSO_3F solutions of the standard base KSO_3F[25] to determine their mode of dissociation. The specific conductance data, concentrations and $K/M(SO_3F)_5$ ($K = KSO_3F$, M = Nb or Ta) ratios are listed in Table 6.II. Plots of the measured conductance vs. $K/M(SO_3F)_5$ ratios are shown in Figure 6.1. Both plots pass through a minimum in conductance, although at different acid-base ratios, and the equivalence points occur at an approximately 1:1 ratio. Therefore, both $Nb(SO_3F)_5$ and $Ta(SO_3F)_5$ behave as *monoprotonic acids* (albeit of different strength) in HSO_3F, with $Ta(SO_3F)_5$ the better conductor in the concentration range studied and therefore the stronger acid.

For a completely dissociated monoprotonic acid, the inversion point will occur at a KSO_3F/Y (Y = Lewis acid) ratio of 1.00 and will coincide with the point of minimum specific conductance.[2,4] If the acid is not completely dissociated, the minimum conductance will occur at a lower K/Y ratio. In the simplest situation, this can be expressed by the following equations:

$$2\,HSO_3F + Y_{(solv)} \overset{K_1}{\rightleftharpoons} H_2SO_3F^+_{(solv)} + [(Y)SO_3F]^-_{(solv)} \qquad (6\text{-}2a)$$

$$KSO_3F + H_2SO_3F^+_{(solv)} \xrightarrow{HSO_3F} K^+_{(solv)} + 2\,HSO_3F \qquad (6\text{-}2b)$$

Table 6.I. Specific Conductance Data in HSO_3F at 25.00 °C

$Nb(SO_3F)_5$		$Ta(SO_3F)_5$	
10^2m, mol/kg	$10^4\kappa$, Ω^{-1}/cm	10^2m, mol/kg	$10^4\kappa$, Ω^{-1}/cm
0	1.57	0	1.55
0.101	1.92	0.119	2.84
0.338	2.97	0.312	4.79
0.546	3.89	0.566	7.37
0.847	5.29	0.822	9.76
0.867	5.38	1.173	13.12
1.175	6.73	1.541	16.37
1.378	7.79	1.770	18.27
1.648	9.18	2.002	20.23
1.660	9.25	2.276	22.48
1.908	10.57	2.549	24.36
2.200	11.72	2.761	26.50
2.416	12.60	2.915	27.53
2.626	13.48	4.002	36.41
2.827	14.33		
3.037	15.27		
3.275	16.36		
3.522	17.44		
3.724	18.40		
3.914	19.30		
4.105	20.18		
4.183	20.56		

Table 6.II. Conductometric Titration of $Nb(SO_3F)_5$ and $Ta(SO_3F)_5$ with KSO_3F in HSO_3F at 25.00 °C

[Nb], 10^2m mol/kg	Mole Ratio, K/Nb	$10^4\kappa$, Ω^{-1}/cm	[Ta], 10^2m mol/kg	Mole Ratio, K/Ta	$10^4\kappa$, Ω^{-1}/cm
7.18	0	30.00	7.62	0	57.18
7.13	0.023	28.53	7.54	0.026	51.74
7.08	0.042	27.44	7.32	0.092	47.56
6.98	0.084	25.48	7.15	0.146	42.68
6.81	0.162	22.69	6.90	0.228	39.72
6.62	0.258	20.69	6.67	0.313	35.59
6.55	0.289	20.27	6.46	0.393	32.20
6.48	0.325	19.99	6.26	0.474	28.80
6.40	0.367	19.71	6.15	0.520	27.60
6.29	0.425	19.58	6.01	0.582	26.30
6.18	0.487	19.67	5.85	0.659	24.77
6.06	0.559	20.01	5.70	0.734	23.25
5.97	0.614	20.47	5.63	0.771	23.03
5.87	0.672	20.95	5.57	0.804	22.80
5.80	0.718	21.41	5.48	0.849	22.64
5.64	0.828	22.72	5.41	0.892	22.76
5.54	0.893	23.67	5.29	0.957	23.34
5.40	0.994	26.69	5.22	1.002	27.22
5.26	1.101	34.52	5.09	1.079	32.72
5.18	1.169	40.28	4.96	1.167	40.80
5.12	1.215	45.45	4.82	1.261	48.85

Since the molal conductance for K^+ (30) at infinite dilution[25] is a factor of 10 smaller than that for $H_2SO_3F^+$ (320),[2] the minimum in specific conductance for a very strong acid, such as $SbF_2(SO_3F)_3$[2] or $Au(SO_3F)_3$,[4] occurs when all the $H_2SO_3F^+$ is replaced by K^+. The increase in conductance at the equivalence point is a consequence of the highly mobile SO_3F^- ion (molal conductance of 235) increasing in concentration. As seen in

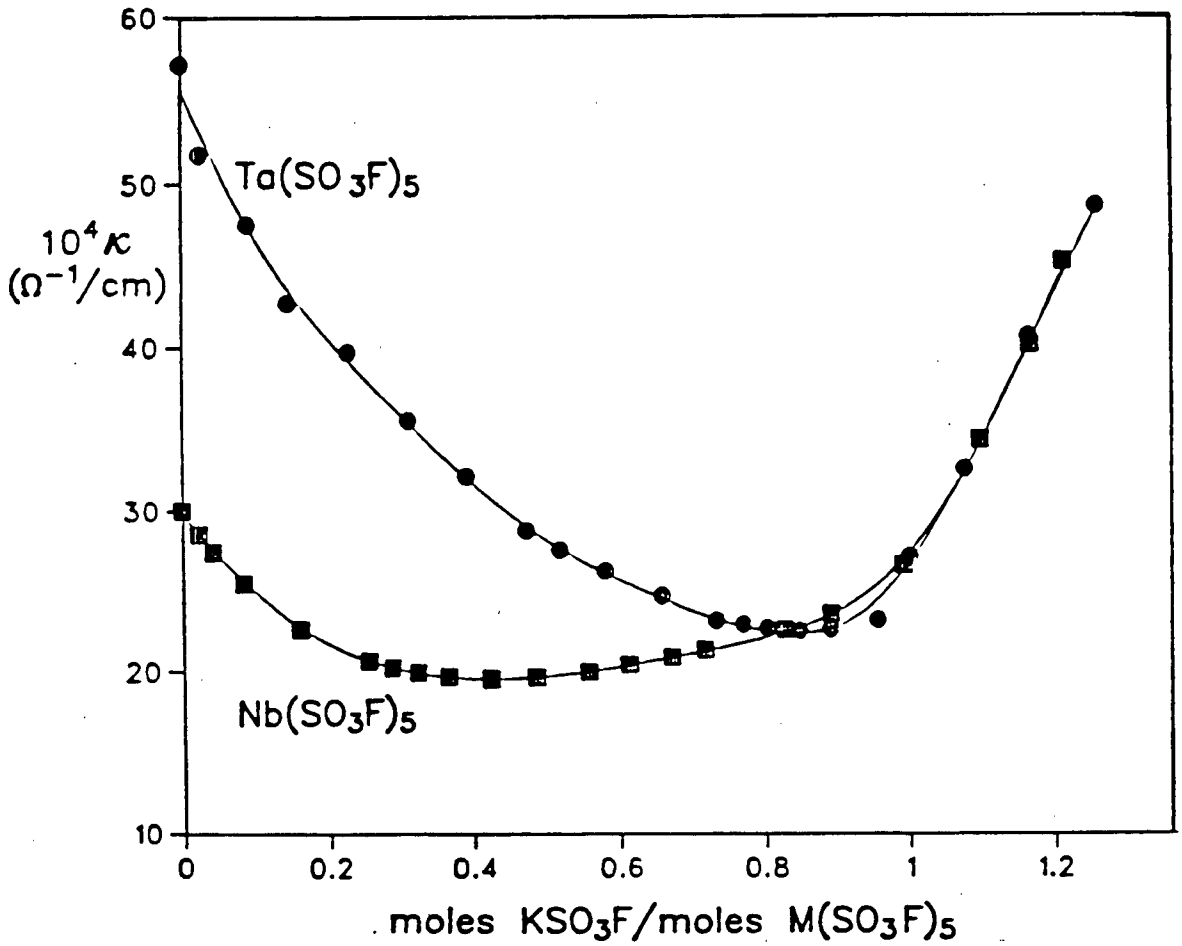

Figure 6.1. Conductometric Titration of $Nb(SO_3F)_5$ and $Ta(SO_3F)_5$ with KSO_3F in HSO_3F at 25.00 °C

Figure 6.1, minimum specific conductances for $Nb(SO_3F)_5$ and $Ta(SO_3F)_5$ occur at K/Y values of 0.43 and 0.85, respectively. This implies that $Ta(SO_3F)_5$ is a stronger acid in HSO_3F, but not quite as strong as either $SbF_2(SO_3F)_3$[2] or $Au(SO_3F)_3$.[4] For SbF_5 ("Magic Acid"), the minimum conductance occurs at a 0.4 ratio,[2] making it comparable in acid strength to $Nb(SO_3F)_5$. The occurrence of the inversion point at K/Y ratios of slightly less than 1.00 in the two acid systems studied may be due to trace basic impurities.

The acidium ion, $H_2SO_3F^+$ (Equation 6-2a), is the principal contributor to the electrical conductivity of acids in HSO_3F, via a proton transfer process.[5] Relative acidium ion concentrations can be evaluated from the slope of a specific conductance vs. Lewis acid concentration plot, which reflects the acid strength in that concentration range. Such a plot is shown in Figure 6.2 for $Nb(SO_3F)_5$ and $Ta(SO_3F)_5$. Reported conductivity data for the acids $Au(SO_3F)_3$,[4] SbF_5[2] and NbF_5[3] are shown for comparison. The relative slopes suggest the following order of solute acidity: $Au(SO_3F)_3 > Ta(SO_3F)_5 \geq SbF_5 > Nb(SO_3F)_5 >> NbF_5$. This is reasonably consistent with a ranking based on conductometric titration data. The curvature of the SbF_5 plot, attributed to solute association,[2] is not observed for any of the other solutes. From Figure 6.2, it is evident that $Nb(SO_3F)_5$ is a considerably stronger acid than NbF_5.[3] The low acidity of NbF_5 has also been attributed in part to its limited solubility in HSO_3F, presumably due to incomplete acidic dissociation of the tetramer. Comparable conductivity data are not available for TaF_5, but its acidity has been measured to be slightly greater than that of NbF_5.[8] This is analogous to the relative acidities of the respective fluorosulfates.

In order to investigate whether F/SO_3F exchange occurs in solution between the highly soluble $Nb(SO_3F)_5$ and the slightly soluble NbF_5, the specific conductance of an

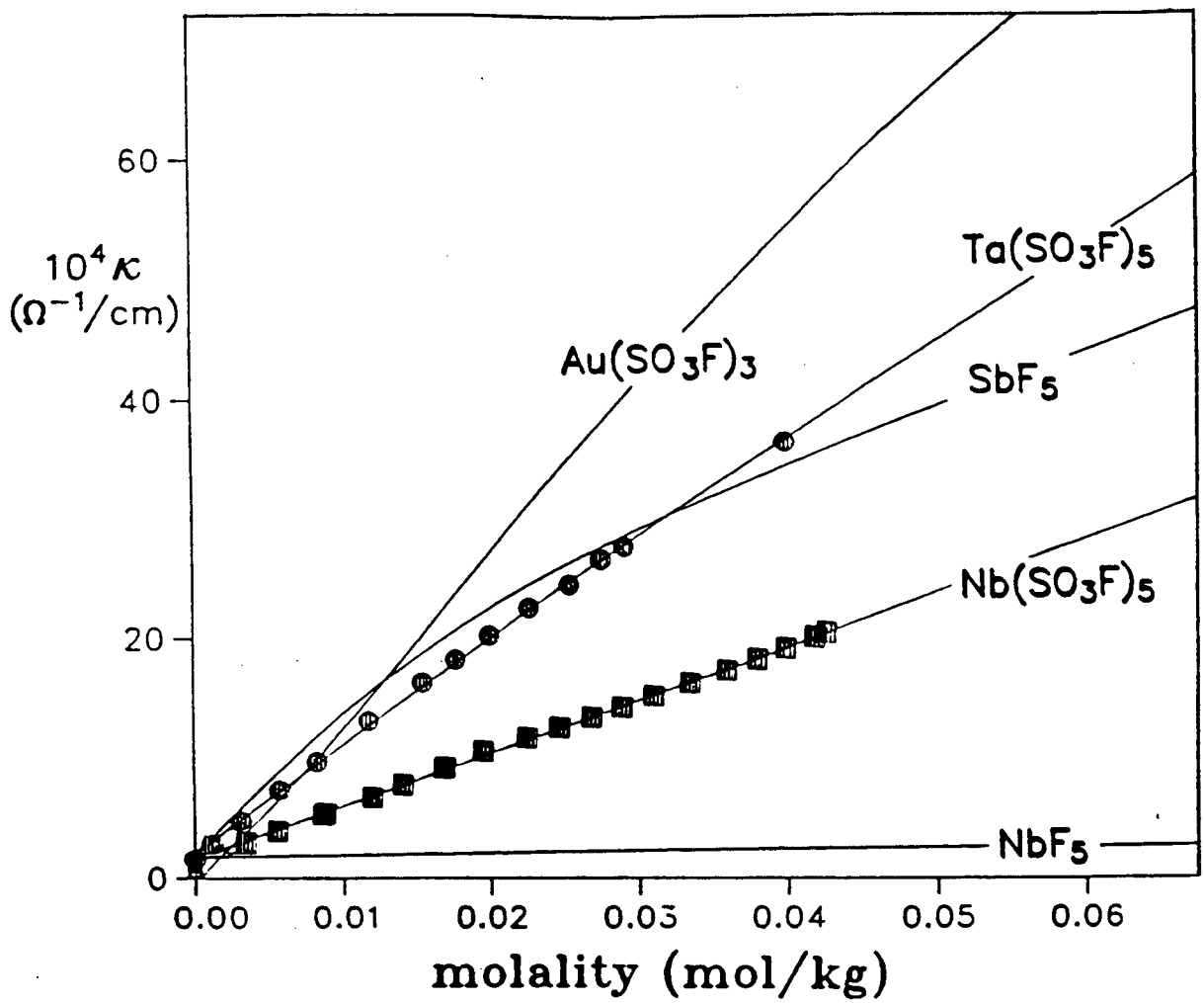

Figure 6.2. Specific Conductance of $Nb(SO_3F)_5$, $Ta(SO_3F)_5$ and Other Lewis Acids in HSO_3F at 25.00 °C ($Au(SO_3F)_3$: ref.4, SbF_5: ref.2, NbF_5: ref.3)

equimolar, dilute HSO_3F solution of $Nb(SO_3F)_5/NbF_5$ was measured. The data are listed in Table 6.III, along with data obtained for $Nb(SO_3F)_5$ and for NbF_5.[3] It is noted that the conductance values for the mixed systems fall approximately halfway between those of the two "parent solutes". Although enhanced solubility of NbF_5 suggests F/SO_3F exchange in solution, electrical conductivities are inconclusive in comfirming such behavior.

Table 6.III. Specific Conductance Data for the Niobium Systems at 25.00 °C

$Nb(SO_3F)_5$		$Nb(SO_3F)_5$ - NbF_5		NbF_5[a]	
10^2m mol/kg	$10^4\kappa$ Ω^{-1}/cm	10^2m mol/kg	$10^4\kappa$ Ω^{-1}/cm	10^2m mol/kg	$10^4\kappa$ Ω^{-1}/cm
0	1.57	0	1.81	0	1.08
0.101	1.92	0.338	3.71	2.30	3.08
0.546	3.89	0.751	4.89	3.20	2.92
0.867	5.38	1.425	6.22	5.46	3.35
1.378	7.79	2.340	7.56	6.90	3.72
1.660	9.25	3.498	9.03	11.10	4.72
2.200	11.72	4.712	10.48		
2.626	13.48				
3.037	15.27				
3.522	17.44				
3.914	19.30				
4.183	20.56				

[a]reference 3

Isolation of the salts $Cs_2[M(SO_3F)_7]$, with M = Nb or Ta, suggests that $Nb(SO_3F)_5$ and $Ta(SO_3F)_5$ behave as diprotonic acids in HSO_3F, in spite of the results from the conductometric titrations, which classify them as monoprotonic Lewis acids that dissociate to form the anion $[M(SO_3F)_6]^-_{(solv)}$ in solution (see Equation 6-2a). However,

it must be remembered that the heptakis(fluorosulfato) metallates are obtained with an excess of the base ion SO_3F^- present, whereas only a weakly basic medium is generated during the acid-base titrations. Furthermore, the second dissociation step to form the $[M(SO_3F)_7]^{2-}_{(solv)}$ species may involve a much smaller equilibrium constant than K_1 (see Equation 6-2a). Analogous to these findings, the systems HF-NbF_5 and HF-TaF_5 are viewed as monoprotonic acids in HF[8,26,27] even though salts like K_2NbF_7 and K_2TaF_7 exist.[28,29] Hence, the superacid system HSO_3F-$Pt(SO_3F)_4$[1] remains the only diprotonic superacid system known thus far. To gain further insight, specific electrical conductance measurements were obtained for solutions of $K[Ta(SO_3F)_6]$, $K_2[Nb(SO_3F)_7]$ and $K_2[Ta(SO_3F)_7]$ and the data are listed in Table 6.IV. Potassium was used instead of cesium as countercation in these studies for two reasons: (i) cesium salts show limited solubility in HSO_3F and (ii) transport numbers and molal conductances in HSO_3F are known[25] for K^+ but not for Cs^+, allowing more accurate interpretation of the data. The greater conductance of the $K_2[Ta(SO_3F)_7]$ salt in solution relative to $K[Ta(SO_3F)_6]$ suggests the presence of more ions in the former solution, as would be expected. Furthermore, the conductance values of $K_2[Nb(SO_3F)_7]$ and $K_2[Ta(SO_3F)_7]$ are very comparable, in spite of the difference in acidity between $Nb(SO_3F)_5$ and $Ta(SO_3F)_5$.

To confirm that $[Ta(SO_3F)_6]^-$ and K^+ are the only conducting species at the equivalence (or inversion) point of the acid/base titration, conductance data of $K[Ta(SO_3F)_6]$ were interpolated to the concentration present at the endpoint in the titration. The value of 22.14 $ohm^{-1}cm^{-1}$ obtained agrees within experimental error ($\pm$ 1-2 $ohm^{-1}cm^{-1}$) with the titration value of 23.40 $ohm^{-1}cm^{-1}$.

Table 6.IV. Specific Conductance of $K[Ta(SO_3F)_6]$ and $K_2[M(SO_3F)_7]$, with M = Nb or Ta, in HSO_3F at 25.00 °C

$K[Ta(SO_3F)_6]$		$K_2[Ta(SO_3F)_7]$		$K_2[Nb(SO_3F)_7]$	
10^2m mol/kg	$10^4\kappa$, Ω^{-1}/cm	10^2m, mol/kg	$10^4\kappa$, Ω^{-1}/cm	10^2m, mol/kg	$10^4\kappa$, Ω^{-1}/cm
0.363	2.61	0.109	2.57	0.140	3.66
0.710	4.74	0.443	9.74	0.510	11.87
1.044	5.95	0.758	17.00	1.045	23.87
1.522	8.47	1.112	26.10	1.492	33.05
1.996	10.01	1.598	39.07	1.899	41.91
2.447	11.97	2.095	49.33	2.375	51.17
2.960	14.43	2.816	64.10	3.001	61.99
3.557	16.97	3.268	73.14	3.492	70.81
4.139	18.99	4.164	87.71	3.959	76.15
4.642	20.96	4.616	95.21	4.681	87.70
5.076	21.79				
5.384	22.62				
5.725	23.24				

6.C.1.b. Interpretation of Electrical Conductivity Data

If it is assumed that the conductivity of dilute solutions containing strong electrolytes varies linearly with electrolyte concentration, it is then possible to calculate the specific conductance for any given solution to a good approximation by the expression:

$$\kappa = 10^{-3}\sum_n \lambda^*_n m_n \qquad (6\text{-}3)$$

where $\lambda^*_n = 1000\kappa_{ion}/m$ is the molal conductance and κ_{ion} is the specific conductance ($ohm^{-1}cm^{-1}$) of an individual ion n at a concentration m (mol kg^{-1}).

Before Equation (6-3) could be used to generate calculated specific conductance curves for the various systems studied, it was first necessary to obtain the λ^* values for the solvated $[(Y)SO_3F]^-$ species in Equation (6-2a), with Y being $Nb(SO_3F)_5$ or $Ta(SO_3F)_5$. These were calculated from each species' specific conductance value at the equivalence point, since the only conducting species in solution have been shown to be K^+ and $[(Y)SO_3F]^-$; the very small contribution of 1×10^{-4} $ohm^{-1}cm^{-1}$ resulting from the solvent's autoprotolysis[5] was also accounted for. Molal conductances for K^+ were calculated at any desired concentration in the range 0 ~ 0.1 m from previously reported values and transport number derivations.[25] Using Equation (6-3), the λ^* values for $[Nb(SO_3F)_6]^-$ and $[Ta(SO_3F)_6]^-$ were estimated to be 20 for 0.054 m $[Nb(SO_3F)_6]^-$ and 19 for 0.052 m $[Ta(SO_3F)_6]^-$. These values are in reasonable agreement with values of 23 and 13 found previously for 0.029 m $[Au(SO_3F)_4]^-$ and 0.084 m $[SbF_5(SO_3F)]^-$, respectively.[2,30,31] Although the molal conductance of any conducting species should theoretically decrease with an increase in concentration (and ionic strength),[25] calculations for the $Au(SO_3F)_3$ superacid system[30] have shown that in the concentration range 0 - 0.05 m, the $\lambda^*([Au(SO_3F)_4]^-)$ value decreases by only about 4%, which is comparable to the minimum experimental error associated with these measurements and hence is not significant. Consequently, the above values were used for all concentrations encountered in this study. Although not completely correct, the assumption that $2\lambda^*([(Y)SO_3F]^-) = \lambda^*([(Y)SO_3F]^{2-})$ is also adequately accurate for the purpose of these studies, since the calculated specific conductance values are much more sensitive to $\lambda^*(H_2SO_3F^+)$ than they are to $\lambda^*([(Y)SO_3F]^-)$, except near the titration equivalence points.[2]

Equation (6-2a) earlier displayed the simplest possible dissociation equilibrium of a monomeric Lewis acid in HSO_3F. Letting m be equal to the molality of the given

Lewis acid and x to the molality of $H_2SO_3F^+$ (which in turn is equal to the molality of $[(Y)SO_3F]^-$), the acidic dissociation constant in Equation (6-2a) can be expressed as:

$$K_1 = \frac{x^2}{(m-x)} \quad \text{mol kg}^{-1} \tag{6-4}$$

Incorporating Equations (6-3) and (6-4), and assuming that $\lambda^*(H_2SO_3F^+) = 320$ in the concentration range 0 - 0.1 m,[2] best fits of K_1 to experimental data are shown as curves A in Figures 6.3 and 6.4 for the Nb and Ta systems, respectively. The values of K_1 in each case are tabulated in Table 6.V, together with values calculated previously for HSO_3F-$Au(SO_3F)_3$[30,31] and the "Magic Acid" system, HSO_3F-SbF_5, for comparison.[2] The calculated curves fit the data of both acids only at concentrations below about 0.01 m; beyond this concentration, the K_1 value would have to increase rapidly to account for the measured conductances. A similar concentration dependency of K_1 reported[2] for the SbF_5 system was not nearly as pronounced as in either of the systems studied here. Furthermore, the magnitude of the Sb system's K_1 value (see Table 6.V) is quite comparable to that of the Ta system and considerably higher than that of the Nb system. Some deviation from theory may be expected as a result of modelling the conductivity of partially dissociated acids on concentrations rather than activities of the ions involved, but the deviation would be expected to be much smaller than observed here, especially over the dilute concentrations studied.[2]

The curve in Figure 6.5 illustrates a close fit of K_1 (recorded in Table 6.V) to the conductance data of the stoichiometrically mixed $Nb(SO_3F)_5/NbF_5$ solution. The slight deviation at the lower concentrations may be explained by the presence of some basic

Table 6.V. Calculated Ionization Equilibrium Constants for Various Association Models in HSO_3F at 25.00 °C

Acid System	Concentration (mol/kg)	10^3K_1 (m)	K_2	10^3K_{12} (m)	10^3K_{13} (m)	10^3K_{14} (m)	10^3K_{15} (m)
$Nb(SO_3F)_5$	0 - 0.045	0.36	–	–	0.70	1.8	2.8*
$Nb(SO_3F)_5/NbF_5$	0 - 0.050	0.23	–	–	–	–	–
$Nb(SO_3F)_5/KSO_3F$	0.055 - 0.075	1.5	–	–	–	2.2*	–
$Ta(SO_3F)_5$	0 - 0.045	1.5	0.50	5.0	15*	–	–
$Ta(SO_3F)_5/KSO_3F$	0.050 - 0.080	5.2	–	6.7*	10	–	–
$Au(SO_3F)_3$[a]	0 - 0.050	3.0	3.3*	24	–	–	–
$Au(SO_3F)_3/KSO_3F$[a]	0.030 - 0.050	51	–	–	–	–	–
SbF_5[b]	0 - 0.085	3.7	0.007*	–	–	–	–

[a]ref. 31, [b]ref. 2 ("K_2" obtained by fitting K_1 and K_2 simultaneously); *best fitting model for given acid system

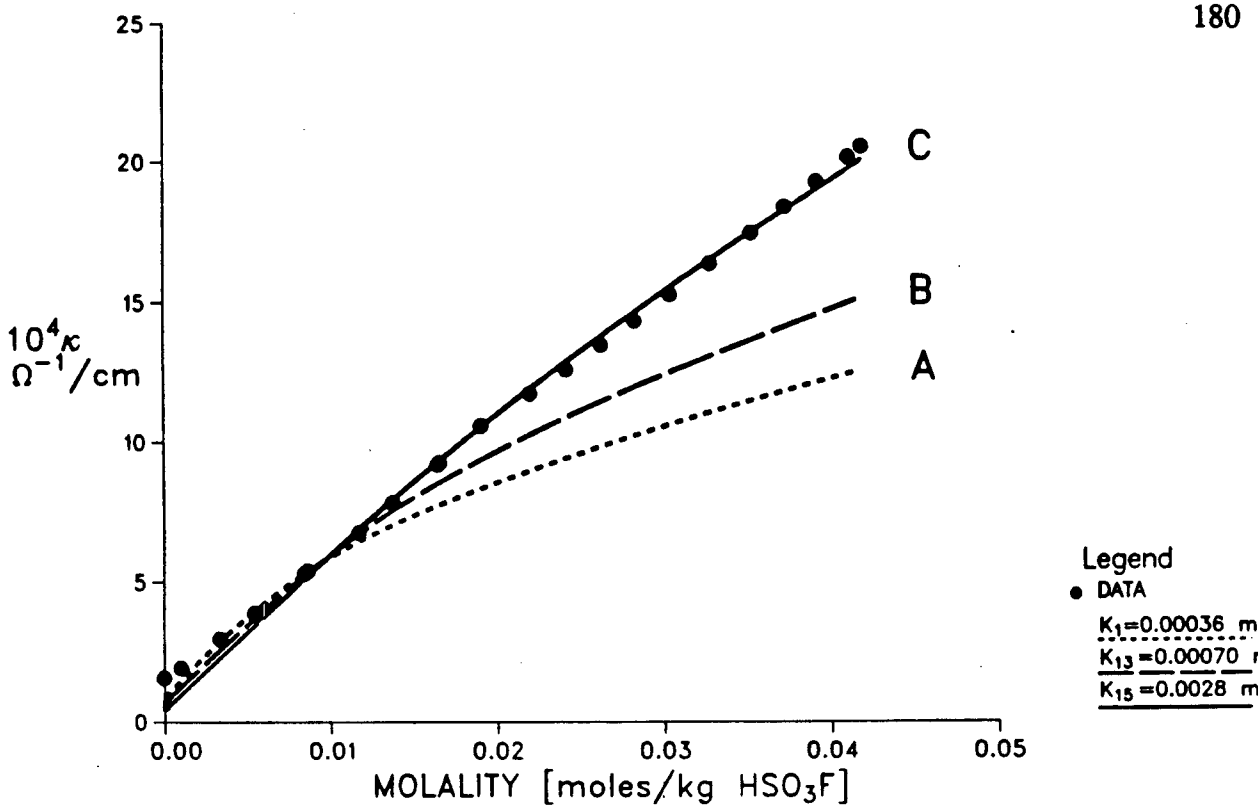

Figure 6.3. Best Fits to Experimental Specific Conductance Data of $Nb(SO_3F)_5$ in HSO_3F at 25.00 °C

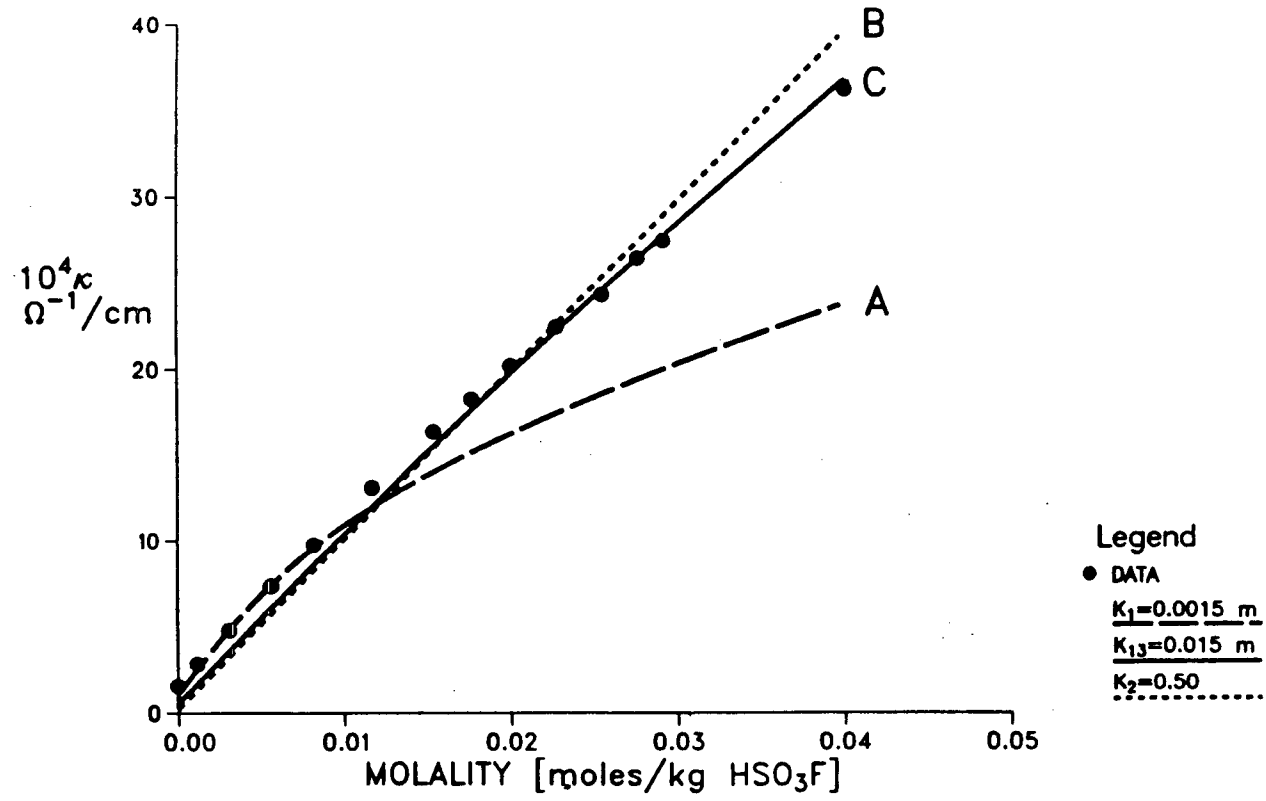

Figure 6.4. Best Fits to Experimental Specific Conductance Data of $Ta(SO_3F)_5$ in HSO_3F at 25.00 °C

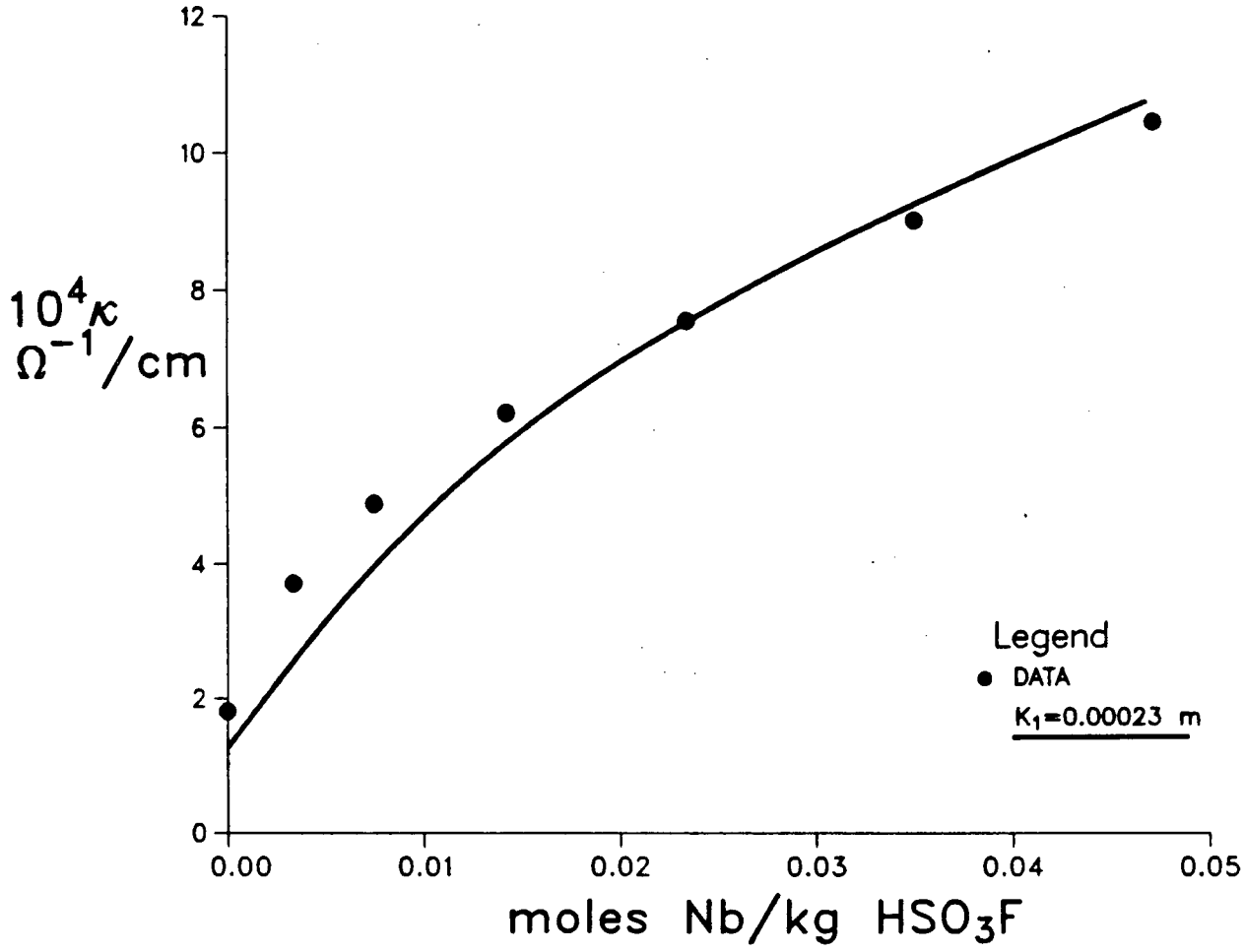

Figure 6.5. Best Fit to Experimental Specific Conductance Data of $Nb(SO_3F)_5$-NbF_5 Equimolar Mixture in HSO_3F at 25.00 °C

impurities in the solution, as indicated by the slightly enhanced background conductance from the expected solvent value of 1.1×10^{-4} ohm^{-1}cm^{-1}.[5] In spite of the large difference in conductance (and therefore acidity) found between $Nb(SO_3F)_5$ and NbF_5, the best fitting $10^3K_1 = 0.23$ m value to the mixed system's data is not much lower than that of $10^3K_1 = 0.36$ m found for $Nb(SO_3F)_5$ at concentrations of < 0.01 m. This, and the poor fit of K_1 to the latter system's data at all but the lowest concentrations, are indicative of ligand exchange between NbF_5 and $Nb(SO_3F)_5$ in the mixed system. It also suggests that both $Nb(SO_3F)_5$ and $Ta(SO_3F)_5$ undergo a more complex acidic dissociation in HSO_3F.

The formation of polymeric or polynuclear acids at higher concentrations has previously been held responsible for the increase in acidity at higher concentrations of both the SbF_5 "Magic Acid" system and aqueous HF solutions.[2] To test for similar behaviour in the $Nb(SO_3F)_5$ and $Ta(SO_3F)_5$ systems, their conductivity data were modelled according to the simplest oligomeric equilibrium for acidic dissociation, in which the Lewis acid exists as a *dimer* in solution according to:

$$\underset{m-2x}{2\,M(SO_3F)_5} + 2\,HSO_3F \underset{HSO_3F}{\overset{K_2}{\rightleftharpoons}} \underset{x}{H_2SO_3F^+_{(solv)}} + \underset{x}{[[M(SO_3F)_5]_2SO_3F]^-_{(solv)}} \qquad (6\text{-}5)$$

with m and x defined as in Equation (6-4) and K_2, the dimeric acidic dissociation constant, defined as:

$$K_2 = \frac{x^2}{(m-2x)^2} \qquad (6\text{-}6)$$

Using Equation (6-3) and (6-5), the best fit of K_2 to experimental data was obtained for $Ta(SO_3F)_5$ as shown by curve **B** in Figure 6.4. Although this fit is closer than the best K_1 fit obtained earlier, it is not yet an accurate fit, indicated in part by the surprisingly large

value of $K_2 = 0.5$ obtained here. Fitting the data of $Nb(SO_3F)_5$ in this manner was not attempted due to the poor nature of the Ta system's fit. An accurate fit using this model simultaneously with the model shown in Equation (6-4) has been obtained previously with $10^3K_2 = 7$ for the SbF_5 system (at concentrations between ~0.02 and 2 m).[2] $Au(SO_3F)_3$ has displayed even more interesting behaviour.[31] When the conductivity of "in situ" solutions was measured directly without first isolating the solid Lewis acid, a good *monomeric* fit was obtained with $10^2K_1 = 5.1$ m in the concentration range 0 - 0.05 m, indicating very high acidity. Yet when solid $Au(SO_3F)_3$ was first isolated and then re-dissolved in HSO_3F, a reasonably accurate *dimeric* fit to the data with $K_2 = 3.3$ was obtained in the same concentration range, suggesting nearly complete acidic dissociation. The dimeric dissociation constants for all these systems are also listed in Table 6.V. $SbF_2(SO_3F)_3$ was found to dissociate completely along a dimeric pathway, but evidence for the co-existence of complete monomeric dissociation was also reported,[2] and equilibrium between the two has been postulated to best describe the system.

The failure to fit the data for both $Nb(SO_3F)_5$ and $Ta(SO_3F)_5$ to either monomeric or dimeric models at low concentrations suggested that perhaps both may be more strongly associated. Support for this argument also comes from Raman spectroscopy and NMR solution studies discussed later in this chapter. A more general approach to the problem is to combine a monomeric dissociation constant with any n^{th} degree oligomeric dissociation constant by obtaining the product of Equation (6-4) with a generalized form of Equation (6-6) and simplifying, with the following results:

$$K_1K_n = \frac{x^4}{(m-x)(m-nx)^n} \quad \text{for } n \geq 2 \qquad (6\text{-}7)$$

$$= \frac{x^4}{(m-x)(m-nx)^{n-2}(m-nx)2} \quad \text{mol}^{(3-n)}\,\text{kg}^{(n-3)}$$

By introducing the term K_{1n} and letting $(K_{1n})^2 = \frac{x^4}{(m-nx)^2}$ $mol^2\,kg^{-2}$ the following is obtained:

$$K_{1n} = [K_1 K_n (m-x)(m-nx)^{n-2}]^{1/2} \qquad (6\text{-}8)$$

$$= \frac{x^2}{(m-nx)} \quad mol\,kg^{-1}$$

This produces a workable method which can describe acidic dissociation of a Lewis acid in HSO_3F in terms of a combined *oligomeric/monomeric dissociation constant*, K_{1n}. Moreover, the dependency of its magnitude on acid concentration is explicitly expressed; such a dependency has previously been suggested for the SbF_5 and $SbF_2(SO_3F)_3$ systems, but never explicitly formulated.[10] The greatest limitation of Equation (6-8) is that it does not allow modelling of conductivity data for highly dissociated acids ($K_n \rightarrow \infty$) with $n > 2$, since nx/m rapidly approaches and then exceeds unity, at which stage K_{1n} becomes undefined. Fortunately, neither of the two systems discussed here fall into this category. In addition, the model does not represent the *exact* degree of oligomerization, but merely the *relative* degree of oligomerization among different acids.

Using Equations (6-3) and (6-8), the best fits to the $Nb(SO_3F)_5$ and $Ta(SO_3F)_5$ conductance data, at least in the concentration range 0 - 0.045 m, were found to be $10^3K_{15} = 2.8$ m and $10^2K_{13} = 1.5$ m, respectively, shown as curves **C** in Figures 6.3 and 6.4. For comparison purposes, the best fit of K_{13} to the $Nb(SO_3F)_5$ data is also shown by curve **B** in Figure 6.3 and is clearly inadequate. It appears that $Nb(SO_3F)_5$ is more highly polymerized than $Ta(SO_3F)_5$, but the latter is a significantly stronger acid, as would be expected from the previous section's results. Interestingly, the ratio of the best fitting constants for the two systems, $K_{13}/K_{15} \sim 5$, is in very good agreement with the earlier found (at lower concentration) K_1 value ratio of about 4, indicating that the relative

strength of the two acids does not change significantly with concentration. These dissociation constants are recorded in Table 6.V, together with a few best fit values for different degrees of oligomerization, clearly of inferior quality to the ones discussed above.

To test the validity of these dissociation constants, similar treatment was given to the acid/base titration data. The Lewis acid concentration of these solutions spanned a range of ~0.05 - 0.08 m, beginning approximately where the previous solutions left off. Slight amendments were made to Equation (6-4) and (6-8) to account for the presence of KSO_3F in solution, as follows:

$$K_1 = \frac{x(x+z)}{m-x-z} \quad \text{mol kg}^{-1} \tag{6-9}$$

$$K_{1n} = \frac{x(x+z)}{m-nx-z} \quad \text{mol kg}^{-1} \tag{6-10}$$

In the above equations, z represents the molality of KSO_3F. Since KSO_3F is completely dissociated in HSO_3F,[25] these constants have exactly the same physical definition as before.

The best fitting K_1 values to data were calculated for $KSO_3F/Nb(SO_3F)_5$ and $KSO_3F/Ta(SO_3F)_5$ using Equations (6-3) and (6-9). They are listed in Table 6.V and plotted in Figures 6.6 and 6.7, respectively. Both fits are seen to be at best satisfactory, with their respective values of 1.5×10^{-3} m and 5.2×10^{-3} m being approximately four times greater than found earlier in the 0 - 0.01 m concentration range.

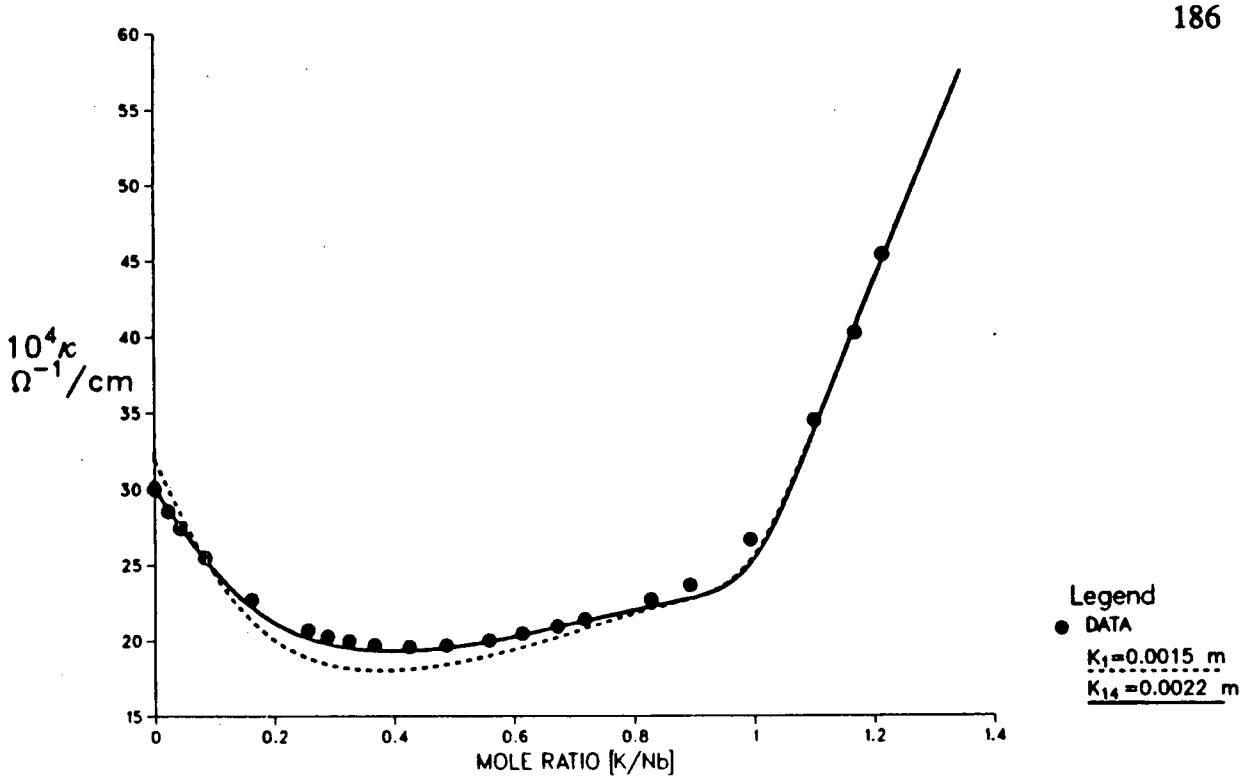

Figure 6.6. Best Fits to Experimental Conductometric Titration Data of $Nb(SO_3F)_5$ with KSO_3F in HSO_3F at 25.00 °C

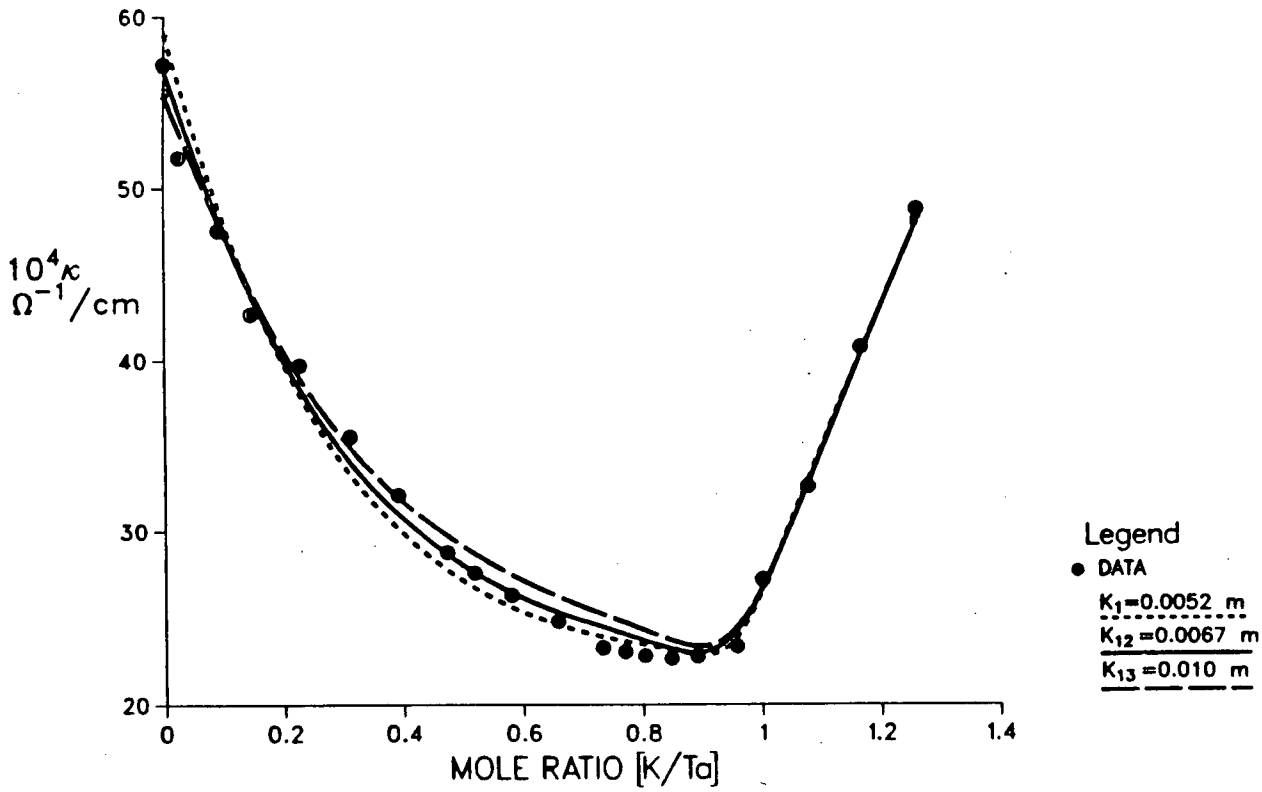

Figure 6.7. Best Fits to Experimental Conductometric Titration Data of $Ta(SO_3F)_5$ with KSO_3F in HSO_3F at 25.00 °C

Better fits to the two acid systems' titration data were obtained from Equations (6-3) and (6-10). 10^3K_{14} = 2.2 m clearly gives the best fit to the $KSO_3F/Nb(SO_3F)_5$ data, in reasonably good agreement with 10^3K_{14} = 1.8 m and 10^3K_{15} = 2.8 m determined earlier for the $Nb(SO_3F)_5$ system at lower concentrations, and is shown in Figure 6.6. Choosing between fits for the $KSO_3F/Ta(SO_3F)_5$ system is more difficult. Both 10^3K_{12} = 6.7 m and 10^2K_{13} = 1.0 m (plotted in Figure 6.7) give reasonably good fits, but neither is as good as the optimal fit to the Nb analog, partially due to more random scatter in the tantalum system's data. K_{12} does however appear to offer a marginally better fit, indicating more dimeric than trimeric character at these concentrations. Again, both values again agree quite well with the respective 10^3K_{12} = 5.0 m and 10^2K_{12} = 1.5 m values found at lower concentrations for this system.

The validity of the different acidic dissociation models presented and the accuracy of the fits shown should now be briefly considered. It appears that a simple monomeric acidic dissociation equilibrium (see Equation (6-4)) best describes both acids' conductivity data at concentrations below about 0.01 m (10^3K_1(Ta) = 1.5 m > 10^4K_1(Nb) = 3.6 m). The same model has also been reported to best describe the conductivity of both SbF_5[2] and $Au(SO_3F)_3$[31] at these very low concentrations. These values also represent the approximate dissociation constants at infinite dilution. At higher concentrations, the dissociation process becomes more complicated, since different models appear to fit better at different concentrations (see Table 6.V and Figures 6.4 - 6.7). By calculating the % error between the best calculated fits and the observed conductance data according to:

$$\% \text{ Deviation from data} = \frac{K_{obs} - K_{calc}}{K_{calc}} \times 100 \qquad (6\text{-}11)$$

and plotting it vs. concentration for both sets of data discussed earlier, a more explicit indication of each model's accuracy in the approximate concentration range 0.01 - 0.08 m is obtained. These plots are shown as Figures A.1 - A.4 in the Appendix for $Nb(SO_3F)_5$ and $Ta(SO_3F)_5$ as well as for their titration data. A few general trends can be seen and conclusions drawn from the information contained in the plots:

(i) In the concentration range 0.01 ~ 0.035 m, the combined pentamer/monomer equilibrium, with 10^3K_{15} = 2.8 m, best describes the acidic dissociation of $Nb(SO_3F)_5$ whereas at higher concentrations, this dissociation is surprisingly best represented by the tetrameric/monomeric model, with 10^3K_{14} = 1.8 - 2.2 m, depending on the exact concentration. Hence, the only conclusion that can be reached is that $Nb(SO_3F)_5$ appears to exist as a highly oligomerized weak acid in HSO_3F solutions spanning the ~0.01 - 0.08 m concentration range.

(ii) Over the whole concentration range 0.01 - 0.08 m, both the combined trimer/monomer and dimer/monomer acidic dissociation equilibria give comparably good descriptions of the acidic dissociation of $Ta(SO_3F)_5$ in HSO_3F: 10^2K_{13} = 1.5 m and 10^3K_{12} = 5.0 - 6.7 m (depending on the exact concentration), respectively. While $Ta(SO_3F)_5$ behaves as a significantly stronger acid in HSO_3F than $Nb(SO_3F)_5$, its degree of oligomerization is somewhat smaller over this concentration range.

(iii) When K_{1n} and $K_{1(n+1)}$ give approximately the same fit to data at a given concentration, the magnitude of the latter is always greater for both systems, suggesting that acid strength does indeed increase with the degree of polymerization. This trend has been suggested previously by Gillespie et al.[2,10]

(iv) A significant degree of experimental error in the $Ta(SO_3F)_5$ system's titration data made the interpretation of its % error plots somewhat difficult; computer generated curve averaging techniques were of great help here, as evidenced from Figure A.4 in the Appendix.

It is unfortunate that the calculation of K_n from K_{1n} at a given concentration is not possible, since K_1 is itself very concentration dependent (see Table 6.V). However, an increase in the magnitude of K_{12} is accompanied by a decrease in K_{13} with increasing concentration for the $Ta(SO_3F)_5$ system, while the accuracy of the constants' description of the system's behaviour remains comparable. This suggests that at higher concentration K_{12} may equal K_{13} and a single acidic dissociation constant, K_a, may be used to express the acidity of the $Ta(SO_3F)_5$ system, derived as follows:

Given that $K_{12} = K_{13}$, then from Equation (6-8):

$$[K_1K_2(m-x)]^{1/2} = [K_1K_3(m-x)(m-3x)]^{1/2} \qquad (6\text{-}12)$$

with m and x as previously defined.

Letting $K_a = K_{12} = K_{13}$, the following is obtained:

$$Ka^2 = K_2(m-x) = K_3(m-x)(m-3x) \qquad (6\text{-}13)$$

Using Equation (6-6), the simplest form of K_a can be expressed as:

$$K_a = \left[\frac{x^2(m-x)}{(m-2x)^2}\right]^{1/2} \text{mol}^{3/4}\,\text{kg}^{-3/4} \qquad (6\text{-}14)$$

It must be remembered that the above dissociation model is based on the assumption that K_{12} and K_{13} will converge at some concentration > 0.1 m in the $Ta(SO_3F)_5$ acid system.

At very low concentrations of ≤ 0.01 m, the following acidity ranking can be established amongst the strongest known monoprotonic acids in HSO_3F, based on their optimal K_1 values listed in Table 6.V:

$$SbF_2(SO_3F)_3{}^2 > SbF_5{}^2 \geq Au(SO_3F)_3{}^{30,31} > Ta(SO_3F)_5 > Nb(SO_3F)_5$$

At concentrations between 0.01 m and 0.1 m, the order of acid strength is somewhat different, based on the various dissociation constants K_n and K_{1n} ($2 \leq n \leq 5$), also listed in Table 6.V:

$$SbF_2(SO_3F)_3 > Au(SO_3F)_3 > Ta(SO_3F)_5 > SbF_5 > Nb(SO_3F)_5$$

Finally, the apparent degree of oligomerization (or polymerization) at low concentrations assumes the order:

$$Nb(SO_3F)_5 > Ta(SO_3F)_5 > Au(SO_3F)_3 \sim SbF_2(SO_3F)_3 \sim SbF_5$$

This is somewhat surprising, since the antimony systems have been reported to undergo oligomerization via both F and SO_3F bridges,[2,9] whereas the other three systems can only bridge via the latter. The complexity of the antimony systems[2,8,10] would nevertheless be expected to alter the above "polymerization ranking" at higher concentrations.

Oligomerization of $Nb(SO_3F)_5$ and $Ta(SO_3F)_5$ in HSO_3F is not completely surprising, since most of the $Cs_x[M(SO_3F)_{5+x}]$ ($x = 1$ or 2) type salts described earlier appear to involve bridging fluorosulfate groups between metal centers, as do the two fluorofluorosulfates $NbF_2(SO_3F)_3$ and $TaF_4(SO_3F)$. Moreover, the analogous fluorides, MF_5, exist as tetramers in solid state with both metals.[32] An important assumption that has been made throughout this section is that $\lambda^*([(Y)SO_3F]^-) \approx \lambda^*([(Y)_nSO_3F]^-)$ which is

in turn based on the assumption that both are involved in hydrogen bridging to HSO_3F and will conduct, like the self-ionization ions SO_3F^- and $H_2SO_3F^+$,[5] by a proton transfer mechanism. The assumption is therefore accurate enough for the purpose of these studies.

6.C.1.c. The $[M(SO_3F)_7]^{2-}$ - $[M(SO_3F)_6]^-$ Equilibrium Systems (M = Nb or Ta)

To establish further the validity of the previous sections' calculations, the conductance data of $K[Ta(SO_3F)_6]$ listed in Table 6.IV of Section 6.C.1.a is fitted with data calculated from Equation (6-3) and the following complete ionization equation:

$$K[Ta(SO_3F)_6] \xrightarrow[HSO_3F]{K_d = \infty} K^+_{(solv)} + [Ta(SO_3F)_6]^-_{(solv)} \qquad (6\text{-}15)$$

The calculated $K_d = \infty$ curve is shown in Figure 6.8 together with the experimental data. Except at concentrations ≥ 0.05 m, the fit is extremely good, indicating that $[Ta(SO_3F)_6]^-$ does not undergo any significant basic dissociation, similar to the $[Pt(SO_3F)_6]^{2-}$ anion in the HSO_3F - $Pt(SO_3F)_4$ superacid system.[1] The reduced accuracy of the fit at the higher concentration is probably due to non-ideal behaviour, as would be expected for more concentrated electrolytic solutions. Even a minimal degree of basic dissociation would result in higher, not lower, experimental values than calculated from Equation (6-15), due to the much larger relative mobility of SO_3F^- over either K^+ or $[Ta(SO_3F)_6]^-$.[25] The monomeric nature of $[Ta(SO_3F)_6]^-$ shown in Equation (6-15) is not too surprising, since in either weakly basic or weakly acidic solutions, monomeric dissociation fits have been found to be at least as good as oligomeric ones at representing the solution behaviour of

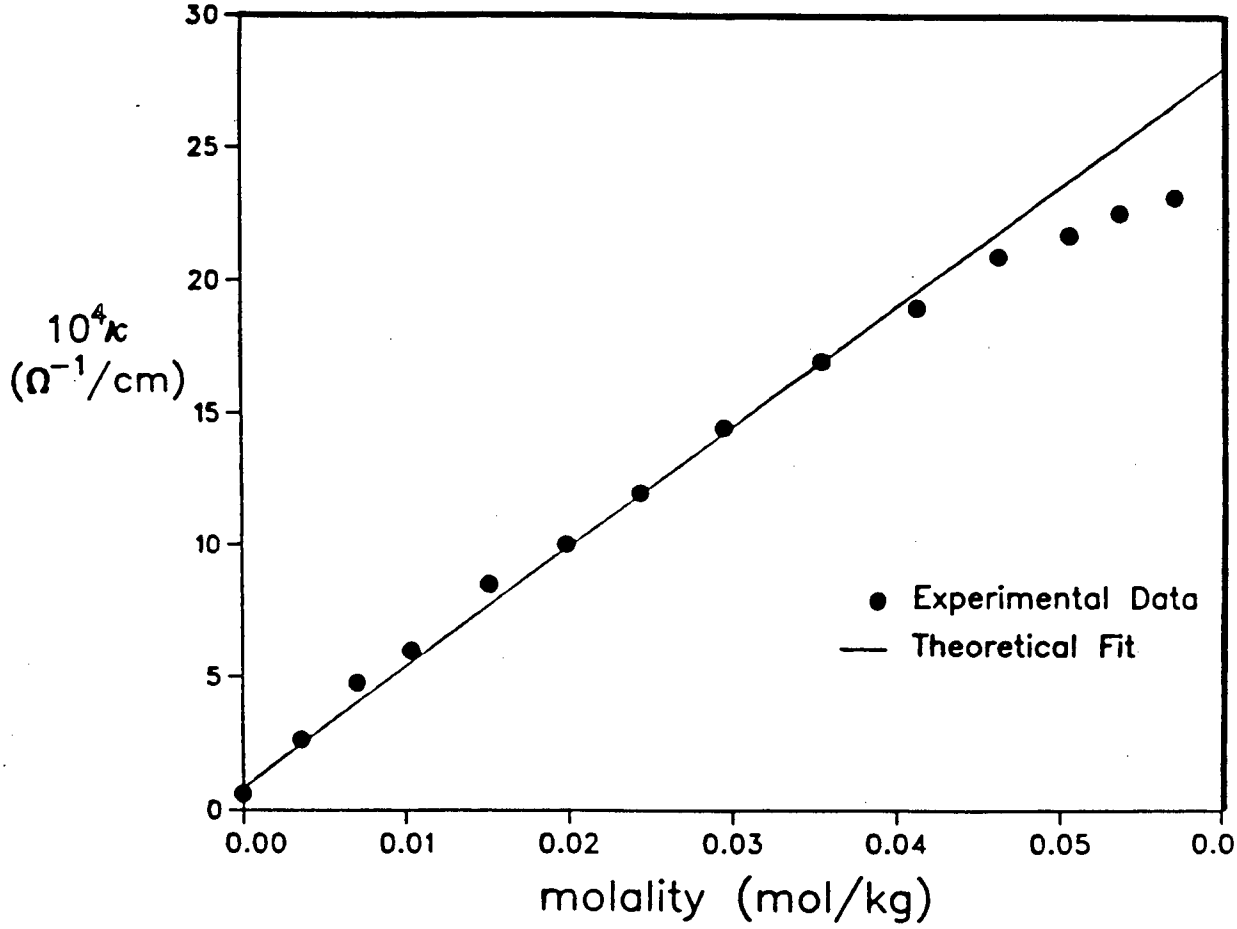

Figure 6.8. Specific Conductance of $K[Ta(SO_3F)_6]$ in HSO_3F at 25.00 °C

$Ta(SO_3F)_5$. $K[Nb(SO_3F)_6]$ is believed to behave in a very similar fashion (see previous two sections).

To address the apparent inconsistency between the measured monobasic acidity of both $Nb(SO_3F)_5$ and $Ta(SO_3F)_5$ and the isolation of analytically pure salts of the type $Cs_2[M(SO_3F)_7]$ with both metals, two equilibria were established by comparing measured with calculated conductance values. The simplest ionization equilibrium according to:

$$K_2[M(SO_3F)_7] \xrightarrow[HSO_3F]{K_d = \infty} 2\,K^+_{(solv)} + [M(SO_3F)_7]^{2-}_{(solv)} \qquad (6\text{-}16)$$

was found to be inadequate, since the calculated conductance values were much lower at a given concentration than the measured values. The basic dissociation equilibrium:

$$2\,K^+_{(solv)} + [M(SO_3F)_7]^{2-}_{(solv)} \underset{HSO_3F}{\overset{K_b}{\rightleftharpoons}} 2\,K^+ + [M(SO_3F)_6]^-_{(solv)} + SO_3F^-_{(solv)} \qquad (6\text{-}17)$$

was found to describe the system more satisfactorily. The above equation can be simplified, since two moles of K^+ are present on both sides of the equilibrium, to the following:

$$\underset{m-x}{[M(SO_3F)_7]^{2-}_{(solv)}} \underset{HSO_3F}{\overset{K_b}{\rightleftharpoons}} \underset{x}{[M(SO_3F)_6]^-_{(solv)}} + \underset{x}{SO_3F^-_{(solv)}} \qquad (6\text{-}18)$$

where: m = molality of $K_2[M(SO_3F)_7]$
x = molality of $[M(SO_3F)_6]^-$ = molality of SO_3F^-
M = Nb or Ta

Using previously reported $\lambda^*(SO_3F^-)$ values[25] and then letting $\lambda^*([M(SO_3F)_7]^{2-}) = 2 \times \lambda^*([M(SO_3F)_6]^-)$ and $[K^+] = 2 \times [K_2[M(SO_3F)_7]]$, Equation (6-3) was used together with:

$$K_b = \frac{x^2}{(m-x)} \quad \text{mol kg}^{-1} \tag{6-19}$$

to calculate the best fits of $10^2K_b = 2.4$ m and $10^2K_b = 4.1$ m for the Nb and Ta systems, respectively. Both calculated curves are shown together with their respective data in Figure 6.9. Both fits appear to be very good over the 0 ~ 0.05 m concentration range, indicating that a substantial amount of $[M(SO_3F)_6]^-$ is present in both solutions; for example, at initial concentrations of 0.04 m $K_2[M(SO_3F)_7]$, the $[Nb(SO_3F)_6]^-/[Nb(SO_3F)_7]^{2-}$ mole ratio present in solution is 1.13 (53% $[Nb(SO_3F)_6]^-$) while the $[Ta(SO_3F)_6]^-/[Ta(SO_3F)_7]^{2-}$ ratio is 1.65 (62% $[Ta(SO_3F)_6]^-$). At a lower concentration of 0.02 m, the respective amounts of $[M(SO_3F)_6]^-$ in solution are an even higher 65 and 74 mole %.

It is now easier to understand the apparent inconsistency between the type of acidic behaviour of these systems and the salts isolated from them. In the absence of very bulky cations such as Cs^+ or Ba^{2+}, $[M(SO_3F)_7]^{2-}$ dissociates mainly to $[M(SO_3F)_6]^-$, even in a highly basic environment. This explains why salts could not be isolated with the smaller cations K^+ or Li^+, since they are not able to delocalize adequately the negative charge of the anion. Furthermore, the higher K_b value found for the Ta system may explain the failure to isolate analytically pure $Ba[Ta(SO_3F)_7]$ and the difficulty encountered during the synthesis of $Cs_2[Ta(SO_3F)_7]$ relative to the Nb analog.

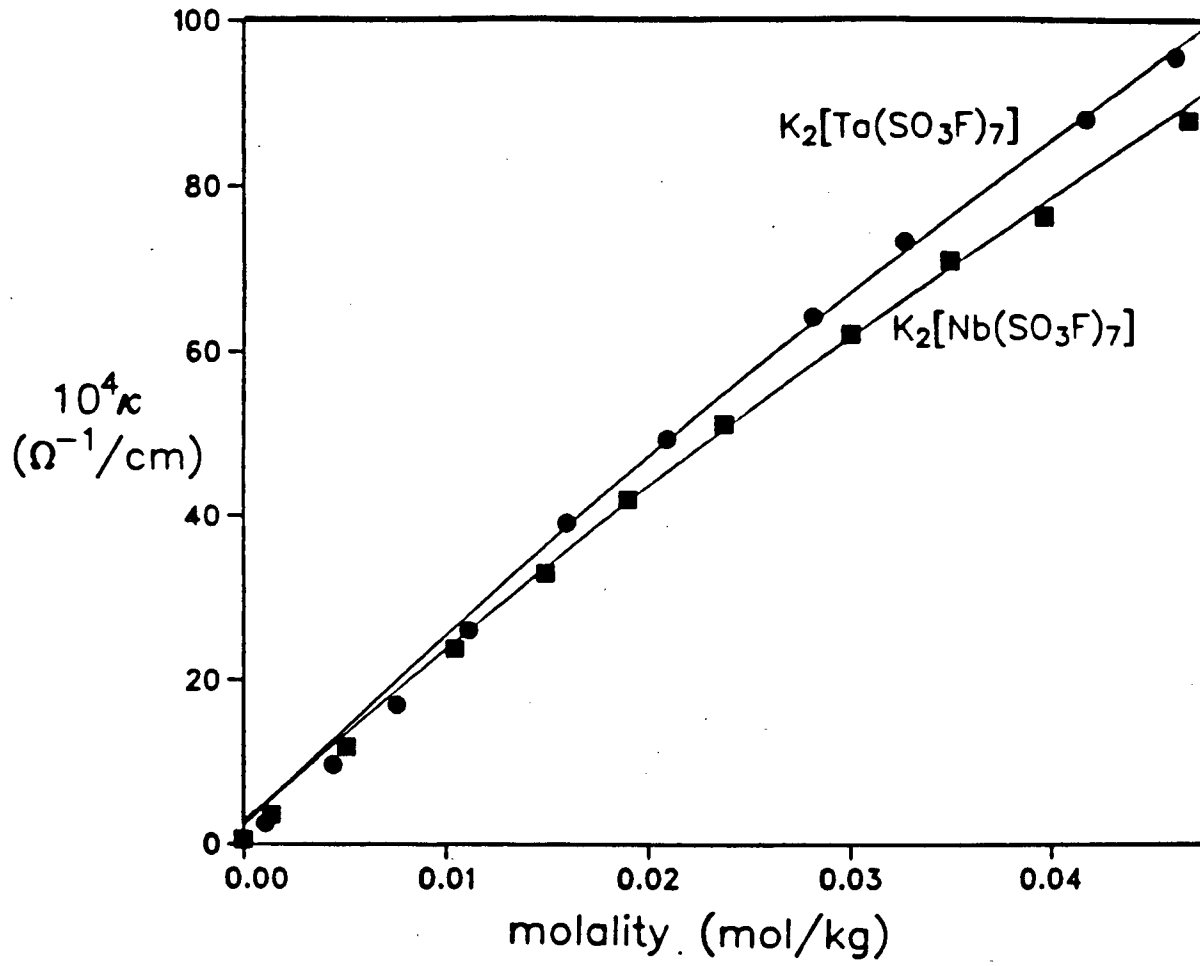

Figure 6.9. Specific Conductance of $K_2[Nb(SO_3F)_7]$ and $K_2[Ta(SO_3F)_7]$ in HSO_3F at 25.00 °C (solid lines indicate best fits- see text)

Although the dissociation pathways shown in Equations (6-15) and (6-18) deal strictly with monomeric species, oligomerization of the anions in solution cannot be completely ruled out, in light of the structural information obtained for the isolated salts in Chapters 4 and 5. However, the formation of a significant concentration of oligomers is not consistent with the accuracy of the fit to data obtained from Equation (6-15). On the other hand, calculations using Equilibrium (6-18) would not be affected even if oligomerization was accounted for, provided the degree of oligomerization remained equal on both sides of the equilibrium; in other words, this type of equilibrium is not suitable as a "polymerization indicator".

It appears that the $Nb(SO_3F)_5$ and $Ta(SO_3F)_5$ superacid systems are surprisingly complex even at low concentrations (< 0.1 m). They exist in various concentration-dependent stages of polymerization, and yield multi-component equilibrium systems in the presence of basic additives. To investigate the acidic behaviour of the stronger of the two systems at higher concentrations, the Hammett Acidity Function of the HSO_3F-$Ta(SO_3F)_5$ system was obtained and is discussed in the next section. Based on the noted complexity, a simple monomeric dissociation equilibrium is not expected to adequately describe the acidic behavior of this system at higher concentrations.

6.C.2. The Hammett Acidity Function of the HSO_3F-$Ta(SO_3F)_5$ System

6.C.2.a. Determination of H_0 Values

The aromatic nitro indicators 2,4-dinitrofluorobenzene (DNFB) and 2,4,6-trinitrotoluene (TNT) were chosen because both exist in mono- and diprotonated forms in very strong acid solutions, with an effective acidity range of about 6 H_0 log units.[10,22]

Before Equation (1-9) of Chapter 1 could be used to calculate the H_o values of various $Ta(SO_3F)_5$ solutions, it was necessary to calculate the respective ionization ratios, I, according to:

$$I = \frac{[BH^+]}{[B]} = \frac{\varepsilon_B - \varepsilon}{\varepsilon - \varepsilon_{[BH^+]}} \qquad (6\text{-}20)$$

where: [B] = concentration of neutral indicator
[BH+] = concentration of protonated indicator
ε_B = extinction coefficient of neutral indicator B
ε_{BH+} = extinction coefficient of protonated indicator BH+
ε = measured extinction coefficient of solution

Previously determined values[10] of ε_B and ε_{BH+} were used; these were obtained at wavelengths where BH+ showed maximum absorption. The ε values were measured at these same wavelengths, whose exact positions were slightly dependent on the $Ta(SO_3F)_5$ concentration in solution. This dependency constituted the primary limitation on the accuracy of the measurements obtained. Since the absorptions due to the individual nitro groups of these indicators are essentially independent,[10] three peaks were observed in the more concentrated solutions' spectra: one due to unprotonated nitro groups, another due to the first protonated nitro group and the last a result of the second protonated nitro group. The wavelength maxima of these three peaks are at a reasonable separation, and resolution of the peaks was therefore adequate enough to allow subtraction of the first protonated nitro group's overlapping absorption from that of the second protonated group's absorption, and thus allowing the calculation of $[BH^{2+}]/[BH^+]$ according to Equation (6-20). Previously determined[10] ε_{BH+} and $\varepsilon_{BH^{2+}}$ values, obtained at the wavelength of maximum BH^{2+} absorptions, were again used. Extinction coefficients for the neutral and protonated bases, λ_{max} values, pK_{BH+} values[10] and -log I values for the four indicators and various $Ta(SO_3F)_5$ solutions are listed in Tables A.I

and A.II of the Appendix. Where the log I value approaches or exceeds ±1 for any of the indicators, a second indicator has been used for verification.

It has previously been shown that all four indicators form a consistent set, although $-H_0$ values above about 17 diminish in accuracy. Furthermore, the behaviour of the protonated indicators DNFBH+ and $TNTH^+$ has been previously demonstrated to be adequately similar to that of other non-protonated indicators to justify their treatment as Hammett bases.[10]

6.C.2.b. The Acidity of HSO_3F - $Ta(SO_3F)_5$

Table 6.VI lists the $-H_0$ values of $Ta(SO_3F)_5$ in HSO_3F up to a concentration of 3.37 mole %. The acidity of HSO_3F is seen to increase with $Ta(SO_3F)_5$ concentration.

Table 6.VI. The Hammett Acidity of $Ta(SO_3F)_5$ in HSO_3F at 20 °C

$[Ta(SO_3F)_5]$, mole %	$-H_0$	Indicator
0	15.07	DNFB, TNT
0.055	15.55	DNFB, TNT
0.154	16.07	TNT
0.318	16.73	TNT, DNFBH+
0.913	18.03	DNFBH+
1.25	18.36	DNFBH+, TNTH+
1.80	18.58	TNTH+
2.11	18.71	TNTH+
3.37	18.91	TNTH+

Higher concentrations of Lewis acid were not suitable for study due to various experimental restrictions, among them problems encountered when trying to quickly dissolve more Ta metal powder in the $S_2O_6F_2/HSO_3F$ mixtures. The reaction times needed were too long, leading to contamination from a slow leakage of air into the reactor or from trace amounts of grease dissolved in the media. It was found that only reactions of less than about 5 days' duration led to reproducible H_o values.

The plot of $-H_o$ vs. mole % Lewis acid is shown in Figure 6.10 for $Ta(SO_3F)_5$, and for the two strong Lewis acids SbF_5 ("Magic Acid") and $SbF_2(SO_3F)_3$.[10] The principal feature of the plot is that beyond a concentration of about 1 mole %, $Ta(SO_3F)_5$ appears to be at least as strong as $SbF_2(SO_3F)_3$. The second striking feature worth noting is that compared to either SbF_5 or $SbF_2(SO_3F)_3$, the rate of $-H_o$ increase is considerably less for $Ta(SO_3F)_5$ in the 0 ~ 1 mole % range, whereas beyond this concentration, it is equal or even greater.

Both features of the $Ta(SO_3F)_5$ acidity can be explained. Its unexpectedly high value at concentrations beyond ~1 mole % (~0.1 m) has already been predicted by the conductance results of Section 6.C.1, which revealed the oligomeric nature of this system in addition to a ten-fold increase of its acidic dissociation constant with a similar increase in concentration (from 0.01 to 0.1 m). By extrapolation of the conductivity results, the acidic dissociation constant, K_a, for $Ta(SO_3F)_5$ should be of the order of 2×10^{-2} m at 1 mole % and 1×10^{-1} m at 5 mole %. From the previously estimated concentration of $H_2SO_3F^+$ in 100% HSO_3F and its $-H_o$ value, the idealized Equations (6-21) and (6-22)[10] shown at the top of page 201 can be used to estimate K_a for $Ta(SO_3F)_5$ in HSO_3F at any given concentration. $[H_2SO_3F^+]$ is equal to $[Ta(SO_3F)_6^-]$ in the latter Equation.

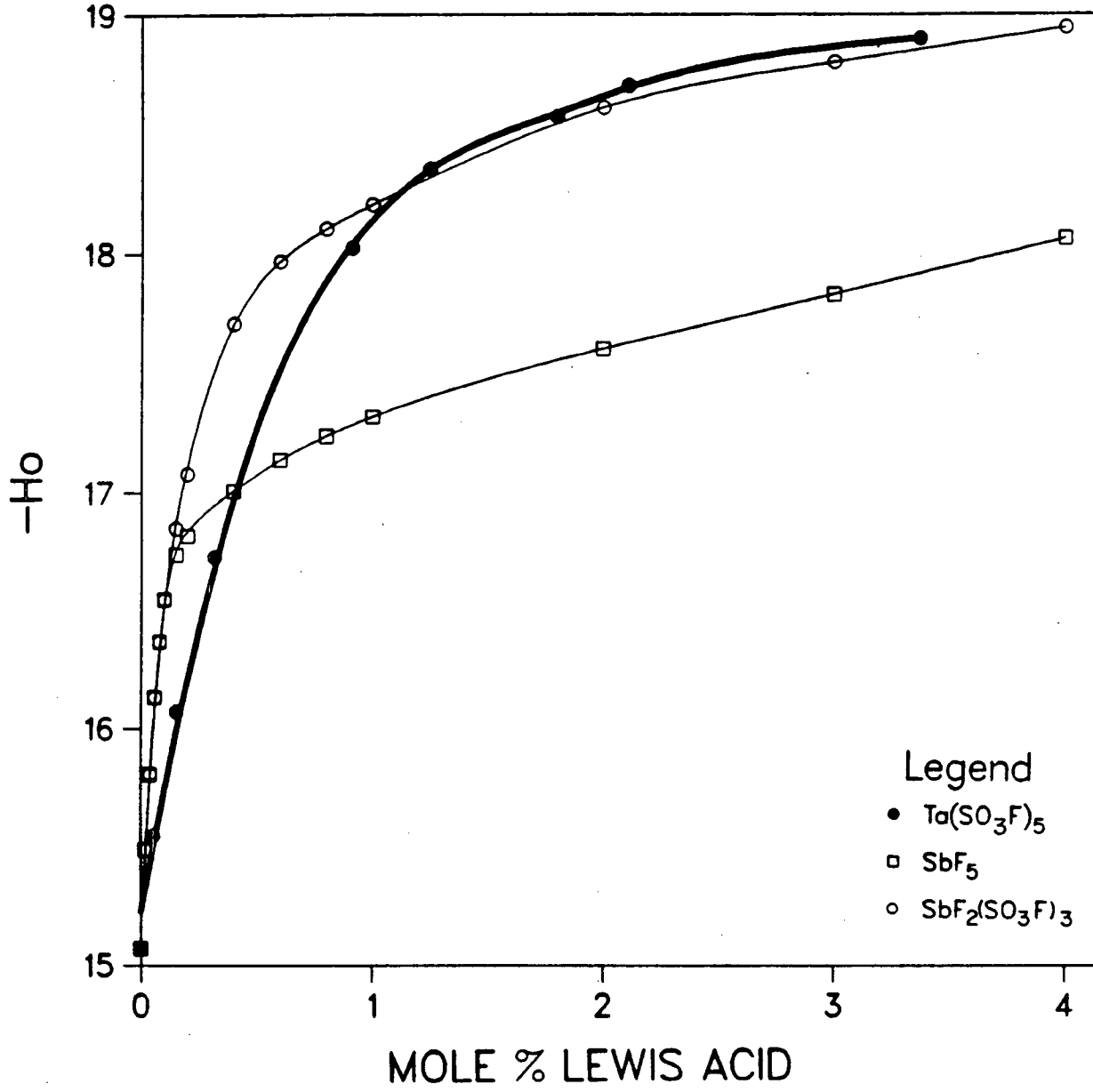

Figure 6.10. Hammett Acidity of $Ta(SO_3F)_5$, SbF_5 (ref.10) and $SbF_2(SO_3F)_3$ (ref.10) in HSO_3F at Ambient Temperature

$$-H_o = \log[H_2SO_3F^+] + 18.79 \quad (6\text{-}21)$$

$$K_a = \frac{[H_2SO_3F^+][Ta(SO_3F)_6^-]}{[Ta(SO_3F)_5]} \text{ mol kg}^{-1} \quad (6\text{-}22)$$

A plot of K_a vs. $Ta(SO_3F)_5$ concentration is shown in Figure 6.11. K_a increases steeply at concentrations greater than ~1 mole %, up to a value of ~5 m at the maximum concentration, indicating virtually complete dissociation of the acid. Furthermore, this value is an order of magnitude greater than the K_a value of ~0.1 m predicted at this concentration from the conductivity studies. The K_a vs. concentration curve is deceiving, however, since the rate of K_a increase at the lower concentrations is hidden by the scale of the plot. For this reason, a plot of $\ln K_a$ vs. concentration is also shown in Figure 6.11 and indicates that the greatest *logarithmic rate of Ka increase* is at concentrations of less than about 1 mole %. Following this "critical point", the rate quickly decreases and $\ln K_a$ approaches a constant value. Extrapolation of the $\ln K_a$ plot to infinite dilution leads to a very approximate K_a value of 8×10^{-5} mol kg^{-1}, which is about an order of magnitude less than that estimated from the conductivity measurements. This suggests a large dependence of the acidic dissociation constant shown in Equation (6-22) on concentration, which in turn implies that it is not a very accurate representation of the system's acidity, as was already indicated from the conductivity measurements.

The increase in magnitude of this system's acidic dissociation constant with concentration can be partially attributed to formation of stronger polymeric acids at higher concentrations, as suggested for the SbF_5 systems.[10] The slope difference between the three systems' $-H_o$ vs. concentration curves (Figure 6.10) at ≤ 1 mole % Lewis acid concentration reflects the lower initial K_a value of the tantalum system.

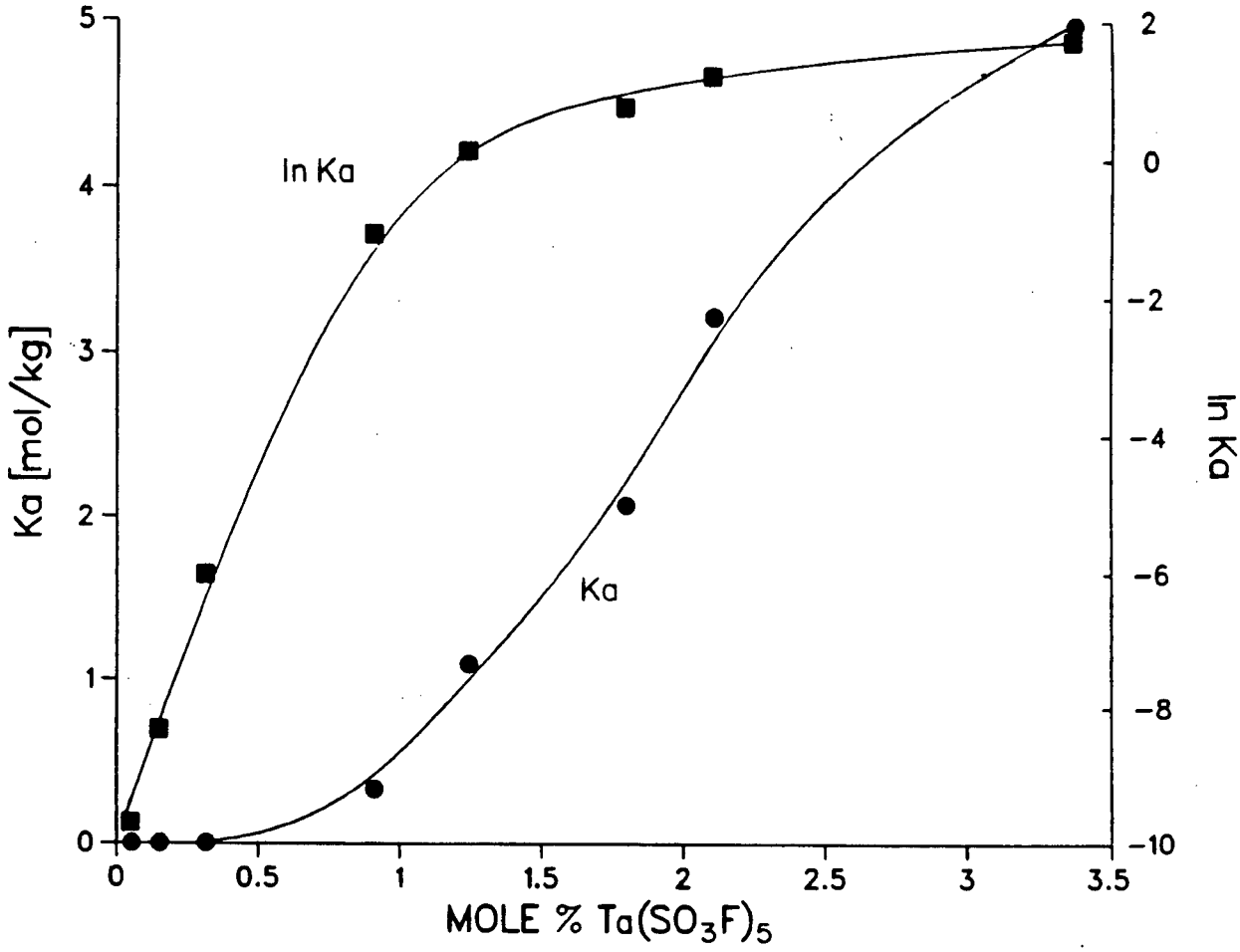

Figure 6.11. Dependence of the Acidic Dissociation Constant, K_a, on $Ta(SO_3F)_5$ Concentration in HSO_3F at Ambient Temperature

The formation of $H_x[Ta(SO_3F)_{5+x}]$ (with $x > 1$) type acids (and/or polymeric analogs) in solution at higher $Ta(SO_3F)_5$ concentrations is not inconceivable, since $Cs_2[Ta(SO_3F)_7]$ is isolable. This could result in two or even three moles of $H_2SO_3F^+$ forming per mole $Ta(SO_3F)_5$ upon acidic dissociation, leading to an approximate two- or three-fold increase in the acidity expected from simple acidic dissociation, and thus further contributing to the magnitude of the $-H_0$ values at higher concentrations. Species of this type are not known to exist in either the SbF_5 or $SbF_2(SO_3F)_3$ systems. However, it must be stressed that the conductometric titration results do not provide any evidence for such polybasic acids in the neutral range.

Previous acidity studies with the HSO_3F-MF_5 (M = Sb[2,10] or As[3]) systems have shown that acidity increases steadily with the number of moles of SO_3 added, but a maximum of only three moles SO_3 could be inserted into the Sb-F or As-F bonds. Hence, the presence of an unprecedented five fluorosulfate groups per metal center may also be partly responsible for the high acidity of $Ta(SO_3F)_5$.

The Hammett Acidity Function could not be determined at meaningful concentrations for the HSO_3F-$Nb(SO_3F)_5$ system, due to the gradual elimination of SO_3 and the visible formation of $NbF_2(SO_3F)_3$, which was consequently isolated and characterized.

The remaining sections of this chapter will deal with less rigorous investigations into the solution behavior of the $Nb(SO_3F)_5$, $Ta(SO_3F)_5$ and other related fluorosulfuric acid systems.

6.C.3. Multinuclear NMR Studies

6.C.3.a. $M_x'[M(SO_3F)_{5+x}]$ Solutions, with M' = Cs or Ba and x = 1 or 2

Variable temperature ^{19}F NMR data for solutions of $Cs[Nb(SO_3F)_6]$, $Cs_2[Nb(SO_3F)_7]$, $Ba[Nb(SO_3F)_7]$, α-$Cs[Ta(SO_3F)_6]$, β-$Cs[Ta(SO_3F)_6]$ and $Cs_2[Ta(SO_3F)_7]$ are listed in Table 6.VII. Concentrations are as close to saturation as possible. At ambient temperature (usually about 293-298 K), one combined solvent/solute resonance is observed for each species, within ± 0.3 ppm of the ^{19}F resonance for pure HSO_3F at 40.74 ppm. Rapid fluorosulfate exchange between the solute anion and the solvent is the likely cause. Fluorosulfate group exchange in HSO_3F was previously observed[7] only for solutions of $K[Sn(SO_3F)_5]$, while solutions of the salts $K_2[Sn(SO_3F)_6]$[33] and $Cs_2[Pt(SO_3F)_6]$[1] both gave rise to a separate solute peak, due to the existence of the coordinatively fully saturated species $[M(SO_3F)_6]^-$. It hence appears that adherence to a strict, stable octahedral coordination is not found for $[M(SO_3F)_{5+x}]^{x-}$ in HSO_3F solution with either Nb or Ta.

Signals of varying intensity and shape attributed to the solute become visible at 253 K (within about 3 ppm *upfield* of the solvent resonance) for all species studied except $Cs[Nb(SO_3F)_6]$ and $Cs_2[Ta(SO_3F)_7]$. At 218 K, solute peaks appear for all the salts, with more than one signal present in some cases. The $Cs_2[Nb(SO_3F)_7]$ solution exhibits the solvent resonance shifted by about 1 ppm downfield from its normal position at this temperature. This suggests that some fluorosulfate exchange between solute and solvent may still occur even at 218 K. This exchange may also persist for the other solutions and, together with overlap between solvent and solute peaks, makes definite assignment of the solute peaks difficult. Spectra could not be investigated at lower temperatures due to solute precipitation.

Table 6.VII. ^{19}F NMR Chemical Shifts for the Salts $M_x'[M(SO_3F)_{5+x}]$, with M′ = Cs or Ba, M = Nb or Ta and x = 1 or 2, in HSO_3F

Salt	Molarity	Temp.(K)	HSO_3F (δ, ppm)	Solute (δ, ppm)
$Cs[Nb(SO_3F)_6]$	0.2	293	40.79	-
		273	40.73	-
		253	40.73	-
		218	40.75	39.8(st), 39.1(st,b), 36.6(st,b)
$Cs[Ta(SO_3F)_6]$ (β-form)	0.07	293	40.60	-
		253	40.68	-
		218	40.65	37.9(st,b)
$Cs[Ta(SO_3F)_6]$ (α-form)	0.3	293	40.98	-
		253	41.02	40.3(st), 39.3(st,b)
		218	40.80	40.2(st), 39.5(st), 38.8(st), 37.9(st)
$Cs[Ta(SO_3F)_6]$ (α-form + filtrate)	?	293	40.69	-
		253	40.70	39.9(st), 39.0(st,b), 37.8(st,b)
		218	40.67	40.3(st), 39.8(st), 39.1(dt,b), 38.5(dt), 37.7(st)
$Cs_2[Nb(SO_3F)_7]$	0.1	293	40.98	-
		253	41.45	40.5(sh)
		218	41.49	40.4(st), 39.8(dt), 39.4(dt), 37.5(st,b)
$Ba[Nb(SO_3F)_7]$	0.1	293	40.67	-
		253	40.86	-
		218	40.85	39.6(st), 38.7(st), 36.9(st,b)
$Cs_2[Ta(SO_3F)_7]$	0.1	293	40.57	-
		253	40.64	-
		218	40.60	39.6(st), 39.1(st), 38.0(st)

Intensity-expanded portions of representative ^{19}F NMR spectra of the salt solutions are shown in Figures 6.12 and 6.13. Figure 6.12 shows the spectra of α-$Cs[Ta(SO_3F)_6]$ and "ß-$Cs[Ta(SO_3F)_6]$" at three different temperatures. Although the purity of the latter salt is questionable, the simplicity of its NMR spectra suggests that the discrete anion $[Ta(SO_3F)_6]^-$ is present in solution at 218 K, as indicated by the singlet peak *d*, assigned to six equivalent fluorosulfate groups. In contrast, the analytically pure salt α-$Cs[Ta(SO_3F)_6]$ exhibits four solute resonances *a*, *b*, *c* and *d* of progressively decreasing intensity at this temperature. The ^{19}F NMR spectrum of $Cs[Nb(SO_3F)_6]$ at 218 K appears quite similar to that of the α-salt solution, although only three solute peaks are resolved. Scales between the spectra of the different solutions shown in Figures 6.12 and 6.13 are not identical and consequently only line shapes and chemical shifts, rather than linewidths, are meaningful.

The ^{19}F NMR spectra of α-$Cs[Ta(SO_3F)_6]$ re-dissolved in the filtrate solution obtained during its isolation (see Chapter 5) are shown in Figure 6.13 together with spectra obtained for a solution of $Cs_2[Nb(SO_3F)_7]$. Already at 253 K, hints of the three solute peaks *b*, *c*, and *d* are seen in the α-isomer/filtrate spectrum. At 218 K, five peaks labelled *a*, *b*, *c'*, *c"* and *d* occur at approximately the same chemical shifts as the four peaks found for the α-isomer at this temperature, with peak *c* now forming a "doublet". Their relative intensities and shapes, however, are different. Peak *b* is now the most prominent, with peak *a* the least intense and most poorly resolved, due to the partial overlap of the solvent signal. Similarly, the spectrum of $Cs_2[Ta(SO_3F)_7]$ at 218 K exhibits the solute peaks *b*, *c'*, *c"* and *d* with very comparable intensities and shapes to those found for the α-isomer/filtrate solution; peak *a* may be present but hidden by the nearby solvent peak. The 0.5 - 0.8 ppm downfield shift of these peaks in the latter

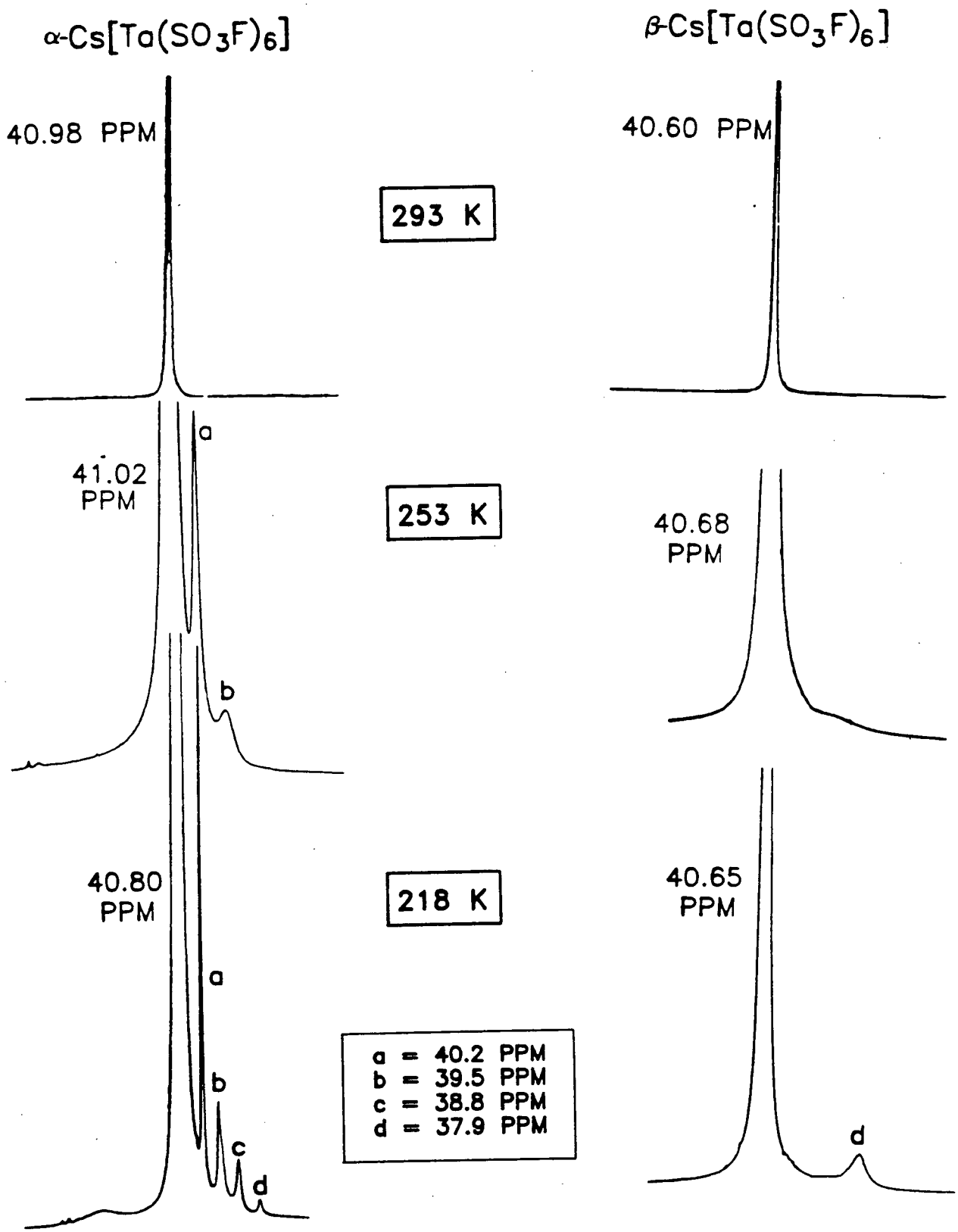

Figure 6.12. Variable Temperature ^{19}F NMR Spectra of α-$Cs[Ta(SO_3F)_6]$ (0.3 M) and β- $Cs[Ta(SO_3F)_6]$ (0.07 M) in HSO_3F

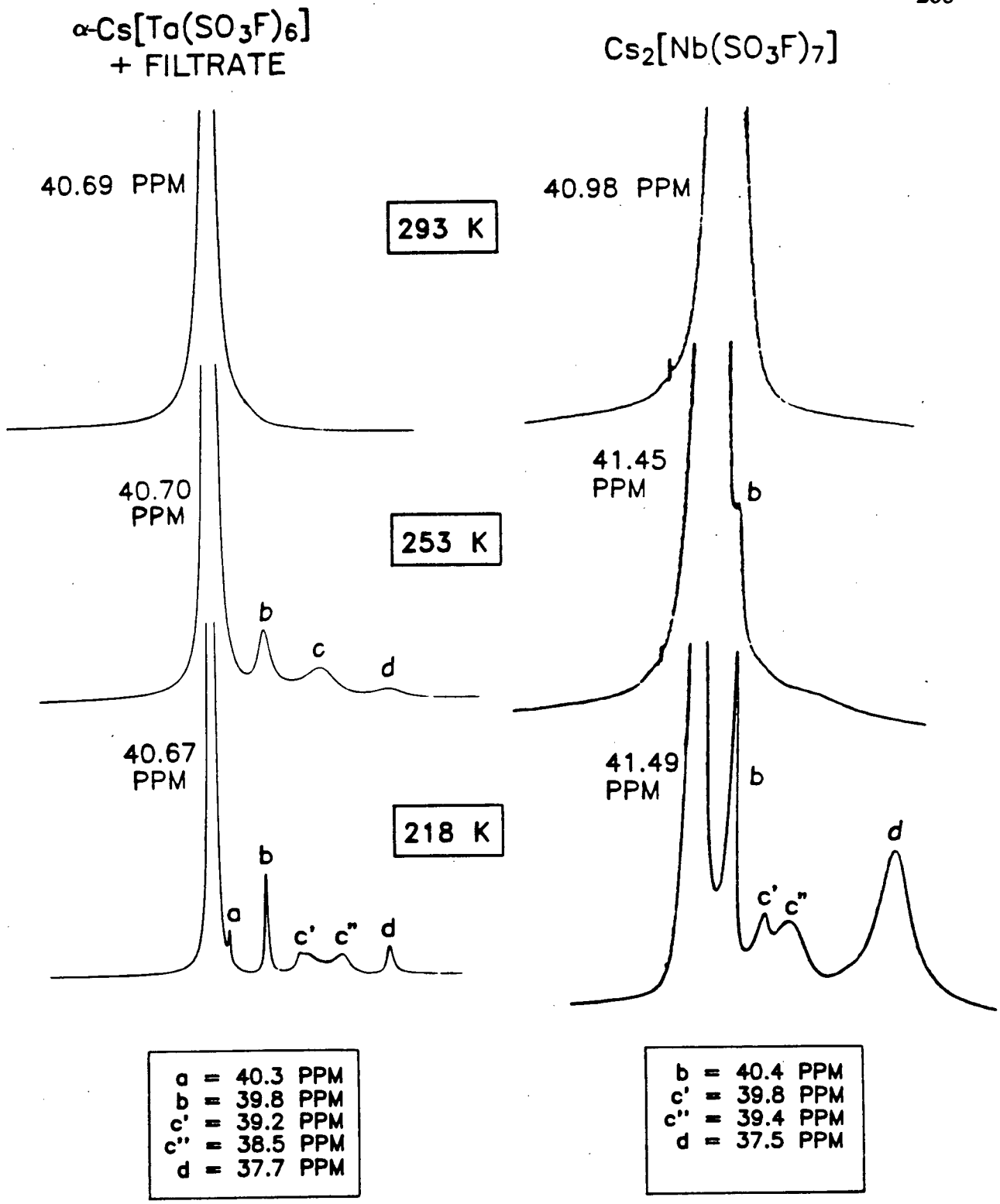

Figure 6.13. ^{19}F NMR Spectra of α-$Cs[Ta(SO_3F)_6]$/Filtrate and $Cs_2[Nb(SO_3F)_7]$ (0.1 M) in HSO_3F

system may be expected from the similar shift of the solvent resonance, as mentioned earlier; the chemical shifts may also be slightly dependent on the metal present. Incidentally, the spectra (218 K) of both $Cs_2[Ta(SO_3F)_7]$ and $Ba[Ta(SO_3F)_7]$ are similar to that of $Cs_2[Nb(SO_3F)_7]$, with the only noteworthy difference being the absence of peak *c* splitting.

The greater similarity between the spectra of the α-$Cs[Ta(SO_3F)_6]$/filtrate and $Cs_2[Nb(SO_3F)_7]$ solutions than between those of the former and the pure α-isomer solution is surprising. It suggests that in solution, both the α-hexakis- and heptakis-fluorosulfato anions exist in equilibrium with each other, with the relative abundance of each being a function of the redissolved salt's initial composition. The α-isomer/filtrate mixture appears from its spectra in Figure 6.13 to be a mixture of both of these anionic types. The presence of one or two moles of Cs^+, and hence the basicity of the solution, appears to determine which of the equilibrium species present will precipitate preferentially at high solute concentrations. The presence of peak *d* at 218 K in both the spectra of α-$Cs[Ta(SO_3F)_6]$ and $Cs_2[Nb(SO_3F)_7]$ serves to illustrate this point. This observation raises the question: why do all the solutions except ß-$Cs[Ta(SO_3F)_6]$ exhibit more than one solute peak in their spectra at 218 K?

The single solute peak *d* of the salt ß-$Cs[Ta(SO_3F)_6]$, prepared in an acid-free medium, is attributed to the species $[Ta(SO_3F)_6]^-$; the absence of any exchange equilibrium is indicated by the solvent resonance matching that of pure HSO_3F. The seemingly oligomeric salt, α-$Cs[Ta(SO_3F)_6]$, was however isolated from HSO_3F solution, which could consequently result in an equilibrium of oligomeric anions upon redissolution, as was found earlier for $Ta(SO_3F)_{5(solv)}$. The multicomponent spectra of the other three salts studied (see Table 6.VII) indicate similar equilibria occurring.

Based on the low-temperature spectra in Figures 6.12 and 6.13 as well as on the electrical conductivity studies of Section 6.C.1.c, the solution behaviour of these salts can be summarized by the following general set of equilibria:

$$\underset{\mathbf{A}}{[[M(SO_3F)_5]_x(SO_3F)_{2x}]^{2x-}_{(solv)}} \overset{K_1}{\underset{HSO_3F}{\rightleftharpoons}} \underset{\mathbf{B}}{[[M(SO_3F)_5]_x(SO_3F)_x]^{x-}_{(solv)}} + x\, SO_3F^-_{(solv)} \qquad (6\text{-}23a)$$

$$\underset{\mathbf{A}}{[[M(SO_3F)_5]_x(SO_3F)_{2x}]^{2x-}_{(solv)}} \overset{K_2}{\underset{HSO_3F}{\rightleftharpoons}} x\, \underset{\mathbf{C}}{[M(SO_3F)_7]^{2-}_{(solv)}} \qquad (6\text{-}23b)$$

$$\underset{\mathbf{B}}{[[M(SO_3F)_5]_x(SO_3F)_x]^{x-}_{(solv)}} \overset{K_3}{\underset{HSO_3F}{\rightleftharpoons}} x\, \underset{\mathbf{D}}{[M(SO_3F)_6]^-_{(solv)}} \qquad (6\text{-}23c)$$

$$\underset{\mathbf{C}}{[M(SO_3F)_7]^{2-}_{(solv)}} \overset{K_4}{\underset{HSO_3F}{\rightleftharpoons}} \underset{\mathbf{D}}{[M(SO_3F)_6]^-} + SO_3F^- \qquad (6\text{-}23d)$$

In the equilibria above, type **A** species predominate in the heptakis(fluorosulfato) salt solutions, whereas species **B** are favoured in the hexakis(fluorosulfato) metallate mixtures. Peak *d* is best assigned to the monomeric anion **D**, which is present in all four solutions at varying concentrations. The predominance of resonance *a* in the spectra of the hexakis(fluorosulfato) salt solutions with both metals (see Figure 6.12 and Table 6.VII) suggests that it is due to *terminal* SO_3F groups of species **B**. Based on previous ^{19}F NMR studies of the $SbF_5{\cdot}nSO_3$ (n = 1, 2 or 3) fluorosulfuric acid systems,[2,8] *bridging* SO_3F group resonances are expected upfield of terminal ones and therefore either peak *b* or *c* in Figure 6.12 is best assigned to the bridging SO_3F groups of type **B** species. In light of the predominance of peak *b'* in the spectrum of $Cs_2[Nb(SO_3F)_7]$ (see Figure

6.13), which is best assigned to the *terminal* SO_3F groups of type **A** components, peak *c* is assigned to the bridging fluorosulfate groups of both **A** and **B** type anions, since it is not unreasonable to expect them at more or less the same chemical shift.

The small concentration of species **A** in the α-$Cs[Ta(SO_3F)_6]$ and $Cs[Nb(SO_3F)_6]$ solutions (as indicated by the weak peak *b*) suggests that the magnitude of the equilibrium constants in Equation (6-22) may depend on the nature of the medium. However, the strong intensity of peak *d* in the 218 K spectrum of $Cs_2[Nb(SO_3F)_7]$ is consistent with the fairly large value of K_4 (or K_b) estimated in Section 6.C.1.c for this equilibrium, and supports the already suggested basic dissociation of the heptakis-fluorosulfato anions in HSO_3F.

Peaks *c'* and *c"* in Figure 6.13 are yet to be assigned. One of them is likely due to the *bridging* SO_3F groups of type **A** and/or **B** anions, the other to the nearly equivalent (due to rapid internal exchange) SO_3F groups of the monomeric anion **C** in Equations (6-23b) and (6-23d). The absence of this species from the spectra of all the hexakis-fluorosulfato solutions indicates that the magnitude of K_2 in Equation (6-23) is small while that of K_4 is quite large, verifying earlier arguments.

It should be stressed again that the spectra of the α-$Cs[Ta(SO_3F)_6]$/filtrate solution shown in Figure 6.13 have some characteristics of both the pure hexakis-fluorosulfato and heptakis-fluorosulfato salt solutions, which suggests the existence of the same anionic species in solution, whether one or two moles of $CsSO_3F$ are present, prior to the precipitation of the respective salt. Following the salt's precipitation, the relative abundance of the different solution components changes, as is indirectly

suggested, for example, by differences between the spectra of the pure α-$Cs[Ta(SO_3F)_6]$ solution and that of the filtrate mixture.

Ambient temperature (~293 K) ^{93}Nb NMR spectra of $Cs[Nb(SO_3F)_6]$ (spectrum IV) and $Cs_2[Nb(SO_3F)_7]$ (spectra I-III) are shown in Figure 6.14, the former after 2 hours in solution and the latter after 2 hours, 2 days and 5 days in solution. All the chemical shifts given are relative to that of the $[NbF_6]^-$ anion, as described in Section 6.B.3. The key features of the spectra are: (i) the presence of multiple signals, indicating more than one Nb environment, which is consistent with the ^{19}F NMR study; (ii) the similarity between the spectra of $Cs[Nb(SO_3F)_6]$ and $Cs_2[Nb(SO_3F)_7]$ and (iii) the nearly complete disappearance of the broad downfield signal in spectrum III. Of additional interest are the much smaller linewidth ($w_{1/2}$) of the most upfield signal compared to the other signals as well as the close proximity of this signal to that of the external reference $[NbF_6]^-$. The very large ^{93}Nb chemical shifts (about ± 1000 ppm) which have previously been reported to occur upon changing the chemical environment of niobium[15,16] make the last point more noteworthy.

The shielding for ^{93}Nb increases with the ability of its ligands to donate electrons and hence more tightly ligated complexes are expected to exhibit a higher degree of shielding, resulting in an upfield chemical shift. Based on both this consideration and the results of the ^{19}F NMR and conductivity studies, the resonances present in Figure 6.14 can be assigned. The narrow peak *a* is attributed to the highly symmetric $[Nb(SO_3F)_6]^-$ species, with the niobium nucleus even more shielded than in $[NbF_6]^-$. This could be partially due to the different solvents used (HSO_3F and propylene carbonate, respectively), since a 68 ppm chemical shift difference has been reported between the resonance of $[NbF_6]^-$ dissolved in aqueous HF and in acetonitrile.[16] The

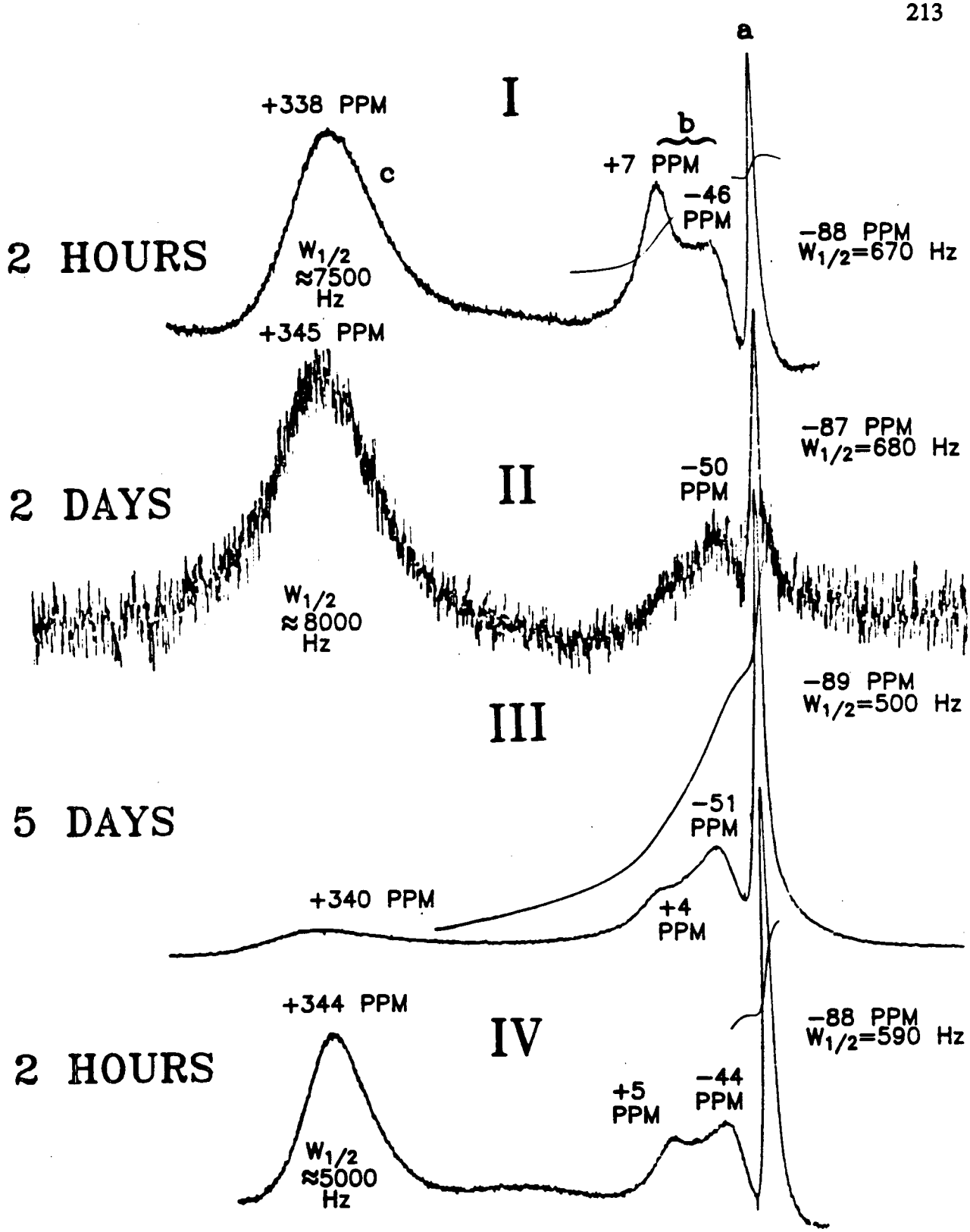

Figure 6.14. ^{93}Nb NMR Spectra of $Cs[Nb(SO_3F)_6]$ (0.2 M) and $Cs_2[Nb(SO_3F)_7]$ (0.15 M) in HSO_3F at Ambient Temperature

narrow linewidth of peak *a* (500-700 Hz) compared to that of $[NbF_6]^-$ (1470 Hz) is probably also a result of the different solvents used.[13] The solvent effect on the shape of the ^{93}Nb NMR signal of $[NbF_6]^-$ has also been studied.[15] A sharp singlet was observed in 48% HF/H_2O at 20 °C,[20] whereas a resolved septet pattern was seen in both ethanol at 0 °C[20] and acetonitrile at ambient temperature.[13] Broadening of the $[NbF_6]^-$ reference signal may be a result of unresolved ^{93}Nb-^{19}F coupling, internal fluorine exchange or the presence of the cation Li^+ in the $[NbF_6]^-$ solution.[13,20]

$[Nb(SO_3F)_6]^-$ is expected to be in equilibrium with species **B** and/or **C** (shown earlier in Equation (6-23)) in these solutions. However, the expected lower symmetry of the two species (especially **C**) would be expected to have a line broadening effect on signal *a* in Figure 6.14, which is not apparent. This suggests that the two respective equilibria's exchange processes are either too slow to affect the line shape[14] of peak *a* and/or that the aforementioned line broadening effects on the ^{93}Nb signal of the external reference $[NbF_6]^-$ are large enough to give the $[Nb(SO_3F)_6]^-$ signal *a* relatively narrow appearance. There appear to be no ^{93}Nb NMR studies reported where niobium is octahedrally coordinated to six identical nuclei with zero nuclear spin. Consequently, the effect of the rapid solvent/solute SO_3F group exchange evident from the ^{19}F NMR study cannot be correlated with confidence to the signal linewidths observed here.

The presence of more than one signal in all spectra shown in Figure 6.14 also suggests that the exchange rates governing the equilibria in Equation (6-23) are probably too slow to affect the ^{93}Nb signal linewidths noticeably. It should be noted that the partial disappearance of peak *c* in spectrum III is accompanied by a slight narrowing of peak *a*, perhaps indicating some effect of the equilibria on signal linewidth, but the narrowing effect is too subtle to allow definite conclusions.

The broadness of peak *c* in addition to its downfield position indicate that it is due to one or both of the two oligomeric species **A** and **B** in Equation (6-23a). They are expected to have the weakest average Nb-O bonds of all four species shown in Equation (6-23) and their symmetry is expected to be significantly reduced due to the presence of SO_3F bridges. The earlier mentioned equilibrium exchange processes may further contribute to the signal's width. The near disappearance of this peak from spectrum III in Figure 6.14 after 5 days in solution may be due to structural rearrangement of the solute anions from oligomers to monomers.[1]

Peak *b* seen in all four spectra in Figure 6.14 can then be assigned to $[Nb(SO_3F)_7]^{2-}$. The peak's doublet-like character may be due to the equilibria shown in Equation (6-23) and/or to the presence of an additional intermediate. The broadness of this peak is not surprising, since the metal coordination environment of $[Nb(SO_3F)_7]^{2-}$ should not be nearly as symmetric as that of $[Nb(SO_3F)_6]^-$ (peak *a*). Although the relatively high intensity of peak *b* in spectrum IV ($Cs[Nb(SO_3F)_6]$) is surprising in light of the equilibria Equations (6-23), and the apparent absence of $[Nb(SO_3F)_7]^{2-}$ from this solution as indicated by its ^{19}F NMR spectrum, it should be recalled that the ^{19}F NMR spectra were obtained at lower temperatures than the ^{93}Nb NMR spectra. If it is assumed that oligomers are favoured over monomers at low temperature, the absence of a resonance due to $[Nb(SO_3F)_7]^{2-}$ from the low temperature 19F NMR spectrum of $Cs[Nb(SO_3F)_6]$ is more acceptable.

The low temperature ^1H NMR spectra of α-$Cs[Ta(SO_3F)_6]$ suggest that proton exchange equilbria are temperature dependent as well. The single resonance (due to the solvent) undergoes an upfield shift from 10.29 to 9.95 ppm when the temperature is lowered from 298 to 203 K. The resonance of pure HSO_3F shifts in the opposite

direction in the same temperature range, from 10.47 to ~10.65 ppm. The increased oligomerization of solvated anions at the lower temperature may be responsible for this shielding effect on the proton resonance.

The previously indicated complexity of these systems is apparent from the NMR spectra as well. A mixture of six, seven or eight coordinated monomers and oligomers appears to form in HSO_3F upon dissolution of the ternary salts, with the relative abundance of each species a function of both temperature and the initial salt composition. Similar equilibria have been reported[2,8,34-37] for the HSO_3F - $SbF_5 \cdot nSO_3$ (n = 0 - 3) systems, where SO_3F - F exchange and the presence of both terminal and bridging fluorines create an even more complicated situation. The appearance of the solute fluorosulfate ^{19}F NMR resonances upfield of the HSO_3F resonance at low temperature does not have a precedent among previously studied metal or metalloid fluorosulfate systems,[1,2,4,7,33,38,39] where the signals are either not resolvable even at low temperature, or occur downfield of the solvent resonance.

6.C.3.b. $M(SO_3F)_5$, $M(SO_3F)_5$-$S_2O_6F_2$ and $M(SO_3F)_5$-MF_5 (M = Nb or Ta) Systems

Both $Nb(SO_3F)_5$ and $Ta(SO_3F)_5$ undergo rapid fluorosulfate exchange with HSO_3F, leading to a combined ^{19}F NMR signal down to 218 K. In a mixture of $S_2O_6F_2$ with HSO_3F, solvent-solute interaction via proton bridging and/or proton transfer as well as fluorosulfate exchange were observed (see Chapter 3). These interactions occur in both neutral and basic (by adding KSO_3F) solutions, but have not been discussed for *acid* media.

To be consistent with the approach of Chapter 3, both ^{19}F NMR and ^{1}H NMR studies of the $M(SO_3F)_5$-HSO_3F-$S_2O_6F_2$ (M = Nb or Ta) solutions were undertaken (the

former at variable temperatures), with the results listed in Table 6.VIII. Two signals are present in the spectra, the downfield one due to the combined $M(SO_3F)_5/HSO_3F$ resonance and the upfield one resulting from the resonance of $S_2O_6F_2$. Again, two parameters are of special interest: (i) the "H/OX" int./stoich. ratios for the two solutions at the various temperatures, which are derived from the following equation:

$$\frac{\text{H/OX int.}}{\text{H/OX stoich.}} = \frac{m_A/m'_{OX}}{(m_H + m_{LA})/m_{OX}} \qquad (6\text{-}24)$$

where: m_H = *stoichiometric* moles fluorine from HSO_3F
m_{LA} = *stoichiometric* moles fluorine from $M(SO_3F)_5$
m_{OX} = *stoichiometric* moles fluorine from $S_2O_6F_2$
m_A = total moles fluorine due to $M(SO_3F)_5$ and HSO_3F, by *integration*
m'_{OX} = moles fluorine due to $S_2O_6F_2$, by *integration*

and (ii) the difference between the chemical shift separating the $HSO_3F/M(SO_3F)_5$ and $S_2O_6F_2$ signals in these solutions and the separation between the signals of HSO_3F and $S_2O_6F_2$ before mixing. This parameter is given as **M-U** in Table 6.VIII. If no interaction were occurring between HSO_3F and $S_2O_6F_2$ in the presence of the Lewis acids, the latter parameter should have a value of zero, whereas the parameter in Equation (6-24) should be exactly equal to unity. It is evident from the data in Table 6.VIII that $Ta(SO_3F)_5$, as the Lewis acid, is capable of inhibiting the interaction between HSO_3F and $S_2O_6F_2$, which is still appreciable even at this temperature. At 253 K and even more so at 298 K, some very limited HSO_3F-$S_2O_6F_2$ interaction appears to occur in the presence of $Ta(SO_3F)_5$, but is less pronounced than in either neutral or basic solutions.

With $Nb(SO_3F)_5$ as Lewis acid, the situation is not quite as straightforward. At 298 K, the degree of HSO_3F-$S_2O_6F_2$ interaction appears to be slightly greater than with

Table 6.VIII. ^{19}F and ^{1}H NMR Data for $M(SO_3F)_5$-HSO_3F-$S_2O_6F_2$ Solutions

Sample[a]	Temperature (Kelvin)	$[M(SO_3F)_5]$ (mol/L)	Molar Ratio (H/OX)	I/S[b]	M-U (ppm)[c]	Δ ^{1}H HSO_3F (ppm)[c]
Nb/H/OX	298	1.00	3.18	1.14	-0.15	+0.22
	253			1.05	-0.01	-
	218			0.92	+0.01	-
Ta/H/OX	298	0.90	1.90	1.09	-0.11	+0.40
	253			1.04	0	-
	218			1.00	0	-

[a]Nb = $Nb(SO_3F)_5$, Ta = $Ta(SO_3F)_5$, H = HSO_3F, OX = $S_2O_6F_2$
[b]I = Integration peak area H/OX ratio, S = H/OX fluorine content ratio from stoichiometry
[c]see text

$Ta(SO_3F)_5$, but less pronounced than in neutral or basic solutions. At 253 K, a similar reduction in the interaction to that found with $Ta(SO_3F)_5$ is observed. However, at 218 K, the "H/OX" int./stoich parameter value is less than unity (by about 8%), while the near zero value of the other parameter suggests absence of any HSO_3F-$S_2O_6F_2$ interaction. The former feature may be due to integration error or may suggest that other species of the form $NbF_x(SO_3F)_{5-x}$ are present in solution rather than $Nb(SO_3F)_5$. This would account for the sub-unity value of the former parameter, since fluorine bonded to niobium is not expected to resonate at the same chemical shift as the fluorine of the SO_3F group.[14] The absence of a detectable Nb-F resonance in the ^{19}F NMR spectra may be due to the high spin (I = 9/2) and quadrupole moment[17] of ^{93}Nb, which can lead to signals too broad for observation.[15-17,20] For comparison, solutions of octahedral $[NbF_6]^-$ in either acetonitrile[13] or dimethylformamide[14] have exhibited ^{19}F NMR decet patterns due to the coupling of the chemically equivalent fluorine nuclei to the quadrupole nuclide ^{93}Nb. Even saturated (~1 M) solutions of NbF_5 failed to show any signals in their ^{19}F NMR spectra. This seems to suggest that this solute undergoes rapid F/SO_3F exchange with the solvent, which leads to a reduction in the average coordination symmetry around the metal center.

The value of 0.92 for the parameter defined earlier in Equation (6-24), which was estimated for the "$Nb(SO_3F)_5$" solution at 218 K, best agrees with the formulation $NbF_2(SO_3F)_3$ for the Lewis acid. This is the same composition that was found earlier for solids formed either from 1.1 M or 2.4 M "$Nb(SO_3F)_5$" solutions. Hence, all evidence indicates that $Nb(SO_3F)_5$ does not exist in HSO_3F solutions beyond concentrations of ~1 M, but tends to dissociate to form primarily $NbF_2(SO_3F)_3$. Conversely, $Ta(SO_3F)_5$ does not seem to undergo dissociation at these concentrations and $TaF_x(SO_3F)_{5-x}$ type precipitates do not form.

The ambient temperature ^1H NMR data of the two Lewis acid solutions (appearing as the parameter $\Delta\,^1H$ **HSO_3F**) are also given in Table 6.VIII and refer to the chemical shift difference between the observed combined solute/solvent resonance and that of pure HSO_3F. The rapid proton exchange between solvent and solute with both metals, which leads to a single resonance, is thought to occur[4,5] primarily according to the equilibrium:

$$M(SO_3F)_5 + HSO_3F \overset{HSO_3F}{\rightleftharpoons} H[M(SO_3F)_6]_{(solv)} \qquad (6\text{-}25)$$

The slight downfield shift of this resonance relative to that of pure HSO_3F may be due either to the interaction between HSO_3F and $S_2O_6F_2$ and/or to the interaction of $M(SO_3F)_5$ and HSO_3F.

The ability of both "$Nb(SO_3F)_5$" and $Ta(SO_3F)_5$ to retard the HSO_3F - $S_2O_6F_2$ interaction at ambient temperature and to stop it at 218 K lends support to the SO_3F exchange mechanism between HSO_3F and $S_2O_6F_2$ suggested in Chapter 3. The presence of a SO_3F acceptor appears to interfere in the exchange process. The residual ambient temperature interaction observed in both Lewis acid systems is probably due to the other interaction mechanisms discussed in Chapter 3.

The rest of this section will deal with multinuclear NMR investigations of the $M(SO_3F)_5$-HSO_3F solutions, with M = Nb or Ta, together with various $M(SO_3F)_5$-MF_5-HSO_3F and MF_5-HSO_3F solutions. The latter studies were carried out for three main reasons: (i) to learn more about the $Nb(SO_3F)_5$ dissociation via SO_3 elimination; (ii) to confirm the absence of such a dissociation in $Ta(SO_3F)_5$ at comparable concentrations and (iii) to investigate to what extent SO_3F/F ligand exchange occurs.

Table 6.IX contains the chemical shift and signal linewidth ^{19}F NMR data for all the solutions studied together with data for pure HSO_3F. None of the species, including NbF_5 nor TaF_5, exhibited any sign of M-F resonances; only the combined SO_3F/HSO_3F resonance was observed at all temperatures in each case. The significant downfield shift and greater linewidth of the $Ta(SO_3F)_5$ solution's signal (1-2 ppm) compared to that of pure HSO_3F and the other species are both indicative of a greater degree of chemical exchange. A downfield shift is expected for HSO_3F solutions rich in $H_2SO_3F^+$, since the addition of the base KSO_3F shifts this resonance upfield.[40] Both features indicate high acidity of the $Ta(SO_3F)_5$ system. Furthermore, this signal's closer proximity to that of pure HSO_3F in the earlier discussed $Ta(SO_3F)_5$-HSO_3F-$S_2O_6F_2$ solutions supports the claim made that $S_2O_6F_2$ behaves as a weak base in HSO_3F, since a large portion of the excess $H_2SO_3F^+$ formed in the presence of a Lewis acid is neutralized by the $S_2O_6F_2$.

The ^{19}F resonance is also found in much closer proximity (within about 0.3 ppm downfield) of the pure HSO_3F signal for each of the $Nb(SO_3F)_5$, $Nb(SO_3F)_5$-NbF_5 and NbF_5 solutions, which indicates lower acidity in these systems. The linewidth of the NbF_5 signal is comparable to that of the pure solvent, indicating a very minimal degree of F/SO_3F exchange, as would be expected for this relatively weak acid.[3] The other two systems' signals exhibit a similar degree of broadening, which suggests a comparable degree of exchange being present in both; this would only be expected if the exchanging species were of very similar composition. This further supports the conclusion that $Nb(SO_3F)_5$ appears to be partly dissociated into $NbF_x(SO_3F)_{5-x}$ at these concentrations.

The ^{19}F signal position and linewidth of TaF_5 is very comparable to that of NbF_5, indicating similarly weak acidity. The narrower than expected linewidth of the signal at

Table 6.IX. ^{19}F NMR Data for Solutions of $M(SO_3F)_5$, $M(SO_3F)_5$-MF_5 and MF_5 (with M = Nb or Ta) in HSO_3F

Solute	Molarity	Temp.(K)	δ (ppm)	$w_{1/2}$ (Hz)	Solute	Molarity	Temp.(K)	δ (ppm)	$w_{1/2}$ (Hz)
None	-	293	40.74	≤ 5	$Ta(SO_3F)_5$	0.9	305	41.98	90
		253	40.68	≤ 10			273	41.94	140
		218	40.64	≤ 15			253	41.97	100
							218	42.29	110
$Nb(SO_3F)_5$	1.0	298	40.88	22					
		273	40.79	30	"$Ta(SO_3F)_5$"	~13	293	40.25	15
		253	40.77	38			253	40.24	40
		218	40.85	90			218	40.19	50
$Nb(SO_3F)_5$-NbF_5 (1:1)	2.2	293	40.80	15	$Ta(SO_3F)_5$-TaF_5 (1:1)	2.5	293	40.71	≤ 10
		253	40.84	40			253	40.63	10
		218	40.80	60			218	40.57	20
NbF_5	0.9	293	41.02	~ 10	TaF_5	0.7	293	40.89	30
		253	41.00	≤ 15			253	40.95	25
		218	41.01	≤ 20			218	40.94	~ 15

218 K may be a result of solute precipitation, resulting in reduced exchange. The resonance observed for the $Ta(SO_3F)_5$-TaF_5 mixed system is similar to that for pure HSO_3F at all three temperatures, suggesting minimal acidity for this system. This also seems to preclude any significant solvent/solute equilibrium, which is very surprising in light of the high acidity of $Ta(SO_3F)_5$. The spectra of the highly concentrated (8 m) $TaF_x(SO_3F)_{5-x}$ solution offer some clues. Its resonance at all three temperatures is observed upfield of HSO_3F, which together with the signal's broad linewidth suggests the presence of a new, less acidic species in equilibrium with the solvent. The differences between the mixed Ta systems' spectra and that of the earlier discussed $Ta(SO_3F)_5$ solution suggests that $Ta(SO_3F)_5$ exists "intact" at least up to a concentration of ~1 M.

The variable temperature ^1H NMR data for $Ta(SO_3F)_5$, "$Nb(SO_3F)_5$" (at two different concentrations) and HSO_3F are given in Table 6.X. Rapid proton exchange is

Table 6.X. ^1H NMR Data for $M(SO_3F)_5$, with M = Nb or Ta, in HSO_3F

Solute	Concentration (M)	Temperature (K)	δ (ppm)	$w_{1/2}$ (Hz)
none	–	298	10.47	≤ 2
		273	10.60	9
		253	10.65	35
		218	10.66	41
$Nb(SO_3F)_5$	2.4	298	10.85, 10.80	3
	1.0	298	10.60	5
	"	273	10.73	13
	"	253	10.77, 10.72, 10.60	52
	"	218	10.59, 10.48	61
$Ta(SO_3F)_5$	0.9	298	11.84	19
	"	273	11.99	28
	"	253	12.04	82
	"	218	12.10	103

evident for $Ta(SO_3F)_5$ from the single resonance obtained at all the temperatures studied. Its downfield shift from that of pure HSO_3F by ~1.5 ppm and the increase in linewidth support this system's high acidity. The 1.0 M "$Nb(SO_3F)_5$" solution, on the other hand, shows an unusual splitting of the solvent proton resonance into two or even three closely spaced signals at the lower temperatures, whereas in the 2.4 M solution, this splitting is already present at ambient temperature.

The results from the ^{93}Nb ambient temperature NMR studies on the niobium-containing solutions are recorded along with data for the external reference, $LiNbF_6$, in Table 6.XI. The most noticeable feature is the broadness of the lone signal observed for each system, which indicates low symmetry around the metal centers[15] and/or rapid exchange between the different species in solution. The observation of only one signal in each case indicates the presence of only one *average* Nb environment in each solution.

Table 6.XI. ^{93}Nb NMR Data for Niobium Fluorosulfates and Fluorides at 293 K

	$Nb(SO_3F)_5$	$Nb(SO_3F)_5/NbF_5$[a]	NbF_5	$LiNbF_6$
Solvent	HSO_3F	HSO_3F	HSO_3F	PC[b]
Molarity (M)	2.4	2.2	1.0	5
δ (ppm)	-80	+20	+60	0
$w_{1/2}$ (Hz)	20,000	27,000	16,000	1470

[a] 1:1 molar ratio
[b] PC = propylene carbonate

The position of the $Nb(SO_3F)_5$ signal at approximately the same chemical shift as that of peak *a* assigned to $[Nb(SO_3F)_6]^-$ in Figure 6.14 suggests that $[Nb(SO_3F)_6]^-$ may be

present in this solution. However, the large $w_{1/2}$ value of 20 kHz found here not only makes the assignment of the exact shift difficult but does not at all correlate with the ~ 600 Hz linewidth found for peak *a* in Figure 6.14. Such a large difference in linewidth can only be explained by assuming that the average symmetry around Nb has been greatly reduced,[15-17] possibly as a result of an equilibrium between species of the type $[NbF_x(SO_3F)_{5-x}]^-$ and/or $[Nb(SO_3F)_5]_nSO_3F^-$ and $[Nb(SO_3F)_6]^-$. The even broader $Nb(SO_3F)_5$-NbF_5 signal supports this, since here the SO_3F/F environment is fully scrambled. The slightly narrower signal of the NbF_5 solution further reflects the relative complexity of the three solutions studied. The apparent tendency of the ^{93}Nb resonances to move upfield with SO_3F content (see Table 6.XI) suggests that the fluorosulfate group is possibly a better π-donor than fluorine, as might be expected.

The ambient temperature ^{19}F NMR spectrum of $TaF_4(SO_3F)$, with its synthesis discussed in Chapter 5, serves as another source of information for the $Ta(SO_3F)_5$-TaF_5 system. The spectrum of a solution obtained *in situ* is shown in Figure 6.15. Three resonances are seen: a broad peak at 119 ppm downfield from $CFCl_3$, an extremely weak line at 40.4 ppm and an intense narrow signal at 38.8 ppm. The intensity integration ratios of the signals are 3.4 : 0.025 : 1.0, respectively. Although the chemical shift of the resonance at 40.4 ppm is very similar to that of HSO_3F (40.74 ppm), its extremely low intensity precludes its assignment as such here. The single broad resonance at 119 ppm is assigned to resonances of fluorine bonded to tantalum. Brownstein et al.[18] found Ta-F resonances of $[TaF_5(SO_3F)]^-$ at 103.9 ppm and 70.4 ppm in SO_2 solution. This suggests that all the fluorines bonded to Ta in $TaF_4(SO_3F)$ are chemically equivalent and that the structure or chemical exchange present must be of a different sort than present for Brownstein's compound. The broadness of the signal at 119 ppm is due to the large quadrupole moment of ^{181}Ta (I = 7/2).[15-17] Since the ^{19}F NMR spectra of Ta-F_x species

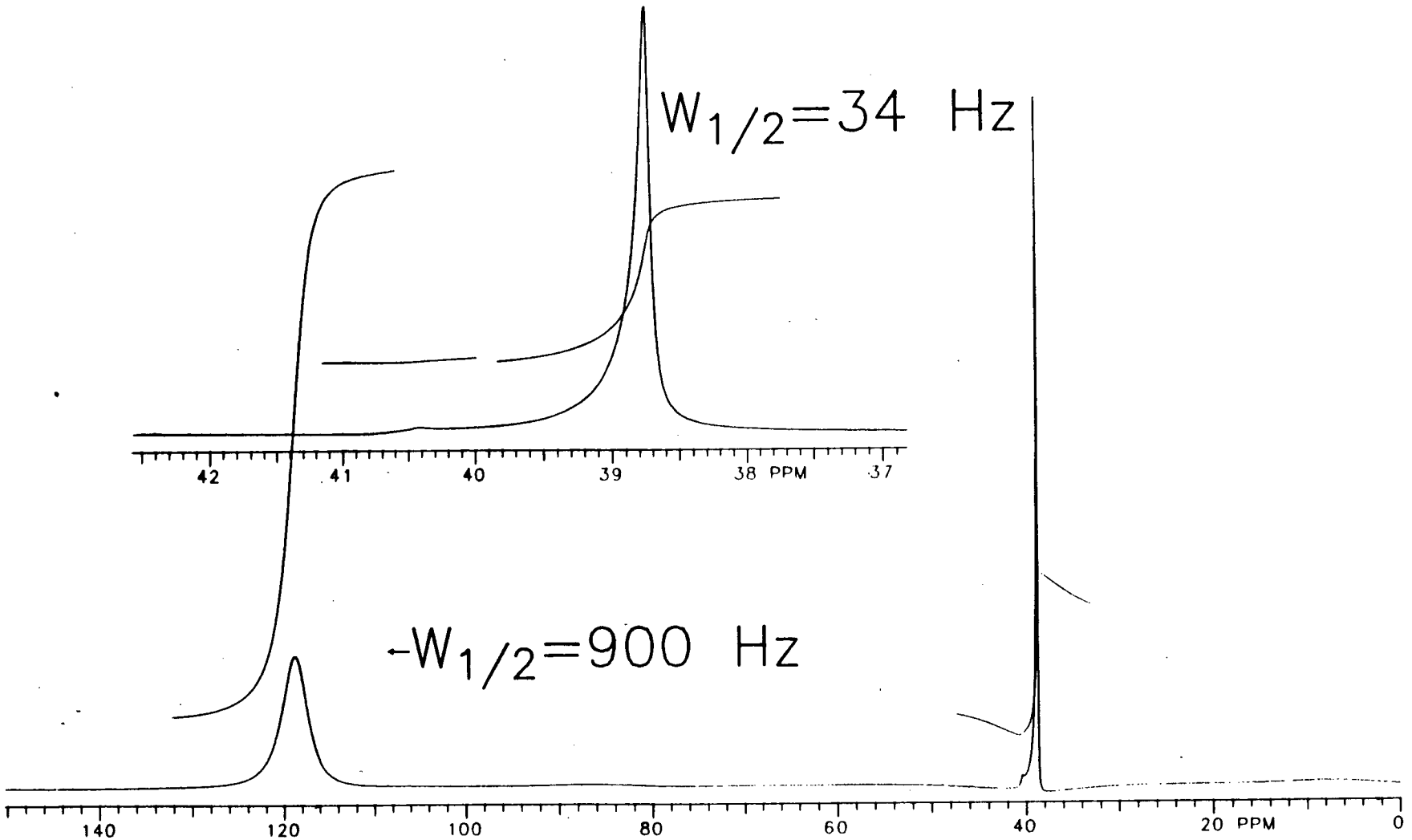

Figure 6.15. ^{19}F NMR Spectrum of $TaF_4(SO_3F)$ in HSO_3F at Ambient Temperature

with low local symmetry show[15,16,20] either extremely broad signals or no signals at all, the present compound must be quite symmetric. This is further verified by the absence of any signals in the spectrum of the octahedral $[TaF_6]^-$ in 48% HF, due to the combined effect from the suspected symmetry-reducing fluoride exchange with the solvent[20] and the high quadropole moment of ^{181}Ta.[15-17] It hence appears quite likely that at least in solution, $TaF_4(SO_3F)$ exists with trans-SO_3F groups, to allow the attainment of maximum symmetry. In solid state, distinction between cis- or trans-SO_3F bridges was not possible for this species (see Chapter 5).

The high symmetry of the solute which is required to explain the resonance at 119 ppm could of course be attained if $TaF_4(SO_3F)$ dissociated in solution to form $[TaF_6]^-$. However, not only is such a dissociation unlikely to occur in HSO_3F, but the ambient temperature ^{19}F resonance of $[TaF_6]^-$ in propylene carbonate was found at a significantly different chemical shift of 31 ppm.

Using vibrational spectroscopy, the oligomeric nature of the solid-state structure of $TaF_4(SO_3F)$ was found to involve bridging SO_3F groups. The signal at 38.8 ppm is therefore attributed to these SO_3F groups, and it is interesting to note that its position agrees very well with that of the resonances earlier attributed to bridging SO_3F groups in the spectra of the $Cs_x[M(SO_3F)_{5+x}]$ salt solutions, shown in Figures 6.12 and 6.13. It is also likely that the solvent HSO_3F is also contributing to this resonance via rapid fluorosulfate exchange with the solute. There is no evidence found in the spectrum for bridging fluorides, which is consistent with the solid state structure.

If $[TaF_4(SO_3F)]_n$ is the composition of the solute in Figure 6.15, then the F : SO_3F intensity ratio should be 4.0:1 and not 3.4:1. This discrepancy can be explained as

follows. Firstly, $[TaF_4(SO_3F)_2]^-_{(solv)}$ is expected in solution as a result of dissociation of the oligomer according to:

$$[TaF_4(SO_3F)]_{n(solv)} + 2n\,HSO_3F \underset{K_a}{\overset{HSO_3F}{\rightleftharpoons}} n\,[TaF_4(SO_3F)_2]^-_{(solv)} + n\,H_2SO_3F^+_{(solv)} \quad (6\text{-}26)$$

In addition, the efficient formation (large K_a) of the monomeric anion with the simultaneous formation of n moles of $H_2SO_3F^+$ per mole of oligomer suggests that the system may behave as an acid in HSO_3F. A similar equilibrium may also contribute in part to the acidity of $Ta(SO_3F)_5$ in ≥1 mole % HSO_3F solutions, as discussed in Section 6.C.2. The resulting 2 : 1 F/SO_3F ratio of the monomer would in part explain the aforementioned ratio discrepancy, since a monomer/oligomer ratio of 0.22 would be enough to lower the integration F/SO_3F ratio to the observed 3.4 value. The contribution from the solvent to the solute's fluorosulfate resonance at 38.8 ppm could also explain this discrepancy. By assuming that half of the discrepancy between the F/SO_3F ratios is due to the monomer's presence and the other half to excess intensity of the solute's SO_3F signal from the solvent contribution, an approximate HSO_3F concentration of 10 mole % was calculated. This implies that 90 mole % of the solution is composed of $TaF_4(SO_3F)$, equal to the highest reported[8] concentration of SbF_5 in HSO_3F. Even if the likely monomeric contribution to this system is completely ignored, the solution still works out to be 80 mole % in $TaF_4(SO_3F)$. It appears that significantly higher concentrations of $TaF_4(SO_3F)$ in HSO_3F are possible than were earlier estimated for $NbF_2(SO_3F)_3$.

This section's results indicate that the following two equilibria best describe the general behavior of the "$M(SO_3F)_5$" species in HSO_3F:

$$[M(SO_3F)_5]_n + 2n/(n-y)\ HSO_3F \overset{HSO_3F}{\rightleftharpoons}$$

$$n/(n-y)\ [M(SO_3F)_5]_{n-y}SO_3F]^-_{(solv)} + n/(n-y)\ H_2SO_3F^+_{(solv)} \qquad (6\text{-}27a)$$

$$n/(n-y)\ [[M(SO_3F)_5]_{n-y}SO_3F]^-_{(solv)} \overset{-HSO_3F}{\rightleftharpoons}$$

$$n/(n-y)\ [[MF_x(SO_3F)_{5-x}]_{n-y}SO_3F]^-_{(solv)} + nx\ SO_3 \qquad (6\text{-}27b)$$

where: $n > y$ and $x \leq 4$

These equations infer the presence of various oligomers in solution, as suggested by the conductivity and NMR studies. The SO_3 elimination becomes noticeable when either the solvent HSO_3F is removed in vacuo or a more concentrated solution is prepared. At higher concentrations, the binary oligomers dissociate to form fluorofluorosulfates. Dissociation appears to be more pronounced in the $Nb(SO_3F)_5$ system than in the $Ta(SO_3F)_5$ system: $NbF_2(SO_3F)_3$ formed from a 1.1 M "$Nb(SO_3F)_5$" solution, whereas $Ta(SO_3F)_5$ appears to remain undissociated up to at least 2 M concentrations, with definite signs of dissociation only observable when solutions of concentrations beyond ~10 M are prepared.

The final section of this chapter will briefly deal with Raman studies of some of these MSO_3F-MF_5 species in HSO_3F solution.

6.C.4. Raman Spectroscopy Studies of $M(SO_3F)_5$-MF_5 (M = Nb or Ta) Solutions

Interpretation of the Raman spectra obtained for HSO_3F solutions of $M(SO_3F)_5$ and $M(SO_3F)_5$-NbF_5 mixtures (M = Nb or Ta) is greatly impeded by the presence of solvent bands in the vicinity of the solute bands. The only spectral region where band overlap is not a serious problem is the ~600 - 800 cm^{-1} region. Some solute bands can also occasionally be resolved at higher wavenumbers. To illustrate this point, the room

temperature Raman data for bands which are not attributable to HSO_3F for all six solutions studied are listed in Table 6.XII. Plausible assignments are also listed. Previously reported[37,41] Raman frequencies for HSO_3F were listed earlier in Chapter 3.

The most intriguing feature in all the tabulated spectra is the presence of a very broad band of variable intensity at ~700 - 740 cm^{-1}, which is the approximate region where terminal M-F (M = Nb or Ta) stretching modes are observed for solid MF_5,[42] as well as for various HF solutions of K_xMF_{5+x} (x = 1 or 2).[12,43] The Raman spectrum of solid $TaF_4(SO_3F)$ discussed in the previous chapter also exhibited three bands assigned to Ta-F stretching modes in this region. If this band is assigned as a M-F stretch in these solutions, its appearance in the mixed 1:1 $M(SO_3F)_5$-MF_5 solutions is not surprising. The presence of this band in the spectrum of the 2.4 M $Nb(SO_3F)_5$ solution is also not too surprising, since $NbF_2(SO_3F)_3$ eventually precipitates out of solution; however, the Raman spectrum (albeit of low quality) of solid $NbF_2(SO_3F)_3$ discussed in Chapter 4 did not show any bands in this region. This indicates that the coordination environment around niobium may be different in solution than it is in solid state, possibly due to a partial break up of the oligomer. However, the presence of a band in this region for the three "$Ta(SO_3F)_5$" solutions is rather puzzling.

The proximity of the 13 M "$Ta(SO_3F)_5$" solutions's only ^{19}F NMR resonance to that of the fluorosulfate in $TaF_4(SO_3F)$ (see previous section) suggests that this solution may at least in part be composed of the latter species. This is supported by its ν(S-F) band (see Table 6.XII) occurring at a comparable frequency to that of solid $TaF_4(SO_3F)$ discussed earlier. The band at ~700 cm^{-1} for this solution is hence reasonably assignable to ν(Ta-F).

Table 6.XII. Raman Vibrational Frequencies ($\Delta\nu$, cm^{-1}) for Assorted $M(SO_3F)_5$ and $M(SO_3F)_5$-MF_5 Mixtures in HSO_3F at Ambient Temperature[a]

$Nb(SO_3F)_5$ (2.4 M)	$Nb(SO_3F)_5$-NbF_5 (2.2 M)	$Ta(SO_3F)_5$ (0.6 M)	$Ta(SO_3F)_5$ (1.6 M)	"$Ta(SO_3F)_5$" (~13 M)	$Ta(SO_3F)_5$-TaF_5 (2.5 M)	Approximate Assignment
			1462 w			
1257 s	1247 m	1245 m	1248 m		1242 m	ν (SO_3)
1072 vw			1078 w		1110 w	
1010 w						
	880 w,sh			890 w		ν (S-F)
				878 w		
734 w,b	747 m	738 w	738 m	738 s	737 m	
714 w,b,sh	725 w,sh			723 m	725 w	? ν (M-F) ?
		702 vw	709 w		699 w	
639 m	642 w,b	645 vw	650 w	642 w	641 w	δ (SO_3F)
			527 w			
290 w,b	311 w		263 w	271 w	271 w	lattice
256 w	240 w,b		240 w	243 m	244 w	vibrations

[a]solvent bands excluded

The previous sections of this chapter as well as the method of preparation of $TaF_4(SO_3F)$ described in the previous chapter suggest that $Ta(SO_3F)_5$ remains intact up to concentrations of ~2 M, which either makes the assignment of the ~700 - 740 cm^{-1} band to ν(Ta-F) doubtful, or leads to the apparent contradiction that the species undergo elimination of SO_3 even at relatively low concentrations of 0.6 - 1.6 M. Unfortunately, SO_3 is undetectable in these solutions because it is removed in vacuo with $S_2O_6F_2$ during preparation of the solutions. The elimination of SO_3 as a result of partial laser-induced decomposition of the solutions cannot be ruled out as a means of resolving the dilemma; some of the solutions did become quite murky within minutes of laser exposure.

It appears that with each completed study, a new level of complexity is revealed for these superacid systems. A few suggestions concerning possible future investigations will be stated in the closing chapter.

6.D. Conclusion

The following conclusions can be drawn from the solution studies described:

(i) $Nb(SO_3F)_5$ and $Ta(SO_3F)_5$ behave as monoprotonic acids in fluorosulfuric acid, leading to two new superacid systems of different strength.

(ii) HSO_3F-$Ta(SO_3F)_5$, the stronger of the two systems, appears to possess even greater acidity than "Magic Acid" HSO_3F-SbF_5 at all but the lowest concentrations studied.

(iii) At the concentrations studied, $Nb(SO_3F)_5$ is more highly oligomerized in solution than is $Ta(SO_3F)_5$.

(iv) The empirical anions "$[M(SO_3F)_6]^-$" and "$[M(SO_3F)_7]^{2-}$" undergo unexpectedly complex behaviour in solution with both metals, seemingly existing as temperature-dependent equilibrium mixtures of coordinatively unsaturated oligomeric species.

(v) Species of the type $[[MF_x(SO_3F)_{5-x}]_nSO_3F]^-$ appear to form with both $Nb(SO_3F)_5$ and $Ta(SO_3F)_5$ as a result of SO_3 elimination at higher concentrations; not surprisingly, this dissociative tendency is more pronounced for the niobium system.

In the next chapter, the conveniently high solubility of both $Nb(SO_3F)_5$ and $Ta(SO_3F)_5$ will be further applied to prepare some analogous (trifluoromethyl)sulfato derivatives.

REFERENCES

1. K.C. Lee and F. Aubke, *Inorg. Chem.* **23**, 2124 (1984).

2. R.C. Thompson, J. Barr, R.J. Gillespie, J.R. Milne and R.A. Rothenbury, *Inorg. Chem.* **4**, 1641 (1965).

3. R.J. Gillespie, R. Ouchi and G.P. Pez, *Inorg. Chem.* **8**, 63 (1969).

4. K.C. Lee and F. Aubke, *Inorg. Chem.* **18**, 389 (1979).

5. R.C. Thompson, in *"Inorganic Sulphur Chemistry"*, G. Nickless, Ed., Elsevier, Amsterdam, 1968.

6. A. Vogel, in *"Quantitative Inorganic Analysis"*, J. Wiley & Sons, N.Y., 1939.

7. S.P. Mallela, K.C. Lee and F. Aubke, *Inorg. Chem.* **23**, 653 (1984).

8. G.A. Olah, G.K.S. Prakash and J. Sommer, *"Superacids"*, J. Wiley & Sons, N.Y., 1985 (and references herein).

9. R.J. Gillespie and T.E. Peel, *Adv. Phys. Org. Chem.* **9**, 1 (1972).

10. R.J. Gillespie and T.E. Peel, *J. Am. Chem. Soc.* **95**, 5173 (1973).

11. J.A.S. Howell and K.C. Moss, *J. Chem. Soc. A*, 2481 (1971).

12. N.A. Matwiyoff, L.B. Asprey and W.E. Wageman, *Inorg. Chem.* **9**, 2014 (1970).

13. K.J. Packer and E.L. Muetterties, *J. Am. Chem. Soc.* **85**, 3035 (1963).

14. D.W. Aksnes, S.M. Hutchison, and K.J. Packer, *Mol. Phys.* **14**, 301 (1968).

15. D. Rehder, in *"Multinuclear NMR"*, J. Mason, Ed., Plenum Press, N.Y., 1988.

16. *"NMR and the Periodic Table"*, R.K. Harris and B.E. Mann, Eds., Academic Press, London, 1978.

17. E.A.V. Ebsworth, D.W.H. Rankin and S. Cradock, *"Structural Methods in Inorganic Chemistry"*, Blackwell Scientific Publications, U.K., 1987.

18. S. Brownstein, J. Bornais and G. Latremouille, *Can. J. Chem.* **56**, 1419 (1978).

19. J.J. Dechter in *Prog. Inorg. Chem.* **33**, 411 (1985).

20. J.V. Hatton, Y. Saito and W.G. Schneider, *Can. J. Chem.* **43**, 47 (1965).

21. L.C. Erich, A.C. Gossard and R.L. Hartless, *J. Chem. Phys.* **59**, 3911 (1973).

22. R.J. Gillespie, T.E. Peel and E.A. Robinson, *J. Am. Chem. Soc.* **93**, 5083 (1971).

23. V.M. Parikh, *"Absorption Spectroscopy of Organic Molecules"*, Addison-Wesley, Reading, U.S., p.15, 1974.

24. D. Bizot and M. Malek-Zadeh, *Rev. Chim. Min.* **11**, 710 (1974).

25. J. Barr, R.J. Gillespie and R.C. Thompson, *Inorg. Chem.* **3**, 1149 (1964).

26. P.L. Fabre, J. Devynk and B. Tremillon, *Chem. Rev.* **82**, 591 (1982).

27. M.F.A. Dove and A.F. Clifford, in *"Chemistry in Non-Aqueous Ionizing Solvents"*, J. Jander, H. Spandau and C.C. Addison, Eds., Vienweg, Braunschweig, Vol. 2.I, 1971.

28. F. Fairbrother, *"The Chemistry of Niobium and Tantalum"*, Elsevier, London, 1967.

29. D. Brown, *Chemistry of Niobium and Tantalum* in *"Comprehensive Inorganic Chemistry"*, Pergamon Press, N.Y., Vol.III, 1973.

30. K.C. Lee, Ph.D. Thesis, University of British Columbia, 1980.

31. W.V. Cicha, K.C. Lee and F. Aubke, *J. Solution Chem.*, submitted April, 1989.

32. A.J. Edwards, *J. Chem. Soc.*, 3714 (1964).

33. P.A. Yeats, J.R. Sams and F. Aubke, *Inorg. Chem.* **12**, 328 (1973).

34. R.J. Gillespie and P.A.W. Dean, *J. Am. Chem. Soc.* **92**, 2362 (1970).

35. R.J. Gillespie and P.A.W. Dean, *J. Am. Chem. Soc.* **91**, 7264 (1969).

36. R.J. Gillespie and P.A.W. Dean, *J. Am. Chem. Soc.* **91**, 7260 (1969).

37. A. Commeyras and G.A. Olah, *J. Am. Chem. Soc.* **91**, 2929 (1969).

38. S.P. Mallela, S. Yap, J.R. Sams and F. Aubke, *Inorg. Chem.* **25**, 4074 (1986).

39. R.J. Gillespie and J.B. Milne, *Inorg. Chem.* **5**, 1236 (1966).

40. A.M. Qureshi, H.A. Carter and F. Aubke, *Can. J. Chem.* **49**, 35 (1971).

41. A.M. Qureshi, L.E. Levchuk and F. Aubke, *Can. J. Chem.* **49**, 2544 (1971).

42. I.R. Beattie, K.M.S. Livingston, G.A. Ozin and D.J. Reynolds, *J. Chem. Soc. A*, 958 (1969).

43. O.L. Keller, Jr., *Inorg. Chem.* **2**, 783 (1963).

CHAPTER 7

TRIFLUOROMETHYL SULFATE DERIVATIVES OF NIOBIUM(V) AND TANTALUM(V)

7.A. Introduction

Trifluoromethyl sulfuric acid, HSO_3CF_3, is of comparable acidity to HSO_3F and has many chemical and physical properties in common.[1-3] It has also been used as the Brönsted acid in superacid systems.[1] There are, however, two important differences between the two acids in terms of their chemical reactivity.[4,5]

(i) Whereas the dissociation equilibria of HSO_3F in water leading to HF and H_2SO_4 have been discussed in Section B of Chapter 1, HSO_3CF_3 ionizes completely according to:

$$HSO_3CF_3 + H_2O \longrightarrow H_3O^+ + CF_3SO_3^- \qquad (7\text{-}1)$$

Hence, it is miscible with water and readily forms well defined, crystalline hydrates. More importantly, the S-C linkage, unlike the S-F linkage in fluorosulfates, is hydrolytically stable.

(ii) The S-C linkage of HSO_3CF_3 systems appears to be sensitive to oxidation, resulting in instability towards strong oxidizing agents such as $S_2O_6F_2$. It is not surprising that the peroxide $S_2O_6(CF_3)_2$ will readily decompose at room temperature into a series of products. Therefore, solvolysis of suitable precursors in HSO_3CF_3 is the only route to trifluoromethyl sulfates ("triflates").

A relevant and suitable general method used to prepare triflates involves the solvolysis of fluorosulfates in a large excess of CF_3SO_3H.[4] In combination with the known degradation reaction[6,7] between CF_3SO_3H and HSO_3F, this reaction pathway suggests that it may be possible to isolate binary triflate derivatives of the highly soluble $M(SO_3F)_5$ species (M = Nb or Ta) from the reaction of their HSO_3F solutions with a large excess of HSO_3CF_3. Furthermore, it was thought that the *exploratory study* discussed in this chapter may lead to crystalline materials suitable for single crystal X-ray diffraction studies.

7.B. Experimental

7.B.1. Synthesis of Tetrafluoro(trifluoromethylsulfato)tantalum(V), $TaF_4(SO_3CF_3)$

A 1.54 M solution of $Ta(SO_3F)_5$ in 1.14 ml HSO_3F was prepared according to the method outlined in the previous chapter. About 5 ml of HSO_3CF_3 were vacuum distilled onto the solution which was allowed to stir for 1 week at 25 °C. By this time, a precipitate had formed. The excess acid and any other volatile by-products were removed in vacuo at room temperature overnight. The white amorphous solid was isolated in quantitative yield. $TaF_4(SO_3CF_3)$ melted at 312-318 °C and appeared to go through a physical change at 255-265 °C.

Analytical Data for $TaSO_3CF_7$:

	Ta(%)	S(%)	C(%)	F(%)
Calculated:	44.57	7.90	2.96	32.76
Found:	44.70	8.20	2.76	32.42
S:C = 1.11				

7.B.2. Attempted Synthesis of Cesium Hexakis(trifluoromethylsulfato)tantalate(V)

About 5 ml of HSO_3CF_3 were vacuum distilled onto 486 mg (0.535 mmol) of α-$Cs[Ta(SO_3F)_6]$ and the solution was stirred at 40 °C for 2 days, during which time all of the starting material was consumed. The solvent and any other volatile by-products were completely removed in vacuo at 40 °C over a 2 day period and a beige/white powdery material was isolated in 93% yield.

Analytical Data for $CsTaS_6O_{18}C_6F_{18}$:

	S(%)	C(%)
Calculated:	15.92	5.96
Found:	14.64	5.70
S:C = 0.962		

7.B.3. Attempted Synthesis of Tetrafluoro(trifluoromethylsulfato)niobium(V)

Synthesis of this material was attempted by distilling ~10 ml of HSO_3CF_3 onto a ~1.2 M solution of $Nb(SO_3F)_5$ in HSO_3F and stirring the mixture for one week at 30-35 °C. Removal of all volatiles led to a product of mixed and uncertain composition.

Analytical Data for $NbSO_3CF_7$:

	S(%)	C(%)
Calculated:	10.08	3.78
Found:	8.01	2.14
S:C = 1.40		

7.B.4. Attempted Synthesis of Pentakis(trifluoromethylsulfato)tantalum(V)

The solvolysis of $TaCl_5$ with excess HSO_3CF_3 for 2 days at 35 °C was attempted. A white solid of mixed and uncertain composition was isolated by slowly removing all the volatiles at ~30 °C over a 3 week period in vacuo.

Analytical Data for $TaS_5O_{15}C_5F_{15}$:

	S(%)	C(%)	Cl(%)
Calculated:	17.31	6.48	0
Found:	11.69	4.51	4.16
S:C = 0.971			

7.C. Results and Discussion

7.C.1. Syntheses and General Discussion

7.C.1.a. $TaF_4(SO_3CF_3)$

The formation of this material according to:

$$Ta(SO_3F)_5 + \text{excess } HSO_3CF_3 \xrightarrow[\text{1 week, 25°C}]{HSO_3F} TaF_4(SO_3CF_3) + SO_2, CF_3SO_3F, COF_2, CO_2, CF_3SO_3CF_3, SiF_4 + \ldots \quad (7\text{-}2)$$

was somewhat unexpected. Previously reported[4] solvolysis reactions of binary fluorosulfates in HSO_3CF_3 have all led to the respective binary trifluoromethylsulfato ("triflate") complex. However, in all these precedents, solid fluorosulfates were treated with triflic acid and during many of these reactions solid material remained in the vessel. $Ta(SO_3F)_5$ was used in HSO_3F solution and a starting mixture consisting of

HSO_3CF_3:HSO_3F:$Ta(SO_3F)_5$ in an approximate 30:10:1 molar ratio was present. Since the degradation reaction of HSO_3CF_3 with HSO_3F is known to yield SiF_4 (via reaction of the by-product HF with glass) among many other fragments,[6,7] it is quite possible that the hydrofluoric acid formed by the degradation of HSO_3F or of the SO_3F group in $Ta(SO_3F)_5$ became involved in the solvolysis reaction. The possibility that some of the $Ta(SO_3F)_5$ dissociated via SO_3 elimination during the reaction or prior to it, forming species of the type $TaF_x(SO_3F)_{5-x}$, also cannot be ruled out.

The volatile degradation by-products with IR active modes which formed during this reaction[4] provide a convenient method by which to gauge the progress of the reaction. Identification of the resulting IR bands was not attempted. The rather high S:C ratio of 1.11 that was analytically obtained for this complex suggests that the reaction did not quite go to completion and that there may be residual amounts of fluorosulfate species left unreacted; the agreement between calculated and found elemental composition is however sufficiently good.

The successful synthesis of $TaF_4(SO_3F)$ via ligand redistribution described earlier was accomplished in a controlled reaction with a predetermined stoichiometry of the reactants. Formation of $TaF_4(SO_3CF_3)$, however, was rather incidental. It would also be of interest to investigate whether the conversion of solid $TaF_4(SO_3F)$ to $TaF_4(SO_3CF_3)$, via solvolysis in HSO_3CF_3, is feasible. The preparation in this solvent of $GeF_2(SO_3CF_3)_2$ from $GeF_2(SO_3F)_2$ serves as a precedent.[4]

Both the high melting point (~315 °C) and the limited air stability (for up to about 15 minutes) of $TaF_4(SO_3CF_3)$ are unusual. $GeF_2(SO_3CF_3)_2$, for example, is reportedly[4] very hygroscopic and melts at 150 °C. All the known $M(SO_3CF_3)_n$[4,8-10] species, with

M = Sn, Pd, Au, Ag, or Hg and n = 2, 3, or 4, are also very hygroscopic and, with the exception of $Sn(SO_3CF_3)_2$ and $Pd(SO_3CF_3)_2$, melt or decompose in the 140 - 235 °C range. The high fluoride content of this material does not in any way explain its high thermal stability, since TaF_5[11] melts at only 97 °C while $TaF_4(SO_3F)$ melts at ~215 °C. The relative thermal stability of this compound is however not without precedent; $I(SO_3F)_3$ melts at 33.7 °C while $I(SO_3CF_3)_3$ melts at 119 °C.[12]

7.C.1.b. Attempted Syntheses of $M(SO_3CF_3)_5$ (M = Nb or Ta) and $Cs[Ta(SO_3CF_3)_6]$

The reaction pathway shown in Equation (7-2) was also unsuccessfully tried in the attempted synthesis of $Nb(SO_3CF_3)_5$. The mixed product which was isolated in vacuo and analyzed for both sulfur and carbon appeared to have an overall composition of $NbF_{4.3}(SO_3F)_{0.2}(SO_3CF_3)_{0.5}$, indicating incomplete substitution of SO_3F by SO_3CF_3, as well as an elevated fluorine content. This may be the result of interference from HF as described above, or due to partial formation of $NbF_2(SO_3F)_3$ (and perhaps other fluoro(fluorosulfates)) in the 1.2 M HSO_3F solution. Nevertheless, both solvolysis reactions of $M(SO_3F)_5$ with M = Nb or Ta take a similar course, even though no well defined product results with niobium as the metal.

An alternative route to $Ta(SO_3CF_3)_5$, the reaction of $TaCl_5$ with excess HSO_3CF_3, was tried to eliminate interference from HF. This method has been previously employed to prepare $Sn(SO_3CF_3)_2$.[9] Unfortunately, an incomplete reaction occurred, with the resulting mixed product being partially decomposed in vacuo. The elemental analyses best agreed with the overall composition $TaO_{1.3}Cl_{0.6}(SO_3CF_3)_{1.8}$ or approximately $TaOCl(SO_3CF_3)_2$. The presence of oxygen may be explained by the elimination of species of the type $S_2O_5(CF_3)_2$ during product isolation.

The availability of salts of the type $Cs_x[M(SO_3F)_{5+x}]$ (x = 1 or 2) with both niobium and tantalum (see Chapters 4 and 5) allows a further application of the general conversion of fluorosulfates to trifluoromethyl sulfates via solvolysis in excess trifluoromethyl sulfuric ("triflic") acid.[4] α-$Cs[Ta(SO_3F)_6]$ was the first of these four salts chosen for this purpose. The reaction and subsequent volatile evolution in vacuo was carried out at 40 °C over a period of four days and yielded nearly a quantitative amount by weight of what appeared to be α-$Cs[Ta(SO_3CF_3)_6]$, but based on carbon and sulfur analyses the product was impure. Both values were too low, with the sulfur value being markedly worse (a S:C ratio of 0.962 was found). It appears that the solvolytic conversion of fluorosulfates into triflates takes a complex course, with possible side reactions. Further work is needed to ensure a complete and successful conversion of the cesium fluorosulfato metallates.

7.C.2. Vibrational Spectroscopy Studies

7.C.2.a. $TaF_4(SO_3CF_3)$

Strong fluorescence, which is common for triflic acid and many previously studied triflates,[4,8,9] prevented the recording of a Raman spectrum while the IR spectrum was very poorly resolved. The data from the latter are listed in Table 7.I. Attempts to use Nujol as a mulling agent were unsatisfactory because "new", very intense bands (not found in the solid film spectrum) were observed and reaction of the solid with Nujol was suspected. Although the listing in Table 7.I may be incomplete, the ν(S-C) band does seem to be present at its typical position[4,8,9] between 750 and 800 cm^{-1}. The

Table 7.I. Infrared Vibrational Frequencies for $TaF_4(SO_3CF_3)$

ν (cm^{-1})		Approx. Assignment
1415	s,sh	$\nu(SO_3) + \nu(CF_3)$
~1350	s,vb	
1255	sh	
1210	s,vb	
~1170	m,sh	
1150	s	
1090	w,sh	
980	s,b	
865	m,b	?
770	w,b	ν (S-C)
~650	m,vb	ν (Ta-F)
605	m,sh	ν (Ta-O) + $\delta(SO_3F)$
572	m	
509	w	
480	w,sh	
465	w	

$\nu(SO_3)$ modes also occur at very "standard" positions. However, the broadness of all the bands makes any further interpretation somewhat difficult.

7.C.2.b. "$Cs[Ta(SO_3CF_3)_6]$"

Although acceptable analytical data have not been obtained for this salt, its bulk composition as shown has been suggested earlier and is further verified by its infrared spectrum, data from which are listed in Table 7.II. The spectrum is shown in Figure 7.1. The most telling evidence for the presence of SO_3CF_3 groups is the sharp band at

Table 7.II. Infrared Vibrational Frequencies of "$Cs[Ta(SO_3CF_3)_6]$"

ν (cm^{-1})		Approx. Assignment
1407	s,b	ν (SO_3)
1307	w	ν (SO_3) + ν (CF_3)
1245	s,sh	
1215	s	
1178	s,sh	
1146	s	
1058	m	
~935	s,vb,sh	
885	s,vb	
774	m	ν (S-C)
680	m	ν_s (Ta-O) + δ (SO_3F) + δ (CF_3)
631	m	
602	m	
567	w,sh	
530	w	δ (SO_3F)
498	m	
~400	vw,vb	δ (CSO)
373	vw,b,sh	
350	w	δ (CF_3)

774 cm^{-1}, attributable to a S-C stretch mode,[4] and the absence of a broad band at ~840 cm^{-1}, which was assigned in Chapter 5 to the S-F stretch mode of the starting material α-$Cs[Ta(SO_3F)_6]$. Due to the frequent overlap of bands resulting from SO_3 and CF_3 fundamentals, it is very difficult to make any definite structural conclusions about this salt; similar problems have been encountered with many of the previously studied binary and ternary triflates.[4,8,9]

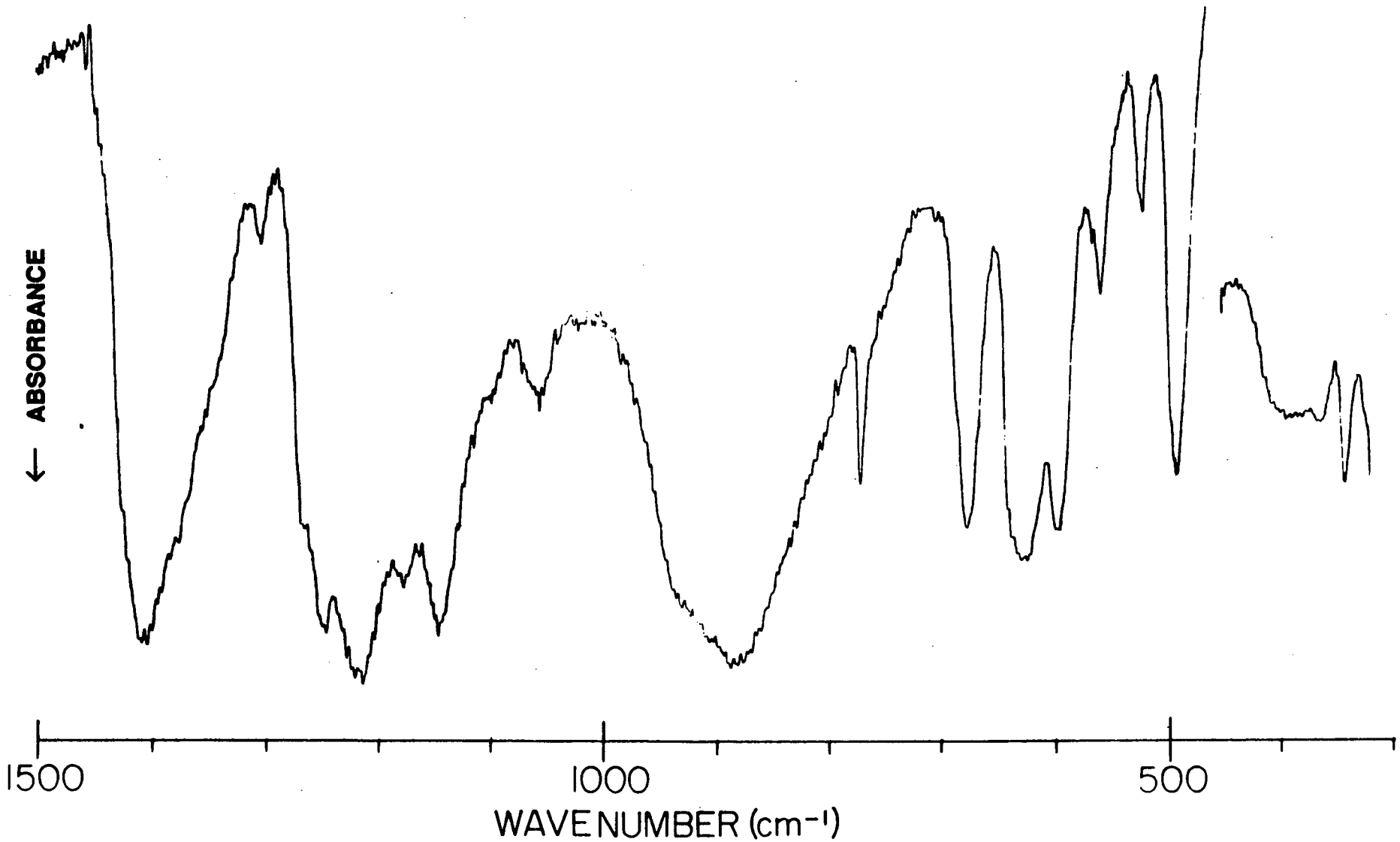

Figure 7.1. Infrared Spectrum of "$Cs[Ta(SO_3CF_3)_6]$" from 300 to 1500 cm^{-1}

7.D. Conclusion

Preliminary exploration of two possible routes to binary trifluoromethyl sulfates of niobium(V) and tantalum(V) has been discussed. Although neither led to the preparation of the desired species, the novel material $TaF_4(SO_3CF_3)$ was prepared and found to have interesting properties. The pathway involving the reaction of MCl_5 with excess HSO_3CF_3 needs to be further investigated, since it holds some promise.

Impure $Cs[Ta(SO_3CF_3)_6]$ also appears to have been prepared from the corresponding fluorosulfate salt, which suggests that $Ta(SO_3CF_3)_5$ may behave as a SO_3CF_3 acceptor in HSO_3CF_3. However, the generation of $Ta(SO_3CF_3)_5$ even "in situ" may not be possible. It would hence seem worthwhile to attempt systematically the preparation of the other $Cs_x[M(SO_3CF_3)_{5+x}]$ type salts, with M = Nb or Ta and x = 1 or 2, from the respective fluorosulfate precursors that were described in Chapters 4 and 5.

REFERENCES

1. G.A. Olah, G.K.S. Prakash and J. Sommer, *"Superacids"*, J. Wiley & Sons, N.Y., 1985 (and references herein).

2. G.A. Olah, G.K.S. Prakash and J. Sommer, *Science* **206**, 13 (1979).

3. R.D. Howells and J.D. McCown, *Chem. Rev.* **1**, 69 (1977).

4. S.P. Mallela, J.R. Sams and F. Aubke, *Can. J. Chem.* **63**, 3305 (1985).

5. G.A. Lawrence, *Chem. Rev.* **86**, 17 (1986).

6. G.A. Olah and T. Ohyama, *Synthesis* **5**, 319 (1976).

7. R.E. Noftle, *Inorg. Nucl. Chem. Lett.* **16**, 195 (1980).

8. P.C. Leung, K.C. Lee and F. Aubke, *Can. J. Chem.* **57**, 326 (1979).

9. R.J. Batchelor, J.N.R. Ruddick, J.R. Sams and F. Aubke, *Inorg. Chem.* **16**, 1414 (1977).

10. M. Schmeisser, P. Satori and B. Lippsmeier, *Chem. Ber.* **102**, 2150 (1969).

11. *"Handbook of Chemistry and Physics"*, 57th Edition, R.C. Weast, Ed., C.R.C. Press, U.S.A., 1976-1977.

12. J.R. Dalziel and F. Aubke, *Inorg. Chem.* **12**, 2707 (1973).

CHAPTER 8

GENERAL CONCLUSIONS

The conclusions from this study are presented in two sections: the first summarizes the results obtained while the second briefly describes some preliminary exploratory work together with suggestions for future investigations.

8.A. Summary

Many of the specific conclusions from this study have already been summarized in previous chapters. Taken as a whole, the following general conclusions can be reached:

(i) Two new monoprotonic superacid systems, HSO_3F-$Ta(SO_3F)_5$ and HSO_3F-$Nb(SO_3F)_5$, have been developed. The former is the stronger acid of the two, and in this respect exceeds the "Magic Acid" system HSO_3F-SbF_5[1,2] at comparable Lewis acid concentrations beyond about 0.1 molal, as indicated by conductivity and Hammett Acidity Function measurements. The niobium system, however, is still much stronger than the analogous fluoride, NbF_5, in this solvent.[3]

(ii) The high solubility of both $Nb(SO_3F)_5$ and $Ta(SO_3F)_5$ in HSO_3F (far superior to that of NbF_5 and TaF_5) has prevented their isolation from this solvent but has allowed detailed studies of their solution behaviour using conductometry, uv/vis spectrophotometry, multinuclear NMR spectroscopy and Raman spectroscopy.

(iii) As implied by their superacidity, both Lewis acids are good fluorosulfate acceptors which allowed the isolation and full characterization (including complete chemical

analysis) of salts of the type $M_x'[M(SO_3F)_{5+x}]$ with M′ = Cs or Ba and x = 1 or 2. Even though both $Nb(SO_3F)_{5(solv)}$ and $Ta(SO_3F)_{5(solv)}$ behave as monobasic acids in a moderately basic environment, up to two moles SO_3F^- could be added cleanly, while isolation of $Cs_3[M(SO_3F)_8]$, with M = Nb or Ta, failed.

(iv) At higher concentrations, both $Nb(SO_3F)_{5(solv)}$ and $Ta(SO_3F)_{5(solv)}$ tend to dissociate via SO_3 elimination to yield polymeric species of the type $MF_x(SO_3F)_{5-x}$. This tendency appears to be more pronounced for $Nb(SO_3F)_{5(solv)}$ and has resulted in the isolation of solid $NbF_2(SO_3F)_3$.

(v) The successful synthesis of $TaF_4(SO_3F)$ from $Ta(SO_3F)_5$ and TaF_5 in HSO_3F should be expandable and is expected to lead to a general, one-step synthesis according to:

$$n\,MF_5 + (5-n)\,M(SO_3F)_5 \xrightarrow{HSO_3F} 5\,MF_n(SO_3F)_{5-n} \qquad (8\text{-}1)$$

or more simply:

$$n\,MF_5 + (5-n)\,M + 5/2\,S_2O_6F_2 \xrightarrow{HSO_3F} 5\,MF_n(SO_3F)_{5-n} \qquad (8\text{-}2)$$

with either niobium or tantalum as the central metal. The resulting Lewis acids are potentially both F^- and SO_3F^- acceptors and should find use in HF as well as in HSO_3F.

(vi) The role of $S_2O_6F_2$ as a very weak base in HSO_3F has been revealed, together with the observations of a previously unknown in situ acid-peroxide equilibrium complex. Useful information concerning the utility of this system as a reagent medium has also been obtained.

(vii) The successful conversion of $Ta(SO_3F)_5$ to $TaF_4(SO_3CF_3)$ in the combined Brönsted acid solvent HSO_3CF_3/HSO_3F as well as initial studies on the conversion of

α-Cs[Ta(SO_3F)$_6$] into the corresponding triflate suggested the feasibility of tantalum triflates as components of a conjugate triflic acid superacid system. Niobium appeared less promising in these conversion reactions.

In general, it appears that the tantalum superacid system is more promising than the niobium system on account of its higher inherent acidity and lower predisposition towards decomposition via SO_3 elimination.

8.B. Exploratory Investigations and Suggestions for Future Work

8.B.1. Ag-Ta(SO_3F)$_5$ Systems

In the quest to stabilize unusual cations, the *colorless* $Ag^I[Ag^{III}(SbF_6)_4]$ solid (or "$Ag(SbF_6)_2$") has recently been synthesized in our laboratory. Interestingly, $Ag(TaF_6)_2$ is known to exist as a deep *blue* solid.[5] Inspired by the above studies and the highly acidic behaviour of the HSO_3F-Ta(SO_3F)$_5$ system, the following two groups of experiments were conducted:

(i) "$Ag(SbF_6)_2$" was dissolved in a solution of Ta(SO_3F)$_5$/HSO_3F, both with an excess of Ta(SO_3F)$_5$ and in an exact 1:2 (Ag:Ta) molar ratio. The object was to investigate whether any ligand exchange would occur between $[Ta(SO_3F)_6]^-$ and $[SbF_6]^-$ and whether the mixed oxidation state of silver would be retained in the process.

(ii) $Ag(SO_3F)_2$[6] was reacted with a double molar amount of Ta(SO_3F)$_5$ in HSO_3F and a 1:1 molar mixture of Ag and Ta was oxidized by $S_2O_6F_2$ in HSO_3F. It was of interest to investigate whether Ag[Ta(SO_3F)$_6$]$_2$ or Ag[Ta(SO_3F)$_7$] would preferentially form.

In all of the above reactions, a deep *green* solution formed initially, with the color gradually changing to *yellow* within a few days and then completely vanishing; the same sequence of events could be induced by partially removing HSO_3F in vacuo. This suggested the presence of equilibria processes in solution, perhaps involving multiple oxidation states of silver.

The complexity of the ^{19}F NMR spectra (greatest for colorless solutions) and the IR spectra of the light yellow, viscous oils that formed upon in vacuo removal of HSO_3F prevents any conclusions to be made about these systems at present. A more systematic solution study involving electronic spectroscopy, among other techniques, is needed to understand their seemingly complex behavior.

8.B.2. Suggestions for Future Work

The present investigation is expandable into four general areas:

(i) The family of fluoro(fluorosulfates) $MF_x(SO_3F)_{5-x}$ needs to be systematically investigated with both niobium and tantalum; these species hold the promise of having high enough solubility and acidity in HSO_3F to serve as superacid systems while being isolable out of solution and hence available for structural study.

(ii) As suitable anions for the ongoing study[7] of $(CH_3)_2SnY_2$ (Y = conjugate base of strong Lewis acid) type salts via ^{119}Sn Mössbauer, $[Nb(SO_3F)_6]^-$ and especially $[Ta(SO_3F)_6]^-$ are both feasible candidates, particularly since salts with Y being $[NbF_6]^-$ and $[TaF_6]^-$ have previously been made[8] and studied.[7] This would also serve as another method of studying the behaviour and acid strength of the two new superacid systems.

(iii) A more detailed investigation of the trifluoromethyl sulfate system with niobium

and tantalum is needed. Their potential superacidity as well as their value as means of better understanding the structural properties of the analogous fluorosulfates are features primarily responsible for this interest.

(iv) Finally, and perhaps most importantly, the suitability of both of the developed superacid systems for any applications such as were mentioned in section C.3 of Chapter 1 needs to be thoroughly investigated. Based on some fundamental considerations, this work has shown the tantalum system to be more suitable; more detailed acid strength and stability determinations should however be undertaken, perhaps by making use of dynamic NMR techniques. Testing of the stability of these systems in the presence of oxidizable organic materials and attempts at generating unstable cations are also among the areas worthy of investigation before either acid can be seriously considered for widespread use.

REFERENCES

1. R.C. Thompson, J. Barr, R.J. Gillespie, J.R. Milne and R.A. Rothenbury, *Inorg. Chem.* **4**, 1641 (1965).

2. R.J. Gillespie and T.E. Peel, *J. Am. Chem. Soc.* **95**, 5173 (1973).

3. R.J. Gillespie, R. Ouchi and G.P. Pez, *Inorg. Chem.* **8**, 63 (1969).

4. B.G. Müller, *Angew. Chem. Int. Ed. Engl.* **26**, 689 (1987).

5. P.C. Leung, Ph.D. Thesis, University of British Columbia, 1979.

6. S.P. Mallela, S. Yap, J.R. Sams and F. Aubke, *Inorg. Chem.* **25**, 4074 (1986).

7. S.P. Mallela, S. Yap, J.R. Sams and F. Aubke, *Rev. Chim. Min.* **23**, 572 (1986).

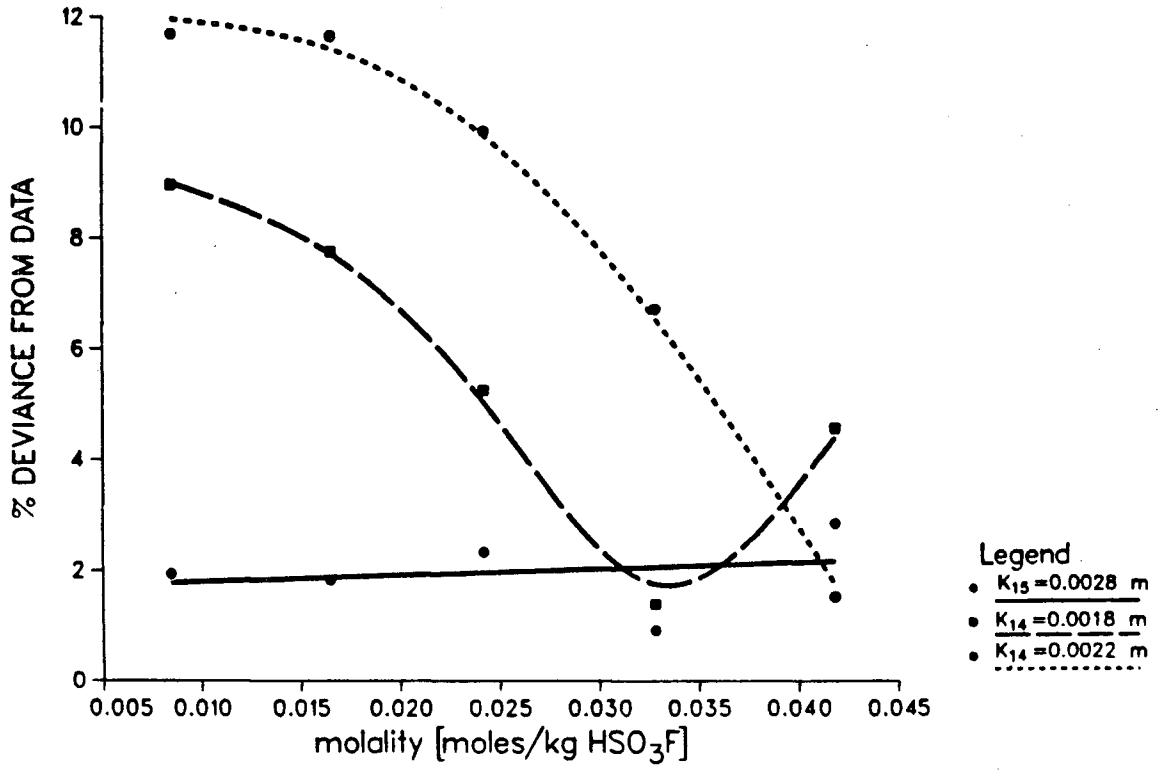

Figure A.1. Comparison of the Deviation from Experimental Data of Optimal Oligomeric Ionization Equilibrium Constants for $Nb(SO_3F)_5$ in HSO_3F at 25.00 °C

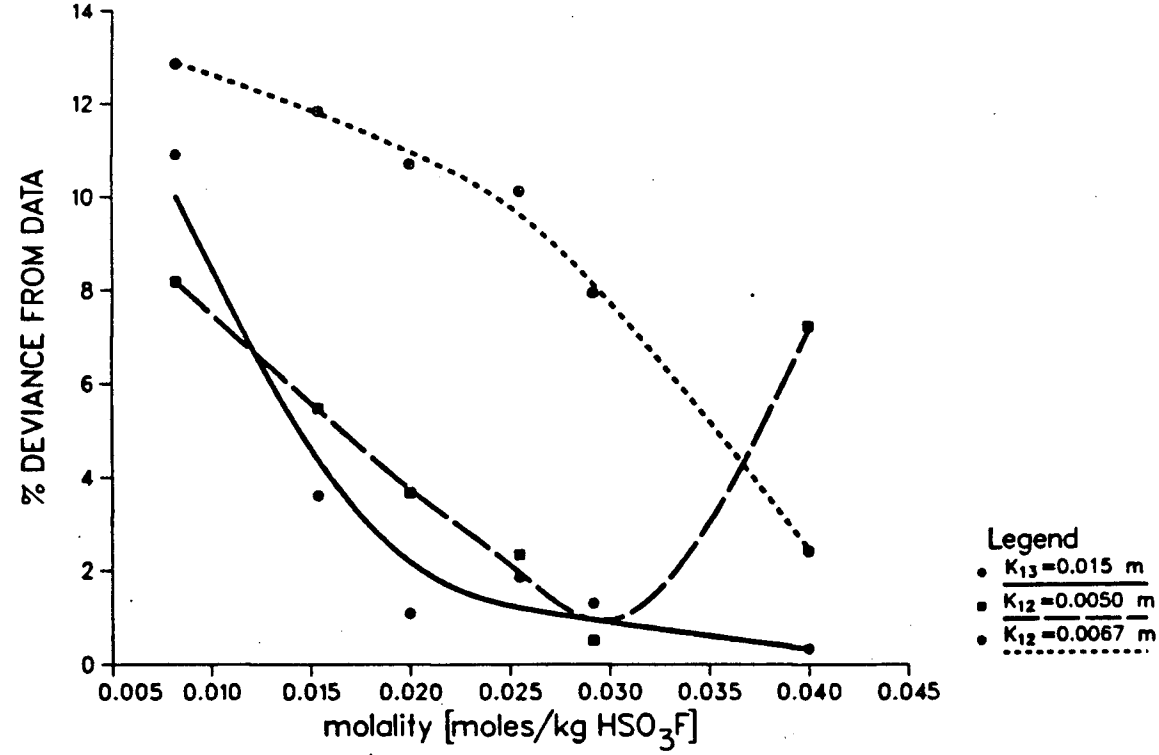

Figure A.2. Comparison of the Deviation from Experimental Data of Optimal Oligomeric Ionization Equilibrium Constants for $Ta(SO_3F)_5$ in HSO_3F at 25.00 °C

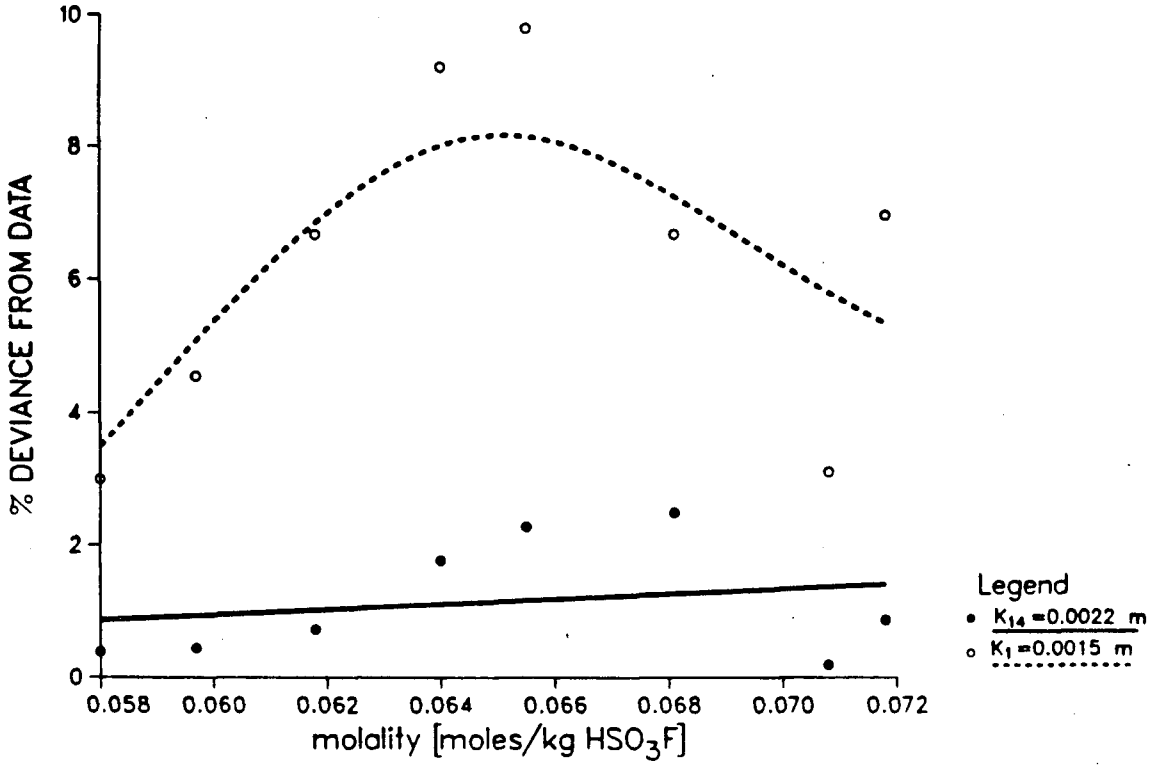

Figure A.3. Comparison of the Deviation from Experimental Data of Best Oligomeric and Monomeric Ionization Equilibrium Constants for $Nb(SO_3F)_5/KSO_3F$ in HSO_3F at 25.00 °C

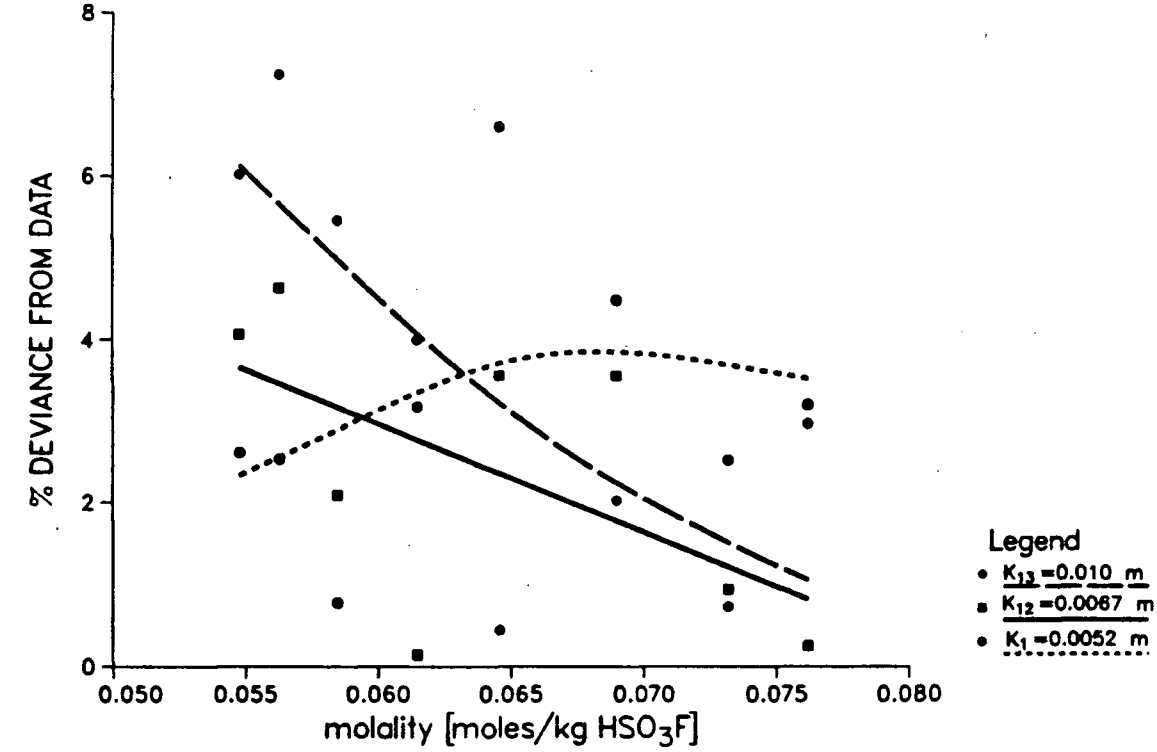

Figure A.4. Comparison of the Deviation from Experimental Data of Best Oligomeric and Monomeric Ionization Equilibrium Constants for $Ta(SO_3F)_5/KSO_3F$ in HSO_3F at 25.00 °C

Table A.I. Molar Absorptivity and pK_{BH^+} Values for Hammett Indicators Used[a]

Indicator	ε_B	ε_{BH^+}	pK_{BH^+}
DNFB	920	12,100	-14.52
TNT	960	10,600	-15.60
DNFBH+	900	20,450	-17.35
TNTH+	0	14,500	-18.36

[a]reference 10 (chapter 6)

Table A.II. Ionization Data for $Ta(SO_3F)_5$ in HSO_3F[a]

	-Log I			
Mole % $Ta(SO_3F)_5$	DNFB	TNT	DNFBH+	TNTH+
0	-0.56	0.55	-	-
0.055	-1.01	0.03	-	-
0.154	-	-0.47	-	-
0.318	-	-1.12	0.61	-
0.913	-	-	-0.68	-
1.25	-	-	-1.00	-0.02
1.80	-	-	-	-0.22
2.11	-	-	-	-0.35
3.37	-	-	-	-0.55

[a]see Equations (1-11) and (6-20)

N.B. Based on the average publication year of the references cited in the introduction of this thesis, the vintage years for superacid chemistry were 1973 ± 11. Better late than never.